NTNU – Trondheim
Norwegian University of
Science and Technology

Stability Analysis of Diode Bridge Rectifier-Loaded Synchronous Generators Characterized with High Values of Reactances

Torunn Husevåg Helland

Master of Energy Use and Energy Planning
Submission date: June 2015
Supervisor: Trond Toftevaag, ELKRAFT

Norwegian University of Science and Technology
Department of Electric Power Engineering

Problem Description

This thesis concerns the stability of diode bridge rectifier-loaded synchronous generators with the possibility for an attached battery-bank, characterized by large values of generator reactances. A particular system onboard ships with diesel-electric, variable speed propulsion DC-system delivered by Siemens is under study.

The thesis should contain a literature study concerning the stability of synchronous generators, possibly connected to diode-bridge rectifiers and with high reactances. It should also include a collection of operating experience, including analysis of existing measurements/registrations of the system under operation. If time allows, new measurements should be planned, conducted and analyzed. The work from the specialization project conducted fall 2014 should be continued with the introduction of a rectifier into the model already established.

A computer-based model of the system is to be established in a suitable simulation tool, where appropriate simulations is to be conducted and the stability is to be analyzed and discussed. The simulations should try to recreate the observations on the ships. Among others is a sensitivity analysis for variations in parameter values and component analysis to be conducted. The thesis should contain an discussion of the results obtained, recommendations and a final conclusion.

Project time-period: January-June 2015

Supervisor: Trond Toftevaag

Collaborating company: Siemens AS

Preface

This thesis was written in the spring semester of 2015 and is the final work of the 2-year master program "Energy use and energy planning" with orientation energy supply at the Norwegian University of Science and Technology NTNU in Trondheim. The thesis is written at the Faculty of Information Technology, Mathematics and Electrical Engineering IME for the Department of Electric Power Engineering.

The problem addressed in this thesis is the instability of diode-bridge rectifier-loaded synchronous generators with high values of reactances, and was proposed by Siemens as a part of their assessment of the new diesel-electric, variable speed propulsion DC-system developed for ships.

I would like to thank my supervisor Trond Toftevaag for his valuable help, advice and motivating conversations when planning the simulations. I could also thank my co-supervisor Espen Haugan in Siemens for taking time to meet up with us to discuss the problems experienced on the ships, for helping me to understand the researched system, and for providing the model of the system in MatLab/SimPowerSystems.

Torunn Husevåg Helland

Trondheim, June 2015

Abstract

This thesis concerns the stability of diode bridge rectifier-loaded synchronous generators characterized by large values of synchronous, transient and subtransient reactances in the d- and q-axis, with the possibility of connecting a battery-bank. The synchronous reactances are in the range 2.5-5.5pu.

The electrical system studied is installed in two tug-ships using two different types of generators, with different ranges of generator reactances and performance. One of the tugships studied uses generators with a capacity of 3333kVA that has synchronous reactances in the lower layer of 2.5-5.5 pu and is characterized as stable during operation. The other ship uses generators with a capacity of 1940kVA, has synchronous reactances in the upper layer of 2.5-5.5 pu and is characterized as unstable during normal operation. The observed oscillations in this ship have a frequency of approximately 2Hz.

The diesel-electric, variable speed propulsion DC-system used in the two ships is delivered by Siemens. The synchronous generators deliver power to a dc-bus through six-pulse diode bridge rectifiers. The thrusters are supplied by the dc-bus through inverters, and a battery can be attached to the dc-bus for redundancy. The object of this thesis is to find the reason why rectifier-loaded synchronous generators with high reactances become unstable, and what can be done to prevent the observed instability.

The same system was under study for a specialization project conducted at the Department of Electrical Power Engineering during the fall 2014. The main findings in this project are included in the present thesis, where simulations indicate that the studied generators become unstable when the gain of the voltage regulator is increased, and no rectifier is included in the model. This happens faster for the 1940kVA generator than for the 3333kVA generator, and when reactive power is consumed.

A literature study of articles and other work concerning the stability of similar systems is also conducted. It is in literature found that local mode problems often is associated with rotor angle oscillations, and usually has a frequency of 0.7-2Hz. Stability criteria is found in literature concerning diode bridge rectifier-loaded synchronous generators in [1] and [2], given below,

respectively:

$$\frac{X_q}{X`_d} \leq 2 \tag{1}$$

$$X`^2_d I`^2_d + X`^2_q I`^2_q \leq 2X`_d I`_d U_p \tag{2}$$

The stability criteria have requirements for the synchronous and transient reactance, but not for the subtransient reactance. [1] claims that small-frequency oscillations starts in the rectifier causing instability of rectifier-loaded synchronous generators. It is also found a criterion in [3] developed from the criterion in [1] in Eq. 1, saying that stability is easier achieved by adding a short-circuited q-axis winding on the rotor. The criterion is shown below [3]:

$$\frac{1}{X_q} + \frac{1}{X`_q} \geq \frac{1}{X`_d} \tag{3}$$

The work of the specialization project is continued, and a rectifier is added to the model established in DIgSILENT PowerFactory in the fall of 2014. The battery is modeled as a constant DC-voltage source, and the rectifier is modeled as a PWM rectifier with no modulation and a firing angle set to zero. The generator stability is studied when the gain of the voltage regulator is increased from 50-500. The simulation is made for both producing and consuming reactive power, both cases of which the generator produces active power.

The gain directly affects the nature of the linearization constant K_5, making it negative resulting in a negative feedback when the external impedances is high. The hypothesis is that this also happens when the internal reactances in the generator is high. This is shown through simulations to be true. It was expected that the 1940kVA generator reaches instability faster than the 3333kVA generator, as was the result in the specialization project, but this was not the case. It is believed that the rectifier chosen does not imitate the real system well enough.

By using the parameters of the 3333kVA and 1940kVA generators, as well as knowledge of the ship components, simplified models are established in the simulation tool MatLab/SimPowerSystems.

The battery in MatLab/SimPowerSystems is modeled as an infinitely large capacitor and a series resistance, and the rectifier is a diode-bridge rectifier. A sensitivity analysis for parameter values is conducted, by varying parameter values of the main components such as the synchronous generator, battery, rectifier, load and voltage regulator, and the stability is studied. The impact of the presence of the main components on the stability is studied as well. Neither of the criteria found in [1] and [2] has requirements for the subtransient reactance, and the impact of the subtransient reactance on the stability is studied through sensitivity analysis. Different load-situations are simulated and generator stability is examined.

The main phenomena observed on the ship are successfully recreated through simulations, and the model established in the simulation tool is verified due to this. It is through simulations found that the presence of the diode-bridge rectifier is crucial to detect stability problems, and that the load-situation impacts the stability. When the 1940kVA generator supplies a load of 1.9MVA, it becomes stable, but is unstable during no-load and for all other loads less than 1.9MVA.

It is also found that the transient and subtransient reactances play an equally important role as the synchronous reactances when it comes to generator stability in this context. The sensitivity analysis conducted is used as a basis for the development of stability limits. The results found through simulations are compared with stability criterions and theories presented in articles found in the literature study concerning the same problems as addressed in this thesis.

The stability criteria found for the 1940kVA generator with emphasis on the transient and subtransient reactance is given as:

$$\frac{X`_q}{X`_d} \leq 5.41 \qquad \frac{X``_q}{X``_d} \leq 0.46 \tag{4}$$

By combining the stability criterion for transient reactance in Eq. 4 with the equation found in Eq.3 by [3], it is found that the stability criterion obtained in this thesis is fulfilled and that stability can be achieved by adding a short-circuited q-axis winding to the generator rotor.

Recommendations for further work is to replace the PWM rectifier with a diode-bridge rectifier in the DIgSILENT PowerFactory model and redo the varying of the gain in the voltage regulator to study the stability of the 3333kVA and 1940kVA generators. It is also suggested that the interaction between the synchronous generator and diode-bridge rectifier is further investigated. Last, but not least should simulation be conducted, where a short-circuited q-axis winding is added to the generator rotor, to verify the results found in this thesis from the stability criteria obtained.

Sammendrag

Dette diplomarbeidet omhandler stabiliteten til diode-bro likeretter-tilkoblede synkrongeneratorer kjennetegnet ved høye verdier av synkrone, transiente og subtransiente reaktanser i d- og q-aksen, med mulighet for tilkobling av batteribank. Synkronreaktansene er i størrelsesordenen 2.5-5.5 pu.

Det elektriske systemet som er studert er installert i to slepebåter som bruker to ulike typer generatorer, med ulik størrelsesorden av generatorreaktanser og ytelse. En av slepebåtene som er studert bruker generatorer med ytelsen 3333kVA, har synkronreaktanser i det nedre sjiktet av størrelsesordenen 2.5-5.5 pu og er karakterisert som stabil ved drift. Den andre slepebåten bruker generatorer med ytelsen 1940kVA, har synkronreaktanser i det øvre sjiktet av størrelsesordenen 2.5-5.5 pu og er karakterisert som ustabil ved normal drift. De observerte pendlingene på dette skipet har en frekvens på omtrent 2Hz.

Det diesel-elektriske, turtalls-variable framdrifts DC-systemet brukt på de to skipene er levert av Siemens. Synkrongeneratorene leverer effekt til en dc-samleskinne gjennom seks-puls diode-bro likerettere. Hovedmotorene og propellene forsynes av dc-samleskinnen gjennom vekselrettere, og et batteri kan kobles til dc-samleskinnen for å oppnå redundans. Formålet med dette arbeidet er å finne bakgrunnen til hvordan likeretter-tilkoblede synkrongeneratorer med høye reaktanser blir ustabile, og finne ut hva som kan gjøres for å unngå den observerte ustabiliteten.

Det samme systemet ble studert i spesialiseringsprosjektet gjennomført ved Institutt for Elkrafteknikk høsten 2014. Hovedfunnene i dette prosjektet er inkludert i dette arbeidet, hvor simuleringer indikerer at de studerte generatorene blir ustabile ved økning av forsterkningen til spenningsregulatoren, når likeretteren ikke er tilkoblet til modellen. Dette skjer raskere for 1940kVA generatoren enn for 3333kVA generatoren, og når det konsumeres reaktiv effekt.

En litteraturstudie av artikler og annet arbeid som omhandler samme problemstilling er også presentert. Det er i litteraturen funnet at lokale mode-problemer ofte er assosiert med polhjulspendlinger, og har ofte en frekvens mellom 0.7-2Hz. Det er funnet stabilitetskriterier som omhandler diode-bro likeretter-tilkoblede synkrongeneratorer i [1] og [2], og de er gjengitt nedenfor:

$$\frac{X_q}{X`_d} \leq 2 \tag{5}$$

$$X`^2_d I`^2_d + X`^2_q I`^2_q \leq 2X`_d I`_d U_p \tag{6}$$

Stabilitetskriteriene har krav for de synkrone og transiente reaktansene, men ikke for de subtransiente reaktansene. [1] påstår at lav-frekvente pendlinger kan starte i likeretteren, og forårsake ustabil drift av diode-bro likeretter-tilkoblede synkrongeneratorer. Det er også funnet et stabilitetskriterie i [3] utarbeidet fra stabilitetskravet i [1] i Likn. 5, som sier at stabilitet er lettere å oppnå ved å legge til en kortsluttet q-akse vikling på rotoren. Kriteriet er vist under [3]:

$$\frac{1}{X_q} + \frac{1}{X`_q} \geq \frac{1}{X`_d} \tag{7}$$

Arbeidet fra spesialiseringsprosjektet er videreført, og en likeretter er lagt til modellen opprettet i DIgSILENT PowerFactory høsten 2014. Batteriet er modellert som en konstant dc-spenningskilde, og likeretteren er modellert som en PWM likeretter med ingen modulering og en skuddvinkel lik null. Generatorstabiliteten studeres når forsterkningen til spenningsregulatoren økes fra 50-500. Simuleringen er gjennomført for når generatoren produserer og konsumerer reaktiv effekt, hvor den i begge tilfeller produserer aktiv effekt.

Forsterkningen påvirker oppførselen til lineariseringskonstanten K_5 direkte, da den kan bli negativ, noe som fører til negativ tilbakekobling når de eksterne impedansene er høye. Hypotesen er at dette også skjer når de interne reaktansene i generatoren er høye. Dette har gjennom simuleringer vist seg å være sant. Det var forventet at 1940kVA generatoren skulle nå ustabilitet raskere enn 3333kVA generatoren, som var resultatet i spesialiseringsprosjektet, men dette var ikke tilfelle. Det er antatt at typen likeretter valgt ikke speiler det reelle systemet godt nok.

Ved å bruke parametere fra 3333kVA generatoren og 1940kVA generatoren samt kunnskap om komponentene på skipet, er det opprettet forenklede modeller simuleringsverktøyet MatLab/SimPowerSystems.

Batteriet i MatLab/SimPowerSystems er modellert som en uendelig stor kapasitans og en motstand i serie, og likeretteren er en diode-bro likeretter. En sensitivitets-analyse for parameter verdier er gjennomført, ved å variere parameterverdiene i hovedkomponentene slik som synkrongeneratoren, batteriet, lasten, likeretteren og spenningsregulatoren, og stabiliteten er studert. Innvirkningen av tilstedevœrelsen av hovedkomponentene på stabiliteten er også studert. Ingen av kriteriene funnet i [1] og [2] inneholder krav for den subtransiente reaktansen, og påvirkningen av denne er studert gjennom sensitivitets-analyse. Ulike lastsituasjoner er simulert og generatorstabiliteten er undersøkt.

Gjennom simuleringer er det vellykket klart å gjenskape hovedfenomenene observert på skipene, og modellen etablert i simuleringsverktøyet er dermed verifisert. Det er ved hjelp av simuleringer funnet at tilstedevœrelsen av diode-bro likeretteren er viktig for å detektere ustabilitetsproblemer, og at lastsituasjonen påvirker stabiliteten. Når 1940kVA generatoren forsyner en last på 1.9MVA er den stabil, men er ustabil ved ingen last og for alle andre laster mindre enn 1.9MVA.

Det er også funnet at de transiente og subtransiente reaktansene spiller en like viktig rolle som synkronreaktansene når det kommer til generatorstabilitet i denne sammenhengen. Resultatene fra sensitivitets-analysen er lagt til grunnlag ved utviklingen av stabilitetsgrenser. Resultatene funnet gjennom simuleringer er sammenliknet med stabilitetskriteriene og teoriene presentert i artiklene funnet gjennom litteraturstudien som omhandler samme problemstilling som er addressert i dette arbeidet.

Stabilitetskriteriene funnet for 1940kVA generatoren med vekt på de transiente og subtransiente reaktansene er gjengitt nedenfor:

$$\frac{X`_q}{X`_d} \leq 5.41 \qquad \frac{X``_q}{X``_d} \leq 0.46 \tag{8}$$

Ved å kombinere stabilitetskriteriet for transiente reaktanser i Likn. 8, med kriteriet funnet i Likn. 7 av [3], er det funnet at stabilitetskriteriet framarbeidet i dette arbeidet er oppfylt, og at stabilitet kan oppnås ved å legge til en kortsluttet q-akse vikling på rotoren til generatoren.

Anbefalinger for videre arbeid er å bytte ut PWM-likeretteren med en diode-bro likeretter i DIgSILENT PowerFactory modellen, og å gjenta forsøket med varieringen av forsterkningen i spenningsregulatoren for så å studere stabiliteten av 3333kVA generatoren og 1940kVA generatoren. Det er også foreslått å videre studere samspillet mellom synkrongeneratoren og diode-bro likeretteren. Sist, men ikke minst, burde simuleringer hvor en kortsluttet q-akse vikling er lagt til generator-rotoren gjennomføres, for å verifisere resultatene funnet fra stabilitetskriteriene utviklet i dette diplomarbeidet.

Contents

List of Figures

List of Tables

Nomenclature

Abbreviations

SG Synchronous Generator

DC Direct Current

AC Alternating Current

AVR Automatic Voltage Regulator

PWM Pulse Width Modulation

IGBT Insulated-Gate Bipolar Transistor

THD Total Harmonic Distortion

RMS Root Mean Square

DG Distributed Generatorion

AVM Average Value Modulation

pu Per unit

PID Proportional Integration Derivation

VT Voltage Transformer

CT Current Transformer

RPM Rotations Per Minute

THD Total Harmonic Distortion

Symbols

First mentioned in Chapter 1

$X_{d,q}$ Synchronous reactance in d- and q-axis

$X`_{d,q}$ Transient reactance in d- and q-axis

$X``_{d,q}$ Subtransient reactance in d- and q-axis

First mentioned in Chapter 3

K_5 Linearization constant

K_p PID gain

K_g PID gain

First mentioned in Chapter 4

i_{dc} Dc current

v_{dc} Dc voltage

v_d Voltage in d-axis

v_q Voltage in q-axis

i_d Current in d-axis

i_q Current in q-axis

v_{fd} Field winding terminal voltage

i_{fd} Field winding terminal current

i_{kd} d-axis damper winding current

i_{kq} q-axis damper winding current

v_{kd} d-axis damper winding voltage

v_{kq} q-axis damper winding voltage

ω_r rotor velocity

L_l Leakage inductance

L_{ls} Stator leakage inductance

R_l Load resistance

R_s Stator resistance

L_m Mutual inductance

L_{mq} q-axis mutual inductance

L_{md} d-axis mutual inductance

L_s Self inductance

R_{fd} Field winding resistance

L_{lfd} Leakage inductance in field winding

R_{kd} d-axis damper winding resistance

L_{lkd} Leakage inductance in d-axis damper winding

L_{lkq} Leakage inductance in q-axis damper winding

k_i, l_v Current and voltage constants

V_d Constant dc voltage

I_n RMS value of the harmonic n

I_F RMS value of the fundamental current

I_H Harmonic content of I_F

$I_{shortcircuit}$ The short circuit current

I_d Constant dc current

V_{LL} Line-to-line voltage

V_{dc} Dc line-to-line voltage

δ Rotor angle

S_m Stability index

$\rho(M)$ Spectral radius of the Jacobian matrix of the periodic orbit

$X(T_0)$ State vector of the researched system at time T_0 when s mall disturbance occurs

θ_2 Position of SG rotor changes with in the period after small disturbance

ϕ Flux

$X(0)$ state vector of the researched system at time zero when s mall disturbance occurs

θ_1 rotor position of SG at the time a small disturbance occurs

X_t commutation reactance

δ phase lag of the armature voltage at on-load, Eq. 4.11

α controlled delay time

u overlapping angle of the commutation

n revolutions per minute

I_g Current through the rectifier

U_p Stationary source voltage

$U‘_p$ Transient source voltage

$I‘$ Transient current

$I‘_d$ Transient current in the d-axis

$I‘_q$ Transient current in the q-axis

U_{LM} Steady state terminal voltage

I Steady state phase current

U_a Steady state voltage in phase a

U_b Steady state voltage in phase b

U_c Steady state voltage in phase c

f_n Nominal frequency

ϵ Angle between ϕ and δ

First mentioned in Chapter 7

theta load angle/rotor angle

u_{abc} Terminal voltage

i_{abc} Terminal current

First mentioned in Chapter 8

w Rotor velocity

u_i Field voltage

u_{dq} Stator voltage in the d-and q-axis

i_{dq} Stator current in the d-and q-axis

deltay Signal output from governor

e_f Field voltage

i_f Field current

i_s Line current

u_s Line voltage

I_f Current output from rectifier

First mentioned in Chapter 10

J Inertia

H Inertia constant

S_{rated} Machine rated apparent power

F_{rated} Machine rated el. frequency

N Number of machine pole pairs

First mentioned in Appendix

u_{act} Filter output voltage from voltage regulator

$u_{ref,reg}$ Reference value signal into voltage regulator

error Error signal into the PID controller in voltage regulator

reg_{out} Output signal from voltage regulator

Chapter 1

Introduction

This thesis concerns the stability of diode-bridge rectifier-loaded synchronous generators with both salient pole and round rotor, characterized with high values of synchronous, transient and sub-transient reactances i the direct- and quadrature-axis ($X_d, X‘_d, X“_d, X_q, X‘_q, X“_q$). Two synchronous generators types with high values of reactances used in the industry is under study. They are operating onboard ships where the electric system is delivered by Siemens, as a part of their new diesel-electric, variable speed propulsion DC-system for ships. One of the generators is characterized as unstable, and the other one as stable.

1.1 Objective

The objective of this thesis is to understand why diode-bridge rectifier-loaded synchronous generators with high values of reactances operated in isolated systems both with and without battery becomes unstable, and to find what could be done to prevent this type of unstable situations.

1.2 Scope of Work

The work should comprise:

- Literature studies on:
  - Instability of SG possibly with high reactances in per-unit values
  - Instability of rectifier-loaded SG possibly with connection of battery
- Continue the work from the specialization project of fall 2014

  - Simulations on DIgSILENT PowerFactory model of SG with rectifier connected

- Simulations using MatLab/SimPowerSystems
  - Analysis and further development of the received model from Siemens
  - Recreate the phenomena observed on the ships in the simulation model
  - Parameter sensitivity analysis of main system components and investigation of stability
  - Component analysis, investigating stability from the presence/absence of main components
- Discussion, final conclusion, recommendations and suggestions for further work

1.3 Limitations

The studied system is the generator-rectifier-battery configuration. An additional load is connected in parallel with the battery to model the rest of the system onboard the ship. In the real system, the thrusters are connected to the dc-bus through inverters. Two generators feed the dc-bus through rectifiers. These components (converters and thrusters) are not included in the studied system in this thesis, but modeled as an active load.

The system is an isolated system and is not connected to any other grid. Only simulations of the ship are included in this thesis, no measurements onboard the ship is made.

1.4 Simplifications and Assumptions

Several simplifications and assumptions is made during the work on this thesis, and is listed below:

- The system is modeled as ideal, ie. no losses is considered
- When the stability is to be examined, the first 20 seconds of the machine start-up is simulated. If no oscillations are found during this time, the system is considered stable. Sometimes the generateor start-up is simulated for a longer time range to observe the voltage regulator response time, but the algorithms in the simulation tool can make the system go unstable if the simulation is too long.
- An infinitely large capacitor with a series resistance is used to model the battery in the simulation model in MatLab/SimPowerSystems.

- A constant dc-voltage source is chosen to model the battery on the DC-side of the rectifier using the simulation model in DIgSILENT/PowerFactory.
- The thrusters connected to the dc-bus after the converter, as well as the converter itself is not considered. In addition to the battery, only an active load is modeled after the diode-bridge rectifier.
- Only situations linked to the observed problems are simulated.
- Only one generator is studied at a time, even through the generator has the option to operate with another generator in parallel on the ship.
- An exciter generator excites the field of the main generator, instead of a diesel engine

1.5 Software

The simulation models applied in this thesis is built in two different simulation tools; MatLab/SimPowerSystems and DIgSILENT PowerFactory. The models build in SimPowerSystems is parameterized by using Matlab, the control systems used in these SimPowerSystems-models is designed in Simulink and mechanical components is added to the model using Simscape. Information about these softwares can be found on the software web side on www.mathworks.com and www.DIgSILENT.de

The thesis is written in the typesetting system LaTeX

1.6 Report Structure

Chapter 2 presents a description of the system under consideration in this thesis. In Chapter 3 is the highlights of the specialization project conducted in the fall semester in 2014 presented, where the same system was under investigation, considering the same objectives as in this thesis. Chapter 4 contains the relevant theory for the system considered, and summarizes the literature study. The fundamental theory of synchronous generator design and stability is expected known and is not provided. A continuation of the work done in the specialization project in fall of 2014 is conducted, and the model description is shown in chapter 5 and the simulation results is given in Chapter 6.

The model used in MatLab/SimPowerSystems is described and presented in chapter 7. Chapter 8 contains the simulations done using the data from the 3333kVA generator that is considered stable. In chapter 9 is the data from the unstable 1940kVA generator used in the simulation model, and the generator is modeled as salient pole. In chapter 10 is the unstable generator

designed as round rotor. The discussion is found in chapter 11 and the conclusion and recommendations is presented in Chapter 12. Ideas for further work is presented in Chapter 13 and the Appendices is found after the Bibliography.

Chapter 2

System Description

This chapter presents a description of the system under study in this thesis, where the most important components are of interest.

This thesis concerns the stability of synchronous generators characterized with high values of synchronous, transient and subtransient reactances in the direct- and quadrature axis ($X_d, X‘_d, X“_d, X_q, X‘_q, X“_q$), with the possibility of connecting a battery-bank. The synchronous generators supply a load through a 6-pulse diode-bridge rectifier. The synchronous reactances is in the range 2.5-5.5 pu.

The system under research is two particular types of synchronous generators used onboard two different tugships with diesel-electric, variable speed propulsion DC-system, where the electrical installation is called BlueDrive +C and is delivered by Siemens. The generators differs in both range of generator parameters and performance.

One of the tugships studied uses generators with a capacitance of 3333kVA, and has synchronous reactances is the lower layer of 2.5-5.5 pu, and is characterized as stable during operation. The other ship uses generators with a capacitance of 1940kVA, and has synchronous reactances is the upper layer of 2.5-5.5 pu, and is characterized as unstable during operation.

The system consists of two generator sets, with two synchronous generators in each set. A bus-tie switch separates the two generator sets. The generators is run by diesel engines that has the possibility to run at variable speed to obtain an efficient operation of the system. Using this technology, the system losses, costs and emissions is reduced significantly.

With the opportunity to work in both parallel and in singular operation, the generator set feeds a DC-bus through diode-bridge rectifiers. The DC-bus has the ability for battery connection to achieve redundancy. The thrusters is supplied by the DC-bus through inverters. The BlueDrive +C system is shown in a one-line diagram in Fig. 2.1 below.

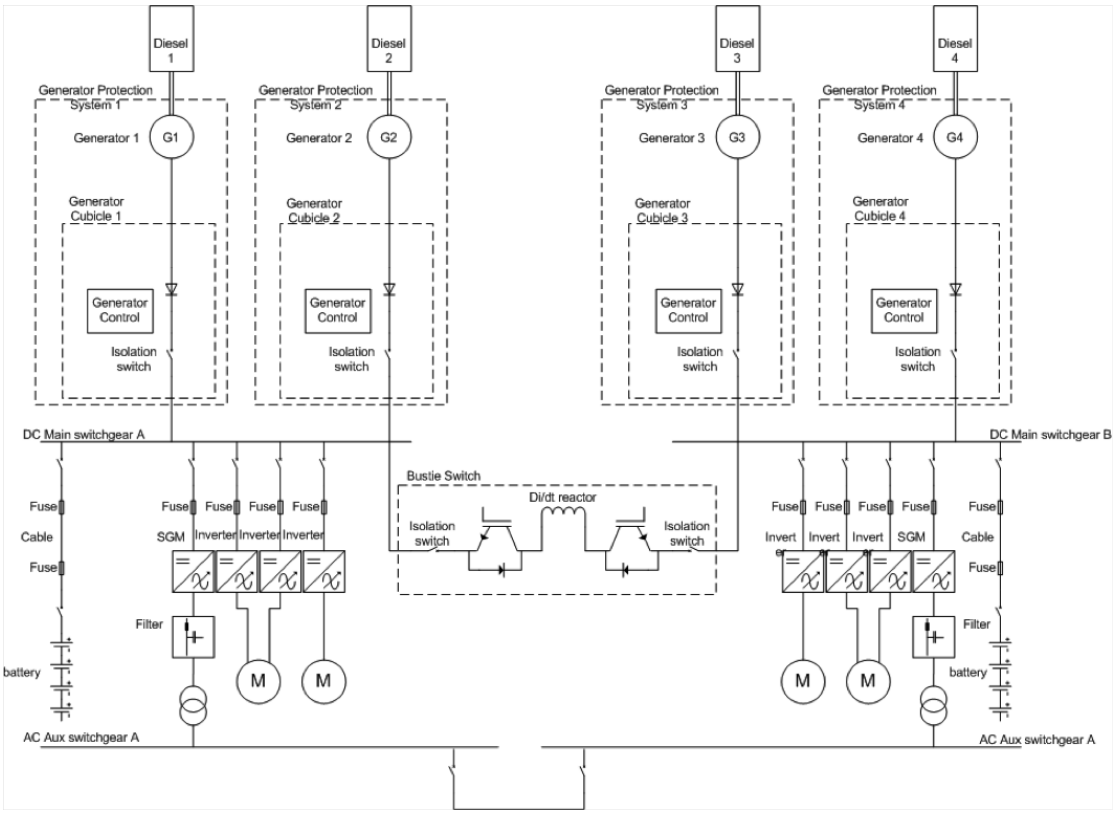

Figure 2.1: One-line diagram of the studied electric system delivered by Siemens, called BlueDrive+C. The electric system is used in tug-ships with diesel-electric propulsion systems. A bus-tie switch separates the two generator-sets, that feed the dc-bus through diode-bridge rectifiers. A battery is connected to the DC-bus to achieve redundancy. The main motors are supplies by the dc-bus through inverters.

The two synchronous generators under study in this thesis is used in two separate tug-ships. Both ships have the same design what matters the electrical system shown in Fig 2.1 above. The generators themselves however, are unique. They differ in both design, rated power and values of reactances, as well as in behavior during operation.

A stable operation of the ship using the 1940kVA generator type in the BlueDrive +C system is not possible at this time, without doing some enhancements of the electric system. Oscillations is found in the output voltage, current and power, indicating oscillations also in rotor angle, in the synchronous generator, as analyzed in [6]. The oscillations have a frequency of around 2 Hz. A transient voltage increase is also detected in the generators on the ship where instability is detected, which has been seen in measurements taken onboard the ship, conducted by the voltage regulator supplier [6].

The use of thyristor-rectifiers has been shown to be an effective, but temporary, solution to prevent instability for this particular ship using the 1940kVA generators. As mentioned earlier, a

diode-bridge rectifier is originally the type of rectifier used in the electric system on the ship. The generators used on this ship where instabilities is observed, has the highest values of reactances of the two generator types studied in this thesis, in the upper range of 2.5-5.5 pu. The generators used in this unstable operating ship, have an apparent power of 1940 kVA and will be referred to as G2 throughout this thesis.

On the ship where the other synchronous generator type is used, oscillations is also detected in voltage, current and power output from the generators, but the oscillations is regulated down to a manageable level by the voltage regulators. However, this happens extremely slowly, which is undesirable. The oscillations have a frequency of around 2 Hz as well. This stable generators used on the ship has an apparent power of 3333 kVA, is of the salient-pole type and will be referred to as G1 throughout this thesis.

The stability problems observed on the two ships increases in strength when the battery in attached to the DC-bus, powered from the generator-sets through the diode-bridge rectifier. When the battery is removed from the dc-bus, the output of the rectifier still oscillates. The battery used on the ship is of the lithium-ion type, and has a capacitance of 150A and a capacitor voltage of 1030V, with a 9V voltage drop. Instability is detected on the ship that uses the generator G2 even when the ship operates with low load.

The 6-pulse diode-bridge rectifier-loaded synchronous generator system is strongly nonlinear and has time-varying characteristics, which makes the problem deeply complex. This makes it harder to understand why the mentioned problem rises, as well as to evaluate it [7] [2].

Chapter 3

Summary of Specialization Project During Fall 2014

The specialization project was conducted during the fall of 2014, as a result of the course TET4510 at the Department of Electric Power Engineering at NTNU. The objective was the same as in this thesis and a summary is presented here. The same system as presented in Chapter 2 was under study, and the system description is not repeated here. Measurements from the unstable ship conducted by the AVR supplier is presented, as well as simulations done in DIgSILENT PowerFactory.

3.1 Measurements Taken Onboard the Unstable Ship

The supplier of the voltage regulator installed on the ship using the 1940 kVA generators, did measurements on the unstable ship in August 2014, at the time when the instability problems were detected. The measurements were taken while one generator-set was operating in parallel on a fixed frequency, and the bus-tie switch was open, isolating the two generator-sets from each other, looking at only one generator-set. A one-line diagram of the system is shown in Fig 2.1 in Chapter 2, describing the electrical system.

The battery was not connected to the DC-bus, and the load during measurements was a mainly active test-impedance connected on the AC-side of the converter, due to the 6-pulse diode-bridge rectifier. In addition is a resistance of 3.3 Ω connected in series with the exciter field winding of the generators during the test. A brushless exciter supplies the DC field current of the generators. The VT is connected between phase C-B and the CT is connected on phase B for both the generators in the generator-set [6].

The voltage measurement used by the voltage regulator attached to the generator is retrieved from an extern winding coupled in parallel with the main winding on the stator inside the synchronous machine. This is done to prevent the voltage measurements going to the voltage regulator to contain disturbances from an eventual pulsating load current. The voltage from the voltage regulator is retrieved from a separate voltage transformer.

The test is conducted with three parameters in mind; the PID gain K_g in the AVR, the speed [RPM] and the setting of the voltage regulator [auto/manual].

The conclusion of the test is that the frequency and amplitude of the oscillations in voltage and current measured from the generator-sets increases as the PID gain and speed is increased. The setting of the regulator also impacts the oscillations, in a decreasing manner, as shown in Fig 3.1 below.

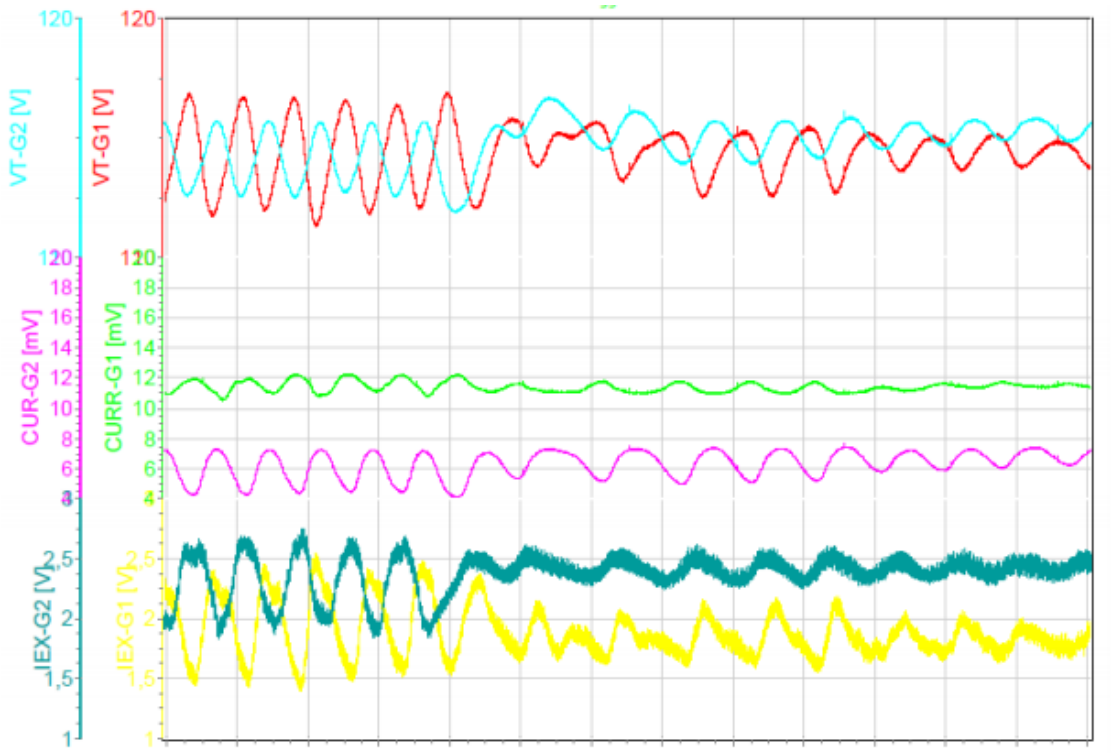

Figure 3.1: The measurement of current and voltage recordings of the two generators in the generator set under operation at 1000 RPM with $K_g = 40$, with change of AVR mode from automatic to manual in one of the generators.

The graphs shown in Fig 3.1 shows, from the top: the RMS voltage measured through the VT, the current measured through the CT and the direct voltage measured over the exciter field resistance, for the two 1940kVA generators in the generator-set, respectively.

The graphs show that the frequency and amplitude of the oscillations in current and voltage decreases as the setting of the AVR is changes from auto to manual mode for one of the generators. The AVR clearly impacts the stability of the generators. The amplitude of the power is not studied, and the origin of the oscillations is not known. The measuring voltage to the regulator is delivered from an auxiliary winding and the feeding voltage of the regulator is delivered from a separately VT.

The frequency of the oscillations when the generator runs at 750rpm (high load) is in the range of 1.756-2.366Hz, and when the generator runs at 1000rpm (low load) the oscillations has a wider frequency-range than during high load, namely 1.171-2.68Hz [6].

Transient voltage increase in the terminal voltage of the synchronous generators on the ship using the generator type G2 is experienced immediately after a load increase is introduced. To explain this, an analytical approach is provided in [6] and is found in Appendix A.1.

3.2 Simulations Using DIgSILENT PowerFactory

The system shown in Fig 3.2 below is based on the system found in [4], where the aim of the article was to decide whether or not high internal impedances in the generator can have the same effect of the stability of the synchronous generator as high external impedances have, such as transformer impedances and lines.

When high external impedances is present, the linearization constant K_5 may become negative, which leads to a negative damping, resulting in an unstable operation of the synchronous generator. The article showed that high internal impedances in the generator also can have this effect on the linearization constant K_5, in the same way as high external impedances do.

The simulations in the specialization project conducted during the fall of 2014 had the same approach as the article [4], and was motivated by the need to see how the large generator reactances in the studied system on the ship impacts the stability, with the same external impedances as in [4]. The parameters of the lines and transformers is given in Table B.1 in Appendix B, and the parameters for the generator is given in Table I.1 and Table I.2 in Appendix I. An external grid is connected to the system to model the battery in the ship.

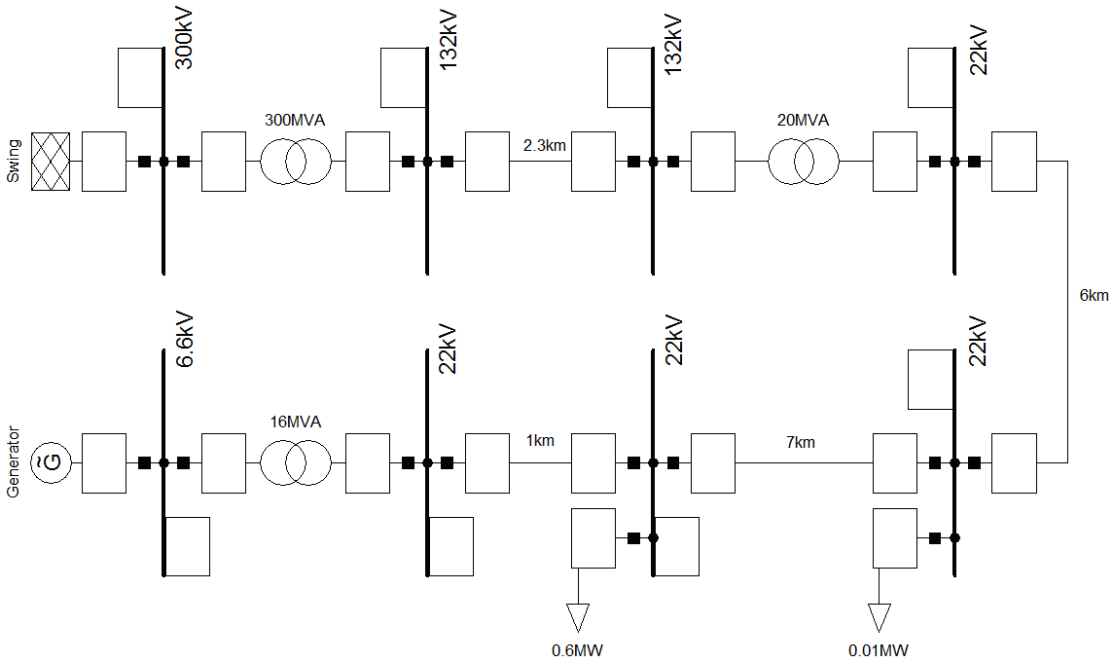

Figure 3.2: The model established in DIgSILENT PowerFactory is based on the system in [4] and simulations where the gain of the AVR, K_p was varied, was conducted in the specialization project during the fall of 2014 [6]. The simulations was motivated by the need to study how high generator reactances impacts the generator stability.

In [6], it is shown that the stability of the generators is affected by several factors; the operation of the generator in the system shown in Fig 3.2, meaning the consumption and production of active power/reactive power, the reactances of the generator and the value of the PID gain K_p in the voltage regulator that directly impacts the linearization constant K_5.

The movement of the critical eigenvalues of the 1940kVA and 3333kVA generators as a results of varying the gain, is shown graphically in the root locus plot in Fig 3.3 below.

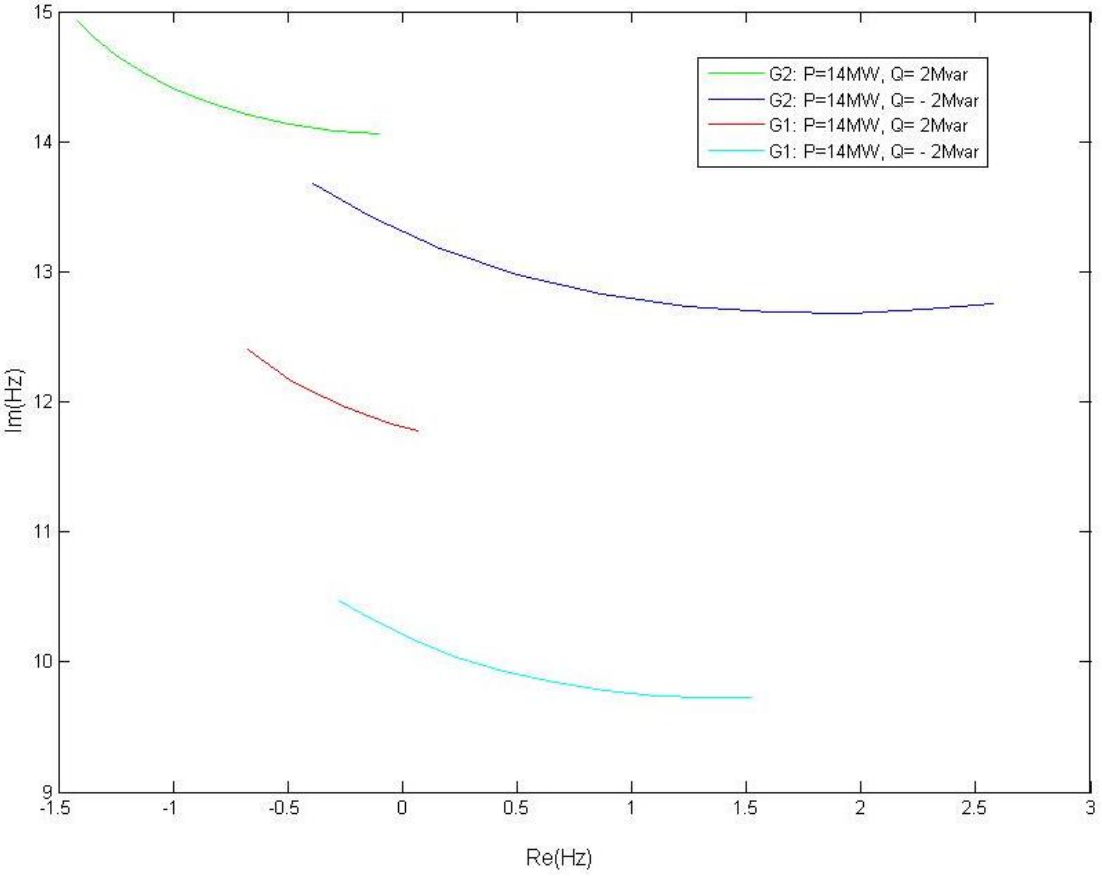

Figure 3.3: This root locus plot shows the eigenvalues of G1 and G2 as a function of the gain in the AVR, directly affecting the linearization constant K_5. The simulations is conducted for two different types of operation; consumption and production of reactive power. In both cases G1 and G2 produces active power. When the eigenvalues move over in the positive half plane of real eigenvalues, the generators are considered unstable.

The root locus plot in Fig 3.3 above shows the eigenvalues of G1 and G2 as a function of the linearization constant K_5 for two different types of operation; consumption and production of reactive power. In both cases G1 and G2 produces active power. The mode that oscillates with around 2Hz is the mode of interest. When the eigenvalues move over in the positive half plane of the real eigenvalues, the generators is defined as unstable.

Fig 3.3 shows that when the gain K_p is increased in its value from 50 to 500, the generators G1 and G2 gradually moves over to the positive half plane and becomes unstable. It is observed that when the generators are consuming reactive power, this instability happens faster. G2 is more sensitive to the change in K_p both when producing and consuming reactive power, which is an interesting observation due to the fact that G2 has higher reactances than G1. [6] concludes that high reactances, consumption of reactive power and high values of gain impacts the generator stability in a negative manner.

Chapter 4

Stability of Rectifier-Loaded Synchronous Generators

This chapter includes theory, literature studies, and relevant background information needed to conduct simulations and to evaluate them, with emphasis on stability of the system studied. Basic theory of stability and synchronous generator design is expected known.

The studied system in this thesis is a synchronous generator with high values of reactances feeding load through a diode-bridge rectifier, as shown in the simplified line diagram Fig 4.1 below [8].

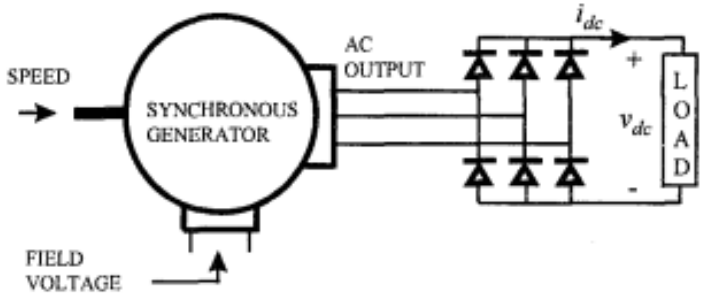

Figure 4.1: Synchronous generator feeding load through diode-bridge rectifier [8].

The theory presented in this chapter concerns the main components of the presented system.

4.1 Six-Pulse Diode Bridge Rectifier Characteristics

The six-pulse diode bridge rectifier is calles "six-pulse" because the resultant voltage output from the input bridge is in the form of DC voltage with six peaks; one peak for each of the positive and negative half cycles of the rectified three-phase input waveform, thus the term "6-pulse drive" [9].

On the ship under study, the battery connected to the dc- bus is supplied through the three phases, six-pulse diode bridge rectifier. The battery can be modeled as a large capacitor. An approximation to this system is shown in Fig 4.2a where the assumptions is that the dc-voltage is a constant dc. For simplicity, another assumption is made; the current i_d on the dc side of the rectifier flows discontinuously, so that only two diodes (one from the top three and one from the bottom three diodes) conducts at any given time. This results in the input voltage being made up by the line-to-line voltages seen in the top graph in Fig 4.2b, giving the resulting phase current waveform in the bottom graph of Fig 4.2b [10].

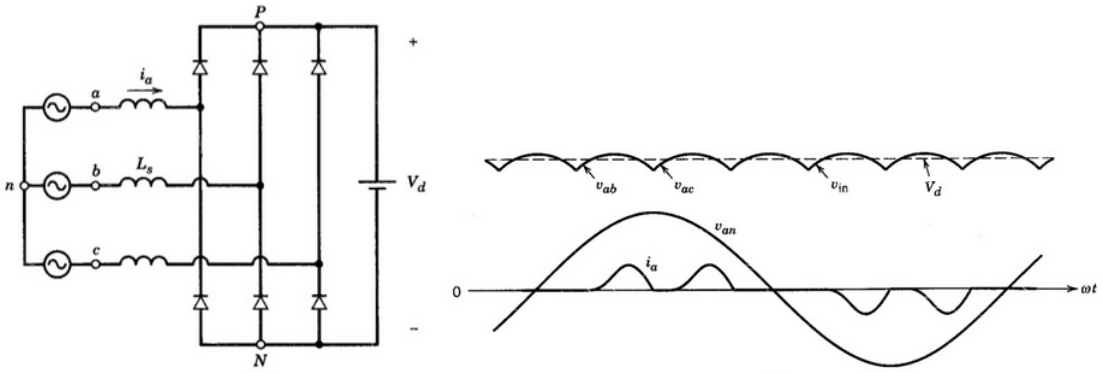

(a) (b)

Figure 4.2: (a) Six-pulse diode bridge rectifier with a finite L_s and a constant dc voltage V_d. (b) The current and voltage waveforms from the rectifier [10].

Power electronic equipment is a source of harmonic distortion in the current, as can be seen in the current waveform in Fig 4.2b. The total harmonic distortion (THD) is defined as [10]:

$$THD = \frac{I_H}{I_F} = \frac{\sqrt{I_2^2 + I_3^2 + ... + I_n^2}}{I_F} = \frac{\sqrt{\sum_{h=2}^{\infty} I_h^2}}{I_F} \tag{4.1}$$

for currents, where I_n is the RMS value of the harmonic n, and I_F is the RMS value of the fundamental current. I_H denotes the harmonic content of the fundamental current I_F. When the voltage or current is purely sinusoidal, there is no harmonic distortion and the value of THD is zero. The THD increases in value as the ratio [10]:

$$\frac{I_{short-circuit}}{I_d} \tag{4.2}$$

increases, where I_d is the constant dc current and $I_{short-circuit}$ is the short circuit current given as [10]:

$$I_{shortcircuit} = \frac{V_{LL}/\sqrt{3}}{\omega_1 L_s} \tag{4.3}$$

An example of a distorted current with harmonic content is shown in Fig 4.3 below, where the current has a pulsed nature is shown in Fig 4.3a from a three-phase diode rectifier in Fig 4.3b [9].

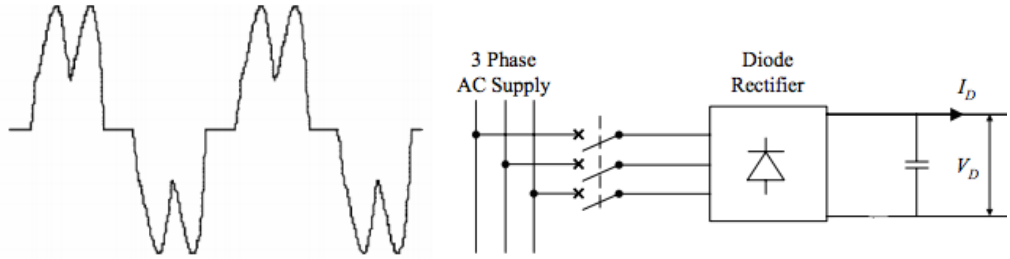

(a) (b)

Figure 4.3: (a) The typical pulsed nature of AC PWM drive input current waveform. (b) The three-phase diode bridge rectifier block diagram [9].

The pulsed nature of the input current is caused by the fact that the power only is drawn from the generator when the voltage in the DC-bus drops below the rectified voltage level [9].

Such waveforms in current can also be caused by a high degree of commutation angle in the rectifier, which can be a result of a large generator inductance and heavy load current. This causes three diodes to conduct at each time, resulting in interval series of the operating generator, where one generator line to line generator is zero, leaving the other two generator line to line voltages being V_{dc} and $-V_{dc}$. The result is a square-shape in the voltage, and the current is characterized by "humps" in the waveform. This can be shown in Fig 4.4 below [8].

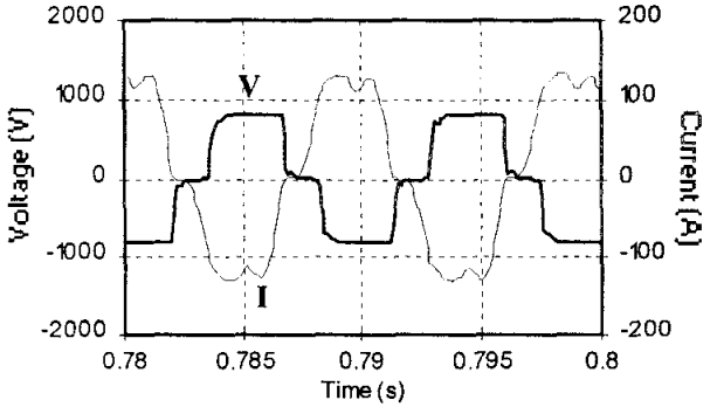

Figure 4.4: The voltage can be characterized by a square-shaped waveform and "humps" can be spotted in the current from the output of the generator feeding a diode-bridge rectifier, caused by high degrees of commutation angle in the rectifier [8].

The characteristics of these waveforms are also load-dependent; meaning that as the operating point changes, the commutation angle varies and the waveforms obtain another shape. More specifically, the commutation angle decreases as the load decreases due to the decreasing output current and frequency. This results in a more sinusoidal waveform in both the current and voltage, where the square-shape in the voltage waveform and the "bumps" in the current waveform diminishes [8].

The average ideal dc voltage from the three-phase, full-bridge rectifier with zero commutation $L_s = 0$, is calculated by Eq. 4.4 below [10];

$$V_d = \frac{3\sqrt{2}V_{LL}}{\pi} = 1.35V_{LL} \tag{4.4}$$

where:

V_d is the average dc voltage

V_{LL} is the rms value of the line-to-line voltage

4.2 Undamped Oscillations in Synchronous Generators Feeding Load in Isolated System

Problems with small-signal stability can be a result of a machine with poorly damping properties of oscillations in the system. Small-signal rotor angle stability is often refried to a machines ability to maintain stability when subjected to small disturbances, such as introducing a load or loss of

load. When a machine is is connected to an infinite bus, the oscillations that occur in the system can be related to local or global modes. They differ in range; local plant oscillation problems are restricted to a small part of the system, for instance rotor angle oscillations in only one generator, while global problems reaches over large groups of generators.

The frequency of the oscillations in local oscillations is larger than the frequency of oscillations linked to global problems. Usually, the local plant mode oscillations have frequencies in the range 0.7-2Hz, and may be related to rotor angle oscillations. The global stability problems often include inter area mode oscillations in the range 0.1-0.4Hz if the generators in large groups oscillate each other, and 0.4-0.7Hz if only generators in one group oscillate each other [11] [4] [12].

The system under study in this thesis is a generator that feeds load through rectifier, with the opportunity for battery-connection. This can be seen as a machine-infinite bus system, where the battery models an infinite bus. Due to the fact that the frequency of the oscillations observed on the ship is around 2Hz, a theory can be stated that local plant mode oscillations related to the rotor angle is, or is a part of the problem, on the ship using the 1940kVA generators. Simulations on the system must be done to further investigate this statement.

4.3 Synchronous Generator Reactances

Table 4.1 below shows typical parameters for SG for both salient pole (hydraulic machines) and round rotor (thermal machines) design [13].

Table 4.1: Typical parameter values for salient pole and round rotor SG

Description	Symbol	Hydraulic Units [pu]	Thermal Units [pu]
Synchronous reactance in d-axis	X_d	0.6-1.5	1.0-2.3
Synchronous reactance in q-axis	X_q	0.4-1.0	1.0-2.3
Transient reactance in d-axis	$X‘_d$	0.2-0.5	0.15-0.4
Transient reactance in q-axis	$X‘_q$	-	0.3-1.0
Subtransient reactance in d-axis	$X“_d$	0.15-0.35	0.12-0.25
Subtransient reactance in q-axis	$X“_q$	0.2-0.45	0.12-0.25

Table 4.1 can be used for finding missing parameters in the simulation models [13].

For typical generators used in hydropower, the generators can be modeled with complete damper winding or with a damper cage. When the generator is modeled with a complete damper winding, the subtransient reactances has approximately the same value: $X“_d \approx X“_q$, giving a ratio between them $\frac{X“_q}{X“_d} = 1$. However, when the generator is modeled as a damper cage, there is a big difference between the subtransient reactances [5].

An example is given in [5] for a hydropower generator (54MVA; $cos\phi = 0.95$, 10.5kV; 600U/min, 50Hz) where typical parameters is found in Table 4.2 below [5].

Table 4.2: Typical parameter values for a hydropower generator with round rotor and complete damper winding/(damper cage) (54MVA; $cos\phi = 0.95$, 10.5kV; 600U/min, 50Hz) [5].

Description	Symbol	Value [pu]
Synchronous reactance in d-axis	X_d	1.04 (1.04)
Synchronous reactance in q-axis	X_q	0.57 (0.57)
Transient reactance in d-axis	$X‘_d$	0.23 (0.23)
Transient reactance in q-axis	$X‘_q$	0.57 (0.57)
Subtransient reactance in d-axis	$X“_d$	0.15 (0.15)
Subtransient reactance in q-axis	$X“_q$	0.16 (0.44)

where it can be seen that $X“_d \approx X“_q$ when the generator is modeled with complete damper winding, and that $X“_d << X“_q$ when the generator is modeled with damper cage. $X‘_q = X_q$ for the salient pole generator because the laminated rotor construction prevents eddy currents from flowing in the rotor body, making the screening effect in the q-axis negligible [5] [12].

When oscillations occur in normally dimensioned synchronous generators, is the effect of the q-axis damper winding much more important than the d-axis damper winding. That is, the damping cage only contributes to a small rotor angle oscillation [5].

By adding a quadrature-axis damper winding, a damping power is added that produces an induced current in the damper windings that introduces a toque which tries to restore the synchronous speed which of the rotor when the rotor speed differs from the synchronous speed, according to Lenz‘s law. Explicit damper windings is often mostly used for SG with salient pole design, because round rotor designed SG have solid steel rotor bodies that provides paths for eddy current, that works in the same way as damper windings [12].

When damper windings is introduced on the q-axis, the screening effect in both the d- and q-axis becomes similar, resulting in a smaller q-axis reactance and that $X“_d \approx X“_q$. This is the reason why the subtransient q-axis reactance is larger for damper cage-designed generators than for complete damper winding-designed generators, where the screening effect in the d-axis is stronger than in the q-axis, and we have that $X“_d < X“_q$ [12].

4.4 Synchronous Generator with Variable Speed

When the diode-bridge rectifier loaded synchronous generator operates at variable speed, as is the case for the studied system on the ship, conventional methods for modeling the system cannot be used. The frequency is not constant, but shifts to achieve optimal operation, and thus

more efficient utilization, of the diesel-engine-generator-system. Consequently, the single-pole transfer function classically used for modeling the synchronous generator equations describing the system cannot be linearized. The single-pole transfer function can only be used when the generator speed is constant and when the generator synchronous reactance is small. Neither of these two assumptions is true in the case with the electrical system on the ship under study in this thesis [8].

A similar system is examined in [8], and a new, average, time-continuous model is proposed. The rotor reference frame model has been used to describe a synchronous generator with one damper winding in each rotor axis, where the equations describing the machine is given as follows [8]:

- $v_d = -R_s i_d + \omega_r(L_{ls} + L_{mq})i_q - \omega_r L_{mq} i_{kq} - (L_{ls} + L_{md})\frac{di_d}{dt} + L_{md}\frac{di_{fd}}{dt} + L_{md}\frac{di_{fd}}{dt}$
- $v_q = -R_s i_q + \omega_r(L_{ls} + L_{md})i_d - \omega_r L_{md} i_{fd} + \omega_r L_{md} i_{kd} - (L_{ls} + L_{mq})\frac{di_q}{dt} + L_{mq}\frac{di_{kq}}{dt}$
- $v_{fd} = R_{fd} i_{fd} - L_{md}\frac{di_d}{dt} + (L_{lfd} + L_{md})\frac{di_{fd}}{dt} + L_{md}\frac{di_{kd}}{dt}$
- $0 = R_{kd} i_{kd} - L_{md}\frac{di_d}{dt} + (L_{lkd} + L_{md})\frac{di_{kd}}{dt} + L_{md}\frac{di_{fd}}{dt}$
- $0 = R_{kq} i_{kq} - L_{mq}\frac{di_q}{dt} + (L_{lkq} + L_{mq})\frac{di_{kq}}{dt}$

The average model of the generator-rectifier system is based on the space-vector diagram of the system presented in Fig 4.5 below.

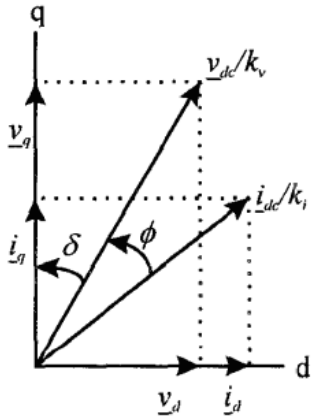

Figure 4.5: The space-vector diagram of the synchronous generator-rectifier system shown in Fig. 4.1 [8]

From this, $\hat{v}_{dc}, \hat{i}_d, \hat{i}_q$ and δ in Fig 4.1 can be expressed as in Equation 4.5, 4.6, 4.7 and 4.8, respectively [8].

$$\hat{v}_{dc} = \frac{\hat{i}_d}{\hat{i}_{dc}}\hat{v}_d + \frac{\hat{i}_q}{\hat{i}_{dc}}\hat{v}_q \tag{4.5}$$

$$\hat{i}_d = \frac{\hat{i}_{dc}}{k_i} sin(\delta + \phi) \tag{4.6}$$

$$\hat{i}_q = \frac{\hat{i}_{dc}}{k_i} cos(\delta + \phi) \tag{4.7}$$

$$\delta = tan^{-1} \frac{\hat{v}_d}{\hat{v}_q} \tag{4.8}$$

Where the $\hat{x}$ denotes the average value of the variable x. The average model is shown to describe the reality well, and simulations using this model matches measured results from experiments. It is found that when the load at the dc side of the rectifier is disconnected during experiments, the dc link voltage rises almost three times due to the large reactances of the synchronous generator. Due to some assumptions and simplifications done when producing the average model, some conditions must be satisfied if the model is to be used validly [8]:

- Generator harmonics other than fundamental deliver negligible power,
- losses in the diode rectifier are negligible,
- diode rectifier output is well filtered (large L or C or both)

The average model is based on the assumption that a complete power transfer happens at the fundamental frequency. The model is nonlinear, and can be linearized around a particular operating point and the system transfer functions can be found, due to the fact that the model is time-continuous [8].

4.5 Stability Criteria for Rectifier-Loaded Synchronous Generators

An isolated power system denotes an independent system used in airplanes, oil drilling platforms, DG systems, electric vehicles and, focused on in this paper, ships. These examples are similar in the fact that they all have restrictions in volume, space and weight. DC power supply consisting of synchronous generators and rectifiers is often used in such isolated power system because of its efficiency and high power density. Diode rectifiers is often used in stead of PWM rectifiers because they are more economic, have smaller volumes, has better electromagnetic compatibility and has a high reliability [7].

The speed and torque of a propulsion load is regulated as constant by the variable-frequency speed regulation system, because the propulsion load generally behaves as a constant power

load. This is however not always the case. This regulation can cause the isolated power system to be unstable when the propulsion load does not behaves as a constant power load [7].

Several models for rectifier-synchronous machine systems is found in the literature. The studied diode rectifiers-synchronous machine system in [7] experiences low-frequency oscillations when critical parameters is applied. Parameters is denoted critical when a small change in value makes the system unstable. [7] proposes equations of a periodic orbit model by using the trapezoidal integration method. The model is established to increase the accuracy in the analysis of small signal stability of diode rectifier-synchronous machine systems. By using theoretical analysis and simulation tests in PSCAD, the proposed model is shown to contribute to modeling and analyze isolated power systems [7].

A stability margin index of the periodic orbit model describing the isolated system consisting of a diode-rectifier-loaded synchronous generator studied in [7], is presented below [7];

$$S_m = 1 - \rho(M) \tag{4.9}$$

where S_m is the stability index, giving a higher stability level the higher the stability index is. $\rho(M)$ is the spectral radius of the M matrix, given by: $M = \frac{\partial Z_2}{\partial Z_1}$ which describes the Jacobian matrix of the PoincarŐ mapping of the periodic orbit given as [7];

$$[X(T_0), \theta_2]^T = \phi([X(0), \theta_1]^T) \tag{4.10}$$

where [7]:

$X(T_0)$: state vector of the researched system at time T_0 when s mall disturbance occurs

θ_2 : position of SG rotor changes with in the period after small disturbance

ϕ : flux

$X(0)$: state vector of the researched system at time zero when s mall disturbance occurs

θ_1 : rotor position of SG at the time a small disturbance occurs

where the discrete periodic orbit equations in found from the Parkńs equations. It is shows through load-analysis that the stability index can reflect the level of stability of the system studied [14] [7].

[14] puts forth a model of a bridge rectifier-loaded synchronous machine connected to a d.c.-link with emphasis on the line-to-line short circuit in the commutation period of the rectifier, that separates the system from a regular synchronous machine. Basic equations are established and

studies on the system is done, with emphasis on commutation reactance, phasor diagram, phasor diagram and basic characteristics. The analysis is based on Park‘s equations [14].

By dividing the two periods of the rectifier into commutation period and the normal conducting period, a commutation reactance is found for the SG during load. This reactance changes during commutation. If the reactance is assumed constant, it can be approximated by the equation [14]:

$$X_t = \frac{X“_d + X“_q}{2} + \frac{X“_d - X“_q}{2} cos(2\delta + 2\alpha + u) \tag{4.11}$$

where [14]:

X_t : commutation reactance

$X“_d$: subtransient d-axis reactance

$X“_q$: subtransient q-axis reactance

δ : phase lag of the armature voltage at on-load

α : controlled delay time

u : overlapping angle of the commutation

The first expression in Eq 4.11 is the classical expression for the commuation reactance, but this does not take the the change in commutation into account. The second expression in Eq 4.11 is therefore added. Since the delay angle α is zero when the bridge rectifier consists of diodes, the commutation angle X_t is approximately the same value as $X“_d$ in the middle of the commutation period, $X_t \approx X“_d$ [14] [3].

Park‘s equations also forms the basis of the parametric average-value method of a rectifier circuit in a synchronous-machine-fed rectifier system, presented in [15]. The method focuses on controllers based on frequency-domain characteristics and can be linearized around a working point. To assume that the parameters in the AVM of a rectifier is independent of the operating situation can lead to great errors [15].

The averaging method is continuous and valid for large-signal time-domain studies, linearization and small-signal impedance characterization for several operation conditions for the studied system. Detailed simulations is done in MatLab/SimuLink and data is measured to verify the proposed model in both time and frequency domain [15].

[1] claims that for rectifier-loaded synchronous generators is not only the synchronous reactances important as it is for regulator synchronous machines, but also the transient, subtransient reactances and the stationary operation influences the stationary operation, unlike a SG with a stiff AC-bus. For each period through the rectifier, a repeative starting process is created, that is

the result from the subtransient behavior in the machine. A consequence of these non-sinusoidal current- and voltage profiles can be large losses in the laminated core and windings inside the machine, which can cause oscillations in the torque in pace with the oscillations in the rectifier [1].

For these reasons can the operation of the rectifier-loaded synchronous machine even during low-speed operations be determined from the subtransient reactance [1].

When an active load is introduced, transient oscillations can occur as a consequent to the repetitive process in the rectifier. The result is a periodic, impulse behaved current flow with large speed-oscillations, that makes it impossible to have a normal operation of the system. A case where the introduction of a rectifier to a synchronous generator makes the voltage and current oscillate, is investigated. [1]

Fig 4.6 shows an oscillating behavior in the voltage U and current I on the ac-side, the rotations per minute n and the current through the rectifier I_g. U_t marks the time, where each time-distance represents 0.1s [1].

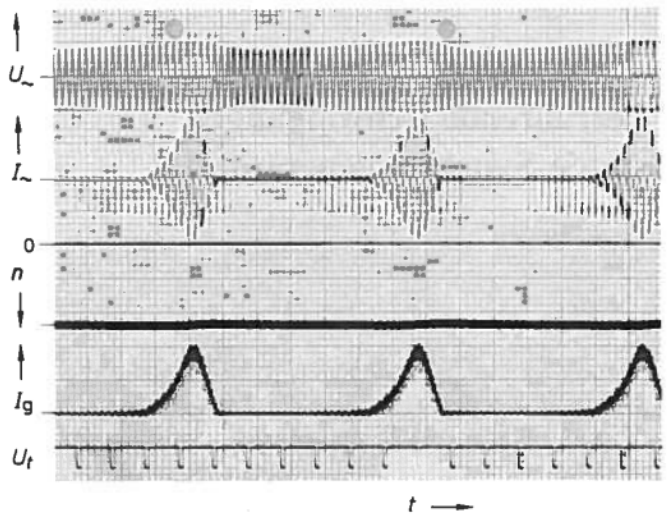

Figure 4.6: The voltage $U_\sim$ and current $I_\sim$ of a generator when a rectifier is introduced in the system, where I_g is the current through the rectifier and n is the rotations per minute [1].

Fig 4.6 shows that when a current I_g is conducted through the rectifier, the voltage and the current starts to oscillate. These processes vary with the nature of the load, i.e., whether it is active or passive. The transient current also impacts the stability of the generator. The withstanding load has an impact on the transient current, and therefore also on the stability [1].

[1] proposes a stability criterion given by the equation:

$$\frac{X`_q}{X`_d} \leq 2 \tag{4.12}$$

and is built on the assumption that under certain conditions during the transient period, super positioning, or an voltage increase can occur in the synchronous machine. This happens even though the excitation of the machine is constant, and both when the current is constant or increasing. The result of this voltage increase is that the generator must be assigned an internal, negative resistance, and the operation becomes unstable [2] [1].

[1] proposes that oscillations that occur in the output voltage of a rectifier-synchronous machine-system is associated with physical oscillations on the rotor angle δ. By performing several tests on the system, it is found that a field damping on the q-axis can reliably and seamlessly prevent the experienced transient oscillatory behavior of a synchronous generator with rectifier [16].

It is claimed by [3] that serious low-frequency current oscillations can occur in rectifier-loaded synchronous generators, resulting in an unstable operation of the generator, although the generator can operate stably without the rectifier.

A new stability criterion is presented in [3], which proposes that system stability is easier achieved when a short-circuited quadrature-axis winding is added to the rotor of a machine with diode-bridge rectifier and back-emf load. The criterion in [3] is obtained for small disturbances and is built on the criterion given in [1] in Eq. 4.12. The stability criterion for round-rotor generators with a short-circuited q-axis rotor winding is given in the following equation: [3]

$$\frac{1}{X_q} + \frac{1}{X`_q} \geq \frac{1}{X`_d} \tag{4.13}$$

with the assumption that usually $X``_q << X_q, X``_d < X_d$ is true. By assuming that $X`_q < X_q$, the stability criterion in Equation 4.13 can be compared with the stability criterion in [1], given in Equation 4.12, where [3] concludes that the criterion given in Equation 4.13 is easier to fulfill. The assumption made to obtain this criterion, is that the commutation angle $\mu = 0$, rotor velocity $\omega = constant$, a short-circuited q-axis winding exists on the rotor and that the disturbance is small. In a practical meaning, when a short-circuited q-axis winding is added to the rotor, the value of the sub-transient reactance in the q-axis reduces significantly. The problems with low-frequency current oscillations can be solved [3].

This is shown through experimental results, where the required critical resistance is less for when the q-axis winding is open-circuited than when the q-axis winding is closed on an inductor, but if the q-axis winding is short-circuited, the system can meet the stability criterion for the whole load range, even if the dc-side series resistance is zero [3].

[8] presents a simplified model of a three-phase, variable-speed synchronous generator-diodebridge

rectifier system. The studied system experiences non-sinusoidal voltages and currents in the ac-output from the generator due to the fact that in variable-speed stand-alone generators is the output impedance in the generator comparable to the load. The model presented is based on the assumption that the generator can not be modeled with a single-pole transfer function when the synchronous reactance is large and the generator-speed is not constant. [8]

4.6 Modified Stability Criterion by Siemens

Siemens in Hamburg, [2], proposes three different modifications to a stability criterion originally presented in [1] and [16]. With the use of vector diagrams of both the stable and transient operation of the system, is the stability criterion solved for three different situations of operation. The stability criterion found in [1] is given in Equation 4.12 and is based on the assumption that oscillations in generator output origins in oscillations in the rotor angle.

Such oscillations in the rotor angle is difficult to discover in a practical meaning. Attempts to detect this rotor angle oscillations is been made by simulations [17], using various values for rotor inertia. Even when the value of the inertia is infinitely high, the voltage oscillations on the generator output is still present. Based on this, the assumption can be made, that the voltage oscillations is created through the transient currents [2].

To investigate the presented assumption, an equivalent circuit of the rectifier-synchronous machine system, and is shown in Fig 4.7 below.

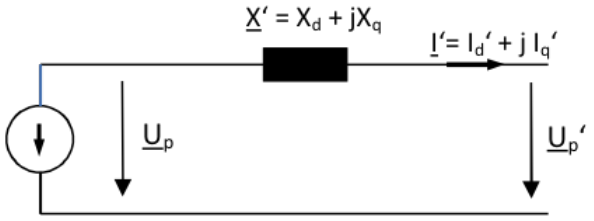

Figure 4.7: Simplified equivalent circuit of the studied system [2].

where [2];

X‘ is the ohmic, transient resistance representing the essential neglected impact, given in d- and q-components

U_p is the stationary source voltage

$U‘_p$ is the transient voltage

I‘ is the transient current given in d- and q-components

By using this circuit as a basis, it can be examined if the transient voltage $U‘_p$, with respect to the stationary source voltage U_p, is changed when a transient current $I‘$ occurs. The vector diagram of this equivalent circuit can be made, and is shown in Fig 4.8 [2].

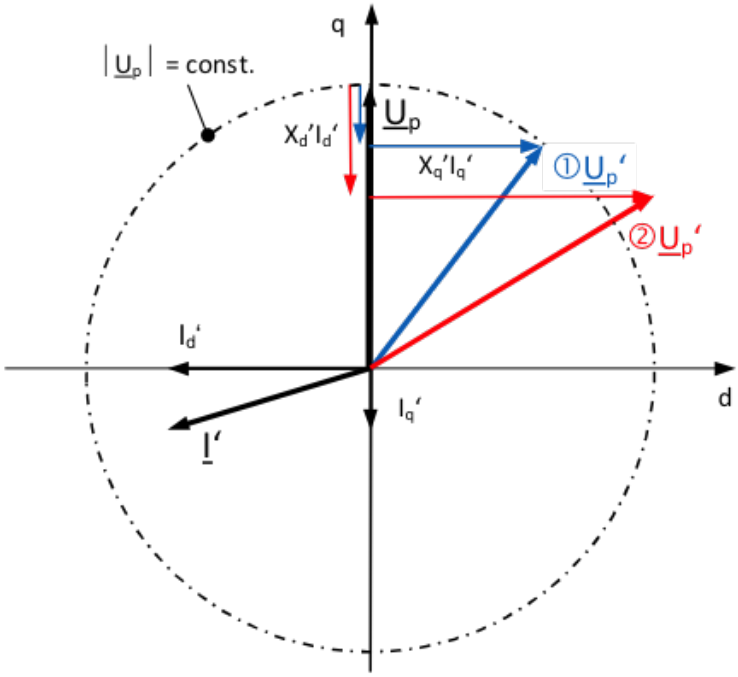

Figure 4.8: The vector diagram given from the simplified equivalent circuit of the studied system [2].

From Fig 4.8 it can be seen that the start of the transient period depend on $X‘(X_d, X‘_q), I‘(I‘_d, I‘_q)$ and U_p, and if $U‘_p$ is bigger or equal to U_p. From this, we can say that stability appears when [2]:

$$| U‘_p | \leq | U_p | \tag{4.14}$$

Which is the case when the transient current $I‘$ does not increase the voltage U_p. When the transient current increases the voltage U_p, instability appears: [2]:

$$| U‘_p | > | U_p | \tag{4.15}$$

By combining Eq. 4.14 and the equation

$$U`_p = \sqrt{(U_p - X`_d I`_d)^2 + (X`_q I`_q)^2} = \sqrt{U_p^2 \underbrace{-2X`_d I`_d U_p + X`^2_d I`^2_d + X`^2_q I`^2_q}_{\text{Must be } \leq 0 \text{ to avoid voltage increase}}} \tag{4.16}$$

a general stability criterion is given by:

$$X`^2_d I`^2_d + X`^2_q I`^2_q - 2X`_d I`_d U_p \leq 0 \tag{4.17}$$

As Eq. 4.17 shows that the stability of the rectifier-synchronous generator system depends not only on the transient reactance $X`$ and the transient current $I`$, but also on the stationary operating point. The value of U_p depends on the excitation of the generator.

The conclusion can be drawn, that the stability criterion is equally dependent on both the transient current $I`$ and the change made in generator excitation. Because of differences in time constants, will the transient current $I`$ change faster than the excitation current. Experiences from the ships in operation shows that the oscillations that leads to instability problems in the system can not be eliminated or dampened by controlling the excitation current [2] [17].

This implies that, to improve the stability of the system, an option is to control the transient current $I`$. Another option is to use controlled rectifiers like thyristor- or IGBT-rectifiers, because of their low deadtime, that is lower or equal to the transient time constants of the generator, which also has shown to be true in praxis [2].

Even though the generators under study is characterized with high values of reactances, the stability criterion in Eq. 4.17 shows that there is not only these reactances, X_d, X_q, that influences the stability of the rectifier-synchronous machine system. Also the stationary operating point influences the stability [2] [17].

4.6.1 Evaluation of the stability criterion

To evaluate the stability criterion in Eq. 4.17, two vector diagrams for both steady state (Fig. 4.9) and transient operation (Fig. 4.10), is used.

The steady state operation is studied to estimate the terminal voltage U_p and the rotor angle δ. It is important to estimate the rotor angle to decide the location of the rotor (in d-q coordinates) relative to the stator winding (in a-b coordinates). To do so, the assumption $cos\phi = constant =$ 0.9...0.95 is made. This is a reasonable assumption because the angle is only weakly dependent on the load because of the diode rectifier. The steady state operation can be found through the steady state terminal voltage U_{LM} and the steady state phase current I [2].

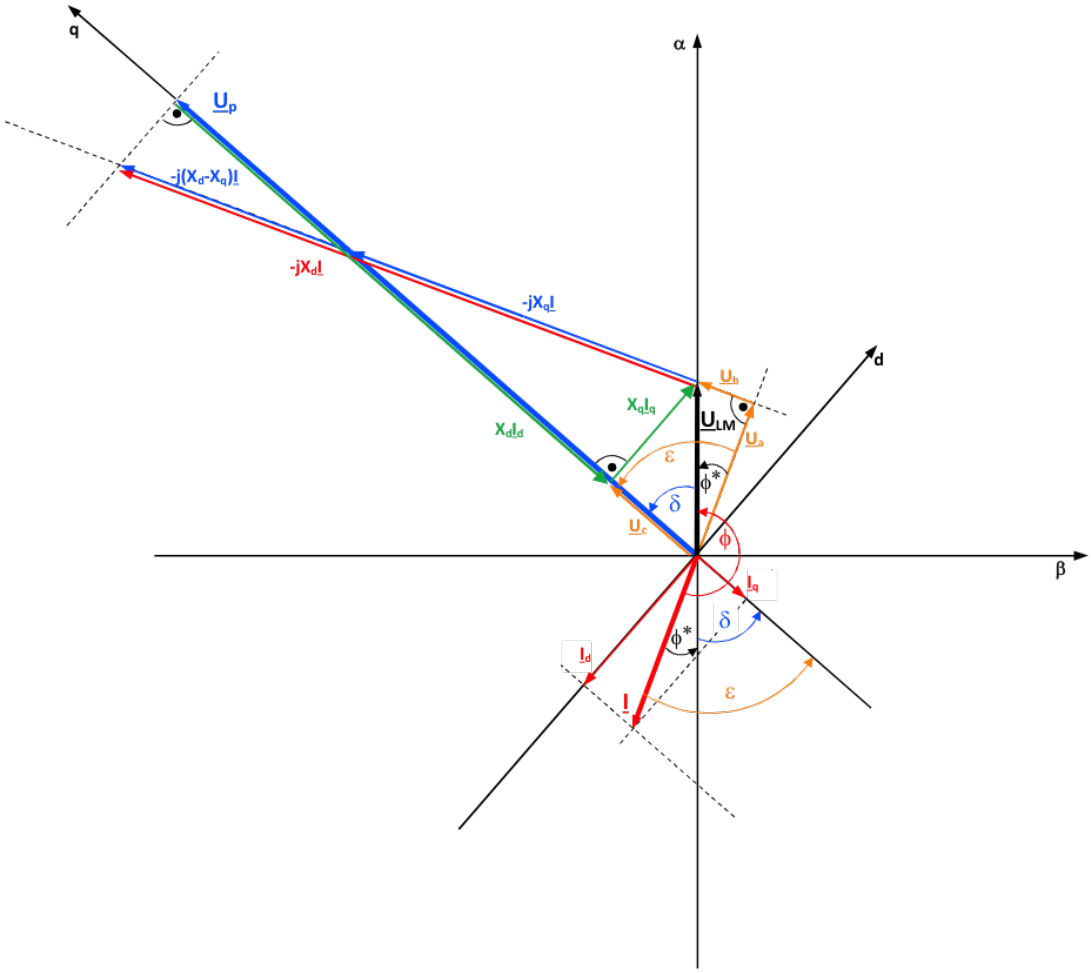

Figure 4.9: The vector diagram of the studied system in steady state [2].

To estimate the steady state voltage U_p, the following evaluations from the steady state vector diagram in Fig 4.9 is made:

- $cos\phi = cos\phi^*$ and $\phi^* = cos^{-1}\phi$
- $U_a = U_{LM}cos\phi = U_{LM}cos\phi^*$

  $U_b = U_{LM}sin\phi^* = U_{LM}sin(cos^{-1}\phi)$
- $X_{d,q} = 2\pi f L_{d,q}$, where

  $L_{d,q} = \frac{X_{d,q}}{2\pi f_n} = \frac{x_{d,q}Z_n}{2\pi f_n}$
- $\epsilon = \delta + \phi = \delta + \phi^* = tan^{-1}(\frac{X_d I + U_b}{U_a})$

- $U_c = U_{LM} cos\delta$
- $I_d = Isin(\delta + \phi^*)$

This results in an expression for the steady state voltage U_p:

$$U_p = X_d I_d + U_c \tag{4.18}$$

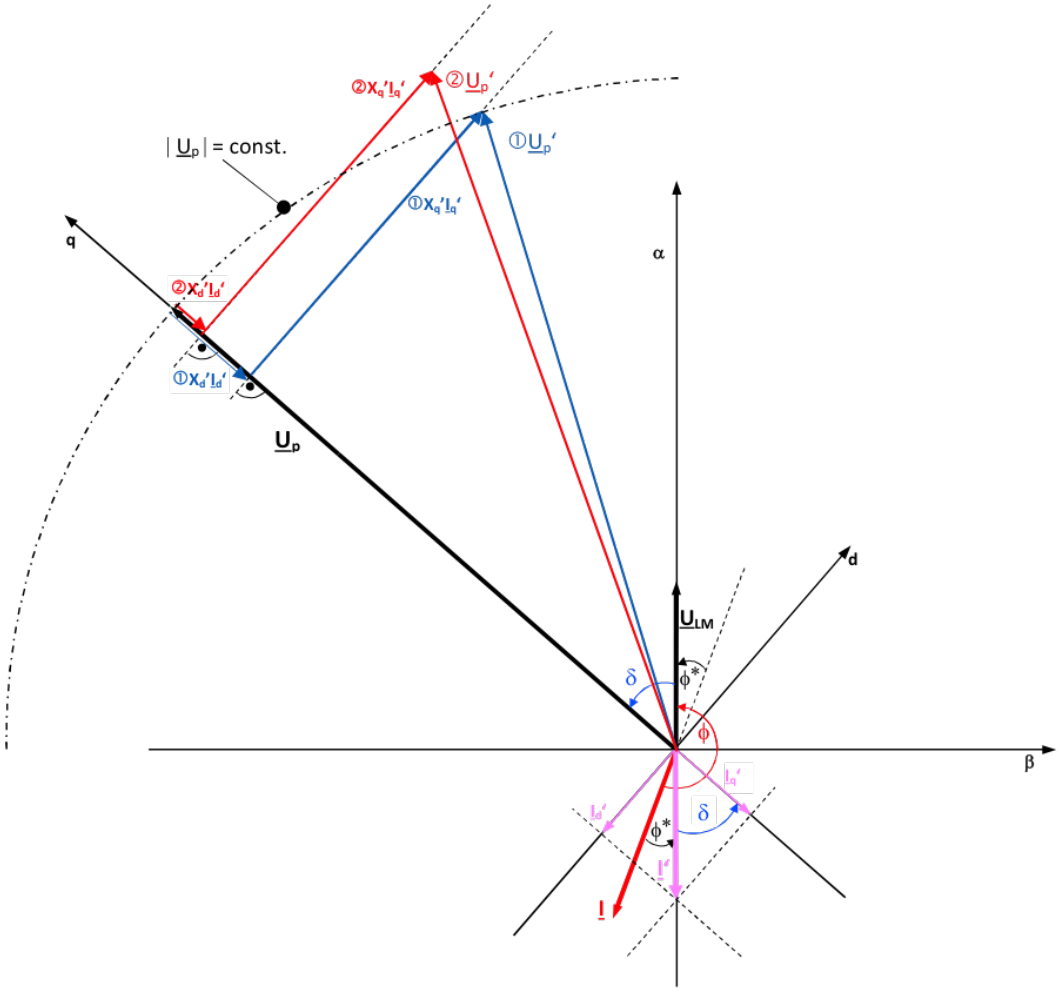

Figure 4.10: The vector diagram of the studied system in the transient state [2].

The following evaluations from the transient vector diagram in Fig 4.10 is made:

- Because the value of the transient current I‘ from the generator through the rectifier is unknown, is the ratio $\frac{I'}{I}$ introduced.

The assumption that $I' \geq I$ must be made, because the steady state current follows the transient current through the rectifier

- The transient current I' is in phase with the assumed terminal voltage U_{LM}, which implies that the transient current only flows in the a-axis.
- The transient currents I'_d and I'_q has the following ratio:

  $I'_d = I' sin\delta$

  $I'_q = I' cos\delta$

The stability criterion given in Eq. 4.14 can now be tested, now that all the components is known.

4.6.2 Stability criterion evaluated for three different operations

The stability criterion in Eq. 4.17 is evaluated to investigate three different types of operation. In the following evaluations, the assumptions $X'_q = X'_d$ and that $\frac{X'_q}{X'_d} = \frac{X_q}{X_d} > 1$ is used, because this is true for most synchronous machines. The assumption that $\frac{I}{I'} = 1$ is also used [2].

Both sides of Eq. 4.17 is multiplied with the expression $\frac{1}{x_d^2 I_d^2}$ and solved by using the expressions for $U_p, I_d, I_q, I'_d, I'_q, X_d, X_q, X'_d$ and X'_q found using the vector diagrams for steady state (Fig. 4.9) and transient state (Fig. 4.10), we have that [2]:

$$\frac{X'_q}{X'_d} \leq \frac{I}{I'}\left(\frac{X_d}{X_q}\frac{sin(\delta+\phi^*)sin\delta}{cos^2\delta}\right) \pm \sqrt{\left(\frac{I}{I'}\left(\frac{X_d}{X_q}\frac{sin(\delta+\phi^*)sin\delta}{cos^2\delta} + \frac{cos(\delta+\phi^*)}{cos\delta}\right)^2 - tan^2\delta\right)} \tag{4.19}$$

That forms the base for the three cases presented next.

Case A

With the assumption $\frac{I}{I'} = 1, cos\phi = cos\phi^* = 1, (\phi^* = 0)$:

$$\frac{X'_q}{X'_d} = \frac{X_q}{X'_d} \leq 1 + \frac{X_d}{X_q}tan^2\delta + \sqrt{\left(1 + \frac{X_d}{X_q}tan^2\delta\right)^2 - tan^2\delta} \tag{4.20}$$

With the assumptions in this case, it is obvious that the ratioship $\frac{X'_q}{X'_d}$ is not only dependent on the machine parameters for stable operation of the diode rectifier-synchronous generator-system,

but depends also on the rotor angle δ [2].

Case B

If in this case, $\delta \to 0$ in Eq. 4.20 and $\frac{I}{I^{\cdot}} = 1$:

$$\frac{X`_q}{X`_d} = \frac{X_q}{X`_d} \leq 2 \underbrace{cos\phi^*}_{cos\phi = cos\phi^* = 1} \leq 2 \tag{4.21}$$

This is the expression that [1] and [3] also proposes. The difference between the expression proposed in [1] and [2] is that [1] assumes an arbitrarily, small load. This is the opposite of what is experienced in praxis with the generators with BlueDrive+C system, which all have the value $\frac{X`_q}{X`_d} \leq 2$ and is stable under operation, except from the non-salient pole generators [2].

Case C

With the assumptions $cos\phi = cos\phi^* = 1$, $\frac{I}{I^{\cdot}} = 1$ and $\delta = 45$:

$$\frac{X`_q}{X`_d} = \frac{X_q}{X`_d} \leq 1 + \frac{X_d}{X_q} + \sqrt{\left(\frac{X_d}{X_q}\right)^2 + 2\frac{X_d}{X_q}} \tag{4.22}$$

With the assumptions presented in this case, it can be observed that the ratio $\frac{X_q}{X`_d}$ only depends on the machine parameters. This may require an evaluation of generators with BlueDrive+C system with critical parameters.

Generators with non-salient poles ($\frac{X_d}{X_q} \approx 1...1,2$) with the ratio $\frac{X`_q}{X`_d} = \frac{X_q}{X`_d}$ must be considered critical. This implies a smaller value of the ratio $\frac{X`_q}{X`_d} = \frac{X_q}{X`_d}$ for a non-salient pole generator than for salient-pole generators ($\frac{X_d}{X_q} \approx 1,5....2$) [2].

Chapter 5

Description of DIgSILENT PowerFactory Model

The models based on the model established in [6], and this work is a continuation on the study done of the impact of the rectifier in the system. The model is based on the model found in [4] as explained and shown in Fig 3.2 in Chapter 3. By implementing a rectifier in the model is it possible to study how the rectifier impacts the same system, with the same internal and external impedances as in Fig 3.2, to compare the stability of the two systems.

The parameters of the lines and transformers is given in Table B.1 in Appendix B, and the parameters for the generators are given in Table I.1 and I.2 in Appendix I. The voltage regulator used is called ESAC8B and the block diagram and the parameter settings is shown in Fig E.1 and Table E.1 in Appendix E. There is no governor added to the generator model.

A voltage source is connected to the system to model the battery in the ship. The rectifier chosen is of the rectangular PWM converter type, and is located in the end of the system, right before the position of the DC voltage source - the battery. This position is chosen to have a better basis for comparison, due to the fact that the impedances is similar in this system as the one shown and described in Fig 3.2 in Chapter 3. The PWM converter model represents a self-commutated, voltage sourced AC/DC converter. The equivalent circuit of the converter is shown in Fig B.4 in Appendix B. [18]

Two loads draws active power from the ac-bus, supplied by the generator. The loads have the magnitudes of 0.6MW and 0.01MW, respectively [4]. No reactive power is delivered through the rectifier, the amount of reactive power produced by the generator is consumed by the rectifier. The system is shown in Fig 5.1 below.

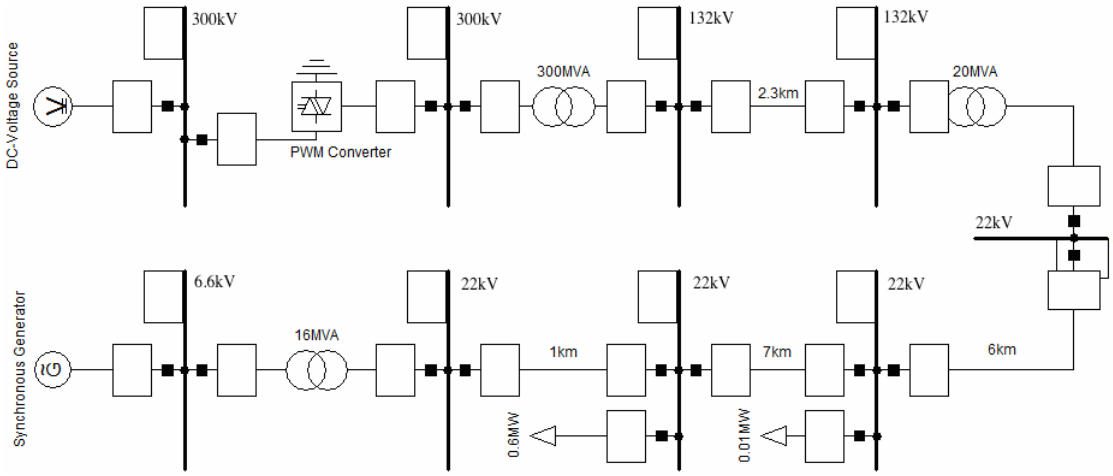

Figure 5.1: This one-line diagram shows the system considered in this K_5-analysis, and is based on the system in [4]. This study is a continuation of the work done in the specialization project conducted in the fall of 2014.

Chapter 6

Simulations in DIgSILENT PowerFactory

The simulations presented in this chapter is based on the model presented in Chapter 5, and is a continuation of the work in [6] presented in Chapter 3.

The same linear analysis as presented in Chapter 3 is made, where the PID proportional gain K_p that directly impacts the linearization constant K_5 is varied from 50 to 1000 for both generators G1 and G2. The mode of interest is the critical mode that oscillates at about 2Hz, and is found using the QR-method. The eigenvalues come in pairs, and are mirrored about the real axis. Only the eigenvalues in the positive half plane is considered. The system is defined as unstable when the real part of the eigenvalues becomes positive ($Re[\frac{1}{s}] > 0$).

A K_5- analysis is done and shown in a mode-plot for G1 and G2 in Figure 6.1 below. The simulations is done when the system is in two different operating scenarios, one where the generators are consuming and the other when the generators are producing reactive power of 2Mvar. In both cases, they produce active power of 14MW. The PID gain K_p of the voltage regulator used called ESAC8B is varied in value from 50-500, and the eigenvalues oscillating around 2Hz is analyzed. When K_p is varied, the linearization constant K_5 is directly affected, The method used for modal analysis is the selective modal analysis type.

The critical modes found in the systems in this simulation oscillated with a frequency of approximately 1Hz. The modes associated with the rotor angle phi oscillates usually with a frequency of around 2Hz. To see what parameter the modes found in this simulation is associated with, a report for the eigenvalues in the system is made and the participation factors for the modes is examined. The report, that is shown for both generators in Appendix B.2, shows what parameters the modes is associated with, and the participation factors. It also provides a bar chart in

addition to the numerical values.

The eigenvalue-report from the modal analysis of the system is created when the gain K_p in the voltage regulator connected to G1 and G2 is at a value of 500. Fig B.1 describes some of the most usual participation factors, and is found in Appendix B.2. The report shows two critical modes. Mode 8 oscillates with 1Hz and mode 10 oscillates with 0.05Hz.

The numerical values for mode number 10 shows that the parameters "avr ESAC8B; xi" and "G1; psie"/"G2; psie" (excitation-flux [pu]) is the parameters with the biggest impact. The numerical values for mode number 8 shows that the parameters "G1; phi"/"G2; phi" (rotor angle [rad]) and "G1; speed"/"G2; speed" (speed [pu]) is the parameters with the biggest impact.

It can be concluded that mode 10 oscillates due to faults in the voltage regulator and in the excitation in the generator, but only with a very small frequency and is not of interest for the object in this thesis. Mode 8 oscillates due to faults in the generator exclusively. Due to this, mode 8 is the mode of interest, and is chosen to represent the oscillations in the rotor angle, with the speed as a participation factor as a consequence to the oscillations in the rotor angle.

The rotor locus plot in Fig 6.1 below shows the displacements of the eigenvalues associated to the critical mode number 8, that oscillates at a frequency of 1Hz, as a result of the varying of the voltage regulator gain K_p.

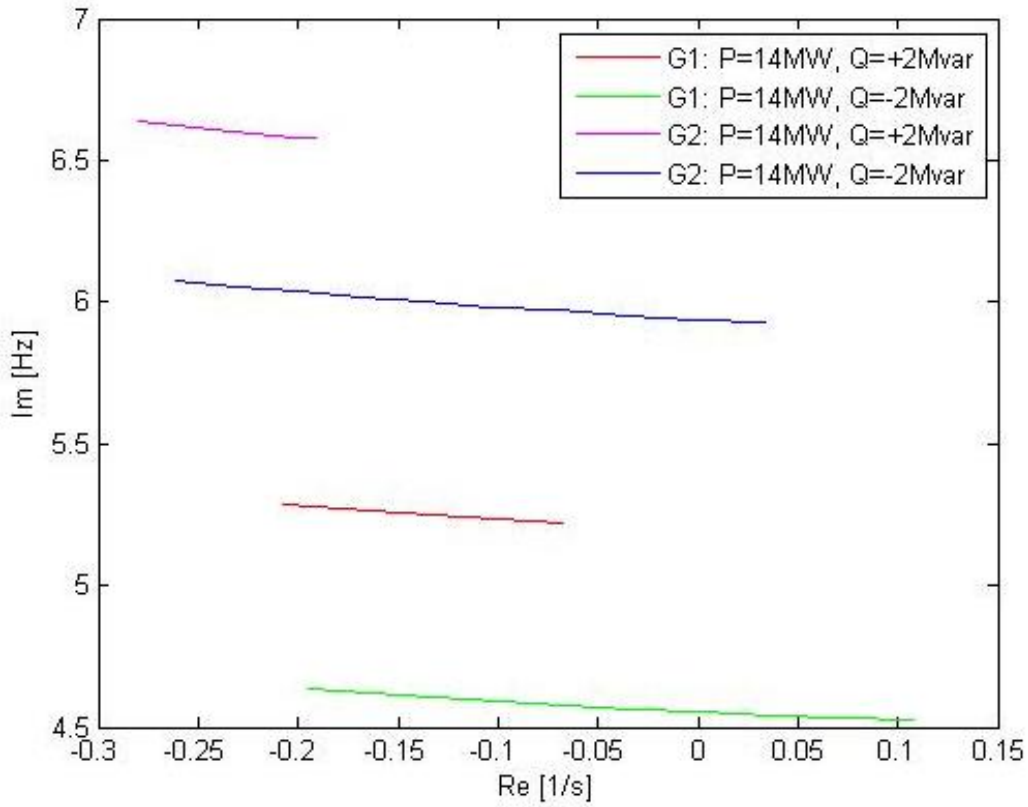

Figure 6.1: This root locus plot shows the eigenvalues of G1 and G2 of critical modes oscillating with approximately 1Hz. Two situations is considered, for the generators producing and consuming reactive power of 2Mvar. In both cases, the generator produces an active power of 14MW.

The root locus plot above shows that the eigenvalues of the critical mode will move to the right in the plane due to a decreasing value in the real part of the eigenvalues, when the gain K_p in the voltage regulator is increased in its value from 50 to 500. The varying of the gain K_p has a direct impact on the linearization constant K_5, as explained in Chapter project. When the real part of the eigenvalues become positive, the generators are considered unstable.

It can be seen that the generators moves faster towards instability when the generator consume reactive power rather than when they produce reactive power. It is remarkable that the generator with the smallest generator reactances (G1) moves faster towards instability than the generator with largest generator reactances (G2) does. This is the case for both operations. This was not the case for when the rectifier is not included in the system, shown in Fig 3.3.

Chapter 7

Description of MatLab/SimPowerSystems Model

Siemens in Trondheim, [17] has through simulations in the simulation tool MatLab/SimPowerSystems made successful attempts to imitate the problem experienced. The model developed is a instantaneous value model, and is the same model mentioned in section 4.6 in Chapter 4.

Two models is created from this model developed by Siemens Trondheim, one with the values for the synchronous generator reactances from G1 and one with the reactances from G2, respectively. The SG with the highest values of reactances, G2, is unstable in the simulations and has an apparent power of 1940 kVA. The other generator, G1 is stable and has an apparent power of 3333 kVA.

The test circuit shows the SM being used as a generator, the terminal voltage is controlled using a simple PID voltage regulator, and the speed is controlled using a simple PI governor. The overall model has been initialized to start in periodic steady state to supply a load increasing up to about 1720kW. The generator have rotating field that operates towards an infinite large capacitor with an inner resistance that represents the battery connected to the DC-bus in the electric system on the ships [17].

The model used for the simulations in SimPowerSystems MatLab is shown in Fig. 7.1 below, where the SM is used as a generator, and the terminal voltage is controlled by an PID AVR and the speed of the generator is controlled by a PI governor. The PID AVR type initially used in the received model from Siemens is throughout the thesis called "AVR type A" to distinguish between this type and other voltage regulators investigated or discussed. The initial setting of the reference voltage value is set to 1.2, meaning that the regulator is to increase the terminal voltage to 20% higher than the nominal voltage of the generator. A rectifier is connected to the

terminals of the generator, and is designed as a six-pulse three-phase rectifier consisting of three bridge arms each with two diodes.

The simulation shows the start-up characteristics of the generators, where the only event except from the generator start-up is in form of the voltage regulator adjusting up the voltage. This up-adjusting of the voltage results in an increasing current into the infinite capacitor with stiff DC-voltage that represents the battery.

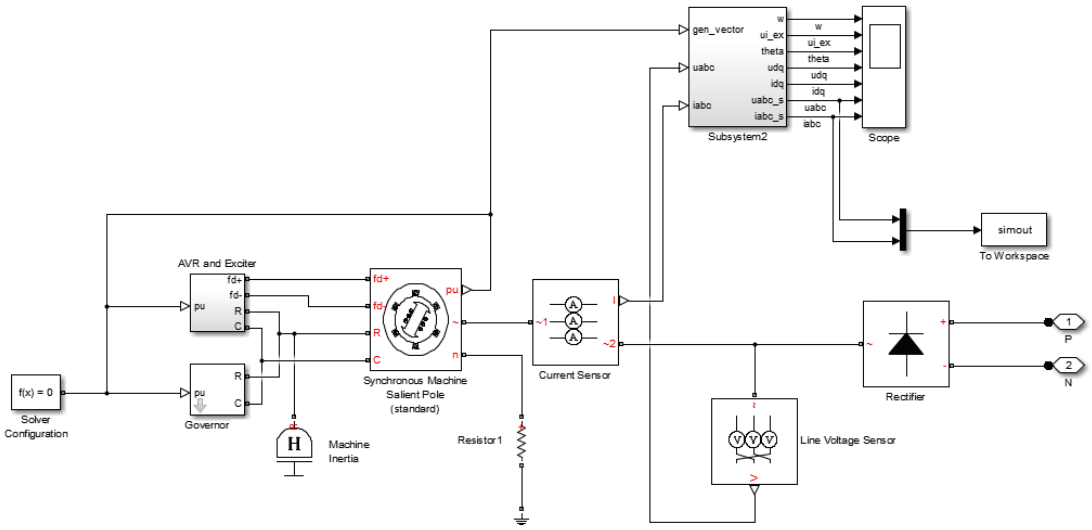

Figure 7.1: The model used in the simulation tool SimPowerSystems

The block diagrams for the governor, exciter and regulator can be found in the Appendix, in Fig C.1, C.2, C.3 and C.4, for G1, and in Fig D.1, D.2, D.3 and D.4, for G2, respectively. The parameters for the exciter generators is found in Table C.1 for G1 and in Table D.1 for G2. The data for the generators are found in Appendix I. The generator parameters for the 3333kVA generator 1940kVA generator is shown in Table I.1 and Table I.2, respectively. The parameters for the components rectifier, battery-arrangement and Resistor4 is found in Appendix F. The parameters for the two generators G1 and G2, as well as the other components used in the origin SimPowerSystems model are obtained from the model received from Siemens in Trondheim, [17].

The generator-block is from SimScape and the machine equations is based on Park's transformation to the rotating reference frame with respect to the electrical angle [19].

The generator feeds a battery C1 through the rectifier, and the connection between the system in Fig. 7.1 and this battery is shown in Fig. 7.2 below, where the system in Fig. 7.1 is represented by the box named "Gen1" to the left. The two connection ports "P" and "N" shown in Fig 7.1 is the same ones that is shown to the left in Fig 7.2 below.

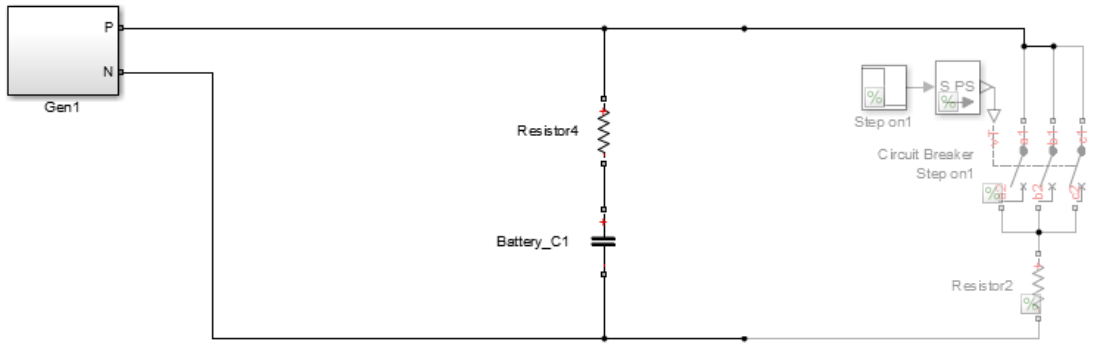

Figure 7.2: One line diagram showing how the generator is connected to the battery C1 and an active load in the model in SimPowerSystems

The battery C1 is the infinite capacitor and is connected in series with a resistor, and the opportunity for connecting load resistance in parallel through a circuit breaker is shown to the right. The load can be added to the model after an optional number of seconds, by setting the desired number of seconds in the circuit breaker.

The solver function used throughout the simulations in this thesis is the ode45-solver, which is a non-stiff problem type, with a medium order of accuracy. This solver is the solver that can be used in most situations according to the help-function in SimPowerSystems [20], and should, quote: "be the first solver you try".

If the problem simulated is stiff and not non-stiff, this solver can still be used, but will be slow. Another solver can then be used, and it is suggested by [20] to switch solver from ode45 to ode15.

The simulation of the generator start-up can be of optional length, but is usually limited to 20 seconds, to examine the stability of the generator. Some simulations is extended to 50 seconds to observe the voltage regulator response time, but this is an absolute maximum simulation time for the dynamic, non-stiff solver used.

Simulations that exceeds this time limitation should not be implemented, because numerical instability might occur, which means that the mathematical equations which the simulation tool is based upon can not handle long time aspects. The algorithms in the system can go unstable if the simulation is set too long. Simulations used for stability analysis is for this reason not longer than 20 seconds.

When the generator stability is analyzed, several parameters is available from the generator output. The load angle *theta* measured from the generator is given in rad and is calculated by: $theta = tan^{-1}(\frac{E_d}{E_q})$. The load angle is also known as the rotor angle.

7.1 Model Verification

The model is tested with a constant, ideal voltage source feeding a load through the rectifier. The reason for this is to verify the model when none of the studied generators is applied. The nominal voltage of the voltage source is set to 690V, and the parameters of the battery, Resistor4 and rectifier is found in Appendix F. The voltage after the rectifier should according to theory found in Chapter 4.1 be: $V_{dc} = \frac{3\sqrt{2}V_{LL}}{\pi} = 1.35 * 690V = 931.5V$.

Load attached on dc-side of the rectifier

The generator start-up of the voltage source feeding load through rectifier is first simulated, without battery. The resistance connected to the dc-side of the rectifier is set to be $R_{Load} = 2.122\Omega$ which corresponds to an active load with magnitude $P_{Load} = \frac{V_{dc}}{R_{Load}} = \frac{(931.83V)^2}{2.122\Omega} = 0.41MW$. It is connected 3 seconds into the simulation. The mean voltage on the dc-side of the rectifier is shown in Fig 7.3 below.

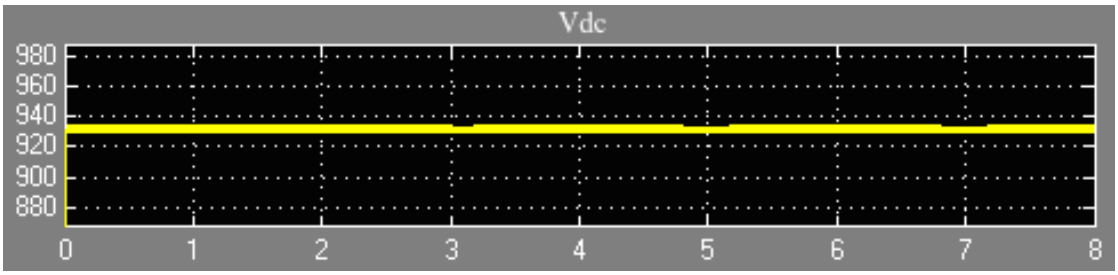

Figure 7.3: The mean dc-voltage for the SimPowerSystems model with constant voltage source and $P_{Load} = 0.41MW$ and no battery connected to the dc-bus.

The mean dc-voltage shows a voltage of 931V after the rectifier, and corresponds to theory found in Chapter 4.1, as mentioned above. The voltage and current delivered from the terminals of the voltage source is shown in Fig 7.4 below.

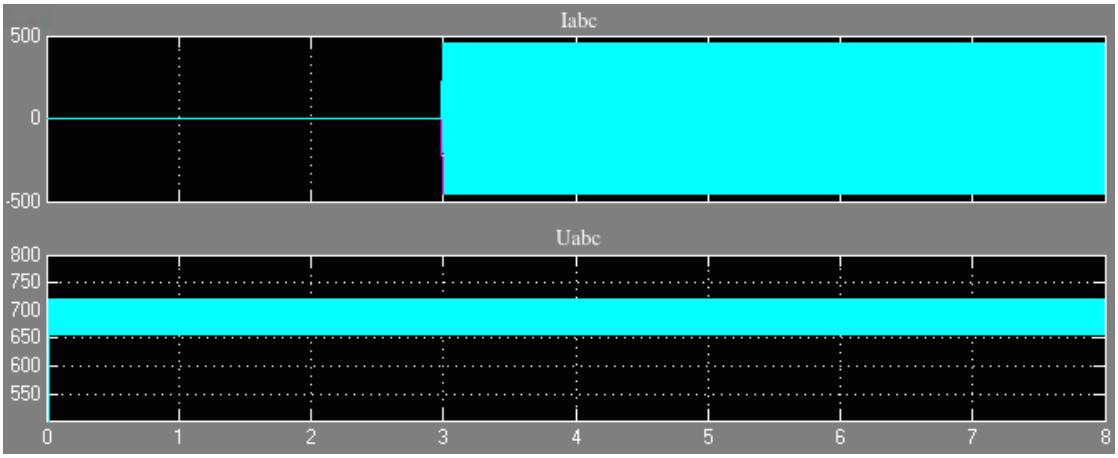

Figure 7.4: The current $Iabc$ and rms voltage $Vabc$ for the SimPowerSystems model with constant voltage source and $P_{Load} = 0.41MW$ and no battery connected to the dc-bus.

The current is zero until the load is connected 3 seconds into the generator start-up simulation, at that point it raises to approximately 500A. The rms voltage shows 690V.

Battery and load attached on dc-side of the rectifier

The load is kept at the same value, but now the battery-arrangement is connected to the dc-bus. The voltage on the dc-side of the rectifier is shown in Fig 7.5 below.

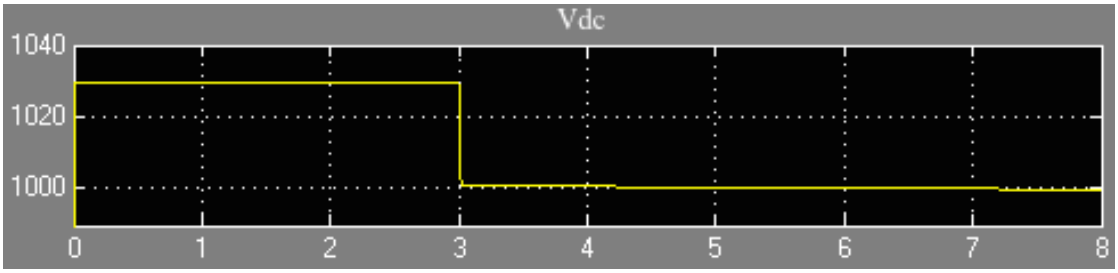

Figure 7.5: The dc-voltage for the SimPowerSystems model with constant voltage source and $P_{Load} = 0.41MW$ and a battery connected to the dc-bus.

The dc-voltage shows a voltage of 1030V before the load is connected at 3 seconds, and the dc-voltage drops to a value of 1000V. The nominal voltage of the battery is set to 1030V, and is the reason why the dc-voltage shows this value. The voltage and current delivered from the terminals of the voltage source is shown in Fig 7.6 below.

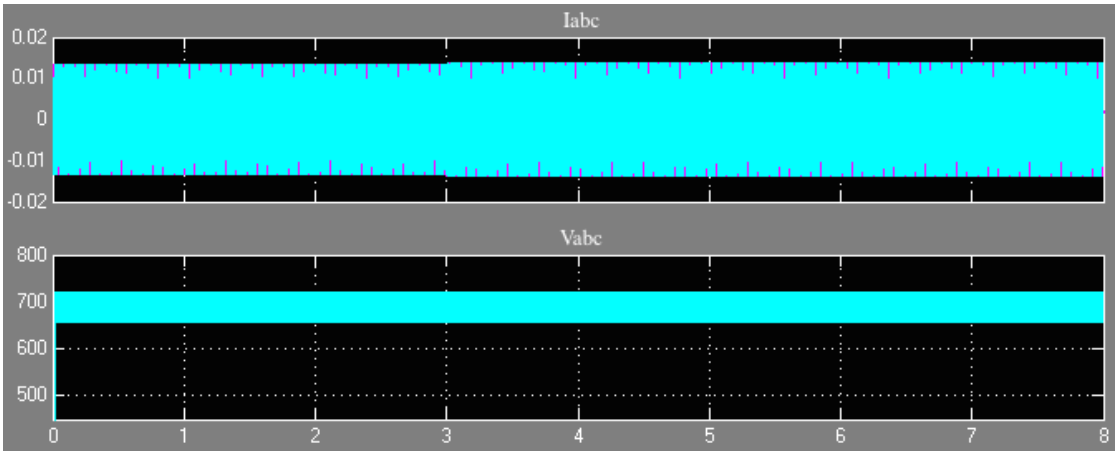

Figure 7.6: The current $Iabc$ and voltage $Vabc$ for the SimPowerSystems model with constant voltage source and $P_{Load} = 0.41MW$ and a battery connected to the dc-bus.

The voltage shows 690V as before. The current is almost zero throughout the simulation, indicating that the battery supplies the load. The current measured between the battery-arrangement and the load is measured and shown in Fig 7.7 below.

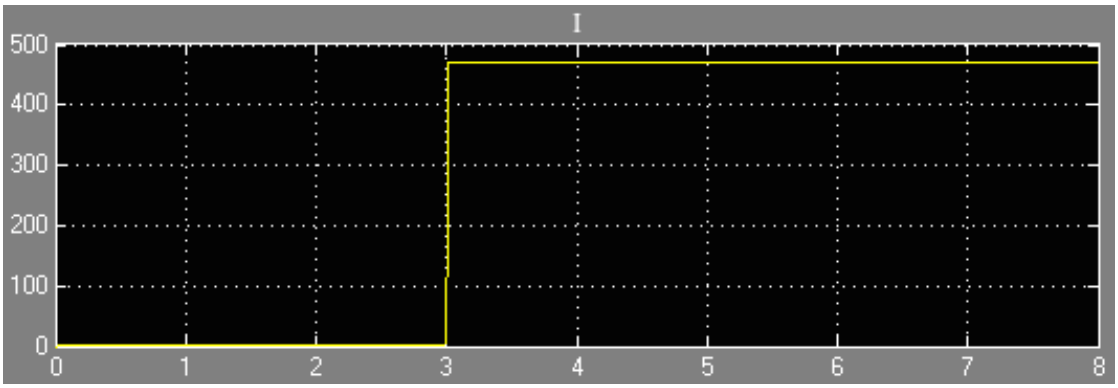

Figure 7.7: The current from the battery to the load in the SimPowerSystems model with constant voltage source and $P_{Load} = 0.41MW$ and battery connected to the dc-bus.

The current flowing towards the load starts to flow when the load is connected after 3 seconds, and is red from the graph to be approximately 470V. This indicates that the battery feeds the load, and not the generator.

Chapter 8

Investigation of 3333 kVA Generator System

The 3333kVA generator is characterized as a stable generator. According to the stability criterion presented in [1], this generator should be unstable: $\frac{X`_q}{X`_d} = \frac{X_q}{X`_d} = 3.51 > 2$. According to [2], this generator should be stable, because it is designed as salient pole, and can have a larger value of the ratio $\frac{X`_q}{X`_d} = \frac{X_q}{X`_d}$ than for round rotor designed machines. The ratio $\frac{X_d}{X_q}$ for the 3333kVA generator ($\frac{X_d}{X_q} = 1.52$) is in the right range compared with most salient pole designed synchronous generators ($\frac{X_d}{X_q} = 1.5...2$). [2]

The ratio between the subtransient reactances in the q- and d-axis is: $\frac{X``_q}{X``_d} = 1.216$. This should ideally be as close to 1 as possible.

By using SimPowerSystems, the generator start-up is simulated, and the output values of G1, modeled as a salient pole synchronous generator, is shown in Fig 8.1 below. There is no load connected to the DC-side of the rectifier except from the battery-arrangement. The voltage regulator and governor is included in the model. The simulation is run for 10 seconds.

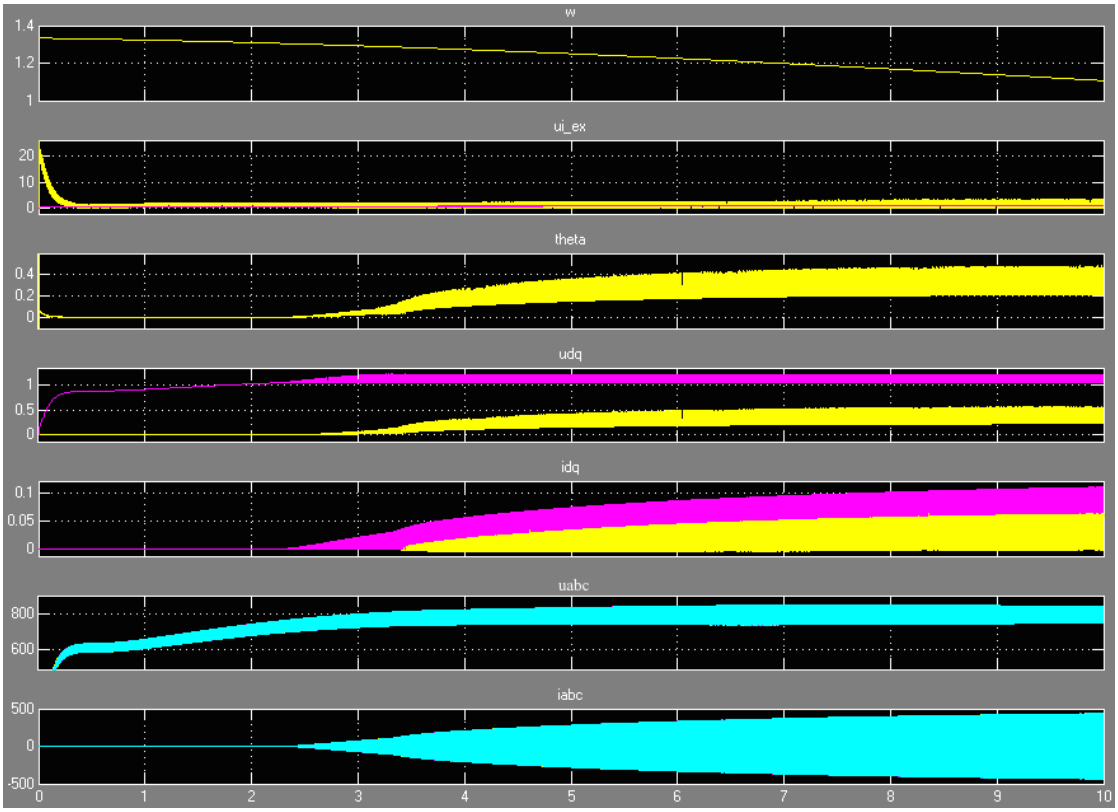

Figure 8.1: 3333 kVA generator system output values, where: w is the rotor velocity in pu, u_i is the exciter field voltage in pu, theta is the rotor angle in rad, u_{dq} is the stator voltage in the d- and q-axis in pu, i_{dq} is the stator current in the d- and q-axis in pu, u_{abc} and i_{abc} is the rms terminal voltage in V and the terminal current in A, respectively.

From the top, Fig 8.1 shows the rotor velocity w [pu], the field voltage u_i [pu], the rotor angle *theta* [rad], the stator voltage in the d- and q-axis u_{dq} [pu], the stator current in the d- and q-axis i_{dq} [pu], the terminal voltage u_{abc} [V] and the terminal current i_{abc} [A] of the 3333 kVA generator, respectively. The graph showing the field voltage u_i contains of a pink and a yellow curve, where the pink curve displays the field current and the yellow curve displays the field voltage. The graphs showing u_{dq} and i_{dq} contains of two curves, one yellow and one pink. The yellow curve is the d-axis for both voltage and current, and the pink is the q-axis for both voltage and current.

From the graph showing the output values of G1, it is observed that there is no oscillating parameters, and the system is stable under these conditions. The voltage reference value is set to increase the terminal voltage to 20% above the nominal voltage of the generator. The nominal voltage of the generator is 690V, so the regulator is supposed to regulate the voltage to $1.2 * 690V = 828V$.

From the graph, the rms terminal voltage increases to a around 790V after a few seconds. This

is 38V below the theoretical value. The terminal voltage oscillates with a frequency of 62.5Hz. The current starts to flow after 2.5 seconds, indicating that the capacitor charges, because there is no load attached.

The simulation results from the governor, voltage regulator and the exciter is shown in Appendix C.2.

The dc-voltage from the exciter feeding the generator field is shown in Fig. 8.2 below.

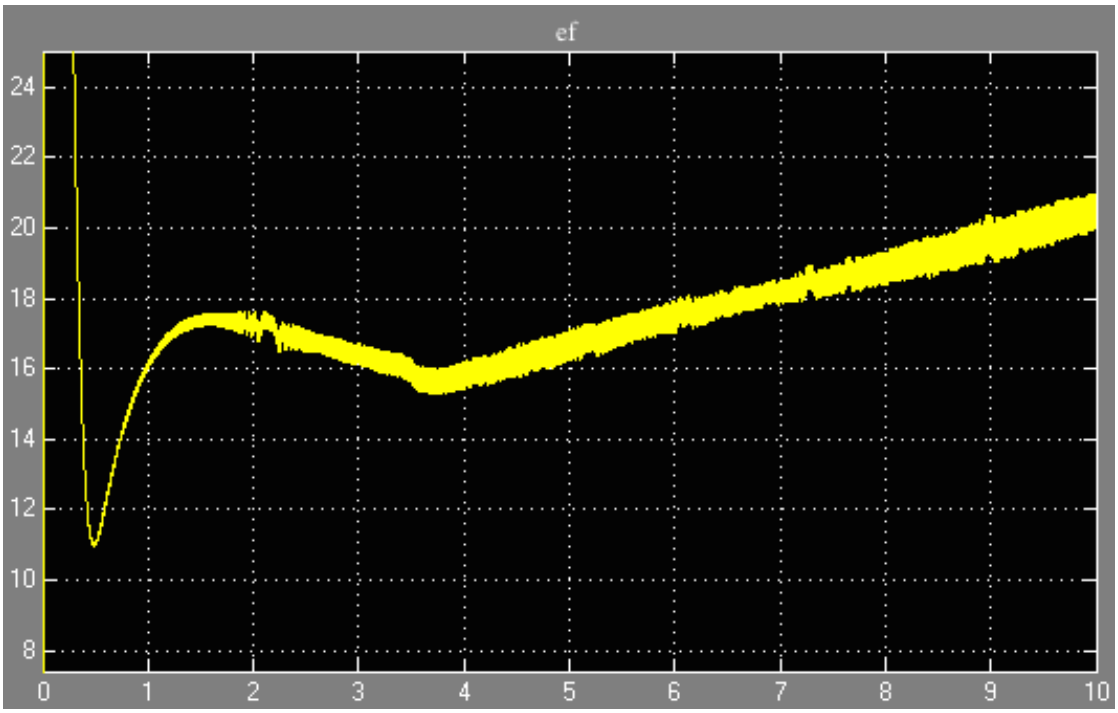

Figure 8.2: ef is the mean dc field voltage from the exciter generator feeding the generator field.

The dc-voltage from the exciter generator feeds the field of the 1940 kVA generator with 21V when the reference value of the AVR is 1.2. The dc-bus voltage is shown in Fig 8.3 below.

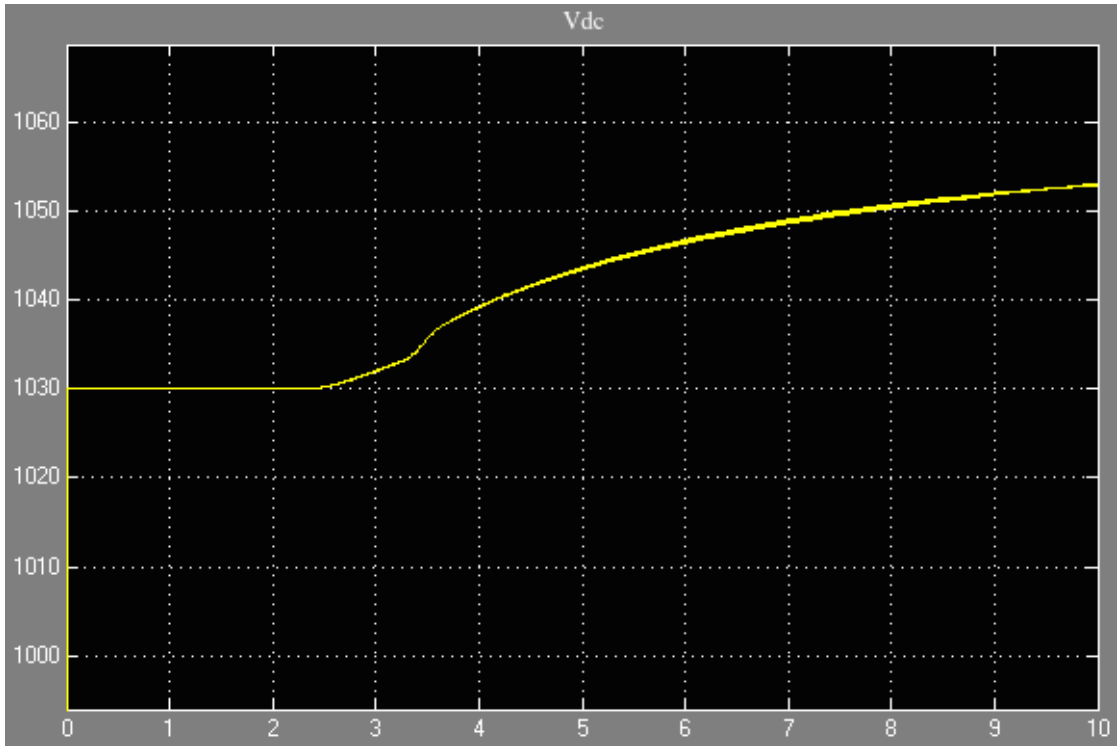

Figure 8.3: V_{dc} is the dc-bus voltage after the rectifier.

The DC-bus voltage shows 1030V, before it increases a bit due to the charging of the large capacitor. This almost corresponds to theory presented in Chapter 4.1 in Eq. 4.4, $V_{dc} = \frac{3\sqrt{2}V_{LL}}{\pi} = 1.35 * 790V = 1067V$. This is a bit higher than the dc-voltage stated in Chapter 2, 1030V. The capacitor voltage in the battery is also set to 1030V.

8.1 Load Step on DC-Side of the Rectifier

An active load R_{Load} is introduced 3 seconds into the generator start-up so see how the dynamics of a stable generator behaves. The equivalent circuit of the system is shown in Fig. 8.4 below. The voltage regulator with a reference value of 1.2 and the governor is included.

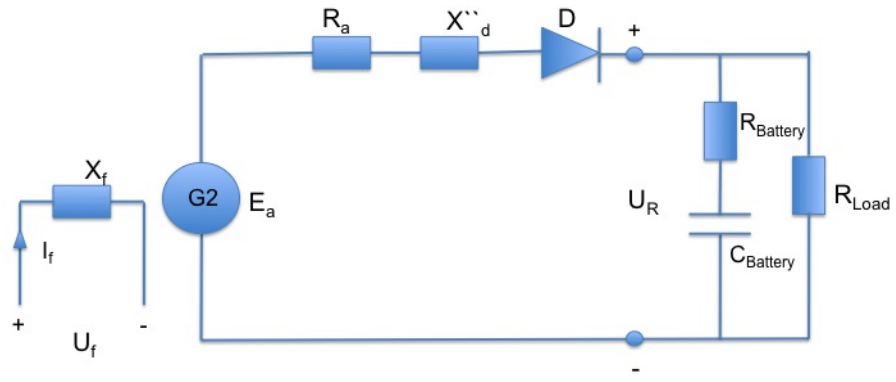

Figure 8.4: The system after the generator-rectifier-arrangement consists of a battery modeled by a series resistance $R_{battery}$ and a capacitor with significant value $C_{battery}$. A resistance R_{load} is placed in parallel with the battery and is adjustable.

The rms terminal voltage and terminal current is studied, and the R_{Load} is varied. First, the load is set to be a step of 0.5MW, which is a load step of 15% of the generator capacity (3.333MW). The resistance load is calculated by $R_{load} = \frac{V^2}{P}$. Since the voltage is 1030V after the rectifier, 0.5MW corresponds to a load resistance of $R_{Load} = \frac{(1030V)^2}{0.5MW} = 2.122\Omega$. It is introduced after 3 seconds and the voltage and current is studied.

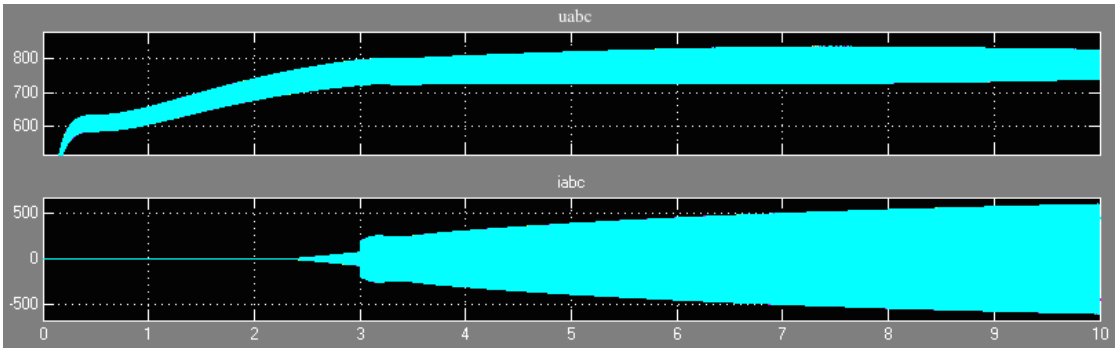

Figure 8.5: 3333 kVA generator system output values, where u_{abc} is the rms terminal voltage and i_{abc} is the terminal current. A load $R_{load} = 2.122\Omega$ which corresponds to an active load of 0.5MW, and is introduced 3s into the generator start-up.

When a load of 0.5MW is introduced after 3 seconds into the start-up simulation, a current starts to flow. The rms terminal voltage value after 10 seconds is 780V. The frequency of the terminal

voltage is 62.5Hz.

The load is increased to 1MW, which is 30% of the total generator capacitance. The resistance load corresponds to $R_{load} = \frac{V^2}{P} = \frac{(1030V)^2}{1MW} = 1.06\Omega$, and the voltage and current is studied.

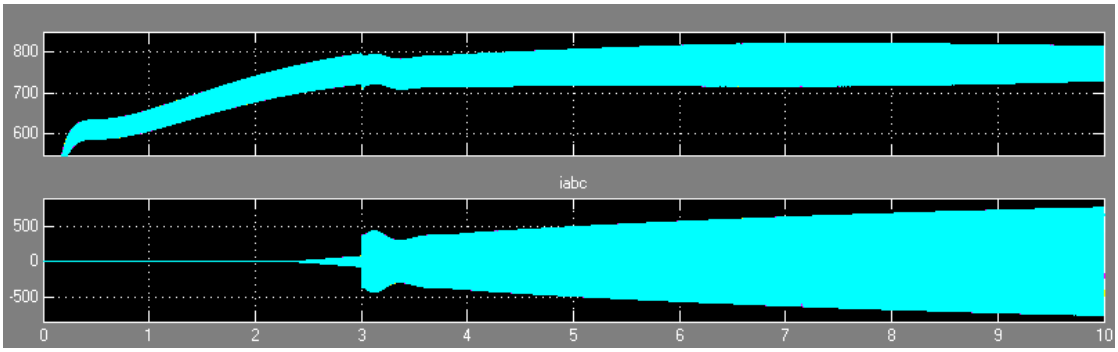

Figure 8.6: 3333 kVA generator system output values, where u_{abc} is the rms terminal voltage and i_{abc} is the terminal current. A load $R_{load} = 1.06\Omega$ which corresponds to an active load of 1.0MW, and is introduced 3s into the generator start-up.

A swell is observed in the current after 3 seconds, and a corresponding dip in the voltage at the the time when the load is introduced. The rms terminal voltage value after 10 seconds is 780V.

The load is increased to 1.5MW, which is 45% of the total generator capacitance. This is a large load step. The resistance load corresponds to $R_{load} = \frac{V^2}{P} = \frac{(1030V)^2}{1.5MW} = 0.707\Omega$, and the voltage and current is studied.

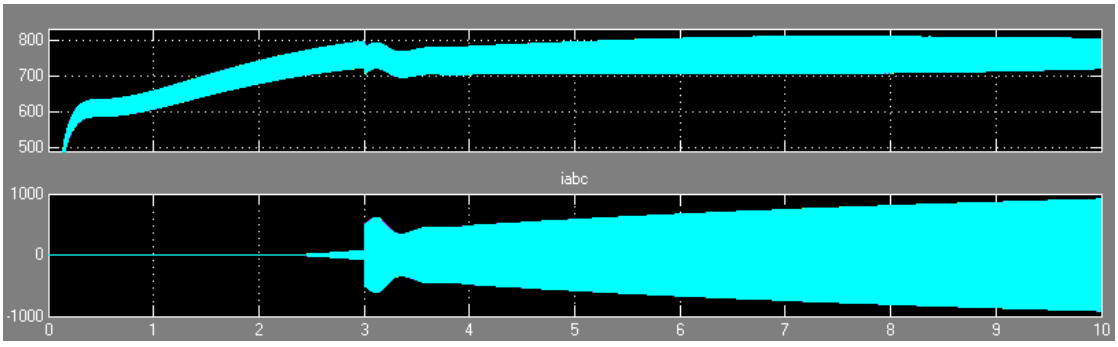

Figure 8.7: 3333 kVA generator system output values, where u_{abc} is the rms terminal voltage and i_{abc} is the terminal current. A load $R_{load} = 0.707\Omega$ which corresponds to an active load of 1.5MW, and is introduced 3s into the generator start-up.

The voltage regulator regulates the voltage to 760V after 10 seconds, and a dip is observed in the voltage and a swell in the current when the load is introduced.

The load is now increased to 3MW, which is 90% of the total generator capacitance. The resistance load corresponds to $R_{load} = \frac{V^2}{P} = \frac{(1030V)^2}{3MW} = 0.354\Omega$, and the voltage and current is

studied in Fig 8.8 below.

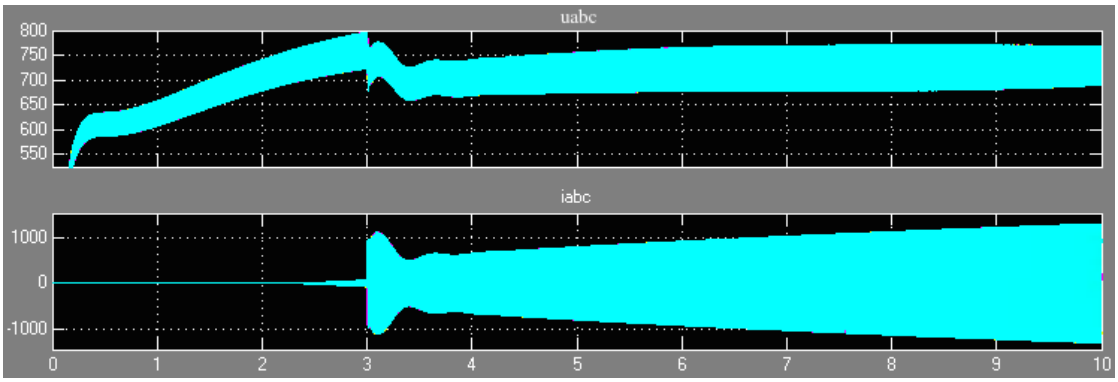

Figure 8.8: 3333 kVA generator system output values, where u_{abc} is the rms terminal voltage and i_{abc} is the terminal current. A load $R_{load} = 0.354\Omega$ which corresponds to an active load of 3MW, and is introduced 3s into the generator start-up.

A large swell is observed in the current and a drop in voltage. The rms terminal voltage value after 10 seconds is 720V when the load is 3MW.

The 333kVA generator is stable for loads. When the load is increased, the voltage regulator does not adjust the voltage at the required value of 828V. Even when the load is quite small, the regulator does not regulate the voltage at the requested value, but the value differs more from the requested voltage value when the load increases. The reference value of the AVR is studied next.

8.2 Influence of Terminal Voltage Value on AVR behavior

The reference value of the regulator is decreased from 1.2 to 1, such that the regulator is to adjust the terminal voltage to the nominal voltage of the generator, instead of to 828V. The terminal voltage and current is studied both when no load is attached, and when a load step is introduced.

No load on dc-side of the rectifier

No load is attached on the dc-side of the rectifier, to only study the dynamics of the generator as a function of the reference value of the voltage regulator, when the battery-arrangement is connected to the dc-bus. The reference value of the AVR is set to 1.0.

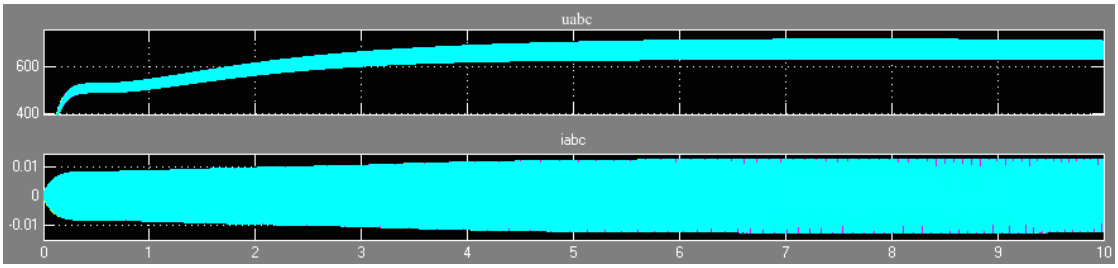

Figure 8.9: 3333 kVA generator system output values, where u_{abc} is the rms terminal voltage and i_{abc} is the terminal current. No load is attached to the dc-side of the rectifier, and the reference value of the AVR is set to 1.0.

The voltage regulator regulates the generator voltage to the nominal voltage 690V, as it is supposed to do. The dc-voltage from the rectifier is studied in in Fig 8.10 below.

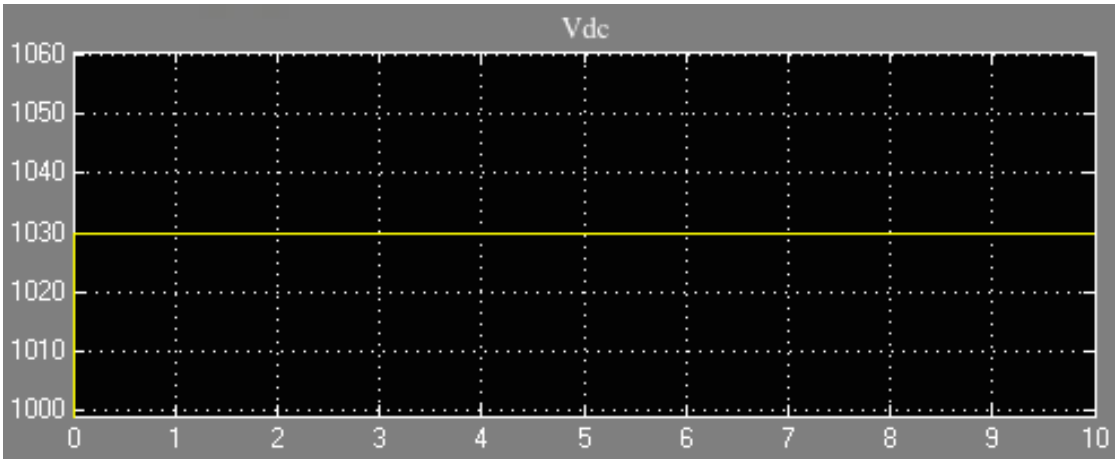

Figure 8.10: V_{dc} is the dc-voltage after the rectifier, supplying the battery-arrangement. The reference value of the AVR is set to 1.0.

The voltage on the dc.side of the rectifier is equal to the nominal voltage of the battery-arrangement, 1030V.

Load attached to the dc-side of the rectifier

A load is attached 3 seconds into the generator start-up, to study the dynamics of the generator as a function of the regulator, battery and load, and to see how the voltage regulator adjusts the terminal voltage when the reference value is set to 1.0. The load is 1.5MW.

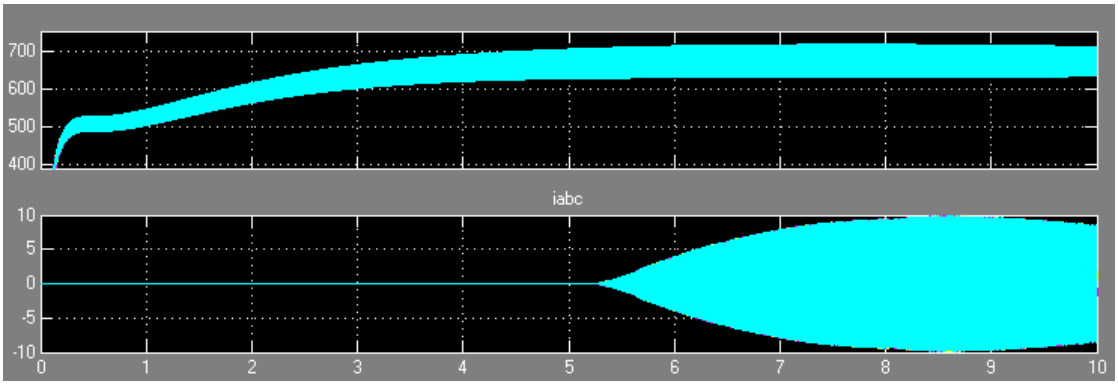

Figure 8.11: 3333 kVA generator system output values, where u_{abc} is the rms terminal voltage and i_{abc} is the terminal current. A load $R_{load} = 0.707\Omega$, which corresponds to an active load of 1.5MW is introduced 3s into the generator start-up, and the reference value of the AVR is set to 1.0.

The voltage settles at 690V when the reference value of the AVR is set to 1.0 and a load of 1.5MW is connected 3 seconds into the generator start-up. The battery supplies the load the first few seconds, due to the fact that the current from the generator starts to flow first after 5 seconds into the start-up. The load is increased to 3MW.

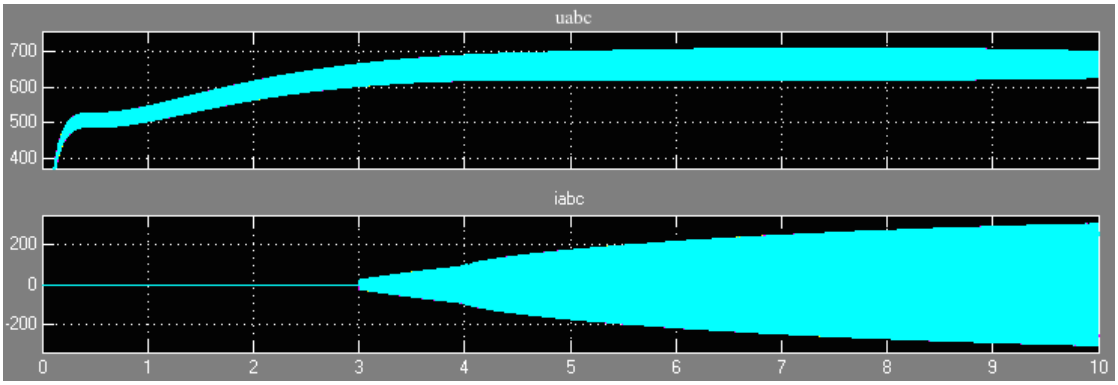

Figure 8.12: 3333 kVA generator system output values, where u_{abc} is the rms terminal voltage and i_{abc} is the terminal current. A load $R_{load} = 0.354\Omega$ which corresponds to an active load of 3MW is introduced 3s into the generator start-up, and the reference value of the AVR is set to 1.0.

The current starts to flow at the moment the load of 3MW is attached, and the battery and generator sloth supplies the load. The voltage settles at 690V.

Next, the voltage and current is studied during no-load and during load when the voltage regulator is not included, to study the generator dynamics when it is not regulated.

8.3 Without AVR Attached to the Generator

A constant DC-source with a voltage $V_{DC} = 21V$ excites the generator field when the voltage regulator and exciter is not present. The generator parameter output is studied both when no load is attached to the dc-side of the rectifier, and when a load is attached and varied.

No load on DC-side of the rectifier

The rms terminal voltage and terminal current is studied, when no load is attached to the dc-side and no AVR regulated the terminal voltage of the generator.

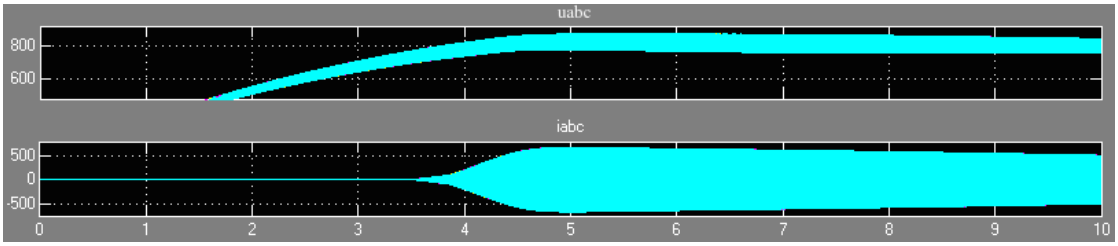

Figure 8.13: 3333 kVA generator system output value during the generator start-up, where u_{abc} is the rms terminal voltage and i_{abc} is the terminal current. The voltage regulator is not included, and no load is attached to the DC-side of the rectifier except from the battery-arrangement.

When no voltage regulator is connected to the generator, and no load is attached to the dc-side of the rectifier, the voltage still rises to a value of approximately 750V. The battery demands a voltage of 1030V, and the generator must raise the terminal voltage up to 800V to supply the battery. If the dc-voltage must be 1030V, the terminal voltage must be: $V_{LL} = \frac{V_d}{1.35} = \frac{1030V}{1.35} = 763V$.

Load on DC-side of the rectifier

The rms terminal voltage and terminal current is studied, and the R_{Load} is varied. First, an active load of 1.5MW, corresponding to a resistance of $R_{load} = 0.707\Omega$ is introduced 3 seconds into the generator start-up simulation.

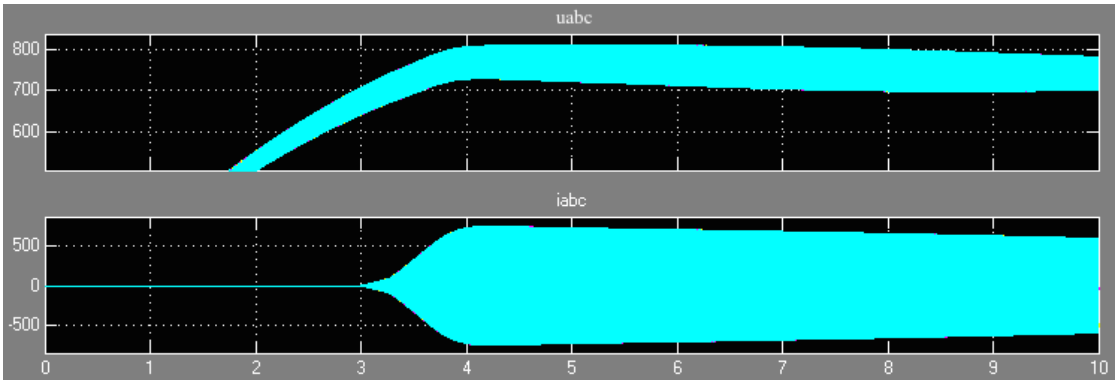

Figure 8.14: 3333 kVA generator system output value during the generator start-up, where u_{abc} is the rms terminal voltage and i_{abc} is the terminal current. The voltage regulator is not included, and a load $R_{load} = 0.707\Omega$ which corresponds to an active load of 1.5MW is introduced 3s into the generator start-up.

After 4 seconds, the voltage value is 740V, but it decreases to a lower voltage value as the time passes. The current also decreases. The reason can be that the battery is fully charged and partly supplies the load in addition to the generator.

The load is increased to 3MW, corresponding to $R_{load} = 0.354\Omega$, and is introduced 3 seconds into the generator start-up simulation.

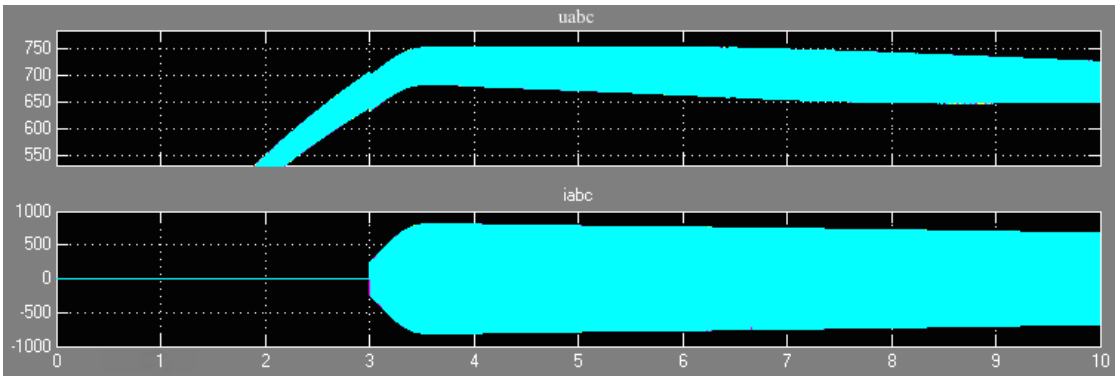

Figure 8.15: 3333 kVA generator system output value during the generator start-up, where u_{abc} is the rms terminal voltage and i_{abc} is the terminal current. The voltage regulator is not included, and a load $R_{load} = 0.354\Omega$ which corresponds to an active load of 3MW is introduced 3s into the generator start-up.

When the load is increased to 3MW, the voltage decreases faster than when the load was 1.5MW, and the battery partly supplies the load. No instability is detected when the AVR is not attached, implying that the 3333kVA generator is not regulated to a stable operation by the AVR, but is stable on its own as well.

8.4 Parameter Analysis; Generator Reactances

It is already mentioned that the ratio between the transient reactances is $\frac{X`_q}{X`_d} = \frac{X_q}{X`_d} = 3.51$. To assume $\frac{X`_q}{X`_d} = \frac{X_q}{X`_d}$ is a normal assumption for generators designed with salient pole. According to the stability criterion presented in [1] this generator should be unstable, because the value of the ratio is larger than 2.0.

8.4.1 Study of Subtransient Reactances on Generator Stability

The ratio between the subtransient reactances is $\frac{X``_q}{X``_d} = 1.216$. This should be an unstable generator according to classical theory, due to the 20% deviation from the ideal value 1.0, but the 3333kVA generator is in fact stable, as shown both in the simulations in Chapter 8.1 and the observations obtained on the ship using these type of generators.

However, the 3333 generator are poorly damped, and uses undesirably long time to stabilize after a load step. For these reasons, the reactances is to be studied. The stability criterion proposed by [2] only take the transient reactances into account. The subtransient reactances is varied and the impact of the stability will be analyzed.

First, the subtransient reactance in the q-axis is varied, while the other reactances is held constant. No load is attached on the dc-side of the rectifier except from the battery-arrangement. The result is shown in Table 8.1 below.

Table 8.1: Parameter analysis, impact of subtransient reactance in the q-axis, $X``_q$, on the stability of the generator G1. The rest of the generator reactances is held constant. Voltage regulator and governor is included. No load is included except from the battery-arrangement.

Parameter	Value [pu]	Operation	Frequency	Comment
$X``_q$	0.1	Stable	-	-
$X``_q$	0.3	Stable	-	-
$X``_q$	0.5	Stable	-	-
$X``_q$	0.6	Stable	-	-
$X``_q$	0.7	Stable	-	-
$X``_q$	0.8	Stable	-	-
$X``_q$	1.0	Stable	-	-
$X``_q$	1.5	Stable	-	-
$X``_q$	3.0	Stable	-	-
$X``_q$	4.0	Stable	-	-
$X``_q$	6.0	Stable	-	-

The 3333kVA generator is stable for all values of $X“_q$.

Now, the subtransient reactance in the d-axis is varied, while the other reactances is held constant. The value of the subtransient reactance in the q-axis is at its initial value. The result is shown in Table 8.2 below.

Table 8.2: Parameter analysis, impact of subtransient reactance in the d-axis, $X“_d$, on the stability of the generator G1. The rest of the generator reactances is held constant. Voltage regulator and governor included. No load is included except from the battery-arrangement.

Parameter	Value [pu]	Operation	Comment	Frequency
$X“_d$	0.1	Unstable	Decreasing amplitude	1.64Hz
$X“_d$	0.2	Stable	-	-
$X“_d$	0.05	Unstable	Standing	0.75Hz
$X“_d$	0.3	Stable	-	-
$X“_d$	0.4	Stable	-	-
$X“_d$	0.6	Stable	-	-
$X“_d$	0.8	Stable	-	-
$X“_d$	1.5	Stable	High initial currents	-
$X“_d$	2.0	Stable	-	-
$X“_d$	3.0	Stable	-	-
$X“_d$	4.0	Stable	High initial currents	-
$X“_d$	6.0	Stable	High initial currents	-

The 3333kVA generator is stable for all values of $X“_d > 0.1pu$. This implies a stability criterion given as:

$$\frac{X“_q}{X“_d} \leq 5.91 \tag{8.1}$$

The ratio with the reactances used in the 3333kVA generators is $\frac{X“_q}{X“_d} = 1.216$, meaning that the generator has a relatively large stability margin. Typical ratios between $X“_q$ and $X“_d$ in synchronous generators with salient pole is 1.3 pu [13].

Now, the ratio between $X“_q$ and $X“_d$ is studied. The ratio is held constant $\frac{X“_q}{X“_d} = 1.216$, but the values of $X“_q$ and $X“_d$ is changed with the same factor. The result is shown in Table 8.3 below.

Table 8.3: Parameter analysis, impact of the ratio $\frac{X“_q}{X“_d}$, on the stability of the generator G1, where the ratio is held constant. but the value of $X“_q$ and $X“_d$ is varied by a factor f. The voltage regulator and governor is included. No load is connected except from battery-arrangement.

ratio	Factor f	Operation	Comment	Frequency
$\frac{X“_q}{X“_d}$	1	Stable	-	-
$\frac{X“_q}{X“_d}$	1.25	Stable	-	-
$\frac{X“_q}{X“_d}$	1.5	Stable	-	-
$\frac{X“_q}{X“_d}$	1.75	Stable	-	-
$\frac{X“_q}{X“_d}$	2.0	Stable	-	-
$\frac{X“_q}{X“_d}$	0.75	Stable	-	-
$\frac{X“_q}{X“_d}$	0.5	Stable	-	-
$\frac{X“_q}{X“_d}$	0.25	Stable	-	-

The generator is stable for all factors of $X“_q$ and $X“_d$ when the ratio between them is kept constant $\frac{X“_q}{X“_d} = 1.216$.

8.4.2 Study of Synchronous and Transient Reactances on Generator Stability

The stability criterion presented in [1] and the transient reactances is to be further examined. According to this criterion, the ratio $\frac{X‘_q}{X‘_d} = \frac{X_q}{X‘_d}$ should be less than 2.0. This is not the case; $\frac{X‘_q}{X‘_d} = \frac{X_q}{X‘_d} = 3.51$. Despite this, the 3333kVA generator is stable. If the stability criterion is to be met anyway, either X_q must be decreased, or $X‘_d$ must be increased. Both cases is tried, and the result is shown in Table 8.4 below.

Table 8.4: Parameter analysis, impact of fulfilling the stability criterion presented by [1] by varying X_q or $X‘_d$, on the stability of the generator G1. Voltage regulator and governor included. No load is connected except from battery-arrangement.

ratio	Parameter	Operation	Comment	Frequency
$\frac{X_q}{X‘_d} = 2$	X_q constant, $X‘_d$ increased	Stable	-	-
$\frac{X_q}{X‘_d} = 2$	$X‘_d$ constant, X_q decreased	Stable	-	-

The generator is stable also when the stability criterion is fulfilled. The ratio $\frac{X_q}{X‘_d}$ is now increased to a value higher than 3.51, to intentionally not fulfill the criterion, and to see if there is a stability limit when X_q is increased or $X‘_d$ is decreased. The ratio between $\frac{X_q}{X‘_d}$ for the 3333kVA generator is first set to be 6.0, and then 8.0. This is three and four times as large as the ideal value should be according to [1], and larger than the real value 3.51. The result is shown in Table 8.5 below.

Table 8.5: Parameter analysis, impact of increasing the ratio $\frac{X_q}{X`_d}$ which is the stability criterion presented by [1] by varying $X_q$ or $X`_d$, on the stability of the generator G1. Voltage regulator and governor included. No load is connected except from battery-arrangement.

ratio	Value	Operation	Comment	Frequency
$\frac{X_q}{X`_d} = 6.0$	X_q constant, $X`_d$ decreased	Stable	-	-
$\frac{X_q}{X`_d} = 6.0$	$X`_d$ constant, X_q increased	Unstable after 10s	-	1.2Hz
$\frac{X_q}{X`_d} = 8.0$	X_q constant, $X`_d$ decreased	Stable	-	-
$\frac{X_q}{X`_d} = 8.0$	$X`_d$ constant, X_q increased	Unstable after 5s	-	0.94Hz

By varying the transient reactance in the d-axis, the generator is still stable even though the ratio $\frac{X_q}{X`_d}$ is increased dramatically from 3.51 to 6.0 and 8.0. However, when X_q is increased, the generator becomes unstable with standing oscillations of frequency 0.94-1.2Hz. This can indicate that the q-axis synchronous reactance is more influential on the G1 stability than the d-axis transient reactance.

This is further examined by increasing the synchronous reactance in the q-axis while the other constants is held constant. The result is found in Table 8.7 below.

Table 8.6: Parameter analysis, impact of synchronous reactance in the q-axis, X_q, on the stability of the generator G1. Voltage regulator and governor included. No load is included except from the battery-arrangement.

Parameter	Value [pu]	Operation	Comment	Frequency
X_q	3.0	Stable	-	-
X_q	5.0	Unstable	After 10s	1.2Hz
X_q	7.0	Unstable	After 5s	0.94Hz
X_q	3.5	Stable	-	-
X_q	4.0	Stable	-	-
X_q	4.5	Stable	-	-
X_q	4.75	Stable	Small oscillations	-
X_q	5.0	Unstable	After 11s	1.2Hz
X_q	4.85	Unstable	After 12s	1.23Hz

The 3333kVA generator is stable when $X_q < 4.85pu$. Two stability criteria can be expressed for the 3333kVA generator with salient pole by looking at the parameters found in Table 8.7:

$$\frac{X_q}{X`_d} < 5.7 \qquad \frac{X_d}{X_q} > 0.94 \tag{8.2}$$

Typical values for these ratios is [13]: $\frac{X_q}{X`_d} = 2$ and $\frac{X_d}{X_q} = 1.5$. The actual values for these ratios using the actual generator parameters obtained from [17] is $\frac{X_q}{X`_d} = 3.51$ and $\frac{X_d}{X_q} = 1.52$. The ratio $\frac{X_d}{X_q}$ is the same as for typical SG with salient poles.

The synchronous reactance in the q-axis impacts the stability of G1 with salient pole more than the transient and subtransient reactances in both q- and d-axis.

The synchronous reactance in the d-axis is now studied.

Table 8.7: Parameter analysis, impact of synchronous reactance in the d-axis, X_d, on the stability of the generator G1. Voltage regulator and governor included. No load is included except from the battery-arrangement.

Parameter	Value [pu]	Operation	Comment	Frequency
X_d	6.0	Stable	-	-
X_d	7.0	Stable	-	-
X_d	8.0	Stable	-	-
X_d	9.0	Stable	-	-
X_d	4.0	Stabil	-	-
X_d	4.5	Stable	-	-
X_d	3.0	Stabil	-	-
X_d	2.0	Stabil	-	-
X_d	1.0	Stabil	-	-

The generator has a stable start-up for any value of X_d. The operation of the G1 generator does rely greatly on the synchronous q-axis reactance, but not on the synchronous d-axis reactance.

Chapter 9

Investigation of 1940 kVA Generator With Salient Pole

According to [2] the 1940kVA generator type is unstable. It has round rotor, and a large ratio $\frac{X`_q}{X`_d} = \frac{X_q}{X`_d} = 9.78$, which should have been less than 2.0 if it was to be stable according to the stability criterion presented in [1]. It should be considered critical. The ratio between the synchronous reactances is $\frac{X_d}{X_q} = 1.12$ for the 1940kVA generator. Machines with salient pole design is in the range $\frac{X_d}{X_q} 1.5 - 2$ and round rotor machines is in the range $\frac{X_d}{X_q} = 1 - 1.2$. In this chapter, the generator is modeled as salient pole, and in that case the ratio $\frac{X_d}{X_q}$ is below the typical ratio value for salient pole machines [2].

The generator start-up of the system with the generator G2, modeled as a salient pole synchronous generator, is shown in Fig 9.1 below. G2 is in reality a round-rotor machine, but is modeled as salient pole in this chapter, to later compare the results found from this salient pole design, to the round rotor design, and to discuss any differences. This is because the stability criterions presented by [2] differ on whether the generators are designed with salient-pole or round-rotor.

The voltage regulator and governor is included in the model, and no load is present at the DC-side of the rectifier except from the battery-arrangement. The reference value of the AVR is set to 1.2.

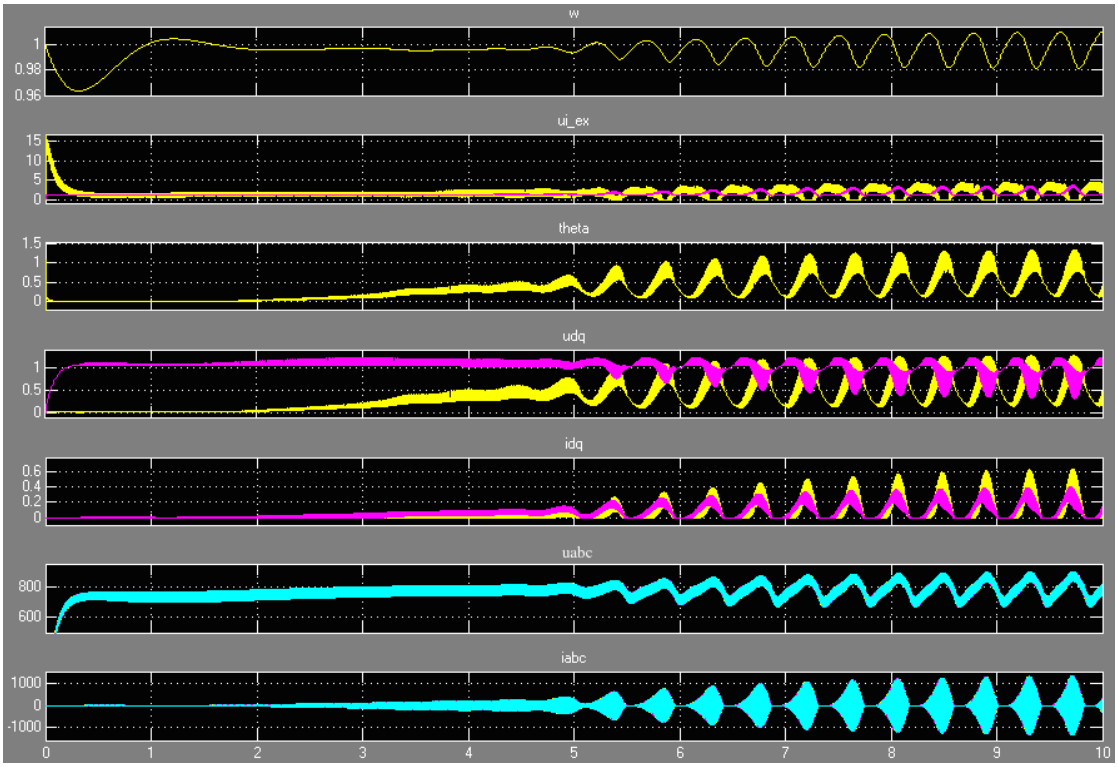

Figure 9.1: 1940 kVA generator system output values, where: w is the rotor velocity, u_i is the field voltage, $theta$ is the rotor angle, u_{dq} is the stator voltage in the d- and q-axis, i_{dq} is the stator current in the d- and q-axis, u_{abc} and i_{abc} is the terminal voltage and current, respectively. No load is attached to the dc-side of the rectifier except from the battery-arrangement.

From the top, Fig 9.1 shows the rotor velocity w, the field voltage u_i, the rotor angle $theta$, the stator voltage in the d- and q-axis u_{dq}, the stator current in the d- and q-axis i_{dq}, the rms terminal voltage u_{abc} and the terminal current i_{abc} of the 1940 kVA generator, respectively. The graph showing the field voltage u_i contains of a pink and a yellow curve, where the pink curve displays the field current and the yellow curve displays the field voltage. The graphs showing u_{dq} and i_{dq} contains of two curves, one yellow and one pink. The yellow curve is the d-axis for both voltage and current, and the pink is the q-axis for both voltage and current.

The rotor velocity w drops from 1 by 4% during the generator start-up, but quickly restores its value back to 1 per unit, before the rotor velocity begins to oscillate when the generator gets unstable, around 5 seconds after start-up. The drop in rotor velocity in the first half second can be caused by the sudden increase in field voltage, and the increase in rotor velocity is due to the governor, that tries to regulate the velocity back to 1 pu. The rotor velocity continues to increase, reaching for a value of 1 pu. The field voltage u_i, the rotor angle $theta$, and the stator voltage and current in the d- and q-axis also starts to oscillate around the same time.

The generator output parameters shown in Fig 9.1 oscillates with the same frequency of 2.3Hz.

The rms terminal voltage in the three phases a, b and c is measured from the plot to be around 740V rms. It oscillates with a frequency of 66.67Hz, which is the rated frequency of the generator.

The current in the three phases a, b and c starts to oscillate in increasing "pulses". This oscillation is in direct ratio to the oscillation seen in the voltage in the three phases.

The supplier of the voltage regulator only measured the current of phase B and the voltage between phases C-B in the measurements done by the onboard the ship where instability is observed. The reason for this, is given by [21] to be that this measurements are representative for all three phases because all the phases is oscillating simultaneously, with 120 degrees phase shift. To take a closer look at the current and voltage, and the ratio between the oscillations in voltage and current, all the three phases of both the voltage and current is simulated and is shown in Fig 9.2 below.

Figure 9.2: 1940 kVA generator system voltage and current in all three phases a, b and c.

Where the top three graphs shows the voltage in phase a, b and c respectively, and the bottom three graphs shows the system current in there three phases a, b and c. The pulsation of the current starts at around 5 seconds after the start-up of the generator. This is, as mentioned above, in direct ratio to what happens in the voltage in the three phases. The voltage in the

three phases starts to oscillate after about 5 seconds into the simulation, which could be a result of the battery on the other side of the rectifier starting to act as a voltage source and delivers power back to the generator, resulting in oscillations in the voltage. The pulsed nature of the current can also be caused by the diode-bridge rectifier.

The fact that the current falls down to zero between each pulse can be that the rectifier in the system can only lead current in one direction, due to the characteristics of the rectifier, which is of the diode bridge type. This behavior of the battery repeats it self, creating oscillations in the voltage resulting in "pulses" seen in the current in phase a, b and c, that increases during the simulation of the unstable start-up characteristics of the 1940 kVA generator. This simulation reflects the observations done on the ship with the 1940 kVA generators.

Each "pulse" in the current oscillates with a frequency of 2.3Hz. Inside each pulse, the current oscillates with a frequency of 66.67 Hz, which is the rated generator frequency.

There is no difference detected in the current or voltage in the three phases, which could be an confirmation of the assumption made by [21], that the measurements taken onboard the ship experiencing instability, where the current is taken in phase B and the voltage between phase C-B, are representative for all three phases because all the phases is oscillating simultaneously, with 120 degrees phase shift. This seems to be true, judging by the results of the simulations.

When the current is zoomed in, the harmonic content of the current can be shown, as explained in Chapter 4.1. Only one phase is shown, due to the similarity of the three phases.

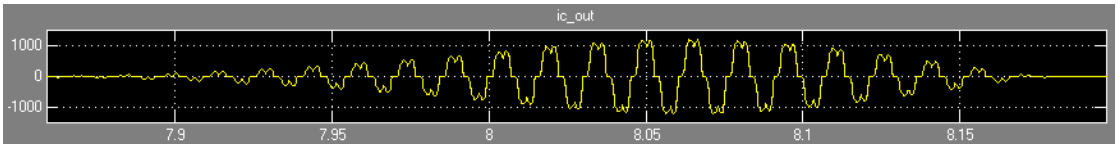

Figure 9.3: 1940 kVA generator system current pulse in phase c

The pulsed nature of the current is distinct, and looks very much alike the input current in Fig 4.3a from a three-phase diode rectifier in Fig 4.3b. The THD of the current can be calculated in Simulink in MatLab, and is 7% at the most, when the pulses occur. Commutation intervals between each wave can be observed in the current characteristic, and will be further investigated later in this chapter.

When the voltage is zoomed for the same period, we see that there is a swell in the voltage and that the top of the waveforms is "clipped" at the same time as the current pulse. Only one phase is shown, due to the similarity of the three phases, as seen from Fig 9.2.

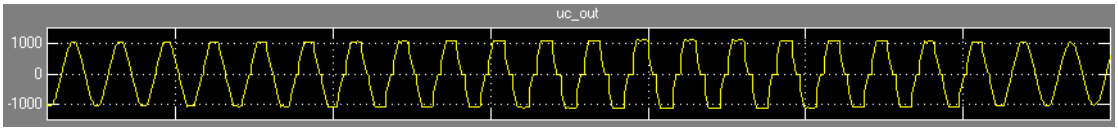

Figure 9.4: 1940 kVA generator system voltage in phase c.

9.1 Parameter Study: Generator Reactances

The ratio between the subtransient reactances in q- and d-axis is: $\frac{X“_q}{X“_d} = 1.048$. From classical theory, the ratio between $X“_q$ and $X“_d$ should ideally be as close to 1 as possible, to achieve stable operation of the generator. The ratio between these two parameters is close to 1 in G2, and fulfills this criterion. If this ratio is increased, the generator should continue to be unstable.

During these tests both governor and AVR is connected to the 1940kVA generator with salient pole. The voltage regulator adjusts the voltage up to 20% of the nominal voltage; 1.2*690V=828V. No load is attached to the dc-side of the rectifier except from the battery arrangement consisting of a series resistance and a large capacitance.

9.1.1 Impact of Subtransient Reactances on Commutation Interval and Stability

Table 9.1 under shows the impact of the subtransient reactance on the commutation intervals observed in the waveforms of current characteristics out from the generator shown in Fig 9.3. The intervals is measured in milliseconds, and is taken in the middle of a current pulse. The table below shows the varying of the parameter $X“_q$, while keeping the value of $X“_d$ constant throughout this experiment. A graphic solution of the numbers in Table 9.1 is shown in Fig 9.5:

Table 9.1: Impact of $X"_q$ on the length of the commutation intervals observed in the current waveform. The length of the commutation intervals is measured in ms.

Parameter	Value [pu]	Length of interval
$X"_q$	0.05	2.3 ms
$X"_q$	0.1	2.19 ms
$X"_q$	0.2	2.0 ms
$X"_q$	0.3	1.58 ms
$X"_q$	0.4	1.57 ms
$X"_q$	0.5	1.49 ms
$X"_q$	0.6	1.29 ms
$X"_q$	0.7	1.21 ms
$X"_q$	0.8	0.81 ms
$X"_q$	0.9	0.6 ms

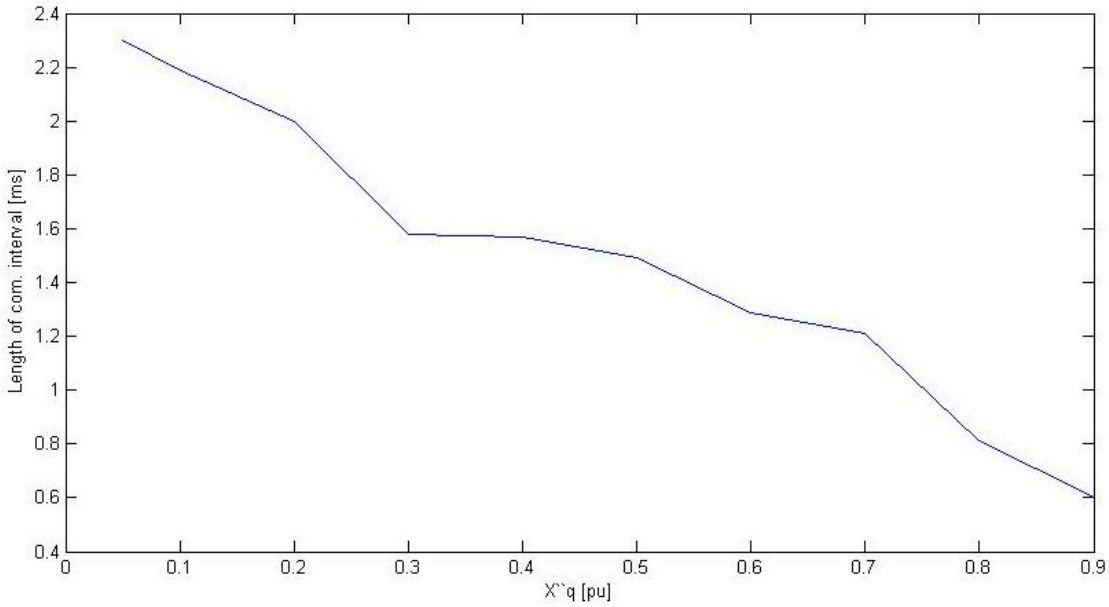

Figure 9.5: The graphic solution of the Table 9.1 shows the impact of $X"_q$ on the length of the commutation intervals observed in the current-curve out from the generator G2.

The current-curve moves towards being more sinusoidal when the subtransient reactances increases, and the commutation intervals decreases in length. The voltage on the other hand, has a more square-formed shape. The pulses in current out from the generator finds place later when the subtransient reactance is small, than when its value is increased.

When a SM is designed and build, there is usually several degrees of freedom when deciding the parameter value of $X"_q$, but none when deciding $X"_d$. This makes the subtransient reactance in the q-axis possible to adjust. The ratio between the subtransient reactances in the q- and d-axis

should as mentioned earlier, ideally be as close to 1 as possible. When $X“_q$ is increased, but $X“_d$ remains it value, the ratio will exceed this criterion, and the generator can become unstable.

This stability limit is examined by the use of iteration, and Table 9.2 below shows how the system responds in terms of unstable/stable, as a consequence to the varying of $X“_q$. When instability is reached, the frequency of the oscillations is calculated and shown in the table. Because all the parameters oscillate with the same frequency, it doesn't matter what parameter is used when finding the frequency, and the rotor angle *theta* is chosen. Only the first 20 seconds is considered in this simulation, if standing or increasing oscillations in speed, rotor angle, voltage and current is detected, it is considered unstable.

On the other hand, if small oscillations occur, but the generator stabilizes during the first 20 seconds, the generator is considered stable. A comment to the operation of the generator is found in the table. The curves in the graphs extracted from the simulations must be used as a basis for stability, and stability is decided by using the graphs.

Table 9.2: Parameter analysis, impact of subtransient reactance in the q-axis, $X“_q$, on the stability of the generator G2. Voltage regulator and governor included. No load is included except from the battery-arrangement.

Parameter	Value [pu]	Operation	Comment	Frequency
$X“_q$	0.1	Stable	-	-
$X“_q$	0.4	Unstable	Standing oscillations after 5s	2.6 Hz
$X“_q$	0.2	Unstable	Standing oscillations after 10s	2 Hz
$X“_q$	0.15	Stable	-	-
$X“_q$	0.175	Unstable	Oscillations after 5s, poorly damped	1.8 Hz
$X“_q$	0.16	Stable	-	-
$X“_q$	0.165	Stable	Poorly damped	-
$X“_q$	0.17	Stable	Very poorly damped	-

From the table above, the value of the subtransient reactance in the q-axis must be $X“_q < 0.175pu$ to achieve generator stability. From tho, a stability-criterion that must be fulfilled to achieve stable operation of G2 with salient pole can be developed;

$$\frac{X“_q}{X“_d} < 0.48 \tag{9.1}$$

From classical theory, this generator should now be unstable because $\frac{X“_q}{X“_d} << 1.0$, but the generator is stable under these conditions. This ratio is typically 1.3 for most synchronous generators with salient poles according to [13], and the stability criterion in Eq. 9.1 is very strict and maybe not realistic. In the 1940kVA generator, this ratio is 1.048 at this time.

The ratio $\frac{X“_q}{X“_d}$ is now studied once more, but this time both reactances is varied by the same factor

f, such that we can study the impact of varying both subtransient reactances while keeping the ratio between them constant. To keep the ratio between the reactances constant, the reactances is varied by the same factor. The governor and AVR is still attached, and no load is connected except from the battery-arrangement on the dc-bus. The result is shown in Table 9.3 below.

Table 9.3: Parameter analysis, impact of the ratio $\frac{X\text{“}_q}{X\text{“}_d}$, on the stability of the generator G2, where the ratio is kept constant but both reactances is varied with the same factor. Voltage regulator and governor included. No load is connected except from battery-arrangement.

ratio	Factor	Operation	Comment	Frequency
$\frac{X\text{“}_q}{X\text{“}_d}$	1	Unstable	-	2.6 Hz
$\frac{X\text{“}_q}{X\text{“}_d}$	0.75	Unstable	-	2.33 Hz
$\frac{X\text{“}_q}{X\text{“}_d}$	0.5	Unstable	-	1.86 Hz
$\frac{X\text{“}_q}{X\text{“}_d}$	0.25	Unstable	-	1.17 Hz
$\frac{X\text{“}_q}{X\text{“}_d}$	0.1	Unstable	-	0.424 Hz
$\frac{X\text{“}_q}{X\text{“}_d}$	1.25	Unstable	-	2.9Hz
$\frac{X\text{“}_q}{X\text{“}_d}$	1.5	Unstable	-	3.17Hz
$\frac{X\text{“}_q}{X\text{“}_d}$	1.75	Unstable	-	3.3Hz
$\frac{X\text{“}_q}{X\text{“}_d}$	2	Unstable	-	3.43

When the ratio $\frac{X\text{“}_q}{X\text{“}_d}$ is kept constant, but $X\text{“}_q$ and $X\text{“}_d$ is varied by the same factor, the generator is still unstable. The frequency decreases as the parameters decrease in value, and increases as the parameters increase in value. The oscillations also increases in amplitude as the parameter values decreases or increases.

It is not accomplished to get a stable operation go G2 when the ratio is held constant and the subtransient reactances is varied by the same factor.

9.2 RMS Values of Voltage and Current

The RMS values of the voltage and current in the three phases a, b and c is similar, and the voltage for phase a and current for phase a is shown in Fig 9.6.

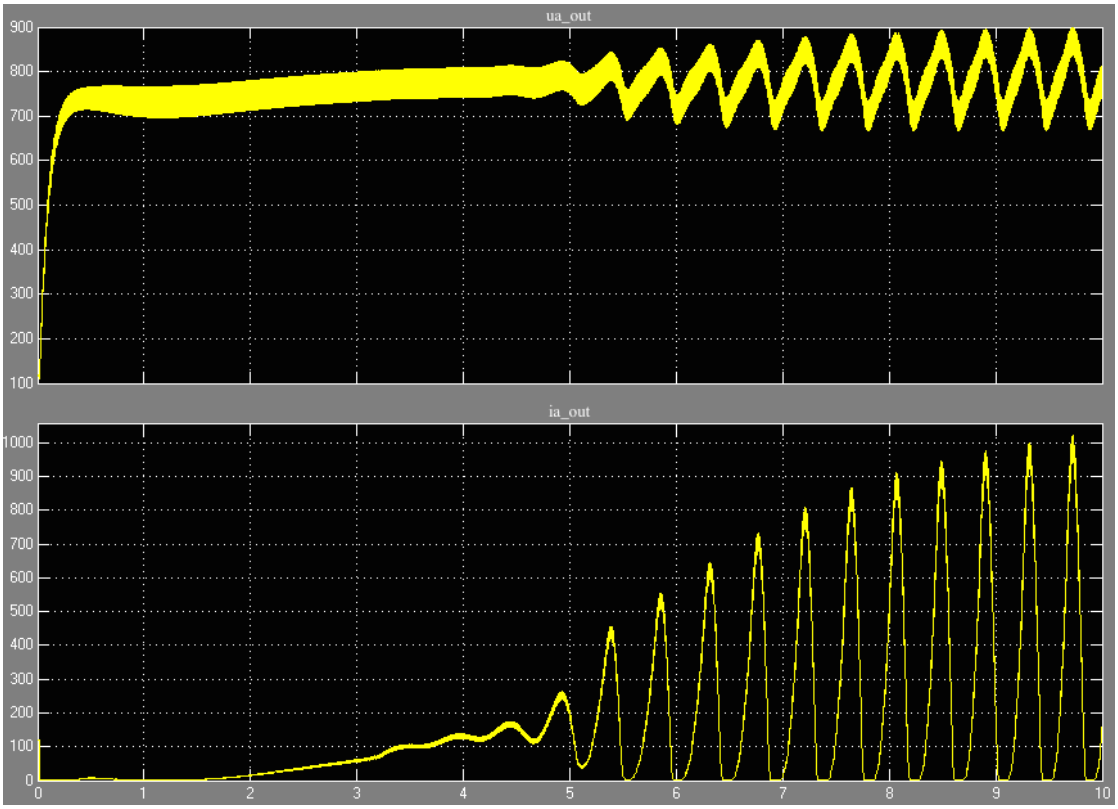

Figure 9.6: 1940 kVA generator system RMS values of the voltage and current in phase a.

The RMS value of the voltage is read to be approximately 740V. There is no distinct difference in either voltage or current in the three phases.

The simulation results from the governor, voltage regulator and the exciter is shown in Appendix D.2.

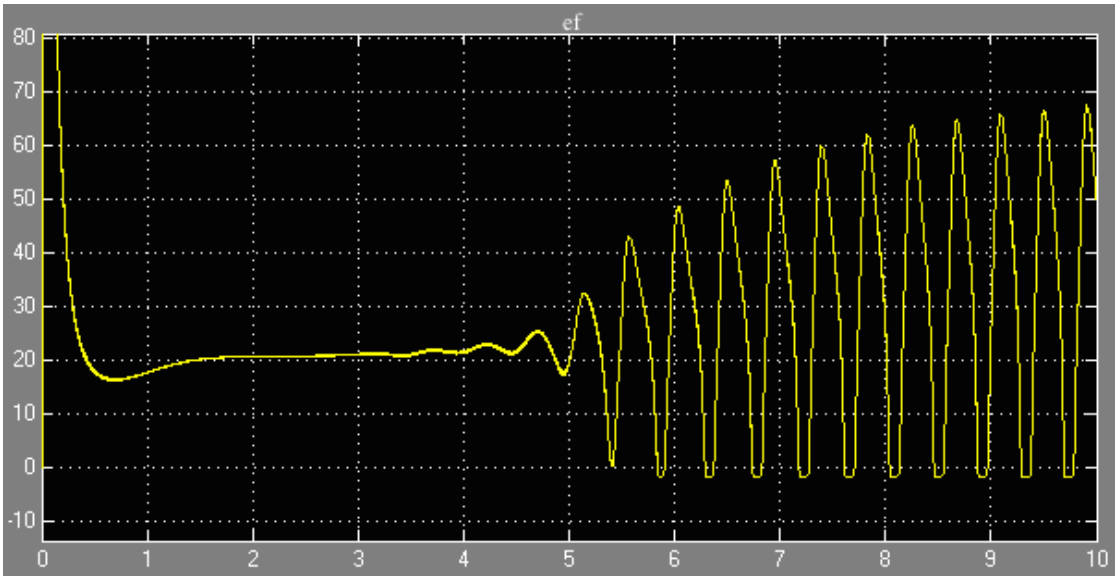

Figure 9.7: 1940 kVA generator system output values from the AVR, where e_f is the mean field voltage.

The mean value of the field voltage supplying the generator field is 21V, before it starts to oscillate with approximately 2.5Hz. It is observed that the generator outputs and the DC voltage from the exciter starts to oscillate at the same time, and with the same frequency. Whether the generator or the voltage regulator starts the instability is not known.

The dc-bus voltage on the dc side of the rectifier is shown in Fig 9.8 below.

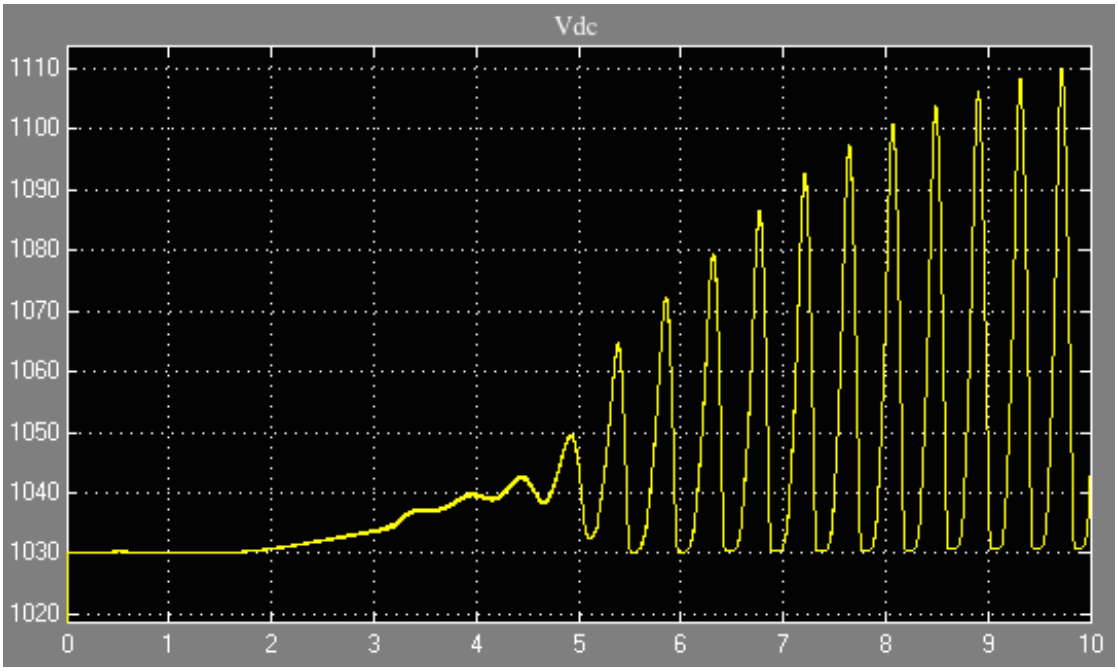

Figure 9.8: The 1940kVA generator feeds the battery through a rectifier, where V_{dc} is the dc-bus voltage.

The dc-bus voltage is 1030V before the instabilities starts.

9.3 Battery Internal Resistance

The d-axis voltage u_d increases significantly in the 1940 kVA generator when the stator current increases. This results in an increased terminal voltage of the generator and the system becomes unstable. This can be prevented by increasing the internal resistance in the battery [17]. This is shown in Table 9.4 below, where the resistance of the battery, modeled by a large capacitor, is increased. The value of the series reactance in the capacitor is initially $1e-9\Omega$. The synchronous generator G2 has the governor and voltage regulator connected during the simulations.

Table 9.4: Parameter analysis; internal resistance of the battery, modeled by a large capacitor.

Parameter value [Ω]	Operation	Frequency DC-side	Frequency AC-side	Comment
$r = 1 * 10^{-9}$	Unstable	2.6Hz	2.6Hz	Standing oscillations after 4.5s
$r = 1 * 10^{-3}$	Unstable	2.5 Hz	2.5Hz	Standing oscillations after 4.5s
$r = 1.0$	Stable	-	-	-
$r = 0.1$	Unstable	2.3Hz	2.3Hz	Standing oscillations after 14s
$r = 0.25$	Stable	-	-	-
$r = 0.15$	Stable	-	-	-
$r = 0.12$	Stable	-	-	-
$r = 0.11$	Stable	-	-	Small oscillations after 16s

It is observed that the generator stabilizes when the internal resistance in the battery of the system is increased. The frequency of the output on the DC-side of the diode-rectifier is 2.3-2.6 Hz when the system becomes unstable. The generator is stable if the internal resistance of the battery is $r > 0.1\Omega$.

The litium-ion battery is infinitely large and acts like a constant voltage source where the voltage drop across is is considered very low. When the internal resistance in the battery is increased as is done above, the voltage drop across the battery increased, and the losses thus increases. If the internal resistance is increased, this must be seen in a direct proportion to the increased losses over the battery. Such an increase as is done in this simulation may be unrealistic and unpractical in praxis.

9.4 Influence of Terminal Voltage Value

When the reference value of the regulator is changed, the voltage in the d- and q-axis of the generator changes characteristics. The initial reference value is 1.2, and the output from the generator G2 salient pole with AVR and governor attached is shown in Fig 9.9 below. No load is attached to the dc-side of the rectifier, except from the battery-arrangement, where both the series resistance and capacitance is at its initial value, $1e - 9\Omega$ and $2100F$.

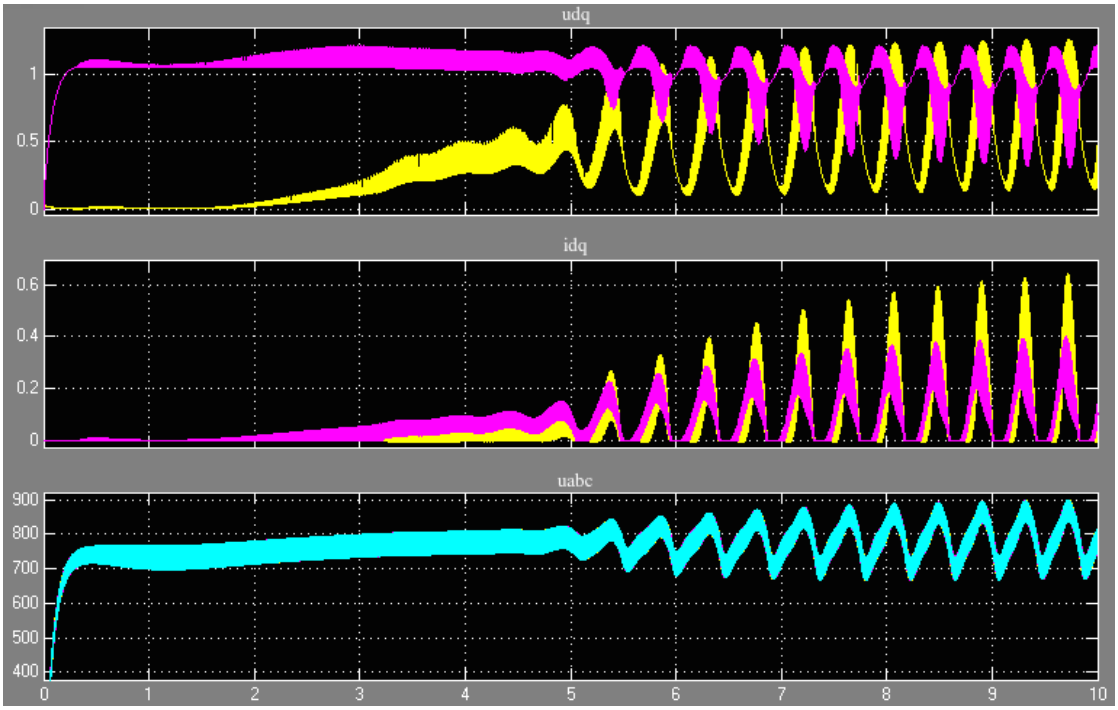

Figure 9.9: 1940 kVA generator system voltage and current in d- and q-axis and the rms terminal voltage in phase a,b and c when the reference value of the regulator is 1.2. The simulation time is 10 seconds and the gain of the avr is 39. Ud and Id is shown in the pink curves, and Uq and Iq is shown in the yellow curves.

The upper graph shows the voltage in the d- and q- axis, the graph in the middle shows the current in the d- and q-axis, and the bottom graph shows the rms terminal voltage in phase a, b and c. The yellow curve is the d-axis for both voltage and current, and the pink is the q-axis for both voltage and current. From the graph, the rms voltage in the three phases is approximately 740V before the generator goes unstable after about 5-6 seconds, when the reference value of the regulator is set to 1.2. The generator output value oscillates with a frequency of 2.6Hz.

When the reference value is set to 1.2, the voltage regulator should adjust the voltage out from the generator up 20% from the nominal rated voltage 690V. Then the line voltage should be $\frac{740V}{1.2} = 617V$. This should ideally be 690V, but it seems as though the generator needs more time to regulate the voltage up the the desired value.

Now, the reference value of the voltage regulator is increased from 1.2 to 1.4, and the output from the generator G2 salient pole with AVR and governor attached is shown in Fig 9.10 below.

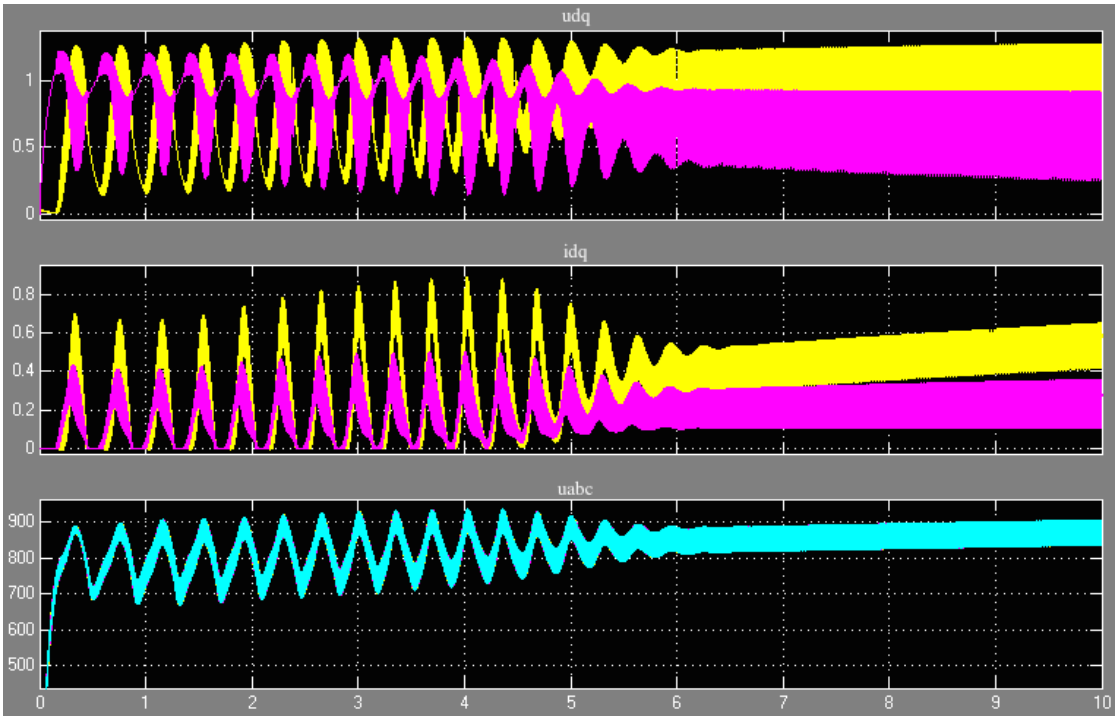

Figure 9.10: 1940 kVA generator system voltage and current in d- and q-axis and the rms line voltage in phase a,b and c when the reference value of the regulator is 1.4. The simulation time is 8 seconds, and the gain of the avr is 39. Ud and Id is shown in the pink curves, and Uq and Iq is shown in the yellow curves.

The upper graph shows the voltage in the d- and q- axis, the graph in the middle shows the current in the d- and q-axis, and the bottom graph shows the rms terminal voltage in phase a.b and c. The yellow curve is the d-axis for both voltage and current, and the pink is the q-axis for both voltage and current. From the graph, the rms voltage in the three phases is approximately 900V when the reference value of the regulator is set to 1.4. The voltage regulator should in reality have increased the voltage to 40% above the terminal voltage, $1.4 * 690V = 966V$.

The voltage changes character when this reference parameter is increased from 1.2 to 1.4. The characteristics of the start-up of the generator is unstable, but changes to stable operation after about 5-6 seconds. The system oscillates with a frequency of approximately 2.6Hz in these first 5-6 seconds. When the system goes stable, the voltage increases, and it might increase up to the theoretical value 966V, but it has only reached 900V when the start up is simulated for 10 seconds.

When the reference value is increased to 1.4, the peak voltage should be $1.4 * 690V = 966V$. This seems to be not the case out from the simulation in Fig 9.10, because the peak voltage is found in this 10s-long simulation to be 900V. But if the simulation is extended, it is shown that the voltage increases slowly, and stabilizes to a value closer to the theoretical value (966V). This

is shown in Fig 9.11 below, where the simulation is run for 50s.

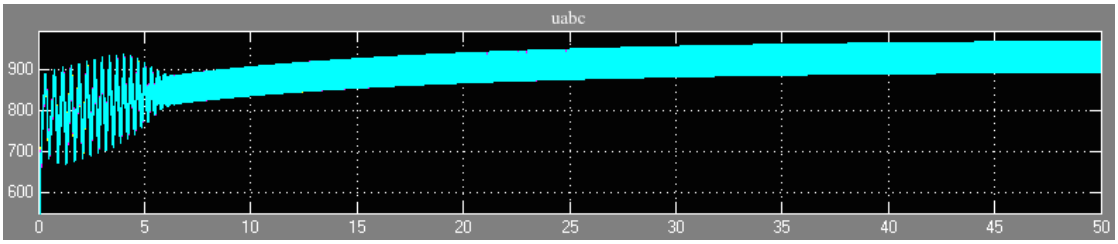

Figure 9.11: 1940 kVA generator rms terminal voltage in phase a, b and c when the reference value of the regulator is 1.4, the gain is 39 and the simulation is run for 50s.

Even though the voltage uses a really long time to stabilize on a definite value, it almost reaches the theoretical value of a rms terminal voltage value of 966V. At 50s, the rms line voltage is red from the graph to be approximately 950V.

The gain in the voltage regulator is increased to 200 from its initial value 39, to see how long time it takes before the generator line voltage stabilizes to the theoretical value 966V when the reference value is set to 1.4 and the gain is increased. The simulation is run for 50s for comparison, and is shown in Fig 9.12 below.

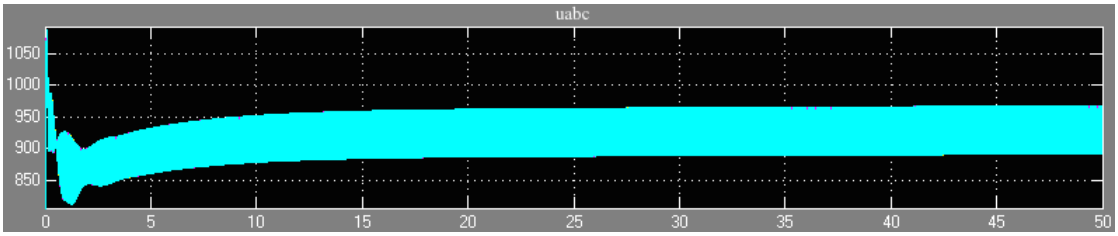

Figure 9.12: 1940 kVA generator rms terminal voltage in phase a, b and c when the reference value of the regulator is 1.4 and the gain is increased from the initial value of 39 to 200. The simulation is run for 50s.

When the gain is increased 200 from 39, the rms terminal voltage still increases at the end of the 50s-simulation, and maybe stabilizes at a value close to the theoretical value 966V, but this still happens slowly. At 50s, the rms line voltage is red from the graph to be approximately 930V. During the first second of the start-up of the generator, a very large voltage spike is observed, with a value of approximately 1240V rms, before if falls down to about 870V rms, and starts to climb slowly towards 966V rms. This spike indicates high start-currents in the generator start-up.

So, by increasing the gain to 200, the voltage does not stabilizes more quickly to a value close to the theoretical value, than when the AVR-gain was at its initial value 39. It is also observed that the output from the generator does not oscillate as before. By increasing the gain, the oscillations in the start-up has vanished.

If the gain of the voltage regulator is is set to the initial value 39 and the reference value of 1.0, the voltage output from the generator should be 690V. The result is shown below.

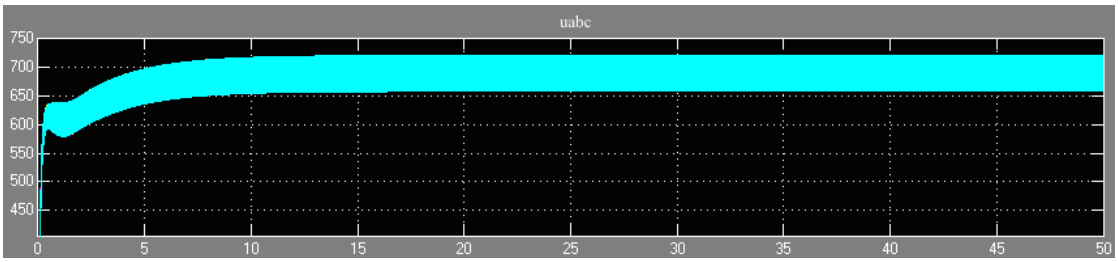

Figure 9.13: 1940 kVA generator rms line voltage in phase a, b and c when the reference value of the regulator is 1.0 and the gain is at its initial value of 39. The simulation is run for 50s.

When the reference value is decreased to 1.0, no oscillations is registered in the generator output, and the generator is stable. The requested value is 690V, and with this demand, the regulator works fairly well, because it regulates the voltage to the requested voltage value. However, this takes 12 seconds, and this should happens much faster. The voltage regulator seems to be working better when the voltage is not to be regulated up to a higher value than the nominal value. Another voltage regulator should be tried out if the voltage is to be regulated up within an acceptable time range.

9.5 Changing the Gain of the Voltage Regulator

The gain in the voltage regulator is initially 39, and the system is unstable, as shown in Fig 9.1. When the gain is increased to 200, the start-up of the generator changes characteristics, as shown in Fig 9.14 below. No load is attached to the dc-side of the rectifier, except from the battery-arrangement. The reference value is set to 1.2.

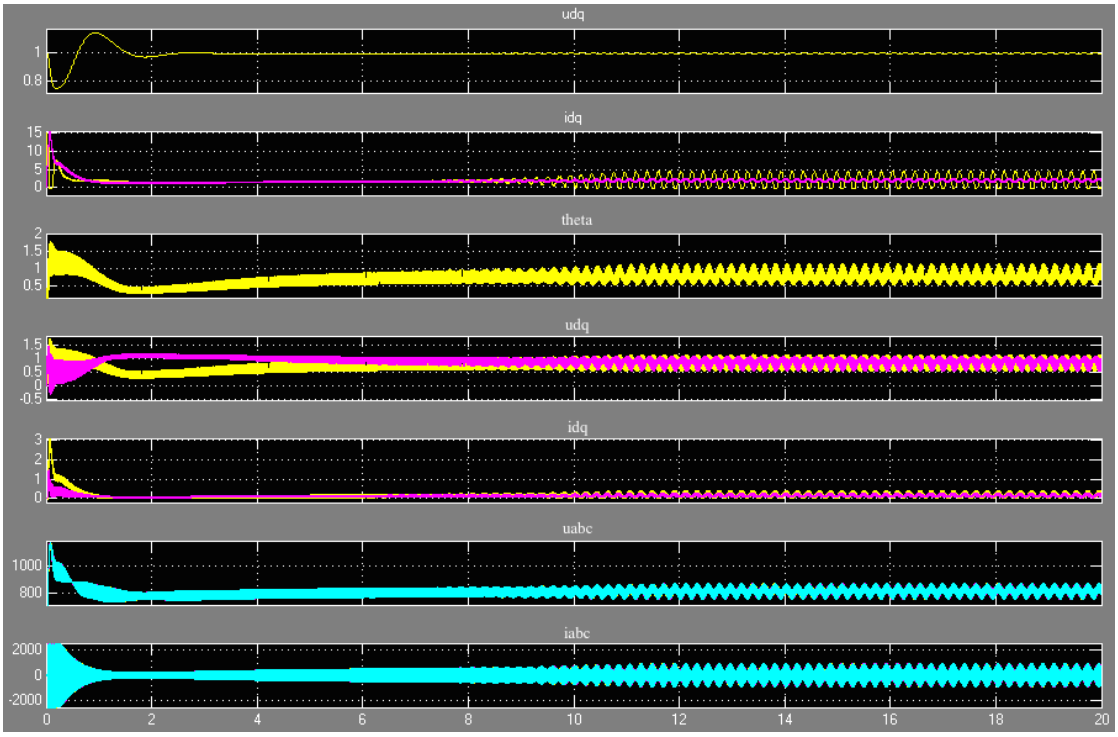

Figure 9.14: 1940 kVA generator output when the gain of the voltage regulator is changed from its initial value 39 to 200, and $V_{ref} = 1.2$. The simulation is run for 20s.

From the top, Fig 9.1 shows the rotor velocity w, the field voltage u_i, the rotor angle *theta*, the stator voltage in the d- and q-axis u_{dq}, the stator current in the d- and q-axis i_{dq}, the terminal voltage u_{abc} in rms and the terminal current i_{abc} of the 1940 kVA generator, respectively. The graph showing the field voltage u_i contains of a pink and a yellow curve, where the pink curve displays the field current and the yellow curve displays the field voltage. The graphs showing u_{dq} and i_{dq} contains of two curves, one yellow and one pink. The yellow curve is the d-axis for both voltage and current, and the pink is the q-axis for both voltage and current.

The generator achieves a stable start-up characteristic for about 8 seconds, when the gain of the AVR is increased to 200. The value of the rms terminal voltage during this stable period, is approximately 800V. The reference value of the AVR is set to 1.2, and the rms voltage should then be $690V * 1.2 = 828V$. The voltage is measured from the plot to be a few voltages below this value.

After 8 seconds into the generator start-up, the generator becomes unstable with standing oscillations. The oscillations of the system has a frequency of 7.25Hz. This frequency of the unstable, oscillating generator frequency differs from the other frequencies registered. Earlier, the generator parameters have a frequency of 2.3-2.6 Hz on the oscillations.

9.6 Load on DC-side of the Rectifier

A load R_{Load} is introduced 3 second into the generator start-up, coupled in parallel with the battery-arrangement. The ability of the voltage regulator to regulate the voltage to a certain value is not studied, only the stability of the system as function of load is studied.

A load of 0.2MW is introduced on the dc-side of the rectifier after 3 seconds. This is 10% of the capacity of the generator (1.94MW). As was shown in Fig. 9.8, the dc-bus voltage is 1030V before the oscillations starts. To introduce a load of 0.2MW, the load resistance corresponds to $R_{Load} = \frac{V^2}{P} = \frac{(1030V)^2}{0.2MW} = 5.3\Omega$.

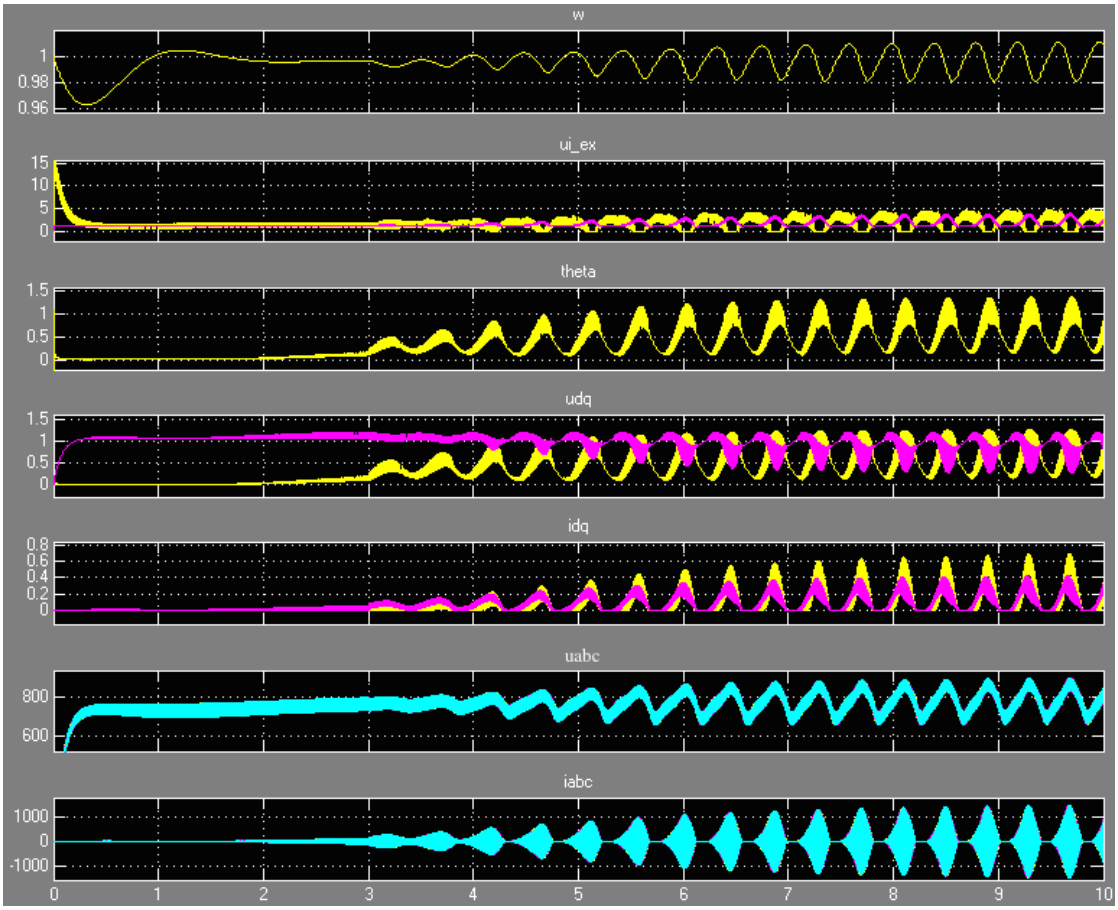

Figure 9.15: 1940 kVA generator modeled as salient pole output values from generator start-up simulation, where : w is the rotor velocity, u_i is the field voltage, $theta$ is the rotor angle, u_{dq} is the stator voltage in the d- and q-axis, i_{dq} is the stator current in the d- and q-axis, u_{abc} and i_{abc} is the rms terminal voltage and terminal current, respectively. A load $R_{Load} = 5.3\Omega$, which corresponds to a load of 0.2MW, is introduced 3s into the simulation.

The frequency of the oscillations is 2.5Hz, and the generator output shows unstability after 3 seconds, immediately after the load of 0.2MW is introduced. Because all the parameters of the

generator oscillates similarly, only the rms terminal voltage and terminal current is studied when the load is further varied.

The load is increased to 0.5MW, which is 26% of the generator capacitance. This corresponds to a load of $R_{Load} = 2.122\Omega$.

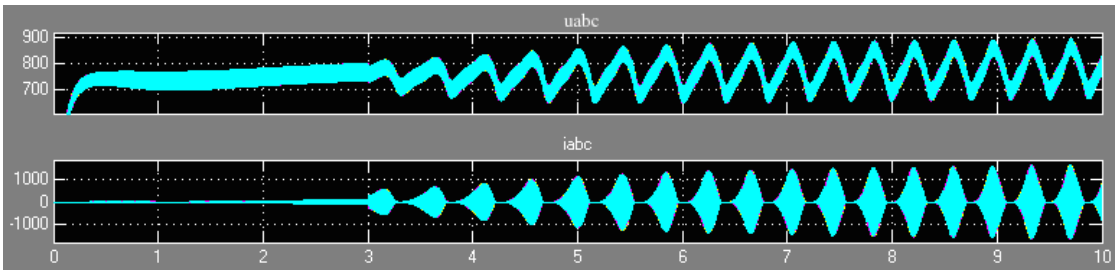

Figure 9.16: 1940 kVA generator modeled as salient pole output values from generator start-up simulation, where u_{abc} and i_{abc} is the rms terminal voltage and terminal current, respectively. A load $R_{Load} = 2.122\Omega$, which corresponds to a load of 0.5MW, is introduced 3s into the simulation.

The generator output shows instability when the load is 0.5MW. The frequency of the oscillations has increased to 2.6Hz.

The load is increased to 1MW, which is 52% of the generator capacitance. This corresponds to a load of $R_{Load} = 1.06\Omega$.

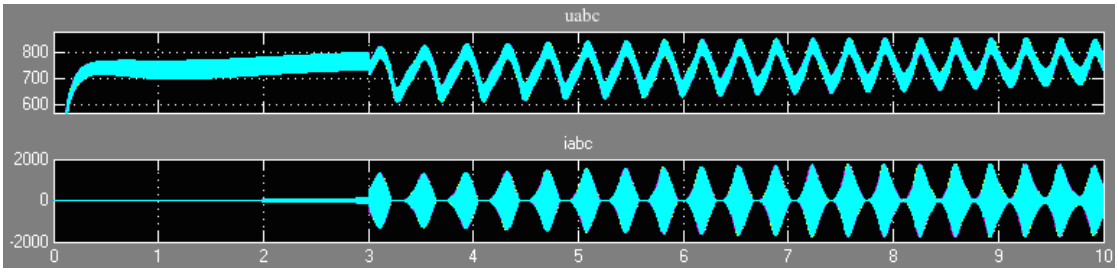

Figure 9.17: 1940 kVA generator modeled as salient pole output values from generator start-up simulation, where u_{abc} and i_{abc} is the rms terminal voltage and terminal current, respectively. A load $R_{Load} = 1.06\Omega$, which corresponds to a load of 1MW, is introduced 3s into the simulation.

The generator output shows instability when the load is 1.0MW, and the frequency of the oscillations has increased further, to 2.7Hz.

The load is increased to 1.5MW, which is 77% of the generator capacitance. This corresponds to a load of $R_{Load} = 0.707\Omega$.

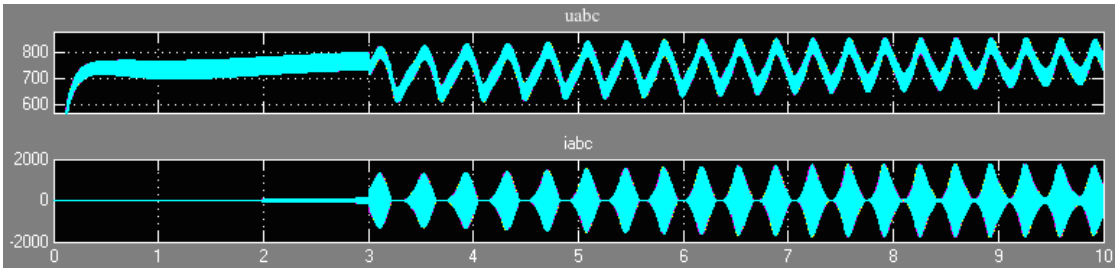

Figure 9.18: 1940 kVA generator modeled as salient pole output values from generator start-up simulation, where u_{abc} and i_{abc} is the rms terminal voltage and terminal current, respectively. A load $R_{Load} = 0.707\Omega$, which corresponds to a load of 1.5MW, is introduced 3s into the simulation.

The generator output shows instability when the load is 1.5MW, with a frequency of 2.7Hz.

The load is increased to 1.9MW, which is 98% of the generator capacitance. This corresponds to a load of $R_{Load} = 0.56\Omega$. This is a very large load. The battery also draws power from the generator, so it is assumed that the generator runs at nominal power, at the limit of what it can deliver.

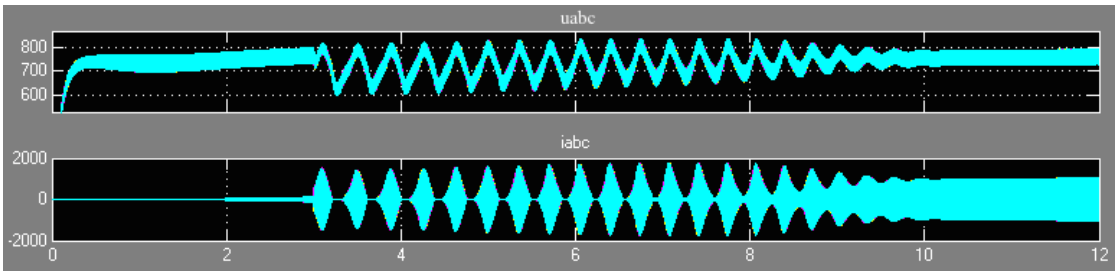

Figure 9.19: 1940 kVA generator modeled as salient pole output values from generator start-up simulation, where u_{abc} and i_{abc} is the rms terminal voltage and terminal current, respectively. A load $R_{Load} = 0.707\Omega$, which corresponds to a load of 1.5MW, is introduced 3s into the simulation.

The generator output shows stability after 10 seconds when the load is 1.9MW.

Summary of the simulations:

Table 9.5: Generator start-up when G2 is modeled as salient pole, governor and AVR is included in the model. The load connected at the DC-side of the rectifier is varied.

Parameter	Value [pu]	Operation	Comment	Frequency AC-side	Frequency DC-side
P_{Load}	$0.2MW$	Unstable after 3s	Increasing	2.5Hz	2.5Hz
P_{Load}	$0.5MW$	Unstable	-	2.6Hz	2.6Hz
P_{Load}	$1.0MW$	Unstable	-	2.7Hz	2.7Hz
P_{Load}	$1.5MW$	Unstable	-	2.7Hz	2.7Hz
P_{Load}	$1.9MW$	Stable after 10s	-	-	-

Table 9.5 shows that when the load is increased up to 1.9MW, at a point where the generator operates at the limit of its capacity, the generator becomes stable.

By rewriting the stability criterion given by [2] in Eq. 4.17, we have that:

$$X`_d^2 I`_d^2 + X`_q^2 I`_q^2 \leq 2X`_d I`_d U_p \tag{9.2}$$

which claims when the source voltage U_p is increased, stability is enhanced. The source voltage is load dependent, meaning that the stability of the 1940kVA generator depends on the load-operation. When the load increases, the source voltage U_p increases and stability is reached according to the stability criterion presented by [2] shown in the equation above. The simulation results presented in Table 9.5 confirms this, saying that the generator becomes stable when the load is increased to 1.9MW. However, instability is observed for all other loads, with an increasing frequency when the load is increased.

Chapter 10

Investigation of 1940 kVA Generator System, Round Rotor

In this chapter, the 1940 kVA synchronous generator is modeled in MatLab/SimPowerSystems with a round rotor design. As mentioned in Chapter 7, the parameters from the generators are obtained from the originally received SimPowerSystems-model from Siemens in Trondheim. In this model, the 1940 kVA generator is modeled as salient pole, but from conversations with Siemens Trondheim, it is understood that this generator is modeled as round rotor.

In addition, the parameters X_d and X_q for the 1940 kVA synchronous generator is close in value, which supports the qualified assumption that the 1940kVA generator in reality is a round rotor. Because the generator is modeled as a salient pole in the model received from Siemens in Trondheim, the parameter-value of the transient q-axis reactance $X`_q$ is missing. This parameter must be found to model the generator as round rotor.

Table 4.1 in Chapter 4 shows typical parameters for SM for both salient pole and round rotor design [13]. As seen from this table, SM with a round rotor design often has values of the parameters X_d and X_q that is very close in value, as is the case with the 1940 kVA generator; $\frac{X_d}{X_q} = 1.12$.

In order to model the 1940 kVA generator as a round rotor machine and not a salient pole machine, the value of the parameter $X`_q$ must be found, and the assumption that $X_d \approx X_q$ must be made, even though they are already very close in value. The value of the transient q-axis reactance can be found using ratios in the parameters given in the Table 4.1 in Chapter 4. By using this table and information about the generator reactances, a qualified guess of the transient q-axis reactance is made: $X`_q = 1.6pu$. A more detailed explanation of the process finding this value is found in the Appendix I.2.1.

Because there is given different values for X_d and X_q, there must be tried both values for X_q, both the original value for X_q and the value of X_d. The value of X_d must throughout the experiment be the originally given value, because there is less degrees of freedom in this axis.

A definition for stability must be found, to classify the generator as stable/unstable. Because MatLab/SimPowerSystems does not have the same way of analyzing eigenvalues in the same way as DIgSILENT PowerFactory, the curves in the graphs extracted from the simulations must be used as a basis for stability. The simulations runs for 20 seconds, and if no oscillations is detected, the generator is considered stable. If instability is observed after 20 seconds is simulated, numerical reasons in the simulation tool could be the reason. Table 10.1 below shows the result of the simulations.

Table 10.1: Parameter analysis, varying $X`_q$ and X_q to investigate generator stability

Parameter analysis		
Parameters	Value	Generator operation
$X`_q$ X_q	1.6 $= X_d$	Stable
$X`_q$ X_q	1.6 $= X_q$	Stable
$X`_q$ X_q	$= X_q$ $= X_d$	Unstable
$X`_q$ X_q	$= X_q$ $= X_q$	Unstable

The table with values in pu-units is given in Appendix I.2.1. From Table 10.1, it can be concluded that the value of $X`_q$ has a great impact on the stability of the generator when designed as a round rotor machine. If the machine is to operate stable, the value of $X`_q$ must be within the limits: $1.6 < X`_q < X_q$. This limit is further examined in the table below, where only $X`_d$ is examined, and the value of X_q is first fixed on $X_q = X_q$, then on $X_q = X_d$. Stability is classified as explained above. If oscillations occur, they will be defined into the following categories: damped, undamped, poorly damped or standing oscillations. The frequency of the oscillations is also calculated. No load is connected to the DC-side of the rectifier, except from the battery-arrangement.

10.1 $1.6 < X`_q < X_q$, $X_q = X_q$

With AVR and exciter

Table 10.2: Parameter analysis, with $1.6 < X`_q < X_q$ and $X_q = X_q$ to investigate the generator stability. Voltage regulator and governor included.

Parameter	Value [pu]	Operation	Comment	Frequency
$X`_q$	1.6	Stable	-	-
$X`_q$	2.0	Stable	-	-
$X`_q$	2.5	Stable	-	-
$X`_q$	3.0	Unstable after 8s	Standing oscillations	3 Hz
$X`_q$	2.75	Unstable after 12s	Increasing oscillations	3 Hz
$X`_q$	2.6	Stable	-	-
$X`_q$	2.65	Stable	-	-
$X`_q$	2.7	Unstable after 12s	Increasing oscillations	2.9 Hz
$X`_q$	4.79	Unstable after 4.5s	Standing oscillations	2.5 Hz

The table with values in pu-units is given in Appendix I.2.1. When G2 is designed as round rotor, with governor and AVR included and $X_q = X_q$, the generator becomes stable when $X`_q < 2.7pu$. A stability criterion for the transient reactances can be obtained:

$$\frac{X`_q}{X`_d} < 5.51pu \tag{10.1}$$

The stability criterion presented by [1] claims that to obtain stability, this ratio should be: $\frac{X`_q}{X`_d} < 2$. When the ratio between the transient reactances is calculated with $X`_q = 2.7$ applied, the ratio becomes: $\frac{X`_q}{X`_d} > 2$ under these conditions. This does not fulfill the criterion presented by [1], but is stable nevertheless.

Without AVR and exciter

The same parameter analysis is done, but now without the voltage regulator connected to the 1940 kVA synchronous generator designed with round rotor. The generator is excited by a constant DC voltage source, providing the generator field with the same voltage as the exciter embedded in the voltage regulator-exciter-block, $V_{dc} = V_{exciter} = 21V$.

The stability is evaluated as before, by simulating 20 seconds of the generator start-up and analyzing the graphs out from the generator. No load is connected to the DC-side of the rectifier, except from the battery-arrangement. The frequency of the oscillation in the parameters is registered when the system becomes unstable. The result is shown in the table below.

Table 10.3: Parameter analysis, with $1.6 < X`_q < X_q$ and $X_q = X_q$ to investigate the generator stability. Only the governor is included. A constant DC-source excites the generator field.

Parameter	Value [pu]	Operation	Comment	Frequency on AC-side
$X`_q$	1.6	Stable	-	-
$X`_q$	2.0	Stable	-	-
$X`_q$	3.0	Stable	-	-
$X`_q$	4.0	Stable	-	-
$X`_q$	5.0	Stable	-	-
$X`_q$	7.0	Stable	-	-
$X`_q$	9.0	Stable	Poorly damped	-
$X`_q$	10.0	Unstable	-	0.22Hz

The table with values in pu-units is given in Appendix I.2.1

The outputs from the generator modeled without AVR all shows that the system is stable when $X`_q < 10.0$ when the AVR is not included and $X_q = X_q$. When $X`_q = 10.0$, spikes appear in the parameters with a very low frequency. Fig 10.1 below shows these spikes in the rotor velocity w during the generator start-up simulation.

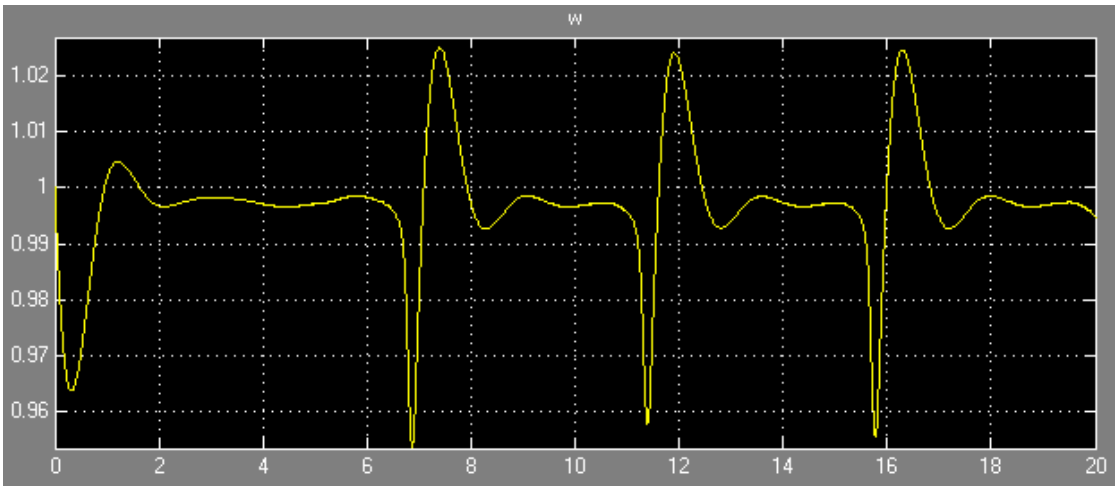

Figure 10.1: 1940 kVA generator modeled as round rotor and $X`_q = 10$, no load is attached to the dc-side of the rectifier and w is the rotor velocity.

10.2 $1.6 < X`_q < X_q$, $X_q = X_d$

With AVR and exciter

A parameter analysis is conducted, varying the transient reactance in the q-axis when $X_q = X_d$. The result is shown in Table 10.4 below.

Table 10.4: Parameter analysis, with $1.6 < X`_q < X_q$ and $X_q = X_d$ to investigate the generator stability. Voltage regulator and governor included.

Parameter	Value [pu]	Operation	Comment	Frequency
$X`_q$	1.6	Stable	-	-
$X`_q$	2.0	Stable	-	-
$X`_q$	2.5	Stable	-	-
$X`_q$	3.0	Unstable after 8s	Standing oscillations	3 Hz
$X`_q$	2.75	Unstable after 10s	Decreasing oscillations	3 Hz
$X`_q$	2.6	Stable	-	-
$X`_q$	2.65	Unstable after 11s	Decreasing oscillations, poorly damped	3 Hz
$X`_q$	2.7	Unstable after 11s	Standing oscillations	3 Hz

The table with values in pu-units is given in Appendix I.2.1. When G2 is designed as round rotor, with governor and AVR included and $X_q = X_d$, the generator becomes stable when $X`_q < 2.65pu$. A stability criterion for the transient reactances can be obtained:

$$\frac{X`_q}{X`_d} < 5.41pu \tag{10.2}$$

Using this parameter, the stability criterion presented by [1] will not be fulfilled with this parameters either. When the ratio between the transient reactances is calculated with $X`_q = 2.65$ applied, the ratio becomes: $\frac{X`_q}{X`_d} > 2$ under these conditions. This does not fulfill the criterion presented by [1], but is stable nevertheless.

Without AVR and exciter

The same parameter analysis is conducted when the AVR and exciter is not included. A constant DC-source excites the generator field with a constant voltage of 21V. The transient reactance in the q-axis is varied when $X_q = X_d$. The result is shown in Table 10.5 below.

Table 10.5: Parameter analysis, with $1.6 < X`_q < X_q$ and $X_q = X_d$ to investigate the generator stability. Only the governor included. A constant DC-source excites the generator field.

Parameter	Value [pu]	Operation	Comment	Frequency
$X`_q$	1.6	Stable	-	-
$X`_q$	2.0	Stable	-	-
$X`_q$	3.0	Stable	-	-
$X`_q$	5.0	Stable	-	-
$X`_q$	7.0	Unstable	-	0.22Hz
$X`_q$	6.0	Unstable	-	0.22Hz
$X`_q$	5.5	Stable after 15s	Poorly damped	-

The table with values in pu-units is given in Appendix I.2.1. The outputs from the generator modeled without AVR all shows that the system is stable when $X`_q < 6.0$ when the AVR is not included and $X_q = X_d$.

The generator becomes unstable for a lower value of $X`_q$ when the AVR and exciter is connected than when it is not. The stability limit is approximately the same for when $X_q = X_q$ and when $X_q = X_d$. From the simulations, it is also seen that when the AVR and exciter is removed, the generator becomes unstable for a lower value of $X`_q$ when $X_q = X_d$ than when $X_q = X_q$, possibly because $X_q < X_d$.

In general, it is observed that when $X_q = X_d$, the generator becomes unstable for a lower value of $X`_q$, both when the AVR and exciter is included and not, than when $X_q = X_q$.

It is also observed that when the generator becomes unstable when the AVR and exciter is included in the model, the generator outputs oscillate with a frequency of 3Hz for both when $X_q = X_q$ and when $X_q = X_d$. When the AVR and exciter is not included in the model and the same parameter analysis is done, the generator outputs oscillate with a frequency of 0.22Hz when the system becomes unstable, for both when $X_q = X_q$ and when $X_q = X_d$.

Despite this, the stability criterions obtained is quite similar in values, indicating that the synchronous reactances X_q and X_q is very close in value and the approximation of $X_q \approx X_q$ can be made.

10.3 Simulation Results of G2 with Round Rotor

The results of the simulations of the generator start-up of the system with G2, modeled as a synchronous generator with round rotor is shown in this chapter. The transient q-axis reactance $X`_q$ is assumed to be the same value as the q-axis synchronous reactance ($X`_q = X_q$). The voltage regulator and governor is both included in the model. The generator start-up is simulated both for when a load is connected on the dc-side of the rectifier, and when no load is attached.

10.3.1 No load at the DC-side

There is no load connected to the DC-side of the rectifier, except from the battery-arrangement consisting of the large capacitance and the series resistance. The reference value of the voltage regulator is set to 1.2, which means that the voltage out from the generator is to be increased from the nominal voltage $690V$ to $1.2 * 690V = 828V$.

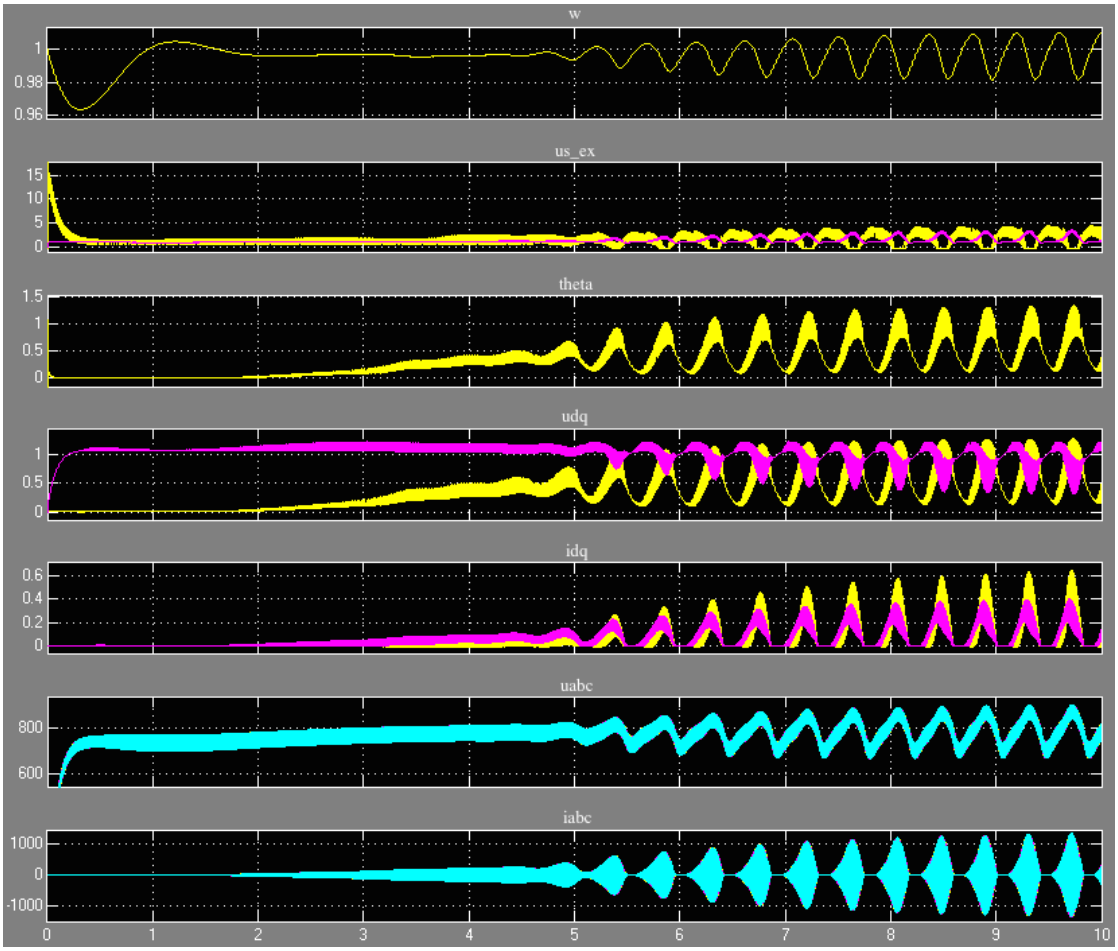

Figure 10.2: 1940 kVA generator system output values, where: w is the rotor velocity, u_i is the field voltage, $theta$ is the rotor angle, u_{dq} is the stator voltage in the d- and q-axis, i_{dq} is the stator current in the d- and q-axis, u_{abc} in rms and i_{abc} is the terminal voltage and current, respectively. No load is connected to the DC-side of the rectifier, except from the battery-arrangement.

From the top, Fig 10.2 shows the rotor velocity w, the field voltage u_i, the rotor angle $theta$, the stator voltage in the d- and q-axis u_{dq}, the stator current in the d- and q-axis i_{dq}, the terminal voltage u_{abc} in rms and the terminal current i_{abc} of the 1940 kVA generator, respectively. The graph showing the field voltage u_i contains of a pink and a yellow curve, where the pink curve displays the field current and the yellow curve displays the field voltage. The graphs showing u_{dq} and i_{dq} contains of two curves, one yellow and one pink. The yellow curve is the d-axis for both voltage and current, and the pink is the q-axis for both voltage and current.

The generator outputs shows an unstable start-up of G2, as expected. The rms voltage in the three phases a, b and c increases up to approximately 740V, before it increases further to about 800V and the system becomes unstable after 5 seconds. When this instability occurs, the generator parameters oscillates with a frequency of 2.5Hz.

The voltage output from the exciter is shown in Fig 10.3 below.

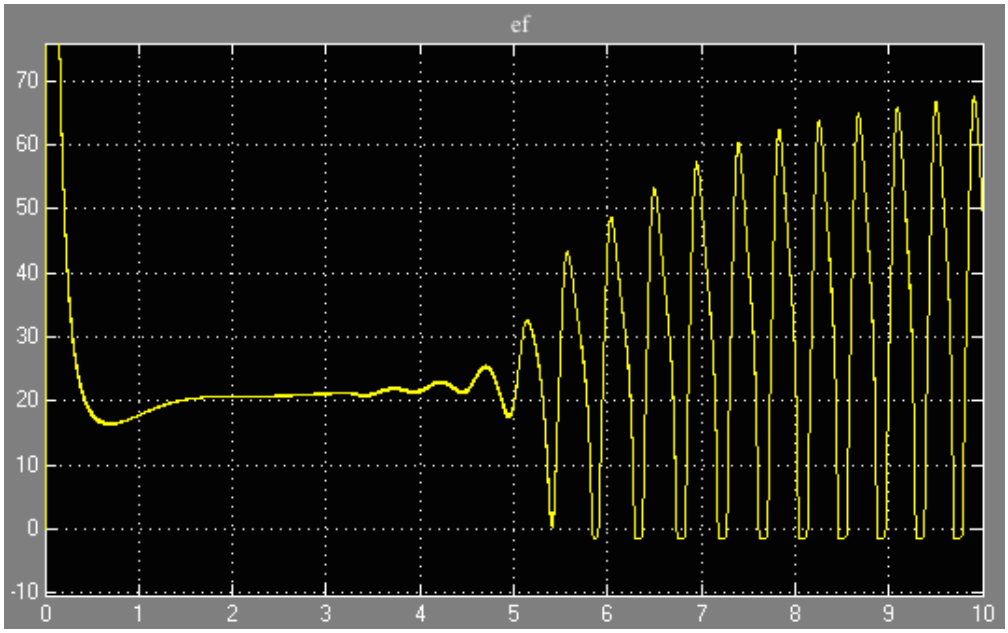

Figure 10.3: 1940 kVA generator system output values from the AVR and exciter where e_f is the field voltage.

The plot shows that the exciter feeds the generator field with a constant DC voltage of 21V DC.

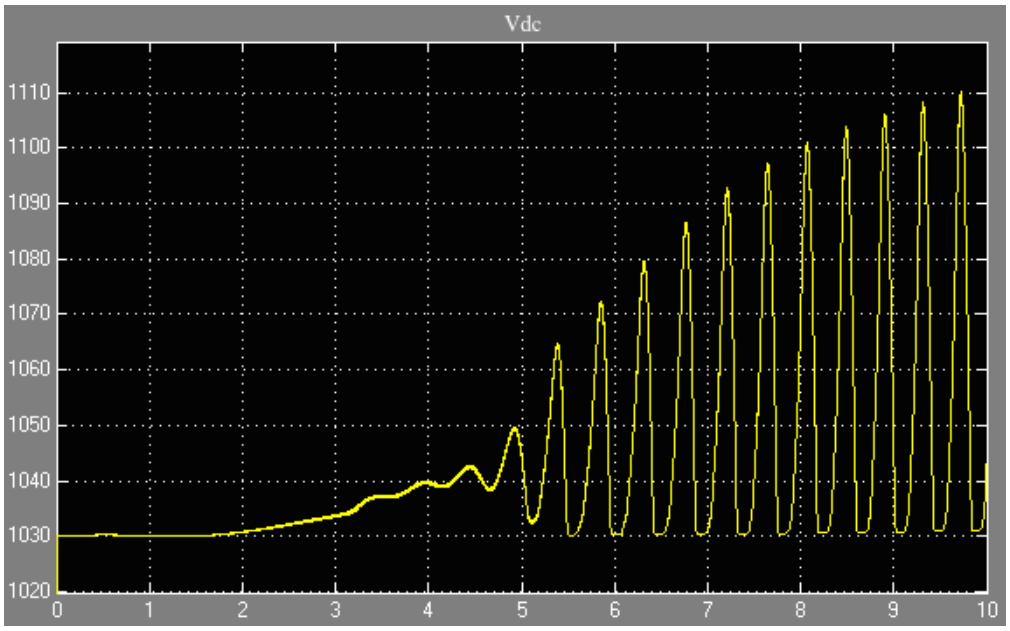

Figure 10.4: The 1940 kVA generator feeds the battery through a rectifier, where V_{dc} is the dc-bus voltage.

The dc-bus voltage shows a value of 1030V before the oscillations begins.

10.3.2 Reference value of the AVR at no load

When the reference value of the voltage regulator is decreased from 1.2 to 1.0, the characteristics of the generator changes from unstable to stable, as shown in Fig 10.5 below.

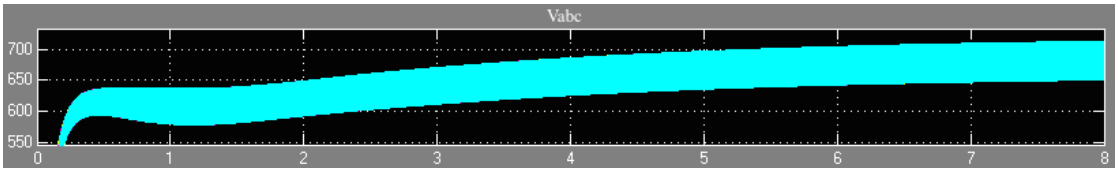

Figure 10.5: The rms terminal voltage uabc in three phases when the generator start-up is simulated, when the voltage regulator is connected and the reference value is set to 1.0. No load is attached to the DC-side except from the battery-arrangement in form of a large capacitor and a series resistance.

The voltage settles at a voltage close to the nominal voltage of the generator, 690V, as requested of the voltage regulator, and the generator output is stable.

The reference value of the voltage regulator is now changed to 1.4, requesting a voltage out from the voltage to be 40% larger than the nominal voltage; $V_{abc} = 1.4 * 690V = 988V$.

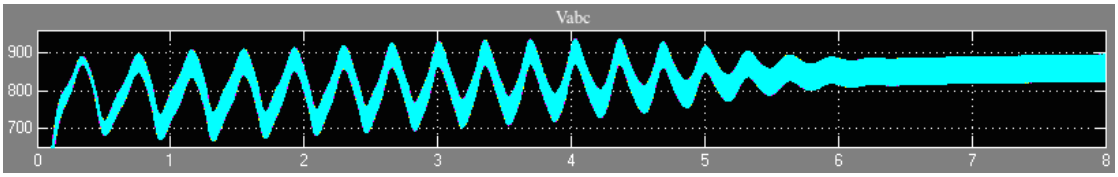

Figure 10.6: The rms terminal voltage uabc in three phases when the generator start-up is simulated, when the voltage regulator is connected and the reference value is set to 1.4. No load is attached to the DC-side except from the battery-arrangement in form of a large capacitor and a series resistance.

The first 6 seconds of the motor-start up is unstable, before the generator output shows a stable characteristics after 6 seconds. At the same time, the voltage regulator tries to increase the voltage up to the requested voltage 966V, but this happens slowly. The simulation is extended to 50seconds, to see if the voltage regulator manages to increase the voltage up to 966V.

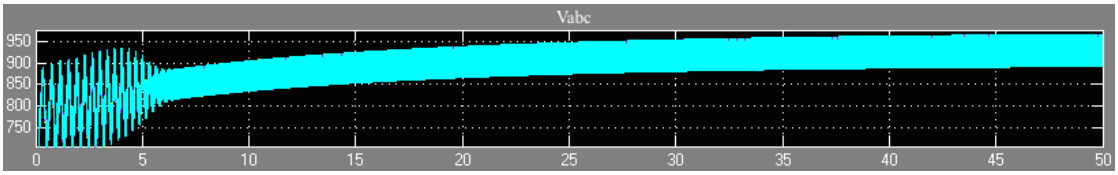

Figure 10.7: The rms terminal voltage uabc in three phases when the generator start-up is simulated for 50 seconds to see if the voltage regulator manages to increase the voltage to the requested voltage $V_{abc} = 1.4 * 690V = 966V$, when the voltage regulator is connected and the reference value is set to 1.4. No load is attached to the DC-side except from the battery-arrangement in form of a large capacitor and a series resistance.

After 50 seconds, the rms terminal voltage is approximately 930V, and the regulator still increases the voltage closer to the requested voltage 966V.

In Chapter 9.4, the same study was done for the 1940kVA generator designed as salient pole. Similarly with the study done above with the 1940kVA generator modeled as round rotor, the salient pole generator G2 was stable when the reference value of the same regulator was set to 1.0, unstable after 5s when $v_{ref} = 1.2$, and stable after 6s when $V_{ref} = 1.4$. The generator characteristics is the same when the voltage regulator is changed, whether or not G2 is designed as round rotor or salient pole.

10.3.3 Load attached to the DC-side

A load of 0.2MW is attached to the DC-side of the rectifier. This is a load step of 10% of the generator capacity. The reference value of the voltage regulator is set back to 1.2, which is its original setting. A load of 0.2MW corresponds to a load resistance of $R_{Load} = 5.3\Omega$ and is introduced 3 seconds into the generator start-up simulation.

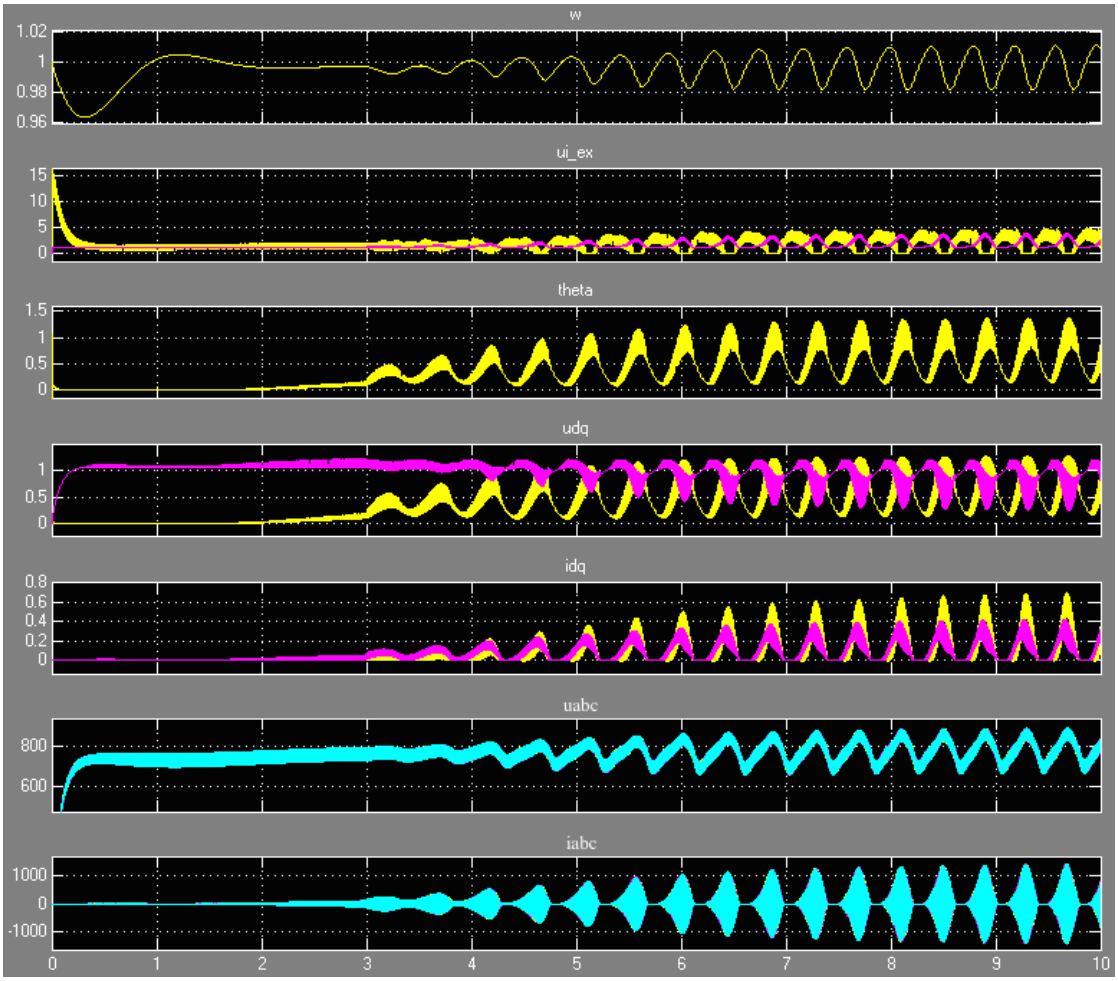

Figure 10.8: 1940 kVA generator system output values, where: w is the rotor velocity, u_i is the field voltage, $theta$ is the rotor angle, u_{dq} is the stator voltage in the d- and q-axis, i_{dq} is the stator current in the d- and q-axis, u_{abc} in rms and i_{abc} is the terminal voltage and current, respectively. A load $R_{Load} = 5.3\Omega$, which corresponds to an active load of 0.2MW, and is attached to the DC-side of the rectifier.

When the load is 0.2MW, the generator is unstable and the parameters oscillate with a frequency of 2.5Hz.

A load of 0.5MW corresponds to a load resistance of $R_{Load} = 2.122\Omega$ and is introduced 3 seconds into the generator start-up simulation. A laid of 0.5MW is a load step of 26% of the generator capacity. The result is shown in Fig. 10.9 below.

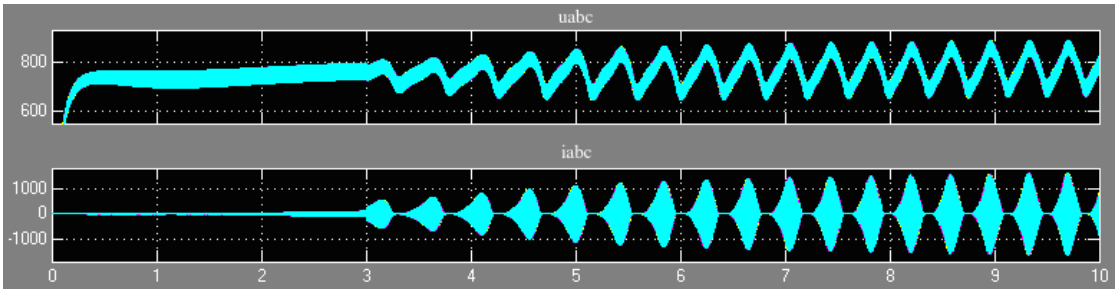

Figure 10.9: 1940 kVA generator system output values, where u_{abc} is the rms terminal voltage and i_{abc} is the terminal current. A load $R_{Load} = 2.122\Omega$, which corresponds to an active load of 0.5MW, and is attached to the DC-side of the rectifier.

When the load is 0.5MW, the generator is unstable and the parameters still oscillate with a frequency of 2.5Hz. The load is increased to 1MW corresponding to a load resistance of $R_{Load} = 1.06\Omega$ and is introduced 3 seconds into the generator start-up simulation.

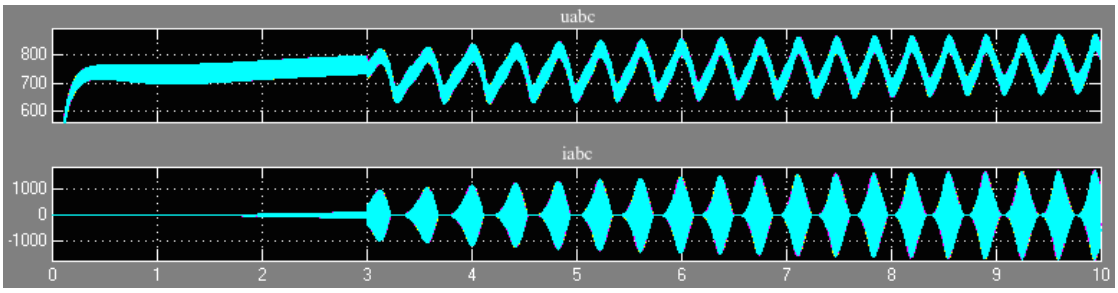

Figure 10.10: 1940 kVA generator system output values, where u_{abc} is the rms terminal voltage and i_{abc} is the terminal current. A load $R_{Load} = 1.06\Omega$, which corresponds to an active load of 1MW, and is attached to the DC-side of the rectifier.

When the load is 1.0MW, the generator is unstable and the parameters oscillate with a frequency of 2.7Hz, which is a small increase in frequency value. The load is increased to 1.5MW, corresponding to a load resistance of $R_{Load} = 0.707\Omega$ and is introduced 3 seconds into the generator start-up simulation. A load of 1.5MW is 77% of the generator capacity.

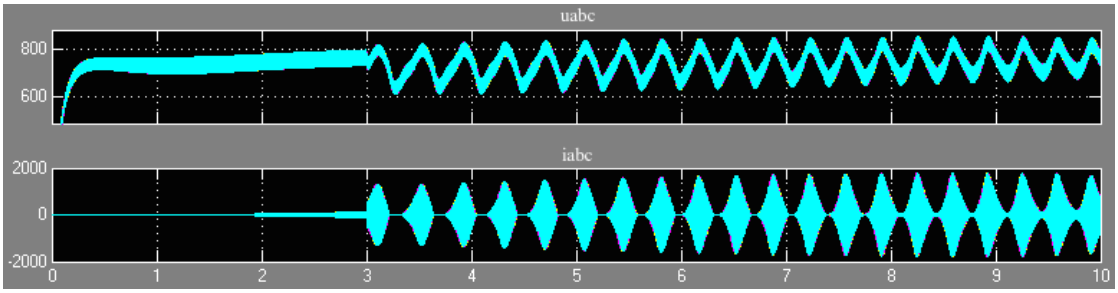

Figure 10.11: 1940 kVA generator system output values, where u_{abc} is the rms terminal voltage and i_{abc} is the terminal current. A load $R_{Load} = 0.707\Omega$, which corresponds to an active load of 1.5MW, and is attached to the DC-side of the rectifier.

When the load is 1.5MW, the generator is unstable and the parameters oscillate with a frequency of 2.8Hz. The load is further increased, to 1.9MW, corresponding to a load resistance of $R_{Load} = 0.56\Omega$ and is introduced 3 seconds into the generator start-up simulation. This is a very large load, making the generator run at the limit of its capacity.

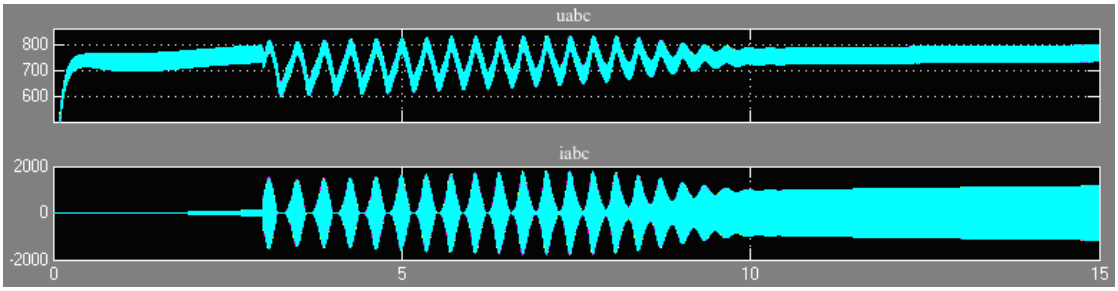

Figure 10.12: 1940 kVA generator system output values, where u_{abc} is the rms terminal voltage and i_{abc} is the terminal current. A load $R_{Load} = 0.56\Omega$, which corresponds to an active load of 1.9MW, and is attached to the DC-side of the rectifier.

When the load is increased to 1.9MW, the generator becomes stable after 10 seconds. This was the case for the 1940kVA generator modeled as salient pole as well. The observations on the ship also corresponds to these simulations.

A summary of the load-step simulations is shown in Table 10.6 below.

Summary of the simulations:

Table 10.6: Generator start-up when G2 is modeled as round rotor, $X`_q = X_q$, governor and AVR is included in the model. The load connected at the DC-side of the rectifier is varied.

Parameter	Value [pu]	Operation	Comment	Frequency AC-side	Frequency DC-side
P_{Load}	0	Unstable	-	2.5Hz	2.5Hz
P_{Load}	$0.2MW$	Unstable	-	2.5Hz	2.5Hz
P_{Load}	$0.5MW$	Unstable	-	2.5Hz	2.5Hz
P_{Load}	$1.0MW$	Unstable	-	2.7Hz	2.7Hz
P_{Load}	$1.5MW$	Unstable	-	2.8Hz	2.8Hz
P_{Load}	$1.9MW$	Stable after 10s	-		

This results corresponds with the results found with G2 designed as salient pole, shown in Table 9.5. The results found in both Table 9.5 for G2 salient pole and Table 10.6 for G2 round rotor confirms the stability criterion found in Eq. 4.17 by [2], due to the fact that stability is enhanced when the load is increased up to a certain value, reaching a high value of the stationary source voltage U_p until the stability criterion presented by [2] is fulfilled.

10.3.4 Infinitely large inertia

This simulation is done to detect oscillations in the rotor angle by varying the rotor-inertia constant H. This test is done by Siemens in Trondheim as well, but according to [2] oscillations was not detected. An infinitely large inertia constant was tried, but the oscillations in the generator output was still intact.

The inertia J is calculated by using the formula [22]: $J = \frac{2*H*N*S_{rated}}{2\pi*f_{rated}}$, where:

J is inertia in $kg*m^2$, H is the inertia constant in sW/VA, S_{rated} is the machine rated apparent power in VA, F_{rated} is the machine rated electrical frequency in Hz, and N is the number of machine pole pairs. The varying of H is shown in the table below. The inertia constant is in direct proportion to the inertia J, so by increasing the inertia constant, the inertia is increased with the same proportion [22].

Table 10.7: Varying rotor intertia to detect oscillations in rotor angle

Parameter	Value [$\frac{sW}{VA}$]	Operation	Comment	Frequency AC-side	Frequency DC-side
H	0.872	Unstable	-	2.5Hz	2.5Hz
H	1000	Unstable	-	2.5Hz	2.5Hz
H	10 000	Unstable	-	2.5Hz	2.5Hz
H	100 000	Unstable	-	2.5Hz	2.5Hz
H	1e6	Unstable	-	2.5Hz	2.5Hz

The system is unstable under these conditions, regardless of the increasing of the rotor inertia, and oscillations for the rotor angle was detected for all values of rotor constants.

10.4 G2 with Round Rotor without AVR

It is of great interest to find how the arrangement with the rectifier coupled generator, feeding the battery on the DC-side, behaves when the voltage regulator, regulating the voltage out from the generator, is removed. As shown in Fig 10.3, the DC voltage from the exciter, exciting the generator field, oscillates greatly, after about 3-4 seconds. At the same time, after 3-4 seconds in to the motor start-up simulation, the oscillations seen in the generator output starts, as seen in Fig 10.2. It is not known, whether it is inside the voltage regulator or the generator the instability arises first. This can be further examined if the voltage regulator is removed and the generator outputs analyzed.

To remove the AVR, the exciter must be replaced by a constant DC voltage source, exciting the generator field with the same DC voltage as the exciter in the voltage regulator did, a constant voltage of 21V, as found in Fig 10.3.

The load step is generated by using a single phase circuit breaker, which opens 3 seconds into the generator start-up. The resistance and capacitance in the battery is set to the initial conditions $2100kF$ and $62.5m\Omega$, respectively. The transient q-axis reactance $X`_q$ is assumed to be the same value as the q-axis synchronous reactance ($X`_q = X_q$).

The resistance R_{Load} on the DC-side of the rectifier, connected in parallel with the battery is to be varied in value to show the generator response.

10.4.1 Simulation results

The output values of the system with G2, modeled as a synchronous generator with round rotor with the AVR not included. This is to show how the generator reacts during the motor-start-up without a regulator. The transient q-axis reactance $X`_q$ is assumed to be the same value as the q-axis synchronous reactance ($X`_q = X_q$). The simulations is first done when the generator operates at no-load, and then during load-operation.

No load attached to DC-side

There is no load connected to the DC-side of the rectifier except from the battery.

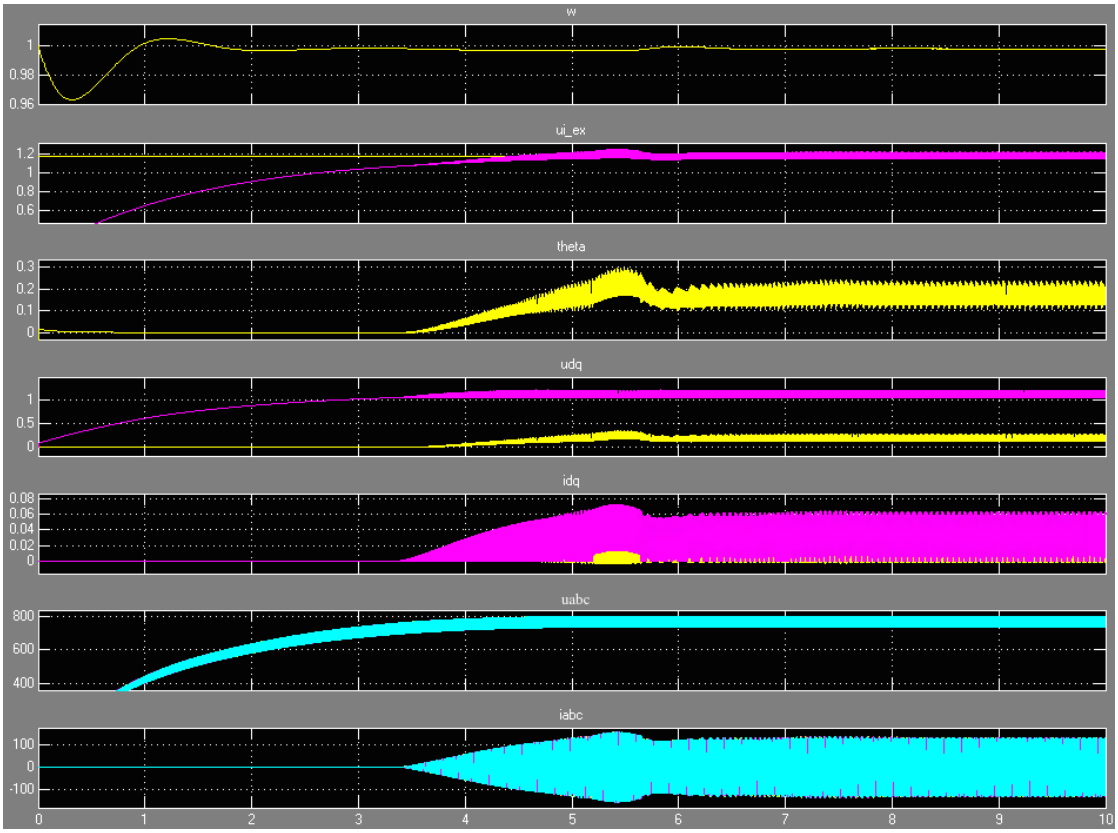

Figure 10.13: The output values from the 1940 kVA generator system with round rotor, modeled without the Voltage regulator, where: w is the rotor velocity, u_i is the field voltage, $theta$ is the rotor angle, u_{dq} is the stator voltage in the d- and q-axis, i_{dq} is the stator current in the d- and q-axis, u_{abc} and i_{abc} is the terminal voltage in rms and the current, respectively. No load is attached to the DC-side of the rectifier except the battery arrangement.

From the top, Fig 10.13 shows the rotor velocity w, the field voltage u_i, the rotor angle $theta$, the stator voltage in the d- and q-axis u_{dq}, the stator current in the d- and q-axis i_{dq}, the rms terminal voltage u_{abc} and the terminal current i_{abc} of the 1940 kVA generator, respectively. The plot of the generator outputs shows that the generator modeled with round rotor has a stable start-up when the AVR is not included and no load is connected to the DC-side of the rectifier.

The voltage output is now not regulated by any AVR and the generator has a stable start-up. The rms voltage from the generator is read from the plot to be 770V when no load is attached to the DC-side of the rectifier, approximately. This is almost 12% higher than the rated frequency of the generator, that is 690V. This is to deliver the voltage requested by the battery, $V_d = 1.35 * V_{LL} = 1030V$.

The period of the oscillations shown in the rms voltage in all three phases in the plot above is found to be 15ms, which corresponds to a frequency of 66.67Hz, which is the nominal frequency of the generator. The mean voltage on the DC-side of the rectifier is shown in Fig 10.14 below.

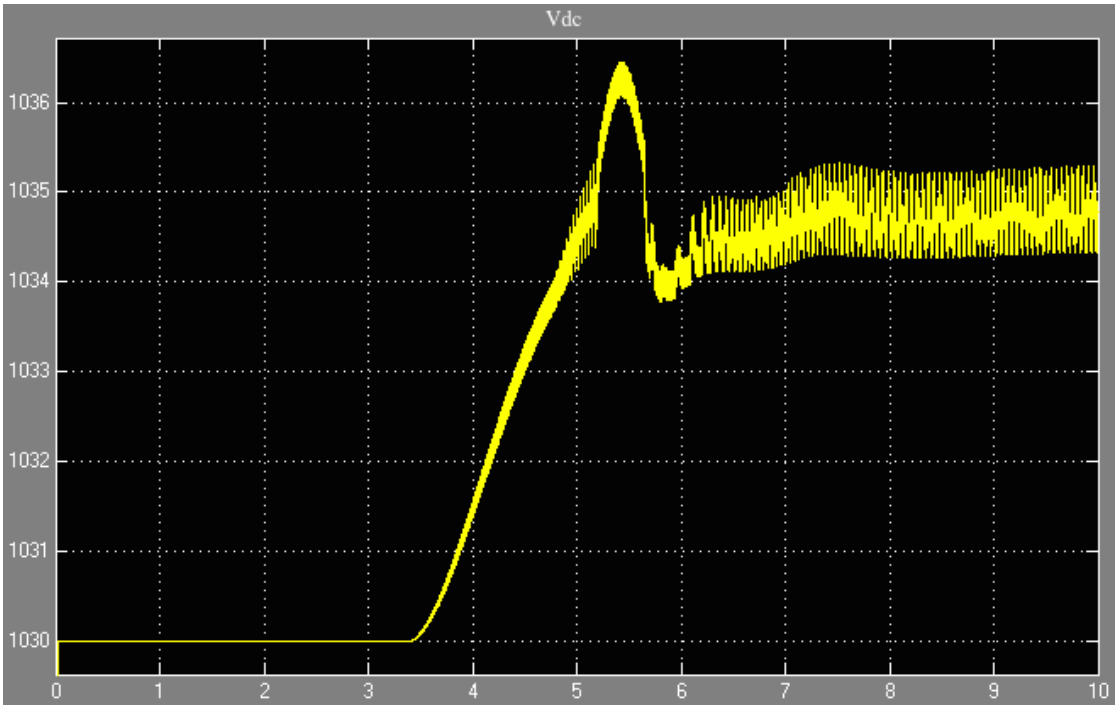

Figure 10.14: The mean DC voltage after the rectifier, supplied from the 1940 kVA generator system with round rotor, modeled without the voltage regulator.

The DC voltage from the rectifier starts at 1030V, and stays at this value in 3.5 seconds, before it increases to 1035V after 3.5 seconds into the generator start-up.

Load attached to DC-side

A load is now attached to the dc-side of the rectifier, and varied.

An active load of 0.2MW corresponds to a load resistance of $R_{Load} = 5.3\Omega$ and is introduced 3 seconds into the generator start-up simulation.

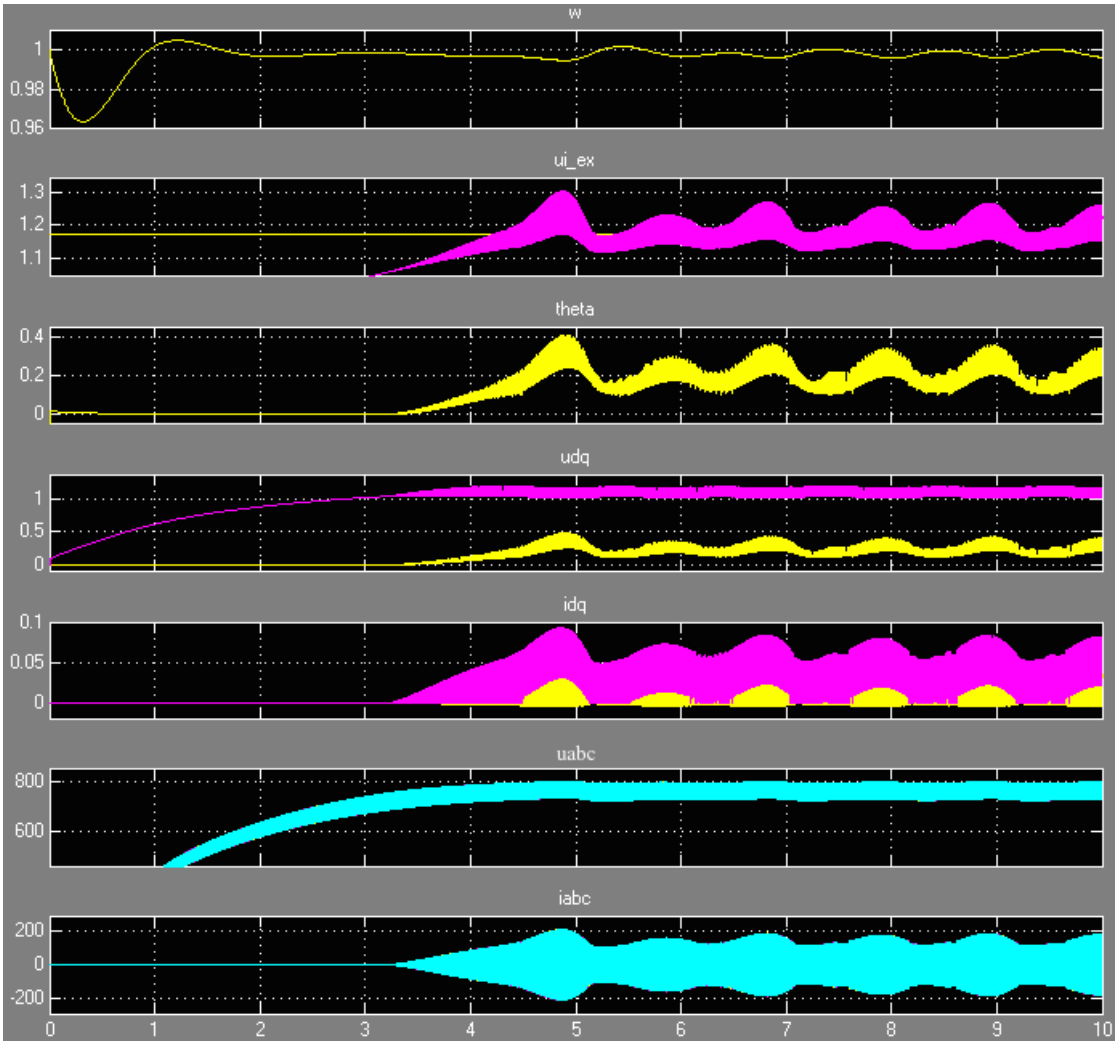

Figure 10.15: The output values from the 1940 kVA generator system with round rotor, modeled without the Voltage regulator, where: w is the rotor velocity, u_i is the field voltage, $theta$ is the rotor angle, u_{dq} is the stator voltage in the d- and q-axis, i_{dq} is the stator current in the d- and q-axis, u_{abc} and i_{abc} is the terminal voltage in rms and the current, respectively. A load $R_{Load} = 5.3\Omega$, which corresponds to an active power of 0.2MW, is attached to the DC-side of the rectifier after 3 seconds into the simulation.

The generator is unstable, and the frequency is lower for this load than when the voltage regulator was attached, only 1Hz.

The load is increased to 0.5MW, corresponding to a load resistance of $R_{Load} = 2.122\Omega$ and is introduced 3 seconds into the generator start-up simulation.

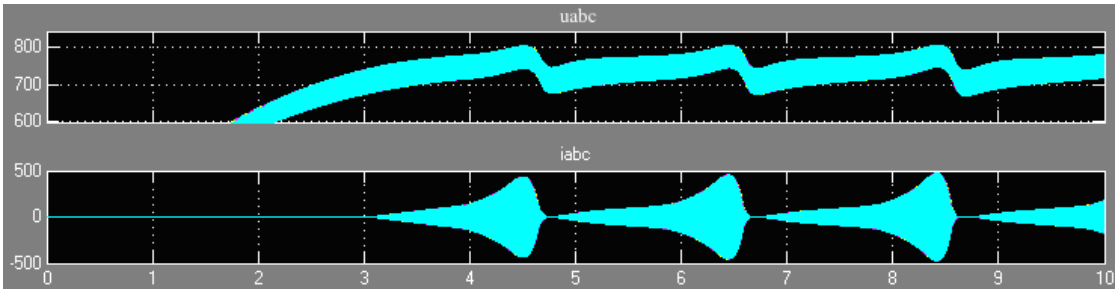

Figure 10.16: The output values from the 1940 kVA generator system with round rotor, modeled without the Voltage regulator, where u_{abc} and i_{abc} is the terminal voltage in rms and the current, respectively. A load $R_{Load} = 2.122\Omega$, which corresponds to an active power of 0.5MW, is attached to the DC-side of the rectifier after 3 seconds into the simulation.

The generator is still unstable, but the parameters only oscillate with a frequency of 0.5Hz.

An active load of 1.0MW corresponds to a load resistance of $R_{Load} = 1.06\Omega$ and is introduced 3 seconds into the generator start-up simulation.

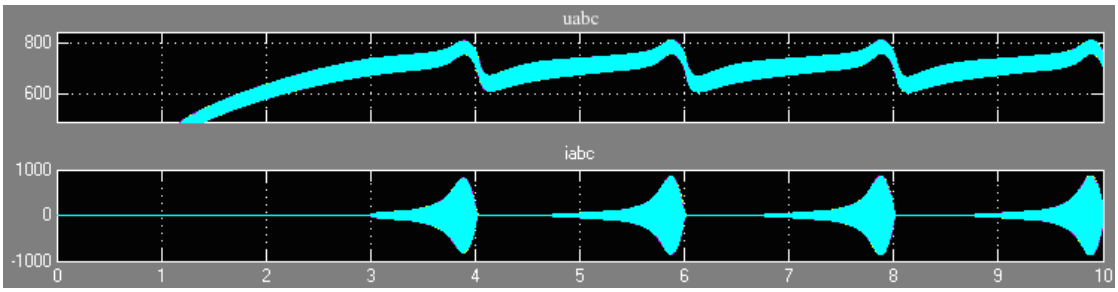

Figure 10.17: The output values from the 1940 kVA generator system with round rotor, modeled without the Voltage regulator, where u_{abc} and i_{abc} is the terminal voltage in rms and the current, respectively. A load $R_{Load} = 1.06\Omega$, which corresponds to an active power of 1.0MW, is attached to the DC-side of the rectifier after 3 seconds into the simulation.

The generator is still unstable, and the parameters still oscillate with a frequency of 0.5Hz.

An active load of 1.5MW corresponds to a load resistance of $R_{Load} = 0.707\Omega$ and is introduced 3 seconds into the generator start-up simulation.

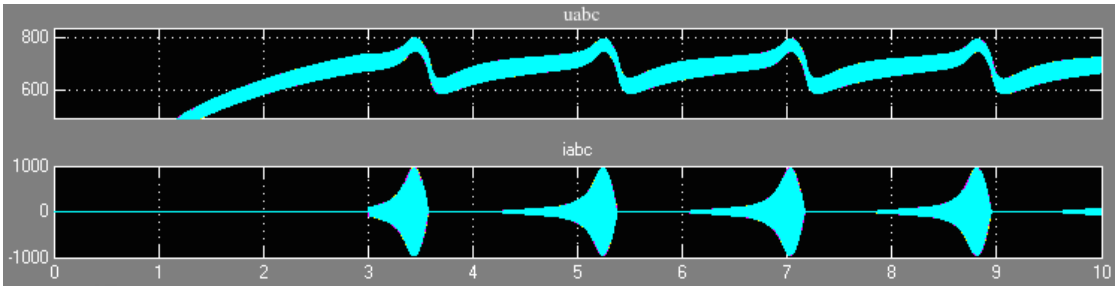

Figure 10.18: The output values from the 1940 kVA generator system with round rotor, modeled without the Voltage regulator, where u_{abc} and i_{abc} is the terminal voltage in rms and the current, respectively. A load $R_{Load} = 0.707\Omega$, which corresponds to an active power of 1.5MW, is attached to the DC-side of the rectifier after 3 seconds into the simulation.

The generator is unstable and has a frequency of 0.6Hz.

The load is increased to 1.9MW, that corresponds to a load resistance of $R_{Load} = 0.56\Omega$ and is introduced 3 seconds into the generator start-up simulation.

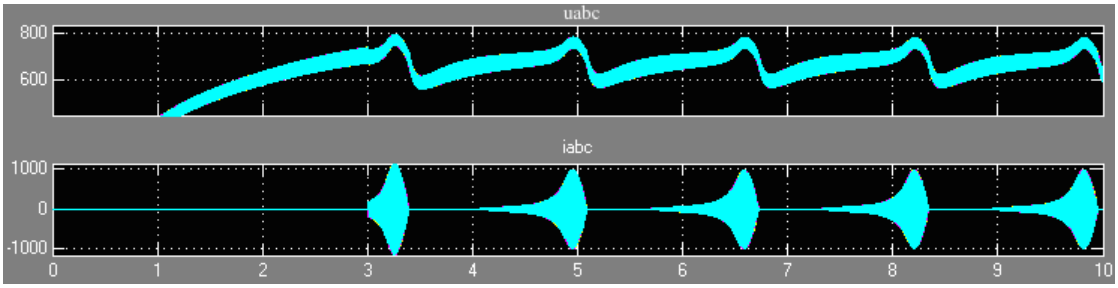

Figure 10.19: The output values from the 1940 kVA generator system with round rotor, modeled without the Voltage regulator, where u_{abc} and i_{abc} is the terminal voltage in rms and the current, respectively. A load $R_{Load} = 0.56\Omega$, which corresponds to an active power of 1.9MW, is attached to the DC-side of the rectifier after 3 seconds into the simulation.

When the load is 1.9MW, the generator is still unstable. A summary of the simulations is shown in the table below:

Table 10.8: Parameter analysis: DC-side load step when no AVR is included.

Parameter	Value [pu]	Operation	Comment	Frequency AC-side	Frequency DC-side
P_{Load}	0	Stable	-	-	-
P_{Load}	$0.2MW$	Unstable	Poorly damped	1Hz	1Hz
P_{Load}	$0.5MW$	Unstable	-	0.5Hz	0.5Hz
P_{Load}	$1.0MW$	Unstable	-	0.5Hz	0.5Hz
P_{Load}	$1.5MW$	Unstable	-	0.6Hz	0.6Hz
P_{Load}	$1.9MW$	Unstable	-	0.63Hz	0.63Hz

To better compare the simulation results from the two situations AVR connected/not connected,

a table is made and shown below.

Table 10.9: Parameter analysis: DC-side load step. Comparison between AVR connected/not connected.

Parameter	Value	With AVR	Frequency AC-side	Without AVR	Frequency AC-side
P_{Load}	0	Unstable	2.5Hz	Stable	-
P_{Load}	0.2	Unstable	2.5Hz	Unstable	1Hz
P_{Load}	0.5	Unstable	2.5Hz	Unstable	0.5Hz
P_{Load}	1.0	Unstable	2.7Hz	Unstable	0.5Hz
P_{Load}	1.5	Unstable	2.8Hz	Unstable	0.6
P_{Load}	1.9	Stable after 10s	-	Unstable	0.63

The generator shows instability when the AVR is included, but is stable when the AVR is not included, when no load is present. The generator is unstable for all loads $0.2MW < P < 1.5MW$ independent on whether the AVR is connected or not. When the load is close to nominal effect of the generator, $P_{Load} = 1.9MW$, the generator becomes unstable when the voltage regulator is not included, and stable when the AVR is included.

The frequencies of the oscillations during instability decreases when the voltage is not regulated by an AVR, from 2.5Hz to 0.5-1.0Hz.

At the outer point, no load and large load, the generator differs in operation when the AVR is included and when it is not. However, the generator becomes unstable for all loads $0.2MW < P < 1.5MW$, which could indicate that the stability problems does not origin in the voltage regulator, but somewhere in the generator-rectifier-battery arrangement. The generator-rectifier-battery-load arrangement must be further examined, the stability problems should be found there.

10.4.2 Parameter analysis of battery on the DC-side of the rectifier

The capacitor and series resistance modeling the battery in the electrical system on the ship under study, is shown in the figure below.

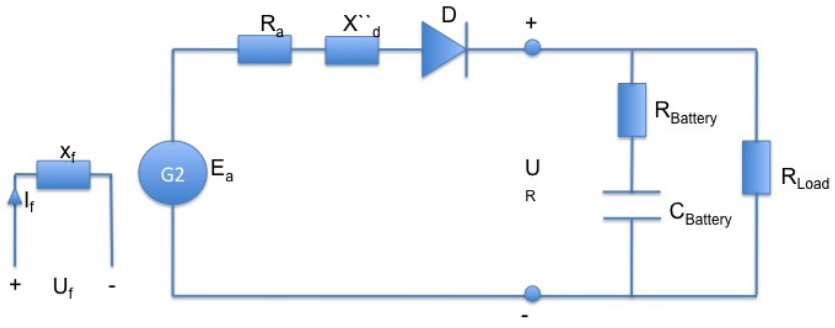

Figure 10.20: The system after the generator-rectifier-arrangement consists of a battery modeled by a series resistance $R_{battery}$ and a capacitor with significant value $C_{battery}$. A resistance R_{load} is placed in parallel with the battery and is adjustable.

Where x_f is the field reactance, I_f is the field current, U_f is the field voltage, E_a is the terminal voltage, R_a is the armature resistance, $X"_d$ is the d-axis subtransient reactance, D is the diode-bridge rectifier, U_R is the DC voltage out from the rectifier, $R_{Battery}$ is the series resistance, $C_{Battery}$ is the capacitance and R_{Load} is the resistance in parallel to the battery.

To investigate why the frequency of the voltage increases in value after the rectifier, the parameters of the resistance $R_{battery}$ and the capacitor $C_{battery}$ must be examined. The generator G2 is still modeled with a round rotor, with $X'_q = X_q$, and with only the governor connected to the generator-model. The voltage regulator is not included. A constant DC-source excites the generator-field with 21V, as shown in Fig 10.20.

The table below summarize the parameter analysis where the value of resistance $R_{battery}$ and the capacitor $C_{battery}$ is varied. The load resistance R_{Load} is not included yet, to analyze only how the battery affects the stability of the system. It will be included later, and analyzed separately, before both the parameters of the battery and the load resistance is analyzed together.

Table 10.10: Parameter analysis of the components on the DC-side of the rectifier. $R_{battery}$ and $C_{battery}$ is varied. G2 is modeled with round rotor with governor connected, and AVR not included. $X`_q = X_q$

Parameter	Value	Operation	Frequency AC-side	Frequency DC-side	Comment
$C_{battery}$ $R_{battery}$	2100 F 62.5 $m\Omega$	Stable	-	-	-
$C_{battery}$ $R_{battery}$	1000 F 0.3 Ω	Stable	-	-	-
$C_{battery}$ $R_{battery}$	500 F 1 Ω	Stable	-	-	-
$C_{battery}$ $R_{battery}$	1 F 10 Ω	Stable	-	-	
$C_{battery}$ $R_{battery}$	0.1 F 100 Ω	Stable	-	-	

As shown in Table 10.9, the generator shows stable operation when no load is connected, but unstable when a battery-arrangement and a load is present. According to Table 10.10 above, the battery parameters does not have such an impact on the generator stability as the load does.

However, the impact of varying the load and the battery parameters at the same time can have an effect on the generator stability, and will be examined next.

10.4.3 DC load step and battery parameter analysis

The load resistance is in parallel with the capacitance $C_{battery}$ and the series resistance $R_{battery}$ that models the battery in the system, and is connected to the system as a load step after 3s into the generator start-up by using a single phase circuit breaker. The AVR is not included, to analyze the generator behavior without the regulator.

The parameter-analysis of the three parameters are shown in Table 10.11 and 10.12 below. The information could not fit in one table, which is the reason why the information is split into two tables. The frequencies noted in the tables is the frequency of both the oscillations of the generator parameters on the AC-side, and the frequency of the oscillations in the voltage and current on the DC-side of the rectifier.

Table 10.11: Parameter analysis of the components $R_{battery}$ and $C_{battery}$ on the DC-side of the rectifier, while a load step in the parallel resistance P_{Load} is simulated. G2 is modeled with round rotor with governor connected, and AVR not included. $X`_q = X_q$

Parameter	Value	Operation	Frequency AC-side	Frequency DC-side	Comment
$C_{battery}$	$2100F$				
$R_{battery}$	0.0625Ω	Unstable	1.0Hz	1.0Hz	Small oscillations
P_{Load}	$0.2MW$				
$C_{battery}$	$3000F$				
$R_{battery}$	0.0625Ω	Unstable	1.0Hz	1.0Hz	Small oscillations
P_{Load}	$0.2MW$				
$C_{battery}$	$1000F$				
$R_{battery}$	0.0625Ω	Unstable	1.0Hz	1.0Hz	Small oscillations
P_{Load}	$0.2MW$				
$C_{battery}$	$500F$				
$R_{battery}$	0.0625Ω	Unstable	1.0Hz	1.0Hz	Small oscillations
P_{Load}	$0.2MW$				
$C_{battery}$	$5F$				
$R_{battery}$	0.0625Ω	Unstable	0.8Hz	0.8Hz	
P_{Load}	$0.2MW$				

Table 10.12: Continuation of Table 10.11: Parameter analysis of the components $R_{battery}$ and $C_{battery}$ on the DC-side of the rectifier, while a load step in the parallel resistance R_{Load} is simulated. G2 is modeled with round rotor with governor connected, and AVR not included. $X`_q = X_q$

Parameter	Value	Operation	Frequency AC-side	Frequency DC-side	Comment
$C_{battery}$	$2100F$				
$R_{battery}$	0.625Ω	Stable	-	-	
P_{Load}	$0.2MW$				
$C_{battery}$	$2100F$				
$R_{battery}$	6.25Ω	Stable	-	-	
P_{Load}	$0.2MW$				
$C_{battery}$	$2100F$				
$R_{battery}$	0.00625Ω	Unstable	0.3Hz	0.3Hz	
P_{Load}	$0.2MW$				
$C_{battery}$	$500F$				
$R_{battery}$	0.0625Ω	Unstable	0.5Hz	0.5Hz	-
P_{Load}	$0.5MW$				
$C_{battery}$	$3000F$				
$R_{battery}$	0.0625Ω	Unstable	0.5Hz	0.5Hz	-
P_{Load}	$0.5MW$				
$C_{battery}$	$500F$				
$R_{battery}$	0.00625Ω	Unstable	0.37Hz	0.37Hz	-
P_{Load}	$1.5MW$				

From the tables above, it is noticed that when a low value of the capacitance is applied to the

model, the frequency of the oscillations decreases, meaning that the period of one oscillation increases. It is also observed that when the resistance in the battery is increased, the system becomes stable, which is shown in earlier simulations. It is also already noted from earlier simulations, that a high load makes the period of the oscillations increases as the load increases, meaning that the frequency decreases.

10.4.4 Without the battery

Table 10.13: DC-side load step without battery.

Parameter	Value	Operation	Comment	Frequency AC-side	Frequency DC-side
P_{Load}	0	Stable		-	-
P_{Load}	$0.2MW$	Stable		-	-
P_{Load}	$0.5MW$	Stable		-	-
P_{Load}	$1.0MW$	Stable		-	-
P_{Load}	$1.5MW$	Stable		-	-
P_{Load}	$1.9MW$	Stable		-	-

When the battery is not included, the generator is stable for all values of the load resistance when the AVR is not included. The observations done on the ship says that the stability problems increases by connecting a battery to the dc-bus, but exists still when the battery is not connected. This observations is however done while the voltage regulator is connected. It is still interesting to note that the simulations shows a stable generator start-up when the battery is not connected when the AVR is not included in the model.

10.5 AC5A Voltage Regulator

Another voltage regulator, named AC5A, is now attached to the generator. The AVR AC5A is typically used in brushless excitation systems, and differs from other ac models in the way that the model uses loaded rather than open circuit exciter saturation data. It is widely used in the industry. The one-line diagram and parameter settings is found in Appendix H, where the parameter settings is found from [23].

10.5.1 Reference value of AC5A

In subchapter 9.4 for salient pole G2 and in subchapter 10.3 for round rotor G2, the reference value of the voltage regulator was changed, and the rms terminal voltage of the generator was studied. When the AVR type A was applied, the response to a change the reference value was

very time-consuming, up to 50s and longer, both when the generator was modeled as salient pole and round rotor. The generator characteristics was similar both for salient pole and round rotor, when the reference value of the voltage regulator was changed, when no load was attached on the DC-side of the rectifier except from the battery-arrangement.

The same reference value is to be changed, to see how long the response of this new voltage regulator, type AC5A, is.

No load

When the reference value of the regulator is set to 1.0, the rms terminal voltage out from the generator should be 690V, as is the nominal voltage.

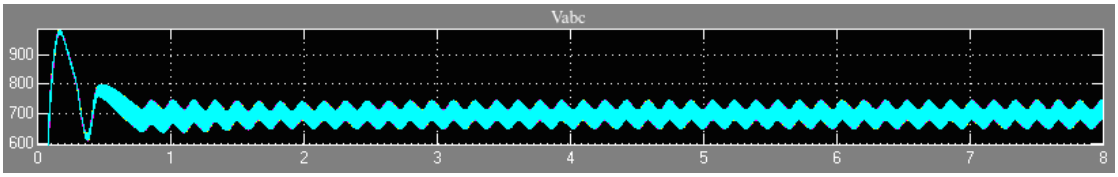

Figure 10.21: The rms terminal voltage uabc in three phases when the generator start-up is simulated, when the voltage regulator AC5A is connected and the reference value is set to 1.0. No load is attached to the DC-side except from the battery-arrangement in form of a large capacitor and a series resistance.

The voltage oscillates with a frequency of 6.2Hz and the generator looks unstable due to the standing oscillations in the rms terminal voltage. The oscillating voltage has a value close to the requested voltage, 690V. However, many of the rest of the generator parameters, including the rotor velocity, the rotor angle, the d-axis voltage, the d-and q-axis current and the current in phase a,b and c, does not oscillate. This is shown in Fig H.2 in Appendix H. For this reason, the generator is characterized as stable for the reference value $V_{ref} = 1$ for AC5A, evan though the rms terminal voltage in Fig 10.21 oscillates with a frequency of 6.2Hz.

When the reference value of the regulator is set to 1.2, the rms terminal voltage out from the generator should be 20% higher than the nominal voltage, i.e. $V_{abc} = 1.2 * 690V = 828V$.

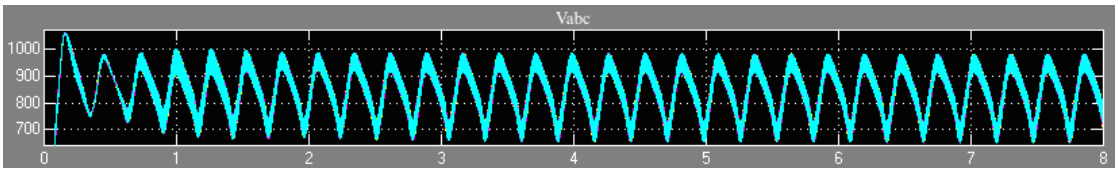

Figure 10.22: The rms terminal voltage uabc in three phases when the generator start-up is simulated, when the voltage regulator AC5A is connected and the reference value is set to 1.2. No load is attached to the DC-side except from the battery-arrangement in form of a large capacitor and a series resistance.

The voltage oscillates with a frequency of 3.7Hz and the generator output shows standing oscillations, indicating instability. The oscillating voltage has a value close to the requested voltage, 828V.

The voltage of the dc-side of the rectifier is shown below.

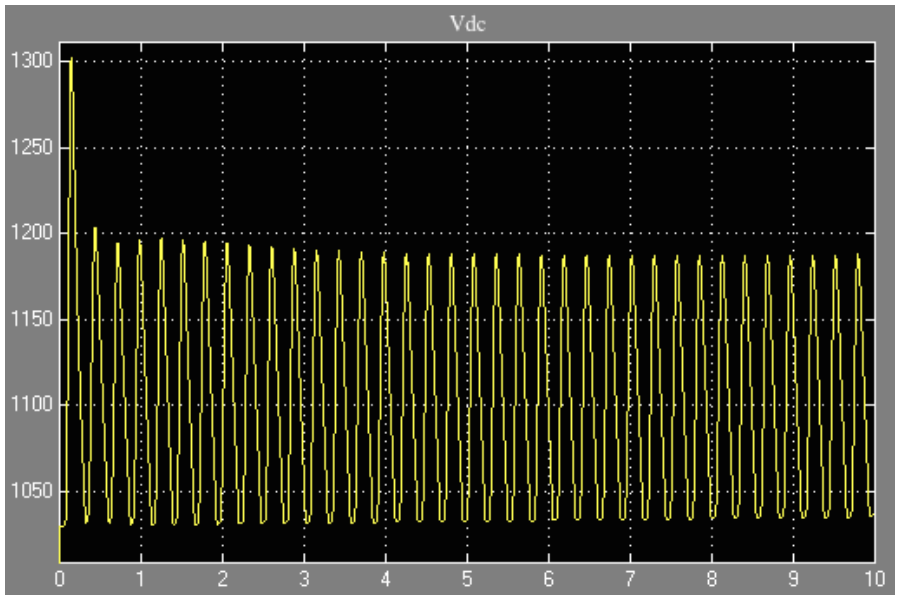

Figure 10.23: The voltage on the dc-side of the rectifier V_{dc} when the generator start-up is simulated, the voltage regulator AC5A is connected and the reference value is set to 1.2. No load is attached to the DC-side except from the battery-arrangement in form of a large capacitor and a series resistance.

The dc-voltage oscillates around the value 1120V. This is higher than the dc-voltage after the rectifier observed for the AVR type A (1030V) when the same battery-arrangement and no load is connected.

When the reference value of the regulator is set to 1.4, the rms terminal voltage out from the generator should be 40% higher than the nominal voltage, i.e. $V_{abc} = 1.4 * 690V = 966V$.

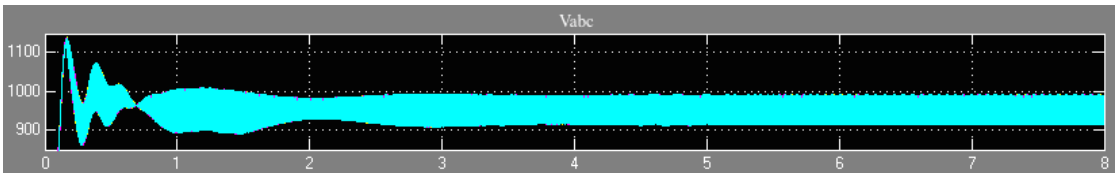

Figure 10.24: The rms terminal voltage uabc in three phases when the generator start-up is simulated, when the voltage regulator AC5A is connected and the reference value is set to 1.4. No load is attached to the DC-side except from the battery-arrangement in form of a large capacitor and a series resistance.

The voltage oscillates with a frequency of 66.67Hz and the generator is stable. The voltage has

a value close to the requested voltage, 966V.

AVR comparison in respect to reference value and no load

The voltage regulator type AC5A reacts much faster than the former voltage regulator type A that was attached to the generator. It rises the voltage to the requested voltage level within 1 second, and keeps it there. This voltage regulator type AC5A has a much lower response time than AVR type A, but the characteristics of the generator differs.

A summary of the results from the study of the voltage reference value with the two types of AVR is shown in Table 10.14 below. The frequency presented in the table is the frequency of the oscillations of the unstable generator parameters of the ac-side of the rectifier. When no frequency is mentioned, the system is stable, and there is no oscillations in the parameters.

Table 10.14: G2 characteristics when changing the reference value of two different types of AVR when no load is attached

Design	$V_{ref}[pu]$	Operation	Comment	Frequency AC-side
AVR type A, salient pole	1.0	Stable	-	-
	1.2	Unstable	after 5s	2.5Hz
	1.4	Stable	after 6s	-
AVR type A, round rotor	1.0	Stable	-	-
	1.2	Unstable	after 5s	2.5Hz
	1.4	Stable	after 6s	-
AVR type AC5A, round rotor	1.0	Stable	-	-
	1.2	Unstable	-	3.67Hz
	1.4	Stable	-	-

The generator becomes unstable when the reference value of both regulators are set to 1.2, and stable when the reference value is set to 1.0 and 1.4. The parameters oscillate with a frequency of 2.5Hz for G2 with round rotor and G2 with salient pole when the AVR type A is used, and the parameters oscillate at a frequency of 3.67Hz when the AVR AC5A is used for G2 with round rotor, when $V_{ref} = 1.2$.

Load on dc-side of rectifier

The voltage reference is set to 1.2. A load is introduced in parallel with the battery-arrangement. The load is 0.5MW. The dc-side voltage oscillated around 1120V, so the resistance load corresponding to 0.5MW is $R_{Load} = \frac{V^2}{P} = \frac{(1120V)^2}{0.5MW} = 2.51\Omega$.

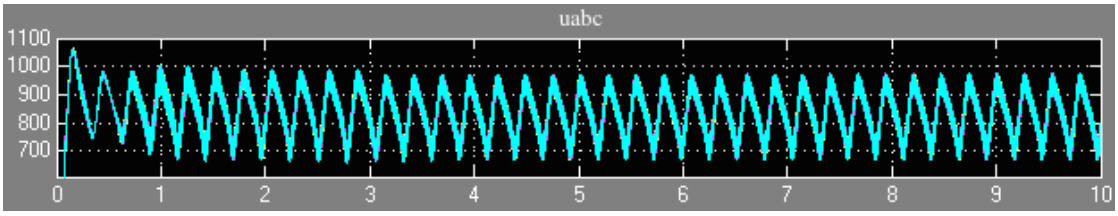

Figure 10.25: The rms terminal voltage uabc in three phases when the generator start-up is simulated, when the voltage regulator AC5A is connected and the reference value is set to 1.2. A load of $R_{Load} = 2.51\Omega$ is attached after 2 seconds in parallel with the battery.arrangement, corresponding to 0.5MW.

The rms terminal voltage oscillates with a frequency of 3.75Hz. The load is increased to 1.5MW, corresponding to $R_{Load} = \frac{V^2}{P} = \frac{(1120V)^2}{1.5MW} = 0.836\Omega$.

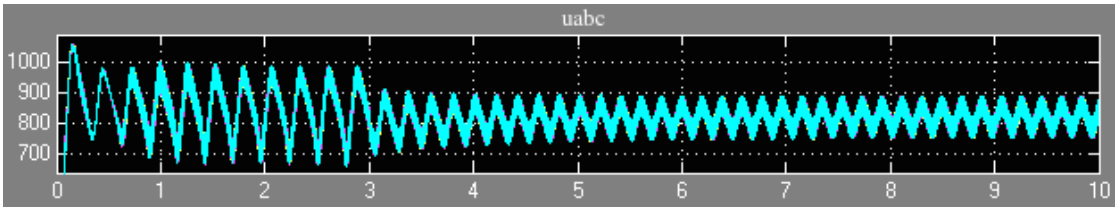

Figure 10.26: The rms terminal voltage uabc in three phases when the generator start-up is simulated, when the voltage regulator AC5A is connected and the reference value is set to 1.2. A load of $R_{Load} = 0.836\Omega$ is attached after 2 seconds in parallel with the battery-arrangement, corresponding to 1.5MW.

The oscillations decreases in amplitude when the load is introduced 3 seconds into the simulation. The frequency of the oscillations increases to 5.5Hz. The load is increased further, to 1.9MW.

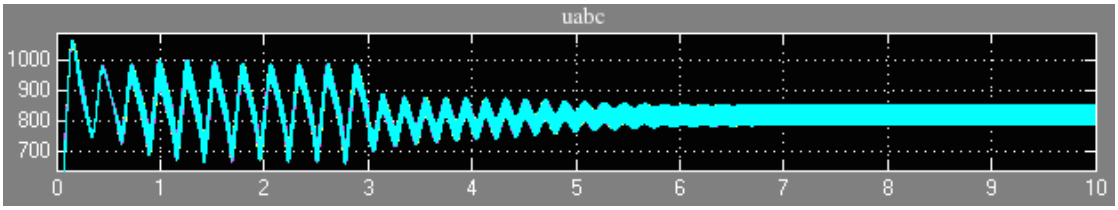

Figure 10.27: The rms terminal voltage uabc in three phases when the generator start-up is simulated, when the voltage regulator AC5A is connected and the reference value is set to 1.2. A load of $R_{Load} = 0.66\Omega$ is attached after 2 seconds in parallel with the battery-arrangement, corresponding to 1.9MW.

The oscillations in the rms terminal voltage out from the generator decreases and vanished completely when the load is increased to 1.9MW. This corresponds to earlier observations done when the AVR type A was used and the generator operates at the limit of its capacity.

10.6 Simulink Battery

A new, more complex version of the battery than the large capacitor-series resistance is added to the model. This new battery-model makes it easier to study what happens inside the battery, and how much the battery can deliver to the load in ratio to the generator. The battery is modeled by a battery-block from the Simscape-library. Both the AVR type AC5A and the AVR type A is applied.

10.6.1 AVR type A

As mentioned earlier, the stability problems in the synchronous generator is increased when the battery is connected to the DC-bus in the ship. It is therefore important to study the impact of the battery on the SM in the SimPowerSystems model, both during no-load and when an adjustable load is attached in parallel with the battery and is supplied from both the generator and battery. The AVR type A is first applied. The reference value of the AVR is set to 1.2.

Earlier, the battery was modeled as a large capacitor and a series resistance, as shown in Fig 10.20. Now, this configuration is replaced by a battery-block from the Simscape-library, as shown in the one-line diagram in Fig 10.28 below. The battery is of the lithium-ion type, similar to the type used on the ship.

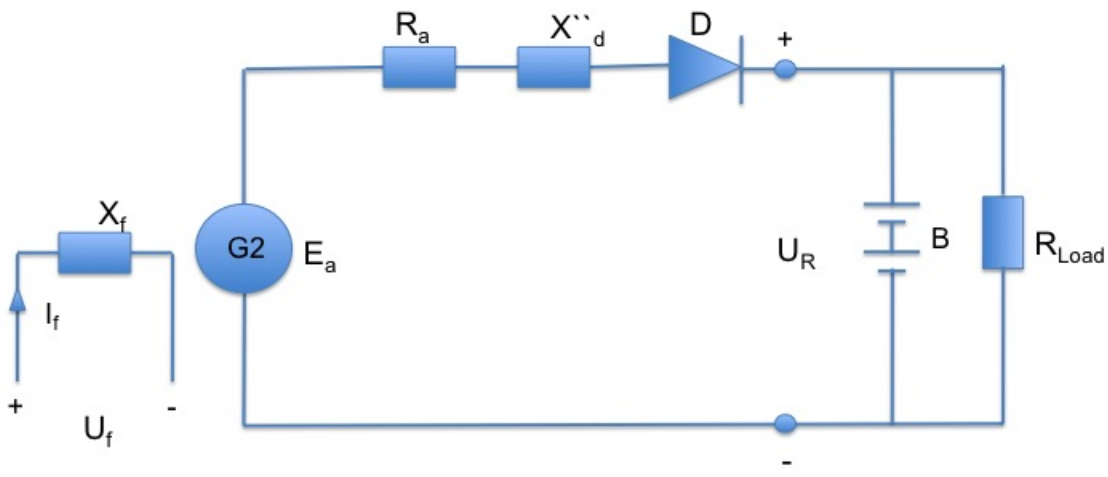

Figure 10.28: The system after the generator-rectifier-arrangement consists of a battery block B. D represents the diode-bridge rectifier. A resistance R_{load} is placed in parallel with the battery and is adjustable.

The size of the battery can be adjusted, but as a first presumption, the battery can be assumed to be 150Ah. Some evaluation of this battery capacity is needed. If it is assumed that the battery can operate in 1h, the current is 150A since $C = h * A$. The voltage that the battery receives

from the generator trough the rectifier is approximately 1000V. This makes the power of the battery $P_{battery} = 150A * 1000V = 150kW$. The nominal power of the generator is 1940kVA, which makes the size of the battery approximately 7-8% of the size of the generator.

With this battery capacity, the battery can take some spikes of the load characteristics when needed. It can support the generator, delivering about 8% of the power needed in one hour, or it can support a larger percentage of the load supplied for shorter periods if redundancy is needed. A battery capacitance of 150Ah seems for these reasons appropriate.

500Ah: P=500A*1000V=500kW –> 26%

The nominal voltage of the battery is set to be 1030V and the initial state of charge is set to 100%. The equivalent circuit, discharge model and charging model of the lithium-ion type battery is shown in Appendix G. The voltage regulator type A and governor is included and connected to the generator, and the reference value of the AVR is set to 1.2.

The discharge characteristics of the battery is shown in Fig 10.29 and Fig 10.30 below.

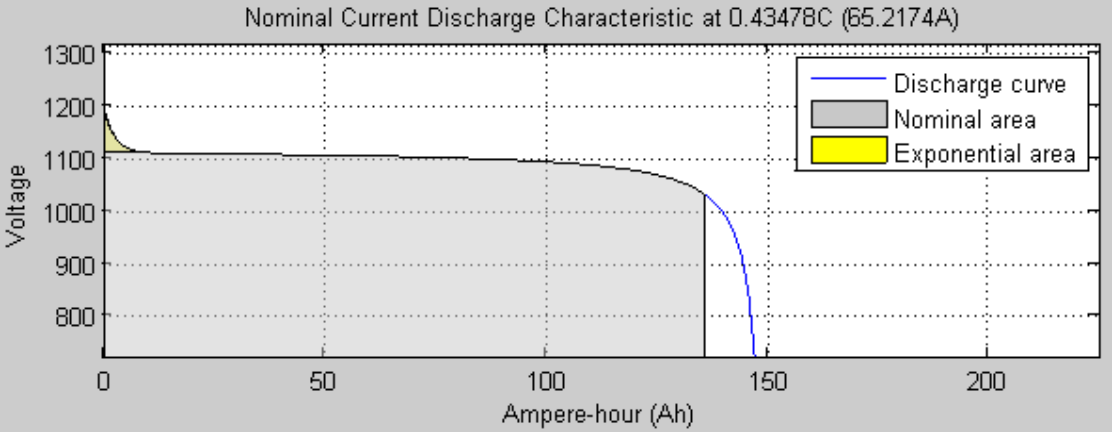

Figure 10.29: The nominal current discharge characteristics of the battery.

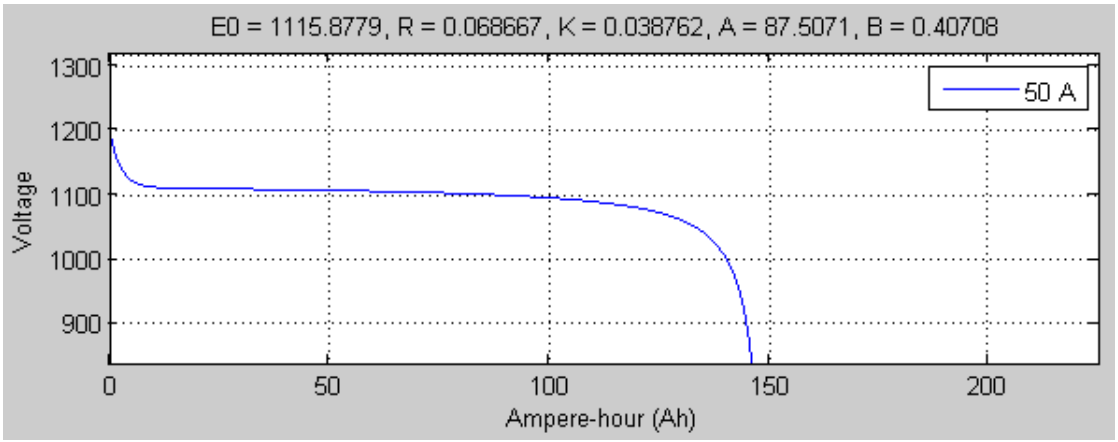

Figure 10.30: The battery profile.

The nominal current discharge characteristic taken from the battery shows the nominal and the exponential area and the discharge current. It can be red from the graph that if the current drawn from the battery is 50A, the battery can deliver 1115V for one hour. If the current drawn is 100A, the battery can deliver 1115V for two hours.

The constant voltage E_0 is 1115V, which is 85V higher than the nominal voltage. If the rated capacity is increased to 300Ah, but the initial voltage is kept to 1030V, the constant voltage is still 1115V, as shown in Appendix G.3. If the initial voltage is decreased to 950V, and the rated capacity is kept at 300Ah, the constant voltage is decreased to 1029V, as shown in Appendix G.4. This is a difference of +80V from the initial voltage. It seems that the constant voltage is increased by some 8% from the initial voltage inserted, and that the capacity (Ah) does not impact the constant voltage.

Because the bus voltage is 1030V dc, the initial voltage of the battery is decreased from 1030 to 950V to get a constant voltage of ≈1030V. The discharge characteristics for the battery with 150Ah and nominal voltage of 950V is shown in Appendix G.5.

No load

The voltage, current and state of charge out from the battery measured during the simulation of the generator start-up is shown in Fig 10.31 below. The load is not yet attached, to see how the charging current and voltage of the battery is, without any load to supply. The initial state of charge is 100%.

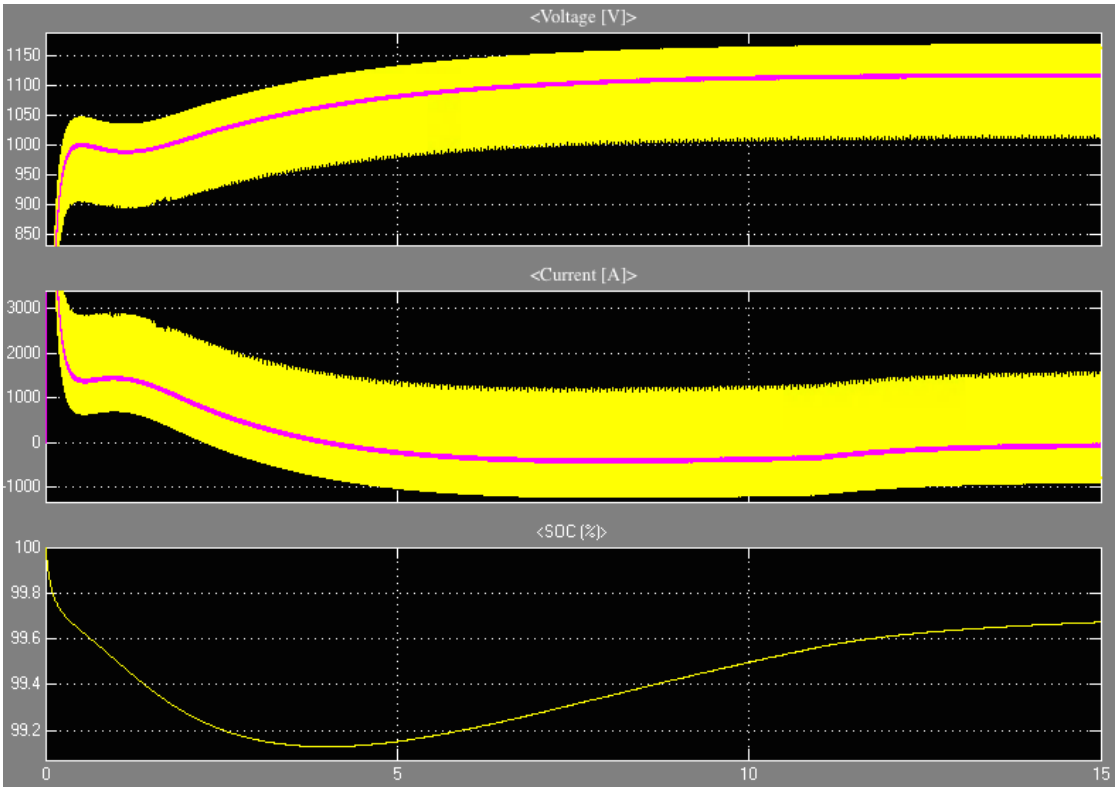

Figure 10.31: From the top: the voltage (yellow), rms voltage (pink), current (yellow), mean current (pink), and state of charge of the battery during the generator start-up, when no load is attached. The battery has a capacity of 150Ah and a nominal voltage of 950V.

From the bottom, it is observed that the state of charge starts at the initial charge of 100%, before it drops 0.8%. The voltage increases as the SoC drops, and the current is positive and decreases. Because there is no load attached, the battery starts to charge after 4 seconds, causing the voltage to increase up to a value of 1100V. The current is defined as positive when the battery is discharging, and negative when the battery charges, and has a value of -100A after 5 seconds. The generator supplies the battery with a power of $P = V * |I| = 1100V * 100A = 110kW$ ($\approx 6\%$ of the generator size, 1.94MW).

It is observed no oscillations from the outputs from the battery. The rms terminal voltage and terminal current from the generator is shown in Fig 10.32 below.

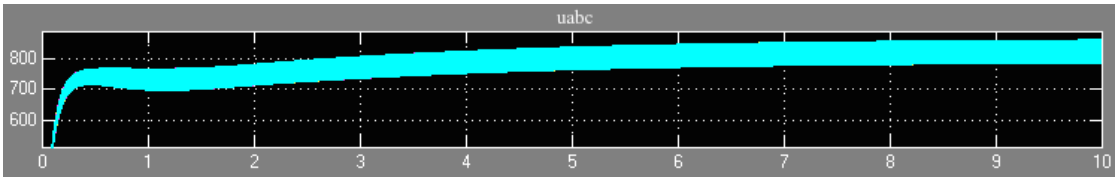

Figure 10.32: From the top: the rms terminal voltage *uabc* from the 1940kVA generator with round rotor, when a SimScape battery-block of 150Ah and no load is attached after the rectifier. The governor and AVR with $V_{ref} = 1.2$ is attached.

No instabilities are observed from the terminal voltage of the generator when no load is attached at the dc-side of the rectifier except form the 150Ah battery. This coincides with earlier observations when simulating the generator start-up of the 1940kVA generator with no load except from a battery-arrangement, and AVR type A attached. The terminal voltage adjusts to approximately 828V, as the regulator is programmed to do.

Next, a load is attached and the stability is studied while the load is varied.

Load at dc-side of rectifier

A load is now introduced after 3 seconds into the simulation. The load is active and have a magnitude of 0.5MW. This is almost 26% of the generator size (1.94MW). The bus voltage is 1030V. Therefore is a load of $R_{Load} = \frac{U^2}{P} = \frac{(1030V)^2}{500kW} = 2.122\Omega$ attached after 3 seconds into the generator start-up simulation. The voltage, current and state of charge out from the battery in this situation is shown in Fig 10.33.

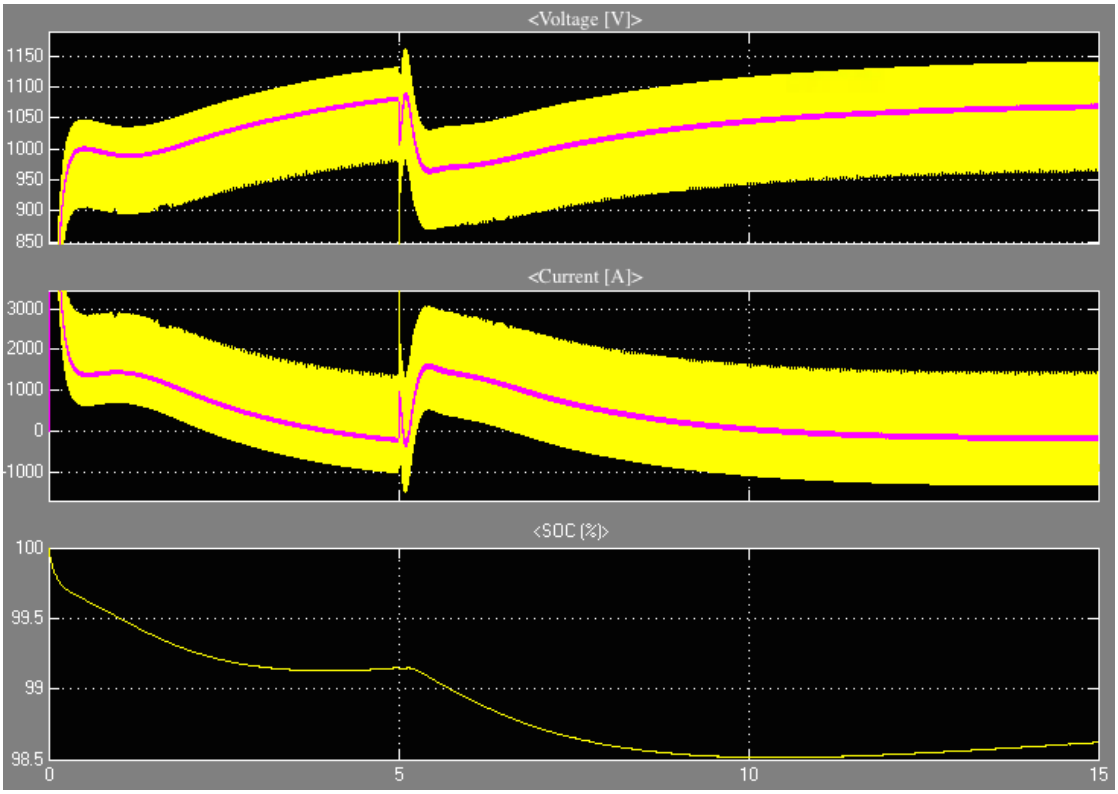

Figure 10.33: From the top: the voltage (yellow), rms voltage (pink), current (yellow), mean current (pink), and state of charge of the battery during the generator start-up, when a load of $R_{Load} = 2.122\Omega$ which corresponds to 500kW, is connected to the dc-side of the rectifier 3 seconds into the simulation. The battery has a capacity of 150Ah and a nominal voltage of 950V.

After 10 seconds, the current is negative, indicating that the battery charges, and that the generator supplies both the battery and load after 10 seconds. This is also shown in the graph at the bottom of Fig 10.33, showing SoC; after 10 seconds the state of charge increases.

The rms terminal voltage and terminal current from the generator is shown in Fig 10.34 below.

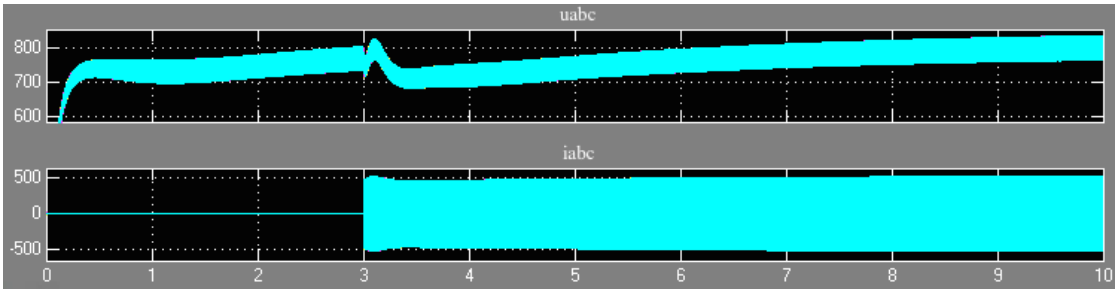

Figure 10.34: From the top: the rms terminal voltage *uabc* from the 1940kVA generator with round rotor, when a SimScape battery-block of 150Ah and a load of 0.5MW is attached after the rectifier. The governor and AVR with $V_{ref} = 1.2$ is attached.

No instability is detected in the output parameters from the generator when the 150Ah battery and 0.5MW load is attached after the rectifier, and the AVR with $V_{ref} = 1.2$ is connected. This is the opposite of the operation situation observed when the same load and AVR type A was attached, but the battery was modeled by a large capacitor and a series resistance, as shown in Table 10.6 in chapter 10.3.

The power from the battery and the power from the generator through the rectifier can be studied to determine which of the two power sources supplies the load of 0.5MW.

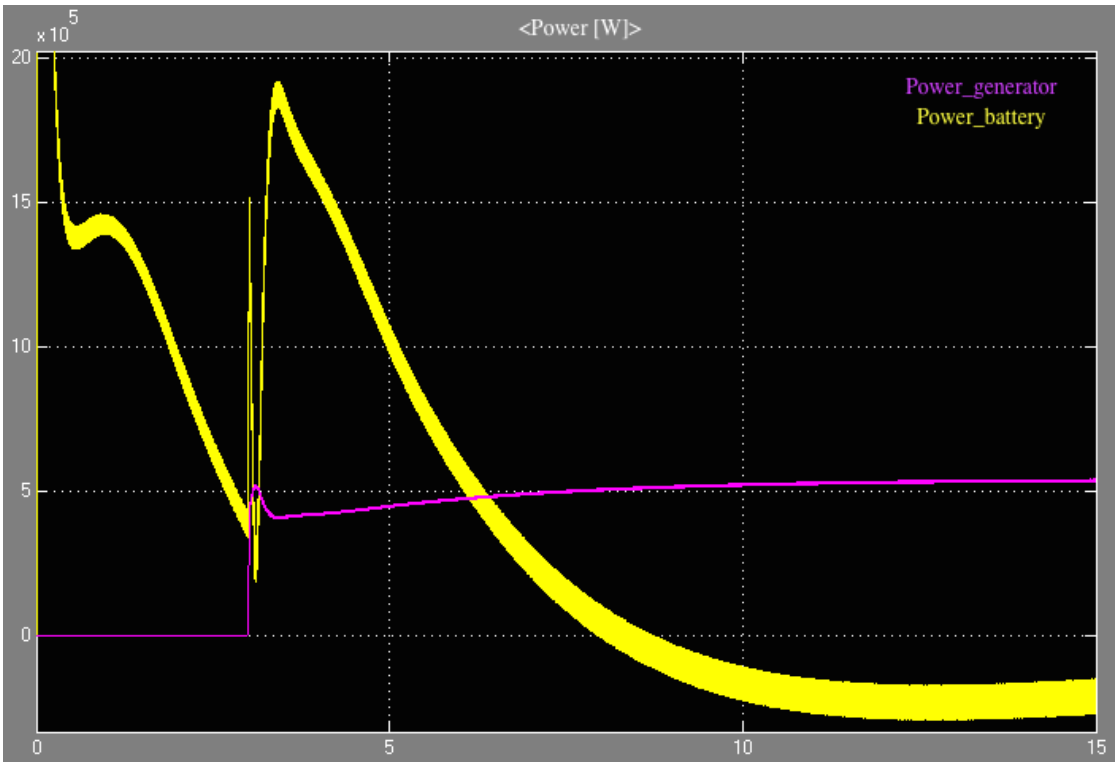

Figure 10.35: Power out from the generator(pink) and power out from the battery(yellow) during the generator start-up, when a load of $R_{Load} = 2.122\Omega$ which corresponds to 500kW, is connected to the dc-side of the rectifier 3 seconds into the simulation. The battery has a capacity of 150Ah and a nominal voltage of 950V, and an initial state of charge of 100%.

When the load is 0.5MW and the 150Ah battery has an initial state-of-charge of 100%, both the battery and the generator supplies the load the first 1,5 seconds, until the generator supplies both the generator and the battery. The battery has an initial large power-peak when the load is introduced, of approximately 1.9MW. After 8 seconds, the power of the battery is negative, indicating that the battery is in charging modus. The power from the generator has a spike of 5.2 before the power decreases to a value of 4.1MW, but as the battery charges it increases to 5.2MW again.

When the same load is introduced after 3 seconds, but the 150Ah battery starts with an initial state-of-charge of 80% instead of 100%, the distribution of the load-supply changes characteristics, as shown from the power-graph below.

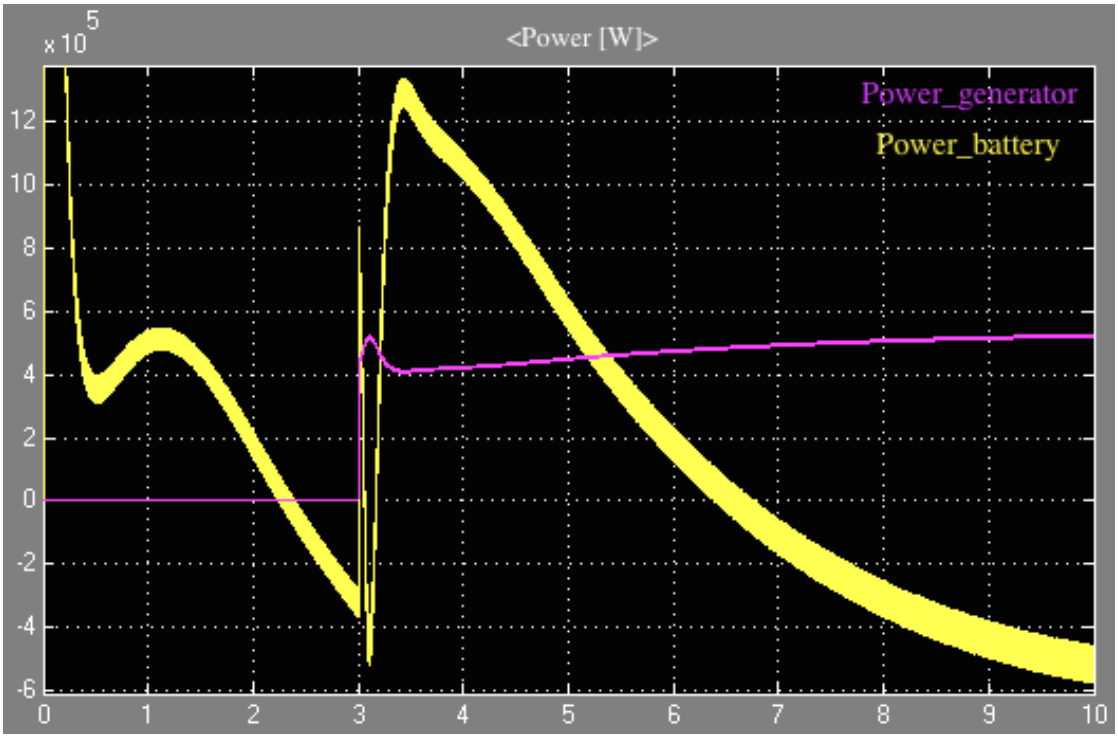

Figure 10.36: Power out from the generator(pink) and power out from the battery(yellow) during the generator start-up, when a load of $R_{Load} = 2.122\Omega$ which corresponds to 500kW, is connected to the dc-side of the rectifier 3 seconds into the simulation. The battery has a capacity of 150Ah and a nominal voltage of 950V, and an initial state of charge of 80%.

The spike of the power delivered from the battery has decreased to approximately 1.35MW, but this is still very high. The spike of the power delivered by the generator is 1.1MW high, going from 4.1MW to 5.2MW. This is the same as before. The generator delivers all the power to the load after 2.3 seconds after it was introduced, i.e 5.3 seconds into the simulation. The battery starts charging after 6.5 seconds into the simulation, and the power from the generator starts to increase towards 6MW, indicating that is supplies both the battery (110kW) and the load (0.5MW).

It is interesting to see how the generator behaves when the battery is not connected at all, but the same load is introduced after 3 seconds.

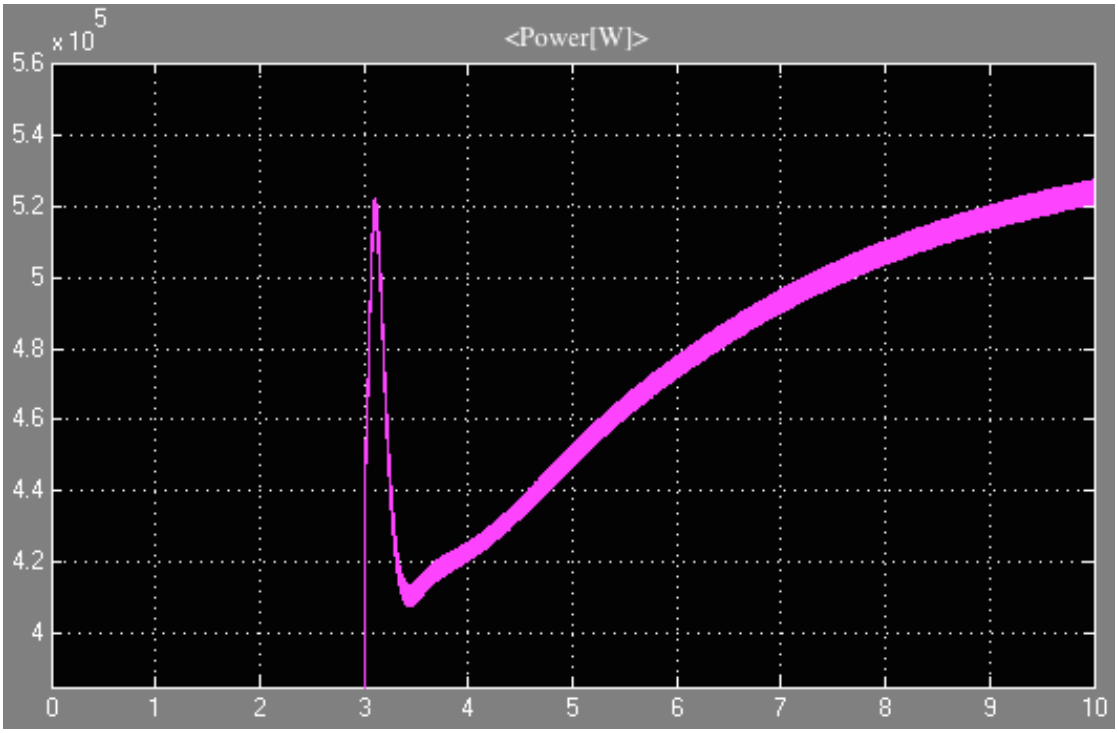

Figure 10.37: Power out from the generator during the generator start-up, when a load of $R_{Load} = 2.122\Omega$ which corresponds to 500kW, is connected to the dc-side of the rectifier 3 seconds into the simulation. The battery is not included.

The spike is 1.1MW high, going from 4.1MW to 5.2MW when the battery is removed. This is the same as it was before, when the battery was included. The generator seem to not have changed behavior when the battery is removed.

The load is increased, to see if the load-supply distribution between the generator and battery changes, and to see if any instability is to be detected, like in earlier simulation including AVR, battery and load. The load is increased to 1.5MW.

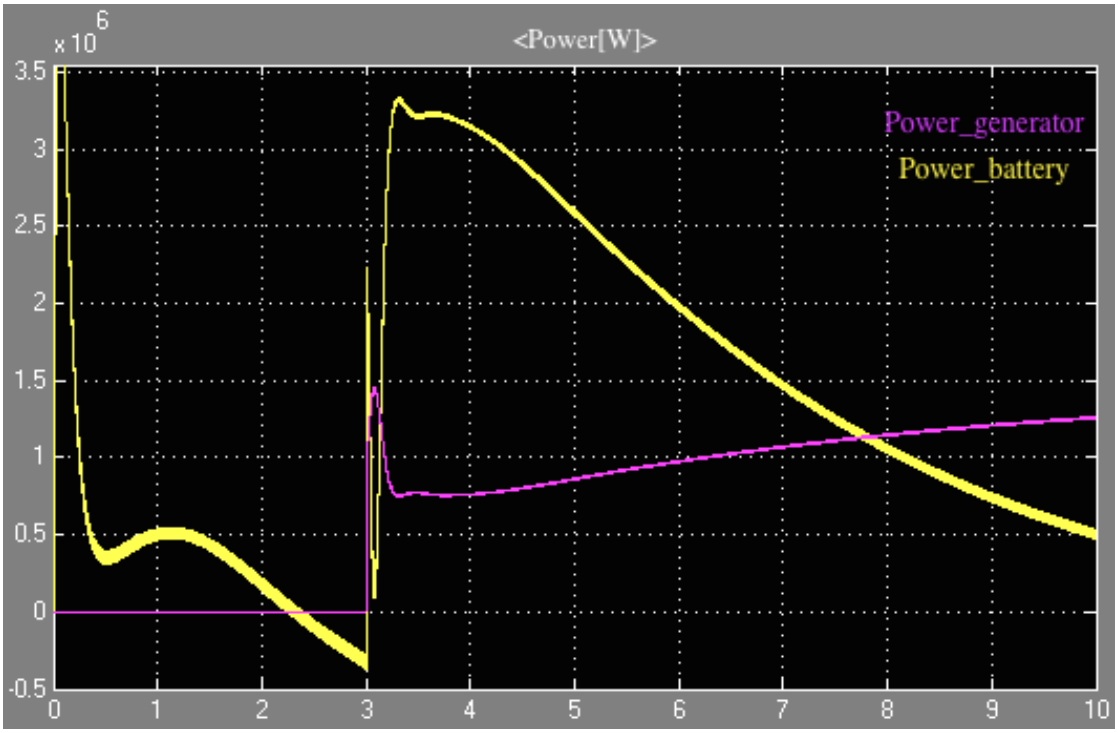

Figure 10.38: Power out from the generator(pink) and power out from the battery(yellow) during the generator start-up, when a load of $R_{Load} = 0.707\Omega$ which corresponds to 1.5MW, is connected to the dc-side of the rectifier 3 seconds into the simulation. The battery has a capacity of 150Ah and a nominal voltage of 950V, and an initial state of charge of 80%.

No instability is detected as a result of the attachment of an increased load. The spike of the power delivered from the generator reaches 1.45MW when the load is introduced after 3 seconds, then it falls down to 0.77MW, before it starts to climb towards 1.26MW. It supplies load alone after 7.8seconds. The spike of the battery reaches 3.3MW before it decharges.

To study the generator stability when the generator operates at the limit of its capacity, the load is increased. The battery draws 110kW. If the generator is to operate at the limit of its capacity, 1.94MW, the load must be 1.94MW-0.11MW=1.83MW. This corresponds to a resistance load of $R_{Load} = \frac{(1030V)^2}{1.83MW} = 0.58\Omega$. The load is attached 3 seconds into the start-up simulation of the motor.

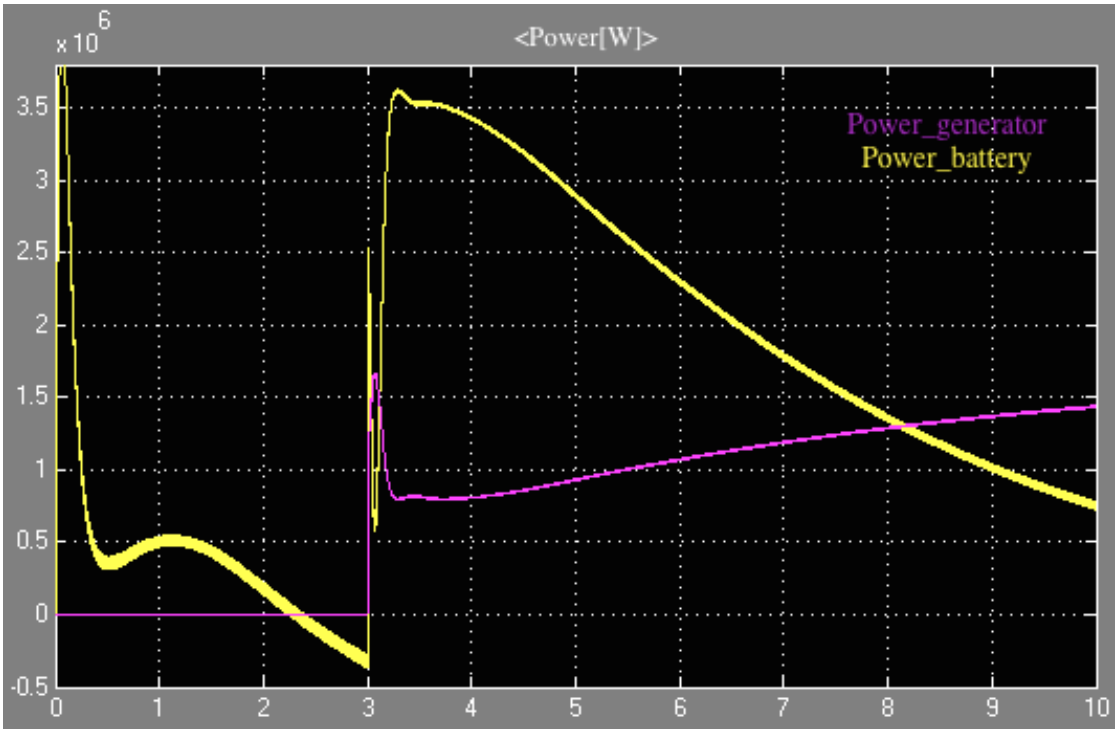

Figure 10.39: Power out from the generator(pink) and power out from the battery(yellow) during the generator start-up, when a load of $R_{Load} = 0.58\Omega$ which corresponds to 1.83MW, is connected to the dc-side of the rectifier 3 seconds into the simulation. The battery has a capacity of 150Ah and a nominal voltage of 950V, and an initial state of charge of 80%.

No instability is detected when the generator runs at its top capacity. The spike of the battery reaches 1.37MW before it decreases. The generator has a spike of 1.67MW when the load is introduced, before it decreases to 0.8MW, and then it increases as the battery-power decreases.

The AVR type A is replaced by the AVR type AC5A, to study the load-supply of the two power-sources.

10.6.2 AVR type AC5A

The AVR type AC5A is applied to the model consisting of generator, governor, rectifier, Simulink-battery and load. The reference value of the AVR is 1.2.

No load

When the reference value of AVR type AC5A is 1.2, the bus voltage is expected to be 1120V as previous simulations shows when no load is attached and the reference value of AC5A is

1.2, in Fig 10.23 in chapter 10.5. No load is attached to the dc-side of the rectifier. The battery has a capacitance of 150Ah, an initial state of charge of 80% and a nominal voltage of 1120V*0.92%=1030V.

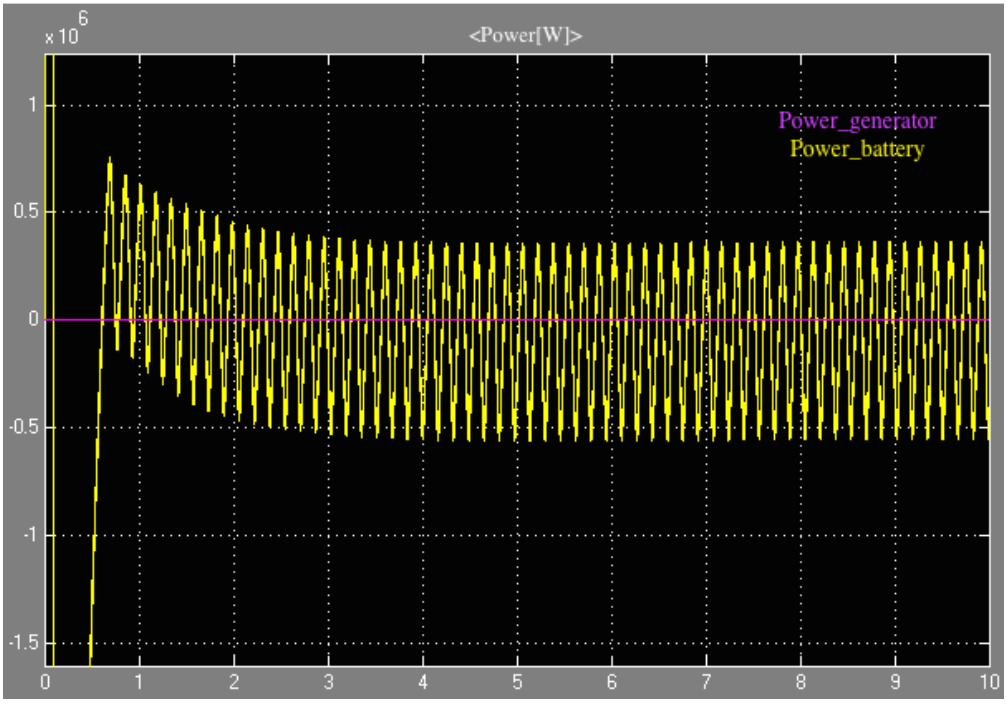

Figure 10.40: Power out from the generator(pink) and power out from the battery(yellow) during the generator start-up, during no-load. The battery has a capacity of 150Ah and a nominal voltage of 1030V, and an initial state of charge of 80%. The AVR type AC5A is applied, and $V_{ref} = 1.2$.

When the generator operates at no load, with no load at the dc-side of the rectifier except from the battery, the generator delivers no power. The power of the battery oscillates with a frequency of 6.2Hz, and shows instability. The rms terminal voltage and terminal current of the generator is shown below.

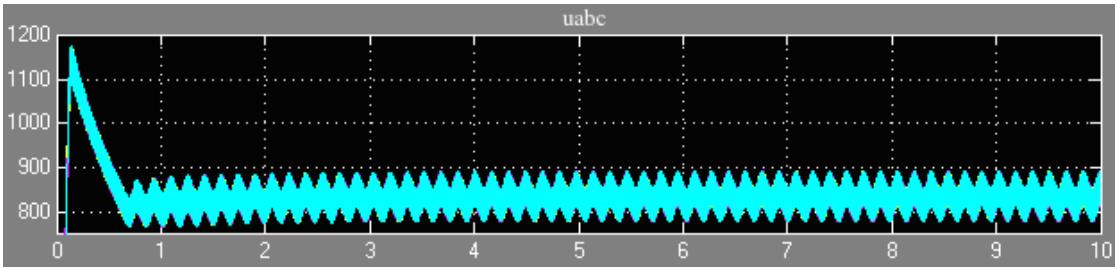

Figure 10.41: The rms terminal voltage *uabc* from the 1940kVA generator with round rotor, when a SimScape battery-block of 150Ah and no load is attached after the rectifier. The governor and AVR AC5A with $V_{ref} = 1.2$ is attached.

The voltage oscillates with a frequency of 6.2Hz and the generator seems to be unstable due to the standing oscillations in the rms terminal voltage. The rms voltage oscillates around the requested voltage, 828V. However, many of the rest of the generator parameters, including the rotor velocity, the rotor angle, the d-axis voltage, the d-and q-axis current and the current in phase a,b and c, does not oscillate. This is shown in Fig H.3 in Appendix H. For this reason, the generator will be classified as stable for the reference value $V_{ref} = 1.2$ for AVR type AC5A when the 150Ah battery is connected, even though the rms terminal voltage in Fig 10.41 oscillates with a frequency of 6.2Hz. This was also the case for $V_{ref} = 1.0$ and no load with AVR type AC5A attached in Chapter 10.5.

Load on dc-side

A load of 0.5MW corresponds to a load resistance of $R_{Load} = \frac{V^2}{P} = \frac{(1120V)^2)}{0.5MW} = 2.51\Omega$ and is attached 3 seconds into the simulation. The battery has a capacitance of 150Ah, an initial state of charge of 80% and a nominal voltage of 1030V.

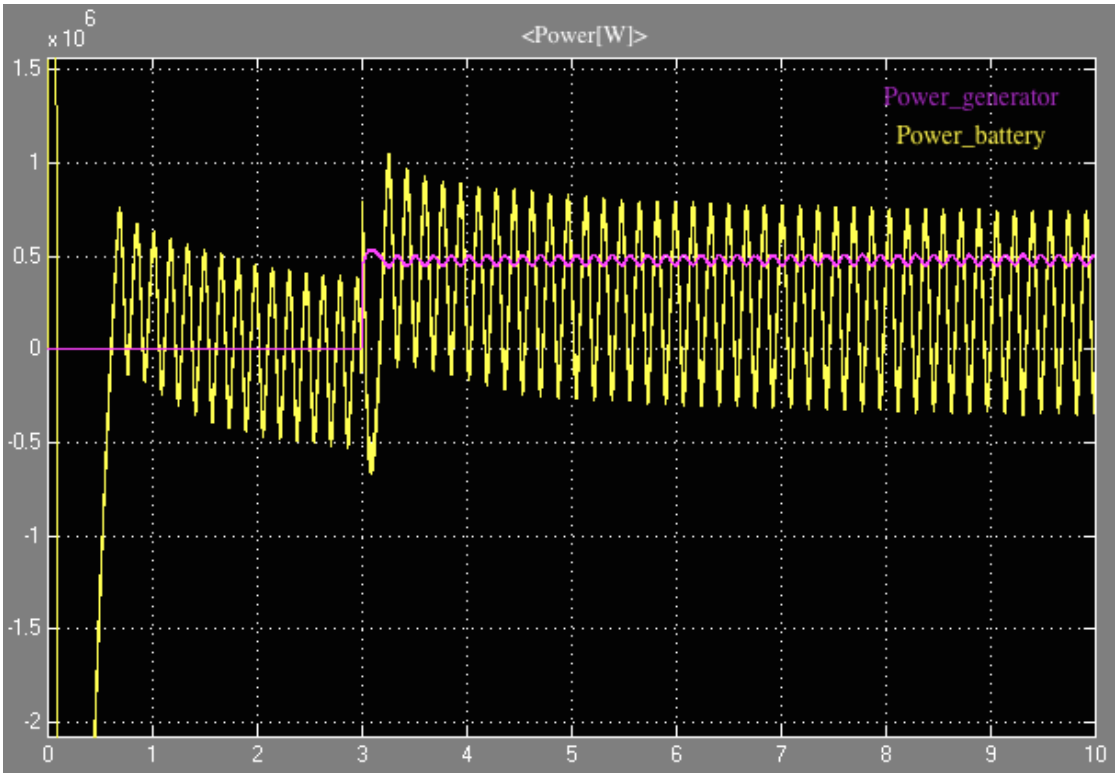

Figure 10.42: Power out from the generator(pink) and power out from the battery(yellow) during the generator start-up, when a load of $R_{Load} = 2.51\Omega$ which corresponds to 0.5MW, is connected to the dc-side of the rectifier 3 seconds into the simulation. The battery has a capacity of 150Ah and a nominal voltage of 1030V, and an initial state of charge of 80%. The AVR type AC5A is applied, and $V_{ref} = 1.2$.

The power from the generator and battery oscillates with a frequency of 6Hz. The power oscillates around the value 0.5MW, the size of the load. The load is increased to 1.9MW corresponding to a resistance load of 0.66Ω.

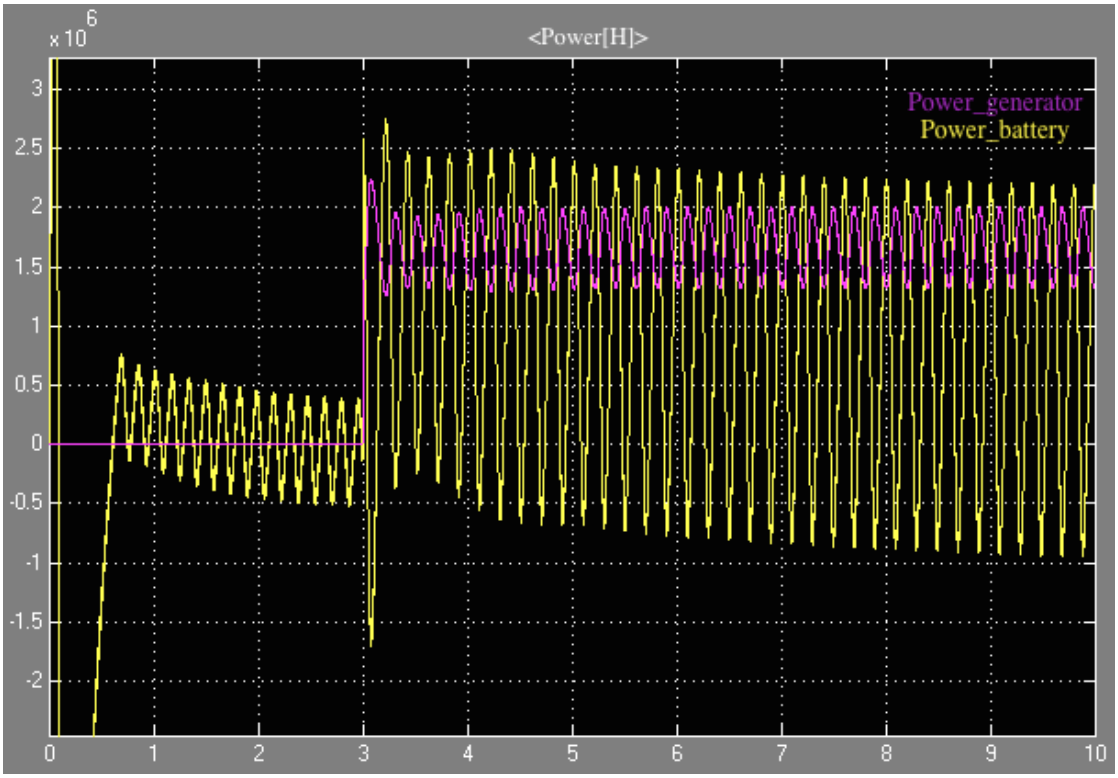

Figure 10.43: Power out from the generator(pink) and power out from the battery(yellow) during the generator start-up, when a load of $R_{Load} = 0.66\Omega$ which corresponds to 1.9MW, is connected to the dc-side of the rectifier 3 seconds into the simulation. The battery has a capacity of 150Ah and a nominal voltage of 1030V, and an initial state of charge of 80%. The AVR type AC5A is applied, and $V_{ref} = 1.2$.

The generator does not show stability when it runs at its capacity limit. This differs from previous simulations. The amplitudes increases in size and the frequency is 5Hz. The power of the generator oscillates around the load size, 1.9Mw.

10.7 Without the Rectifier

The rectifier and battery is replaced by a delta-connected load. The synchronous generator has the initial parameter settings and $X`_q = X_q$, and the load can be varied. Both voltage regulators is tried out, and the reference value of both regulators is set to 1.2.

10.7.1 AVR type A

First, the AVR type A is connected to the 1940kVA generator with round rotor. The load connected to the generator output is 1500kVA.

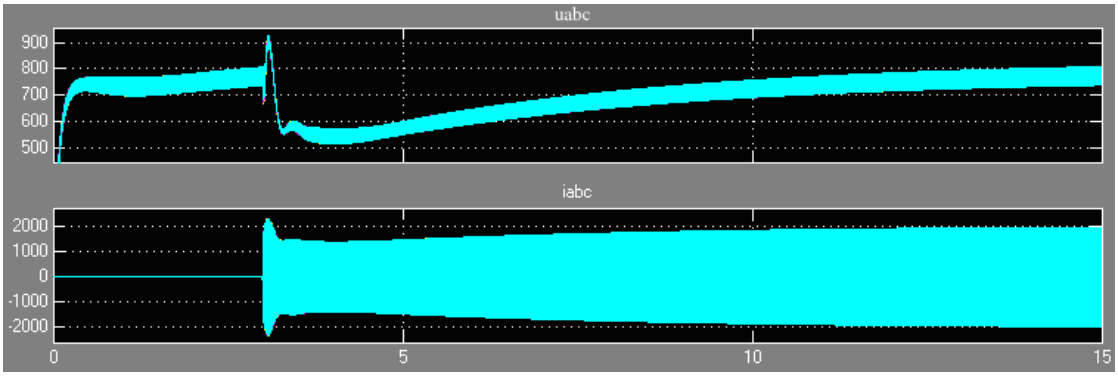

Figure 10.44: The AVR type A is connected to the 1940kVA generator, and a load of 1500kVA is connected to the generator terminals. No rectifier is applied.

The generator shows a stable operation. The regulator does not regulate the voltage back up to 828V after the load step, but is still decreasing after 15s. The load is increased to 1900kVA.

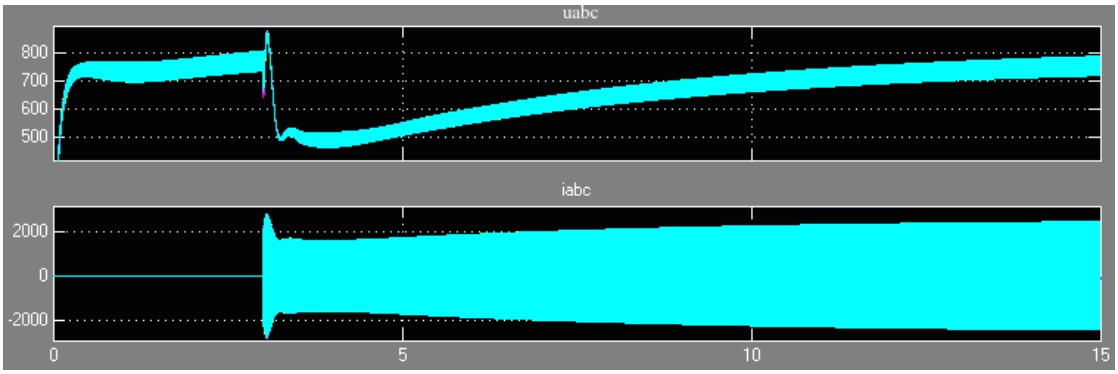

Figure 10.45: The AVR type A is connected to the 1940kVA generator, and a load of 1900kVA is connected to the generator terminals. No rectifier is applied.

The generator is still stable. The generator type AC5A is now connected to the generator, and the load is initially 1000kVA.

10.7.2 AVR type AC5A

The AVR AC5A is applied, with the reference value set to 1.2.

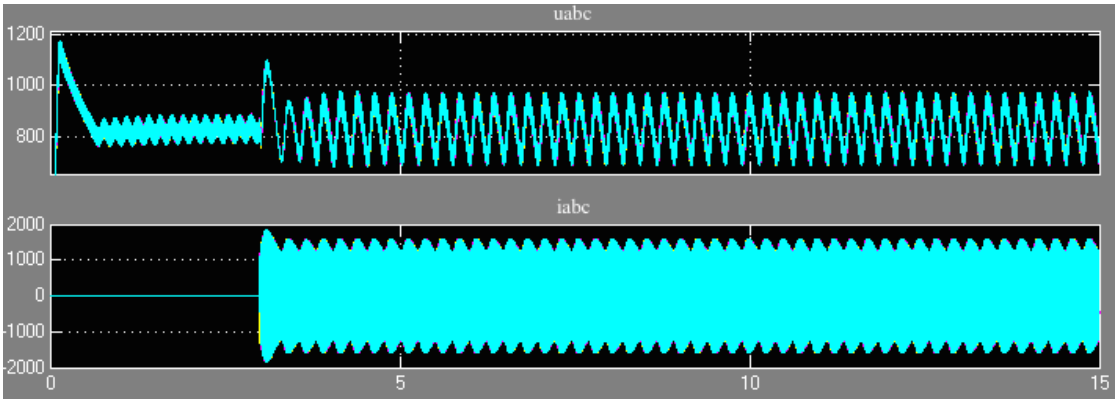

Figure 10.46: The AVR type AC5A is connected to the 1940kVA generator, and a load of 1000kVA is connected to the generator terminals. No rectifier is applied.

The generator is unstable when the AVR type AC5A is applied with no rectifier and a load of 1000kVA. The frequency of the oscillations is of 4.125Hz. The pulsed nature of the current is gone. The load is increased to 1900kVA.

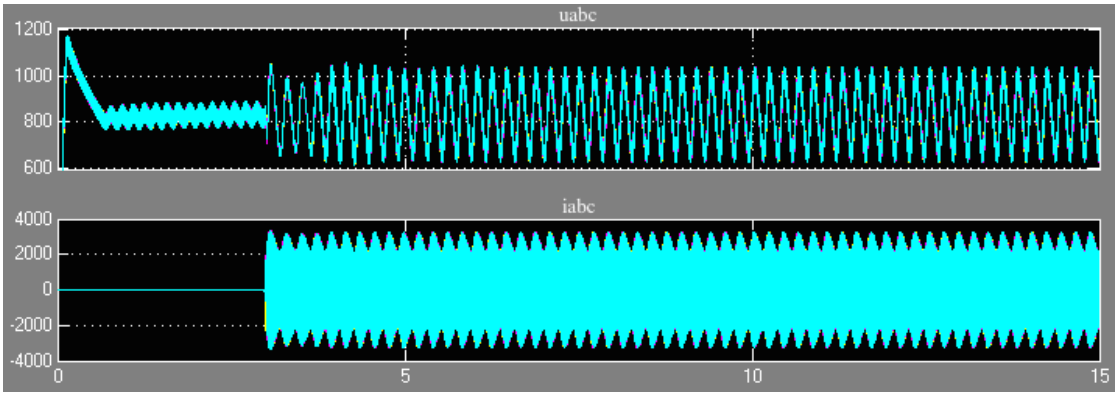

Figure 10.47: The AVR type AC5A is connected to the 1940kVA generator, and a load of 1900kVA is connected to the generator terminals. No rectifier is applied.

The generator is unstable when the AVR type AC5A is applied with no rectifier and a load of 1900kVA. The frequency of the oscillations is of 4.75Hz.

10.8 Excitation of the Generator Field

In the general stability criterion presented by [2], it is suggested that U_d depends on the excitation of the generator. The load is set to 0.5MW, and the voltage of the constant voltage source exciting the generator field is increased. The load resistance corresponds to $R_{Load} = \frac{V^2}{P} = \frac{(1030V)^2}{0.5MW} = 2.122\Omega$.

Table 10.15: Excitation voltage. $P_{Load} = 0.5MW$

$V_{exciter}$	Operation	Frequency	Comment
21V	Unstable	0.5Hz	-
50V	Stable	-	-
40V	Unstable	1.78Hz	-
45V	Unstable	2.2Hz	Decreasing amplitude
47.5V	Stable after 6s	-	-
46.5V	Stable after 5s	-	-
46.0V	Stable	-	-
45.5V	Stable after 18s	-	-

The stability is clearly affected by the value of the dc-voltage exciting the generate field. The generator is stable when the value of the exciter-voltage is $V_{exciter} > 45V$. The load is increased, to see how the operating point affects the stability when the exciter-voltage is varied. The generator is expected to reach instability for a lower value of $V_{exciter}$ for a higher load.

Table 10.16: Excitation voltage. $P_{Load} = 1.5MW$

$V_{exciter}$	Operation	Frequency	Comment
21V	Unstable	0.56Hz	-
50V	Stable	-	-
40V	Unstable	1.8Hz	-
45V	Stable after 6s	-	-
42.5V	Unstable	2.9Hz	-
44V	Stable after 12s	-	-
43V	Unstable	2.17Hz	Decreasing
43.5V	Stable after 19s	-	-

The generator is stable when the value of the exciter-voltage is $43.5V < V_{exciter}$. This is a lower stability-limit than when the load was 0.5MW. This was expected, due to the stability criterion presented by [2]:

$$X'^2_d I'^2_d + X'^2_q I'^2_q \leq 2X'_d I'_d U_p \tag{10.3}$$

that shows that the stability is dependent on the transient current I'_d and the stationary source voltage U_p. U_p depends on the excitation of the generator. The simulations summarized in Table 10.15 and 10.16 coincides with this theory, by the fact that the stability is enhanced when the exciter-voltage increases, which directly affects U_p in an increasing manner, and that the generator reaches instability faster when the load is increased, which directly affects I'_d and I'_q.

The load increase affects both sides of the equation, but because I'_d and I'_q on the left side of the equation is squared, and I'_d on the right side is not, the load increase affects the left side of the equation the most. This affects the stability in a negative manner. Based on experience from the ship has [2] concluded that the stability problems can not be eliminated or damped by controlling the excitation current, because the transient current I' changes much faster than the excitation current.

However, the difference between the stable value of exciter-voltage when the load is 0.5MW and when the load is 1.5MW is not as large as would be expected.

As simulations done in this thesis has shown, reaches the generator stability when it operates at its capacity limit, meaning at high load. The load is increased even further, to 1.9MW. This corresponds to a resistance load of $R_{Load} = \frac{(1030V)^2}{1.9MW} = 0.56\Omega$.

Table 10.17: Excitation voltage. $P_{Load} = 1.9MW$

$V_{exciter}$	Operation	Frequency	Comment
21V	Unstable	0.625Hz	-
50V	Stable	-	-
40V	Unstable	1.85Hz	-
45V	Stable	-	-
42.5V	Stable after 19s	-	-
41.5V	Unstable	1.88Hz	-
42V	Unstable	2Hz	Decreasing

The generator is stable when the value of the exciter-voltage is $42.5V < V_{exciter}$, which is a lower value than when the load was 0.5MW and 1.5MW, but the difference between the stable value of exciter-voltage when the load is 1.9MW compared to when the load is 0.5MW and 1.5MW, is smaller than expected. This can indicate that the load is not as influential on generator stability as the exciter current is. Meaning that increasing U_d affects the stability in a more positive manner, than the increasing of I' affects the stability in a negative manner. The results from the exciter-voltage varying experiment is shown in Table 10.18 below.

Table 10.18: Criterion for exciter-voltage value for a stable operation at different loads.

P_{Load}	Exciter voltage to secure stable operation
0.5MW	$V_{exciter} > 45V$
1.5MW	$V_{exciter} > 43.5V$
1.9MW	$V_{exciter} > 42.5V$

When the load is increased, the value for the exciter-voltage criterion decreases, to keep the generator stable.

10.9 Impact of Subtransient Reactances on Stability

The stability criterion presented by both [1] and [2] only contains requirements for the transient reactances in d-and q-axis, the subtransient reactances is not mentioned in this criteria.

As found in 9.1 for G2 with salient pole does the subtransient reactance in the q-axis impact the stability greatly. The generator behaves unstable when the ratio between the subtransient reactances has the value $\frac{X“_q}{X“_d} = 1.048$. Usually, a ratio of 1.048 between the subtransient reactances $X“_q$ and $X“_d$ would describe a stable generator, but this is not the case for the 1940kVA generator. When the factor between the ratio $\frac{X“_q}{X“_d}$ is varied, but the ratio held constant a the value 1.048, the generator is unstable for all factors. The subtransient q-axis reactance is also varied while other parameters is held constant, and it is found that the generator becomes stable when $X“_q < 0.175pu$.

In Chapter 10.1 and 10.2 the value of the transient q-axis reactance is studied for two scenarios; $X_q = X_q$ and $X_q = X_d$. When $X_q = X_q$, the generator is stable when $X‘_q < 2.7pu$. When $X_q = X_d$, the generator is stable when $X‘_q < 2.65pu$.

The subtransient, transient and synchronous reactances for G1 was studied in Chapter 8.4. It was found, that the synchronous reactance in the q-axis impaced the stability of G1 with salient pole more than the transient and subtransient reactances in the d-and q-axis.

10.9.1 No load

The impact of the subtransient reactances on the stability is to be studied for a round rotor machine. The 1940kVA generator has the AVR type A attached, with a reference value of 1.2. The generator the battery-arrangement through the rectifier, with no other load attached. The battery arrangement consists of the large capacitor-series resistance is connected to the dc-bus.

First, the subtransient q-axis reactance $X“_q$ is varied while the other constants is held constant and the transient q-axis reactance has the value $X_q = X_q$.

Table 10.19: Parameter analysis, impact of subtransient reactance in the q-axis, $X“_q$, on the stability of the generator G2. The other reactances is held constant. Voltage regulator and governor included. No load is included except from the battery-arrangement. The transient q-axis reactance has the value $X_q = X_q$

Parameter	Value [pu]	Operation	Frequency	Comment
$X“_q$	0.4	Unstable	2.6Hz	-
$X“_q$	0.1	Stable	-	-
$X“_q$	0.2	Unstable	1.95Hz	-
$X“_q$	0.15	Stable	-	-
$X“_q$	0.175	Stable	-	Poorly damped
$X“_q$	0.185	Unstable	-	-
$X“_q$	0.18	Unstable	1.77Hz	-

The generator is stable when $X“_q < 0.18pu$ when G2 is modeled as round rotor and $X_q = X_q$. From this, a stability criterion can be obtained for the 1940kVA generator modeled as round rotor during no-load:

$$\frac{X“_q}{X“_d} < 0.48 \tag{10.4}$$

Now, the subtransient q-axis reactance $X“_q$ is varied while the other constants is held constant and the transient q-axis reactance has the value $X_q = X_d$.

Table 10.20: Parameter analysis, impact of subtransient reactance in the q-axis, $X“_q$, on the stability of the generator G2. The other reactances is held constant. Voltage regulator and governor included. No load is included except from the battery-arrangement. The transient q-axis reactance has the value $X_q = X_d$

Parameter	Value [pu]	Operation	Frequency	Comment
$X“_q$	0.4	Unstable	2.67Hz	-
$X“_q$	0.1	Stable	-	-
$X“_q$	0.2	Unstable	1.88Hz	-
$X“_q$	0.15	Stable	-	-
$X“_q$	0.175	Unstable	1.75Hz	Decreasing oscillations
$X“_q$	0.17	Stable	-	Very poorly damped

The generator is stable when $X“_q < 0.17pu$ when G2 is modeled as round rotor and $X_q = X_d$.

From this, a stability criterion can be obtained for the 1940kVA generator modeled as round rotor during no-load:

$$\frac{X\text{“}_q}{X\text{“}_d} < 0.46 \tag{10.5}$$

Now, the ratio between $X\text{“}_q$ and $X\text{“}_d$ is studied. The ratio is held constant, but the values of $X\text{“}_q$ and $X\text{“}_d$ is changed with the same factor. Because there is not much difference in the stability criterions found for the round rotor G2 for $X\text{“}_q$ when $X_q = X_q$ and when $X_q = X_d$, and simulation is simulated with $X_q = X_d$. The result of the simulation is shown in Table 10.21 below.

Table 10.21: Parameter analysis, impact of the ratio $\frac{X\text{“}_q}{X\text{“}_d}$, on the stability of the generator G2, where the ratio is varied by a factor. Voltage regulator and governor included. No load is connected except from battery-arrangement.

ratio	Factor	Operation	Comment	Frequency
$\frac{X\text{“}_q}{X\text{“}_d}$	1	Unstable	-	2.67Hz
$\frac{X\text{“}_q}{X\text{“}_d}$	1.25	Unstable	-	2.88Hz
$\frac{X\text{“}_q}{X\text{“}_d}$	1.5	Unstable	-	3.57Hz
$\frac{X\text{“}_q}{X\text{“}_d}$	2.0	Unstable	-	3.4Hz
$\frac{X\text{“}_q}{X\text{“}_d}$	0.5	Unstable	-	1.83Hz
$\frac{X\text{“}_q}{X\text{“}_d}$	0.25	Unstable	-	1.13Hz

The generator is unstable for all factors of $X\text{“}_q$ and $X\text{“}_d$ when the ratio between them, $\frac{X\text{“}_q}{X\text{“}_d}$, is held constant.

10.9.2 Load on dc-side

The impact of the subtransient reactances on the stability is to be studied for a round rotor machine. The 1940kVA generator has the AVR type A attached, with a reference value of 1.2. The generator feeds a load of 0.5MW through the rectifier. The battery arrangement consisting of the large capacitor-series resistance is connected to the dc-bus. The series resistance is $R_{series} = 0.0625\Omega$, the capacitor is $C_{battery} = 2100F$, and the load resistance corresponding to 0.5MW is $R_{Load} = 2.122\Omega$.

Because there is not much difference in the stability criteria found for the round rotor G2 for $X\text{“}_q$ when $X_q = X_q$ and when $X_q = X_d$, and the load-situation is only simulated when $X_q = X_d$, because this creates the strictest criterion, $X\text{“}_q < 0.17pu$. The result of the simulation is shown in Table 10.22 below.

Table 10.22: Parameter analysis, impact of subtransient reactance in the q-axis, $X“_q$, on the stability of the generator G2. The other reactances is held constant. Voltage regulator and governor included. A load of $P_{Load} = 0.5MW$ is included after 3 seconds into the simulation, on the dc-side of the rectifier. The transient q-axis reactance has the value $X_q = X_d$

Parameter	Value [pu]	Operation	Frequency	Comment
$X“_q$	0.4	Unstable	2.8Hz	-
$X“_q$	0.1	Stable		-
$X“_q$	0.2	Stable after 15s		-
$X“_q$	0.3	Unstable	2.42Hz	Decreasing amplitude
$X“_q$	0.25	Stable after 19s		Very poorly damped

When a load of 0.5MW is connected to the dc-side of the rectifier, the generator is stable when $X“_q < 0.25pu$ when G2 is modeled as round rotor and $X_q = X_d$. From this, a stability criterion can be obtained for the 1940kVA generator modeled as round rotor supplying a load of 0.5MW through diode-bridge rectifier:

$$\frac{X“_q}{X“_d} < 0.67 \tag{10.6}$$

Now, the ratio between $X“_q$ and $X“_d$ is studied. The ratio is held constant, but the values of $X“_q$ and $X“_d$ is changed with the same factor. The result is shown in Table 10.23 below.

Table 10.23: Parameter analysis, impact of the ratio $\frac{X“_q}{X“_d}$, on the stability of the generator G2, where the ratio is varied by a factor. Voltage regulator and governor included. No load is connected except from battery-arrangement.

ratio	Factor	Operation	Comment	Frequency
$\frac{X“_q}{X“_d}$	1	Unstable	-	2.86Hz
$\frac{X“_q}{X“_d}$	1.5	Unstable	-	3.33Hz
$\frac{X“_q}{X“_d}$	2.0	Unstable	-	3.67Hz
$\frac{X“_q}{X“_d}$	0.5	Stable after 19s	-	-
$\frac{X“_q}{X“_d}$	0.25	Stable after 17s	-	-
$\frac{X“_q}{X“_d}$	0.75	Unstable	-	2.5Hz

The generator is stable when the factor of $X“_q$ and $X“_d$ is below 0.75 when the ratio between them, $\frac{X“_q}{X“_d}$, is kept constant, and a load of 0.5MW is connected on the dc-side of the rectifier.

Chapter 11

Discussion

11.1 Model Reliability - Assumptions and Simplifications

It is established several models of the isolated system in the two simulation tools DIgSILENT PowerFactory and MatLab/SimPowerSystems. The models are used to study the presence of different system components and parameters on the stability of the two studied generator types.

Some assumptions and simplifications are made when modeling the isolated system. The generators are modeled in single operation, even if the generators has the possibility to work in parallel onboard the ship. As shown in the measurements taken on the unstable ship by the AVR delivering company, described in Chapter 3.1, is the generators affected by the other when the setting of the AVR is changed from automatic to manual in one of them. However, each generator delivers power to the dc-bus through rectifiers, and no interaction that can affect the stability of the generators is created by this parallel operation due to the one-direction feeding property of diodes. Supporting this theory is that instability is detected during single operation as well, and the simplification is valid.

No losses are taken into account, and the converter and thrusters connected to the dc-bus are modeled as an active load. Because only active power is let through the rectifier, the load consisting of the converters and thrusters connected to the dc-bus is seen as an active load by the rectifier. This simplification is therefore a good assumption.

A large capacitor and a series resistance models the battery connected to the dc-bus in the MatLab/SimPowerSystems model. A capacitor acts as a battery due to the charging- and discharging characteristics, and is able to store energy. Some losses are found in a battery due to some internal resistance, and the series resistance symbolizes this internal resistance. The large capacitor and series resistance mirrors the main properties of a battery in a good way. In the

system modeled in DIgSILENT PowerFactory, the battery is modeled using a voltage source. This is also an assumption used deliberately due to the charging/discharging property of the battery that also can be found in a voltage source, as well as the ability to supply a load.

The rectifier used in DIgSILENT PowerFactory is modeled as a voltage sourced PWM rectifier, consisting of transistors instead of diodes. The reason for this is that it was quite challenging to compute load flow when the diode-rectifier was obtained, and a compromise was made when applying the PWM rectifier by setting the firing angle $\alpha = 0$ and forbid any modulation. Despite this, does a PWM rectifier does not possess the same features as a diode-bridge rectifier, and the results from this model must be interpreted with care.

11.2 Simulations Obtained from PowerFactory

First, the work from the specialization project from the fall 2014 is continued in DIgSILENT PowerFactory, and the impact of the introduction of a rectifier is studied. The rectifier is of the voltage-sourced PWM type. By varying the gain of the AVR, the linearization constant K_5 is directly effected according to [4]. The eigenvalues of the critical modes associated with the rotor angle of the two generators moves towards instability with increasing gain. This study was done for two situations; producing active power of 14MW and producing/consuming reactive power of 2MVar.

From the specialization project conducted during the fall 2014, it was found that the 1940kVA generator becomes unstable faster than the 3333kVA generator. The critical mode oscillates around 2Hz when the rectifier is not included in the model. However, when the rectifier is added to the model and the gain of the AVR is increased, the critical mode associated with the rotor angle oscillates with only 1Hz. As mentioned in Chapter 4, the frequency of the rotor angle oscillations for isolated modes is in the range 0.7-2Hz according to [11]. An oscillation of the rotor angle as a result of the gain increase with a frequency of 1Hz is therefore likely.

The generator moves faster towards instability when reactive power is consumed. In contrast to the result found in the specialization project, does the 3333kVA generator moves faster towards instability than the 1940kVA generator. This was not expected. The PWM converter used in the model uses transistors and are voltage-sourced, but has a firing angle of $\alpha = 0$ and no modulation. The diode-bridge rectifier used on the ship does not have the same properties as the transistor-based PWM converter. The result could have been different if a diode-bridge rectifier was applied.

11.3 Simulations Obtained from MatLab/SimPowerSystems

A simplified model of the system has successfully been established in MatLab/SimPowerSystems. Simple simulations done on the model reflects the observations made on the ship.

3333kVA generator modeled as salient pole

First, the generator that is characterized as stable, was studied in Chapter 8. The system is stable for both no-load operation and when supplying an active load on the dc-side of the rectifier. The generator is also stable when the reference value of the voltage regulator is varied and when no AVR is connected. The generator is stable even if the generator does not satisfy the stability criterion presented in [1]; $\frac{X_q}{X'_d} \leq 2$.

According to [5] most salient pole generator is build with $X''_d \approx X''_q$, which is not the case for the 3333kVA generator, where the ratio is $\frac{X''_q}{X''_d} = 1.216$. Even though it is classified as stable, poor damping is observed on the ship, and the generator reactances has high values. The stability limit for the subtransient reactances was studied, and it is found that to continue a stable operation, the generator must fulfill the criterion $\frac{X''_q}{X''_d} < 5.91$, indicating that it has a large stability limit. It is mainly the d-axis subtransient reactance and not the q-axis subtransient reactance that impacts the stability.

The ratio $\frac{X''_q}{X''_d}$ is held constant while both reactances is varied by a factor f, but the stability is not affected by this experiment. When the synchronous q-axis reactance is varied, a stability criterion is obtained in this thesis; $\frac{X_q}{X'_d} < 5.7$, which is a lot less strict than the criterion given by [1]; 2.0. Using the actual parameters in the generator design this ratio becomes; $\frac{X_q}{X'_d} = 3.51$. The criterion presented by [1] is too strict and can not be used for this type of generators.

Another stability criterion obtained in this thesis is that the 3333kVA generator must fulfill the criterion $\frac{X_q}{X_d} > 0.94$. Using the parameters on the ship, this ratio is actually $\frac{X_q}{X_d} = 1.52$, and has a large stability margin. This is a very realistic criterion.

Because $X'_q \approx X_q$ for salient pole generator, varying X_q means also varying X'_q. This means that the synchronous, transient and subtransient reactances impact the stability of the 3333kVA generator. This coincide with the theory presented in [1], that not only the synchronous reactance, but also the transient and subtransient reactances impacts the stability.

1940kVA generator modeled as salient pole

The 1940kVA generator is characterized as unstable, and is studied as salient pole in Chapter 9. At no-load, the generator is unstable with an oscillation frequency of the output parameters

of 2.3Hz. Prominent "pulses" is observed in the terminal current. The presumption that one phase in voltage or current starts this oscillating behavior due to the rotor angle, is disproved by a voltage- and current-phase simulation. Similar "pulses" is found in the current profile in [1], where a rectifier-loaded synchronous generator with high synchronous reactances X_q, X_d is studied.

The pulsed nature of the current can be the result of the battery starting to act as a voltage source and delivers power back to the generator, in a repetitive manner. The current could obtain this "pulsed" nature due to the fact that the diode-bridge rectifier only conducts current in one direction. Another explanation for the pulsed current can be the commutation process in the diode-bridge rectifier, as suggested by [1]. Oscillations is experienced on the ship even when the battery is not concluded as well, which could imply that the stability problems arise from the interaction between the diode-bridge rectifier and the synchronous generator, where generator reactances affects the stability.

It is found that the commutation interval observed in the current, decreases in length with an increasing subtransient q-axis reactance. The equation for the commutation reactance in Eq. 4.11 found in [14] is dependent on $X“_q$, and may indicate a ratio between the commutation interval length and the commutation reactance.

Due to the impact of the subtransient q-axis reactance on the commutation interval in the current, a parameter analysis is made, and it is found that the generator becomes stable if $\frac{X“_q}{X“_d} < 0.48$. This value is very low and may be unrealistic. A typical value for this ratio is $\frac{X“_q}{X“_d} = 1.3$ for salient pole generators according to [13]. The actual value of this ratio for the generator using the parameters received from Siemems, is $\frac{X“_q}{X“_d} = 1.048$, which is already very low compared to typical ratio values. The ratio $\frac{X“_q}{X“_d}$ is tried held constant while varying both reactances is by a factor f, but this does not impact the stability.

It is found that when the inner resistance in the capacitor modeling the battery is increased, the generator becomes stable when $r > 0.1\Omega$, but this is a large value compared to the initial value $1e-9\Omega$, that may cause large losses over the battery and is unrealistic. By increasing the voltage reference point in the voltage regulator to 1.4, the generator becomes stable. The terminal voltage becomes 966V, and the oscillations stops after 6-7s. However, the oscillations is large in the first seconds and a protection system would likely shut down the system before the generator becomes stable, to avoid damage to electrical equipment.

It is obvious that the voltage and current plays an important role when it comes to stability, and maybe especially when the current is high. This is emphasized by the fact that the simulations show that when the load connected on the dc-side of the rectifier is large, the generator has a stable operation. This phenomenon is also observed on the ship where instabilities is detected, and confirms that the model in MatLab/SimPowerSystems is realistic. The impact of varying the reference value of the AVR also affects the transient current and terminal voltage, and coincides

with the theory presented in [2] saying that the transient current impacts the generator stability.

The frequencies of the oscillations detected during load are in the range 2.5-2.7Hz. This is a bit above the typical frequencies mentioned by [11] for local mode oscillations associated with rotor angle oscillations, which usually is in the range 0.7-2Hz. The reason for this can be that the local mode oscillations often is associated with generators oscillating against each other, but in this case, a single generator interacts with a rectifier and not another generator. The frequency range between these components can be different but still be associated with rotor angle oscillations. The oscillation frequencies registered by the AVR company was 1.171-2.68Hz, hence, the oscillations frequencies found through simulations is in the same range as the observations on the ship.

1940kVA generator modeled as round rotor

The 1940kVA generator was designed as round rotor and was studied in Chapter 10. The parameters for a round machine were examined. $X`_q$ was not given in the original salient pole-model of the 1940kVA generator in MatLab/SimPowerSystems from Siemens Trondheim and an estimated value was found using Table 4.1 found from [13]. A stability criterion for the 1940kVA generator with round rotor becomes is found when varying the transient q-axis reactance; $\frac{X`_q}{X`_d} < 5.41$. This is a very high ratio, typical ratios is found in literature to be $\frac{X`_q}{X`_d} = 2 - 2.5$ [13]. The stability criterion found in [1] is; $\frac{X`_q}{X`_d} < 2$. This is too strict and not realistic for this type of generator, due to the high value of this ratio using the original reactances; $\frac{X_q}{X`_d} = 9.78$.

The generator is unstable for both during no-load and load situation, and is unstable for all loads except from when the generator supplies a load close to the maximum of the generators performance, at 1.9MW. However, the stability is first met after 10 seconds, and the protection system would probably shut down the system to protect electrical equipment because of large start-up currents. The oscillations detected are in the frequency range 2.5-2.8Hz, which is in the same range as when the 1940kVA generator was modeled as salient pole. The oscillations measured from the ship experiencing instability is in the range 2.171-2.68Hz at high load, which matches the frequencies simulated. For local mode oscillations associated with rotor angle oscillations in the frequency range 0.7-2Hz. Both the frequencies measured on the ship and obtained from simulations is a bit lower in value than this.

The generator becomes stable when the terminal voltage is increased to 40% above the nominal voltage, and when the terminal voltage is set equal to the nominal voltage. When varying the reference value of the AVR in this way, the size and behavior of the transient current is affected, which according to [2] is of major importance to the generator stability.

When the AVR is removed, the generator shows stability during no-load, but unstable for all loads. The parameters oscillate with a frequency range of 0.5-1Hz. When the battery is removed,

the generator becomes stable during no-load and for all loads. Observations on the ship shows that the oscillations increases when the battery is connected to the dc-bus, but then the AVR is connected and this simulation results can not be compared. The simulations without AVR were conducted to see how the unregulated generator behaves to load and component analysis.

The influence of the AVR is further studied and the AVR type A was replaced by the AVR type AC5A. Also with this regulator the generator became stable when the terminal voltage was raised by 40% above the nominal voltage and at nominal voltage, and when the load is 1.9MW. However, the frequencies during instability of the generator using AC5A are much higher than for simulations using AVR type A. They are in the range 3.67-5.5Hz. It is clear that the value of the terminal voltage and load situation impacts the generator stability greatly for both regulators, which can imply that the regulator can be tuned to achieve a stable generator.

The battery is studied due to its importance in the stability-question, where observations state that the stability worsens when the battery is attached to the dc-bus. The large capacitor is replaced by a Simulink-model of a battery to better study the power delivered from the battery to the load. No oscillations is found using this battery-type, neither during no-load or during load situation. However, when the AVR type is changed from the original type A to AC5A, the generator is unstable for both no-load and during load situation. The Simulink-battery does not model the battery used on the ship as well as the large capacitor, because it is found that the generator is not affected by the battery-connection when the graphs of the power from the two power-sources is studied, and because no instability is found when it is connected and AVR type A is applied.

The rectifier is removed to study its impact, and to examine the theories presented by [1] saying that the rectifier may be the source of stability problems obtained in rectifier-loaded SG. A load is connected between the terminals of the 1940kVA generator, but no instabilities are found for any load. When the AVR type AC5A is applied, the generator outputs shows instability. The frequency of the oscillations is in the range 4.125-4.75Hz, which is higher than the oscillation frequencies discovered from other simulations using AVR type A. It is also claimed in [3] that generators that are rectifier-loaded can become unstable although they can operate stable without the rectifier connection. The simulations confirm this, and this may be the case for the 1940kVA generator type.

It is claimed in [1] that the rectifier is a part of the stability problems discovered in systems consisting of rectifier-loaded synchronous generators. The simulations obtained show that when removing the rectifier, the generator is only unstable when using the AVR type AC5A. The pulsed nature of the current is completely gone and may indicate that the rectifier is an important component when it comes to both evaluating stability and the current profile, but that the AVR also is of importance.

It is also found that the value of the excitation-voltage has a great impact on the stability. When

a load is connected to the dc-side of the rectifier and the voltage of the constant voltage source is varied, is it found that the excitation voltage must be lower for high load than for low load to achieve stability; $V_{exciter} > 45V$ for a 0.5MW load and $V_{exciter} > 42.5V$ for a 1.9MW load. This is due to the general stability criterion presented by [2];

$$X'^2_d I'^2_d + X'^2_q I'^2_q \leq 2X'_d I'_d U_p \tag{11.1}$$

claiming that when the exciter-voltage $V_{exciter}$ raises, the stationary source voltage U_p increases and the stability is therefore improved. When the transient current is enlarged due to load increase, stability is harder to achieve, because I'_d and I'_q is squared on the left side of the equation. This coincides with the simulation because to compensate for a larger load, the exciter-voltage must be greater. This emphasizes the credibility of the given stability criterion in [2].

The stability criterion given in [2] only impose requirements for the transient reactances, not for the synchronous and subtransient reactances. [5] suggests that the q-axis reactance has a larger impact on the stability than the d-axis reactance. Due to this, the subtransient q-axis reactance is examined, and a stability criterion is obtained; $\frac{X''_q}{X''_d} < 0.46$ for no load. This is a very strict and maybe unrealistic criterion. Typical values for the same ratio of subtransient reactances is $\frac{X''_q}{X''_d} = 1$, and the actual ratio between these reactances in the 1940kVA generator is $\frac{X''_q}{X''_d} = 1.048$.

Also during no-load, it is found that by varying the factor of X''_q and X''_d while keeping the ratio $\frac{X''_q}{X''_d}$ constant, the generator is unstable for all factors f. This emphasizes the theory in [5] that the q-axis reactance is more influential on the stability than the d-axis reactance.

By doing the same parameter analysis when the generator supplies a 0.5MW load, another stability criterion for the subtransient reactances is found; $\frac{X''_q}{X''_d} < 0.67$. This is a less strict criterion than during no-load, but it is still far from both the actual ratio-value and typical value of this ratio. This contradicts with the criterion given by [2], saying that the transient current is enlarged due to load increase, making stability harder to achieve. The equation given by [2], rendered in Eq. 11.1 above, does however have no criterion for the subtransient values, which can indicate that Eq. 11.1 does not capture all causes of instability.

When the ratio $\frac{X''_q}{X''_d}$ is kept constant, and a factor of X''_q and X''_d is varied, the factor must be $f < 0.75$ to achieve stability during load. However, the stability happens after 19s and 17s for $f = 0.5$ and $f = 0.25$, respectively, and this is a very long time, but this simulation shows that the generator is not unstable for all factors f, as is the case during no-load.

As presented in [1] the simulations confirms that both the transient and subtransient reactances, as well as the operation and the presence of a rectifier has great impact on the generator stability.

11.4 Uncertainty Regarding Simulation Results

Throughout the simulations done in this thesis is the frequency of the oscillations is in the range 2.3-2.8Hz when applying AVR type A. This corresponds to the frequency ranges observed on the ship; 1.71-2.68Hz. When AVR type AC5A is applied, the frequencies range is 3.67-5.5Hz, and differs from other simulation and observations, as well as theory. According to [11] is the frequency range 0.7-2Hz for local modes of machine-infinite bus systems, where the oscillations can be associated with the rotor angle. The difference between the frequencies found in simulation and in [11] can indicate that something else than rotor angle oscillations and poorly damped machine can be the source of the stability problems experienced. It can also indicate that the frequency range is different for the interaction between a single generator and rectifier than generators interacting with each other, and that a poorly damped machine still is the main source for the instabilities.

[1] claims that the rectifier can be a source of instability when a rectifier-loaded synchronous generator system is studied.Simulations done in DIgSILENT PowerFactory from the Specialization project shows instability when the rectifier is excluded and the gain of the AVR is increased. When it is connected, the generators still becomes unstable when the gain is increased, but the result differs in the way that the 3333kVA generator becomes unstable faster than the 1940kVA generator. The reason can be the use of a PWM rectifier instead of a diode-bridge rectifier, even if the firing angle $\alpha = 0$ and there is no modulation. Due to this, is the simulation results studying the rectifier in DIgSILENT PowerFactory not fully credible.

Simulations performed in MatLab/SimPowerSystems when the rectifier is removed, shows that the 1940kVA generator is only unstable when the AVR type AC5A is used, and can indicate that the stability problems originates in the diode-bridge rectifier-SG system. The pulsed nature of the current in simulations outputs from the 1940kVA generator also indicates that the rectifier has a major impact on the behavior of the generator terminal values. This conclusion is supported by the fact that the ship operates stable when the diode-bridge rectifier is replaced by thyristor-controlled rectifiers, and that the same conclusion is drawn by [1].

The simulations using the Simulink-battery does not mirror the behaviors observed on the ship as well as the large capacitor does, and is not as valuable. The reason for this may be that there is some setting in MatLab/SimPowerSystems deciding which of the two power sources generator or battery is supposed to supply the load.

11.5 Comparative Analysis

11.5.1 Stability criteria obtained in this thesis regarding generator reactances

According to [1] the stability of rectifier-loaded generator systems is affected by both transient and subtransient reactances in addition to the synchronous reactance. It is claimed that the stability problems originate in the rectifying-process. The stability criterion presented in [1] is given as: $\frac{X_q}{X'_d} \leq 2$.

It is claimed by [2] that the stability of rectifier-loaded generator systems is influenced by the transient current I' and the stationary source voltage U_p. I' is directly influenced by the load-operation, and U_p is directly influenced by the excitation of the generator. A stability criterion is given in Eq. 11.1.

None of the two generators studied in this thesis fulfill the stability criterion given in [1]. The 3333kVA generator has a value of $\frac{X_q}{X'_d} = 3.51$, which is much higher than the proposed value in [1], but it is still stable, though poorly damped. The 1940kVA generator which is characterized as unstable, has a ratio of $\frac{X_q}{X'_d} = 9.78$ and is far from fulfilling the requirement proposed by [1].

From the results in the MatLab/SimPowerSystems model it is found, as also stated in [1], that the theory saying that the stability of the diode-bridge rectifier-loaded synchronous generator depends on the presence of the rectifier, is true. The generator becomes stable during load-operation when the rectifier is disconnected. It is also found that the stability depends on the load-situation of the generator, as proposed by both [1] and [2]. The 1940kVA generator is unstable for both no-load and during most load-scenarios except from when it feeds a load close to its capacity, for which it will become stable.

Via a parameter analysis of the DC-voltage feeding the excitation field of the 1940kVA generator the stability criterion given in [2] is enhanced, saying that by increasing the stationary source voltage U_p, the generator becomes more stable. This is found to be true via simulations and parameter-analysis.

Through a sensitivity analysis of the generator reactances the postulate in [1] is confirmed, claiming that the transient and subtransient reactances is important in addition to the synchronous reactances. The stability criterion in [2] is only dependent on the transient reactances.

Stability criteria for 1940kVA generator

The stability criterion obtained in this thesis for the unstable, 1940kVA generator during no-load with emphasis on the transient reactance is given as:

$$\frac{X`_q}{X`_d} \leq 5.41 \tag{11.2}$$

The stability criterion obtained for this generator during no-load with emphasis on the subtransient reactance is given as:

$$\frac{X``_q}{X``_d} \leq 0.46 \tag{11.3}$$

The stability criterion obtained for this generator when supplying load, with emphasis on the subtransient reactance is given as:

$$\frac{X``_q}{X``_d} \leq 0.67 \tag{11.4}$$

Eq. 11.2 confirms the theory presented in [2] and [1], claiming that the transient reactance is important for the stability. Typical values for this ratio is $\frac{X`_q}{X`_d} = 2 - 2.5$ for round rotor design, according to [13]. The stability criterion presented in [1] is stricter than Eq. 11.2; $\frac{X`_q}{X`_d} \approx \frac{X_q}{X`_d} \leq 2.0$. The actual value of the ratio between this ratio for the 1940kVA generator types is $\frac{X_q}{X`_d} = 9.78$ and is far from fulfilling this criterion by [1], but closer to fulfilling the criterion presented in Eq. 11.2.

Eq. 11.3 and Eq. 11.4 shows that not only requirements for the transient reactances is important for a stable operation of the 1940kVA generator type, but also the subtransient reactances. The value of $X``_q$ can be larger when a load is connected, than when the generator supplies a load, indicating as also shown via simulations and by [2], that a load can improve the operation of the 1940kVA generator. However, both criteria is very strict, on the verge of being unrealistic. Typical values for this ratio is $\frac{X``_q}{X``_d} = 1$ for round rotor machines. The actual value is $\frac{X``_q}{X``_d} = 1.048$.

Stability criteria for 3333kVA generator

The stability criterion obtained for the stable, 3333kVA generator with salient pole, with emphasize on the synchronous reactance is given as:

$$\frac{X_d}{X_q} \geq 0.94 \tag{11.5}$$

The stability criterion obtained for this generator with emphasize on the subtransient reactance is given as:

$$\frac{X“_q}{X“_d} \leq 5.91 \tag{11.6}$$

The stability criterion obtained for this generator with emphasize on the synchronous and transient reactance is given as:

$$\frac{X_q}{X‘_d} \leq 5.7 \tag{11.7}$$

Eq. 11.5 confirms the theory presented in [1] claiming that the synchronous reactance is important for the stability. Typical ratios of these reactances is $\frac{X_d}{X_q} = 1.5$ according to [13]. This is very close to the actual ratio; $\frac{X_d}{X_q} = 1.52$, and the generator has a good stability limit.

Eq. 11.6 shows that also the subtransient reactances are important in this context. This ratio is $\frac{X“_q}{X“_d} = 1.216$ in this generator, and fulfills the criterion obtained. Typical ratios is $\frac{X“_q}{X“_d} = 1.3$ [13].

Eq. 11.7 shows that the criterion presented in [1] is too strict; $\frac{X_q}{X‘_d} \leq 2$. The actual ratio of these reactances in the generator are $\frac{X_q}{X‘_d} = 3.51$ and would be characterized as unstable if the criterion in [1] was used.

11.5.2 Stability enhancement of 1940kVA generator

To fulfill the stability criteria obtained for the unstable 1940kVA generator in Eq. 11.2 or Eq. 11.3 either the transient or the subtransient q-axis reactance must be decreased.

According to [3] the stability criterion can be easier fulfilled if a short-circuited q-axis rotor winding is added to the rotor of a diode bridge rectifier-loaded synchronous generator. The result of an added short-circuited q-axis winding on the rotor winding will lead to a decreased value of the transient q-axis reactance, as is a proposal to achieve stability for the 1940kVA generator, and to fulfill the stability criterion obtained in this thesis for the transient reactances, given in Eq 11.2.

The stability criterion found in [3] is given by:

$$\frac{1}{X_q} + \frac{1}{X‘_q} \geq \frac{1}{X‘_d} \tag{11.8}$$

This stability criterion only contains requirements for the synchronous and transient reactances. When the design values for X_q and $X‘_d$ for the 1940kVA generator are used in Eq. 11.8 and the equation is solved for $X‘_q$, the value of $X‘_q$ is:

$$X`_q \leq 0.549pu \tag{11.9}$$

By using this value for the stability criterion developed in this thesis shown in Eq. 11.2, and the original value for $X`_d$ is used, the equation will be as follows:

$$\frac{X`_q}{X`_d} = 1.12 < 5.41 \tag{11.10}$$

This implies that adding a short-circuited q-axis rotor winding to the generator rotor will fulfill the stability criterion found in this thesis. Because $1.12 < 5.41$, the stability margin becomes quite large if this short-circuited q-axis winding is added to the rotor.

Chapter 12

Conclusion

This thesis concerns the stability of diode-bridge rectifier-loaded synchronous generators characterized with high values of synchronous, transient and subtransient reactances in the d- and q-axis. Two generator types used in the industry are investigated. The synchronous reactances of these two generator types are in the range 2.5-5.5 pu. Two electrical systems for ships have been studied, where one ship uses 3333kVA generator types with synchronous reactances in the lower range of 2.5-5.5pu and has a stable operation. The other ship uses 1940kVA generator types with synchronous reactances in the upper range of 2.5-5.5 pu and is unstable during normal operation.

The generators supplies power to a dc-bus through rectifiers. The thrusters are supplied from the dc-bus through inverters. The connection of a battery bank to the dc-bus is a possibility to achieve redundancy. This electrical system is delivered by Siemens and is a part of their new diesel-electric, variable speed propulsion dc-system. The objective of this thesis was to understand why diode-bridge rectifier-loaded synchronous generators with high values of reactances become unstable, and to find what could be done to prevent the observed instability.

Simplified models of the electrical system are established in the simulation tool MatLab/SimPowerSystems, and suitable simulations and parameter-analysis of the synchronous generators, battery, voltage regulator and load is conducted. The simulation results are compared to theories found in literature concerning the same problems as addressed in this thesis.

It is found through simulations that the interaction between the synchronous generator and diode-bridge rectifier is the reason for the instabilities observed in the studied system. This was a theory presented in [1], and is verified through simulations conducted in this thesis. The 1940kVA generator becomes unstable only when the rectifier is connected. The operation of the generators regarding load also impacts the stability greatly; it is found that the 1940kVA generator can obtain stable operation when the load is close to the generator capacity, 1.9MVA,

but is unstable for all other loads as well as during no-load.

It is claimed by [2] that the transient current affects the stability in a negative manner, and that a high amplitude of the stationary source voltage affects the stability in a positive manner. The load situation directly affects the transient current and the excitation voltage directly affects the stationary source voltage. Through simulations it is found that high load worsen the stability and that high excitation voltage enhances the stability. The statements found in [2] is thus verified.

By conducting a sensitivity analysis of the reactances of the synchronous generators it is found that the values of the synchronous and subtransient reactances is as important as the values of the synchronous reactances to achieve stability. The following stability criteria for the transient and subtransient reactances are obtained for the 1940kVA generator with round rotor during no-load:

$$\frac{X`_q}{X`_d} \leq 5.41 \qquad \frac{X``_q}{X``_d} \leq 0.46 \tag{12.1}$$

By introducing the stability criterion for the transient reactances to a stability criterion found in literature, it is found in chapter 11.5.2 that by adding a short-circuited q-axis rotor winding on the generator rotor this stability criterion can be fulfilled and a stable operation can be achieved.

Suggestions for further work is found in Chapter 13.

12.1 Recommendations

A recommended solution to prevent unstable situations in electrical systems on ships using the 1940kVA generator type is to add a short-circuited q-axis rotor winding on the generator rotor. This is recommended due to the fulfillment of the stability criterion of the transient reactance given in Eq. 12.1 and was investigated in Chapter 11.5.2.

Chapter 13

Further Work

1. Diode-bridge rectifier type in PowerFactory model instead of PWM rectifier
2. Further examine the dynamic interaction between the synchronous generator and diode bridge rectifier
3. Simulate the impact of an added short-circuited q-axis rotor winding on the stability
4. Simulate two generators working in parallel to capture any interactions between them
5. Study the impact of AVR parameters and investigate if the unstable generator can be regulated to run with stable operation
6. Development of a power system stabilzer (PSS) solution for a diode bridge rectifier-loaded synchronous generator system
7. Study the difference in instability when the battery is connected compared to when it is removed, for the unstable 1940kVA generator
8. Study the tuning of the AVR to possibly obtain a stable operation of the 1940kVA generator

Chapter 14

Bibliography

[1] H. Auinger and G. Nagel. *Vom transienten Betriebsverhalten herrührende Schwingungen bei einem uber Gleichrichter belasteten Synchrongenerator. Teil 1.* Theoretische Untersuchungen. 1980.

[2] Dr. Reinhard Vogel. Einfaches modell zur erklärung des instabilen verhaltens von bestimmten generatoren bei bludrive+c - anlagen. *Siemens, Hamburg, Germany*, (PD OM DM NC TI), 2015.

[3] Ma Weiming, Hu An, Liu Dezhi, and Zhang Gaifan. Stability of a synchronous generator with diode-bridge rectifier and back-emf load. *IEEE Transactions on Energy Conversion*, 15(4):458–463, 2000.

[4] Trond Toftevaag, Emil Johansson, and Astrid Petterteig. The influence of impedance values and excitation system tuning on synchronous generator stability in distribution grids. *SINTEF Energy Research*, 2008.

[5] Kurt Bonfert. *Betriebsverhalten der Synchronmaschine*. Springer-Verlag, 1962.

[6] Torunn Helland. *Dynamic analysis of the stability of a diode bridge rectifier connected synchronous generator with high synchronous reactances*. 2014.

[7] Gang Wang, LiJun Fu, XueXin Fan, ZhiHao Ye, and Fan Ma. Periodic orbit model of diode rectifiers-synchronous machine system. *Science China Technological Sciences*, 56(1):245–252, 2012.

[8] Ivan Jadric, D. Borojevic, and Martin Jadric. *A simplified model of a variable speed synchronous generator loaded with diode rectifier*, pages 497–502. IEEE, 1997.

[9] ABS American Bureau Shipping. Guidance notes on control of harmonics in electrical power systems. *Houston, USA*, 2006.

[10] Ned Mohan, Tore M Undeland, and William P Robbins. *Power electronics*. Wiley, 1995.

[11] P Kundur, Neal J Balu, and Mark G Lauby. *Power system stability and control*. McGraw-Hill, 1994.

[12] Jan Machowski, Janusz W Bialek, and J. R Bumby. *Power system dynamics*. Wiley, 2008.

[13] P Kundur, Neal J Balu, and Mark G Lauby. *Power system stability and control, table 4.2 p. 153*. McGraw-Hill, 1994.

[14] S. Moriyasu and C. Uenosono. An analysis on the characteristics of a synchronous machine connected to a d.c.-link. *Archiv f. Elektrotechnik*, 69(2):111–120, 1986.

[15] J. Jatskevich, S.D. Pekarek, and A. Davoudi. Parametric average-value model of synchronous machine-rectifier systems. *IEEE Trans. On Energy Conversion*, 21(1):9–18, 2006.

[16] H. Auinger and G. Nagel. *Vom transienten Betriebsverhalten herrührende Schwingungen bei einem uber Gleichrichter belasteten Synchrongenerator. Teil 2*. Abhilfemassnahmen. 1980.

[17] Espen Haugan. *SimPowerSystems Model*. Siemens, Trondheim, 2014.

[18] DIgSILENT PowerFactory. User-manual, "pwm converter".

[19] SimPowerSystems The MathWorks, Inc. User-manual, "synchronous machine round rotor (standard)".

[20] Inc. SimPowerSystems The MathWorks. User-manual, "solver".

[21] Espen Haugan. *Conversation 2/3-2014*. Siemens.

[22] SimPowerSystems The MathWorks, Inc. User-manual, "machine inertia.

[23] IEEE. *IEEE recommended practice for excitation system models for power system stability studies*. IEEE Power Engineering Society, Sponsored by the Energy Development and Power Generation Committee, 2006.

Appendix A

Specialization Project During Fall 2014

A.1 Transient Voltage Increase

If a synchronous generator with salient poles is considered first to be in no load, i.e. open circuit, we have that $I_d = I_q = 0$, $V_q = E`_{q0} = 1$ and $V_d = 0$. In $t = t_0$, equation A.1 and A.2 describes the system [12]:

$$E`_{q0} = V_q + R_a I_q - X`_d I_d \tag{A.1}$$

$$0 = V_d + R_a I_d + X_q I_q \tag{A.2}$$

When a resistive load R is connected to the terminals of the generator, we have that at the time $t = t_{0t}$:

$$V_q = RI_q \tag{A.3}$$

$$V_d = RI_d \tag{A.4}$$

If equation A.3 and A.4 is introduced into equation A.1 and A.2, we have that:

$$E`_q = E`_{q0} = (R + R_a)I_q - X`_d I_d \tag{A.5}$$

$$0 = (R + R_a)I_d + X_q I_q \tag{A.6}$$

Equation A.5 and A.6 is solved for I_d and I_q:

$$I_d = -\frac{X_q}{(R + R_a)^2 + X`_d X_q} E`_{q0} \tag{A.7}$$

$$I_q = \frac{R + R_a}{(R + R_a)^2 + X`_d X_q} E`_{q0} \tag{A.8}$$

If this is introduced in to equation A.3 and A.4, we get that

$$V_d = -\frac{RX_q}{(R + R_a)^2 + X`_d X_q} E`_{q0} \approx -\frac{X_q}{R} E`_{q0} \tag{A.9}$$

$$V_q = -\frac{R(R + R_a)}{(R + R_a)^2 + X`_d X_q} E`_{q0} \approx -\frac{R^2}{R^2 + X`_d X_q} E`_{q0} \tag{A.10}$$

with the assumption that $R >> R_a$. This shows that the contribution from $V_d > 0$ and that

$$V_g = \sqrt{V_d^2 + V_q^2} > 1 \tag{A.11}$$

which means that the voltage increases after the load is introduced.

Appendix B

Simulations in PowerFactory

B.1 External System Parameters used in PowerFactory Model [4]

Table B.1: Summary of external impedances in pu, ref. $U_B = 6.6kV$ and $S_B = 16MVA$ [4]

Component	R [pu]	X [pu]
Transformer (22/6.6kV)	0.00469	0.08
Cable (22kV)	0.0023	0.0051
Line (22kV)	0.0304	0.1433
Transformer (132/22kV)	0.0038	0.1042
Line 132kV	0.0001	0.007
Transformer (300/132kV)	0.0001	0.007
Sum without generator	0.0391	0.3353

B.2 Modal Analysis in PowerFactory, Participation Factors

Name	Unit	Description
s:speed	p.u.	Speed
s:phi	rad	Rotor-angle
s:psie	p.u.	Excitation-Flux
s:psiD	p.u.	Flux in D-winding
s:psix	p.u.	Flux in x-winding
s:psiQ	p.u.	Flux in Q-winding

Figure B.1: Variables accessible for eigenvalue calculation

Participations G1

```
| Modal-Analysis, Participations;                          Max.Damping:    10,000 Max. Period:    30,00 s Min.Part:    0,001 |

|                 |                                                          |   DIgSILENT   | Project:                  |
|                 |                                                          | PowerFactory  |---------------------------|
|                 |                                                          |    14.1.6     | Date:  4/20/2015          |

| System Stage: Study Case                  | Study Case: Study Case                                  | Annex:                 / 1  |

| Element                              Folder              Magnitude/Angle                    Participation                        |

|                                                                                                                              |
|System Mode   8     Tp=   1,388 s    Dp=   -0,108        A1/A2=      0,861                                                   |
|  avr ESAC8B; xder      Plant_G1                            0,036/-173,69                                                    |
|  avr ESAC8B; xe        Plant_G1                            0,052/  -3,40                                                    |
|  avr ESAC8B; xi        Plant_G1                            0,012/   6,31                                                    |
|  avr ESAC8B; xr        Plant_G1                            0,015/   2,95                                                    |
|  G1; phi               grid                                1,000/   0,00                                                    |
|  G1; psiD              grid                                0,046/  90,48                                                    |
|  G1; psie              grid                                0,112/-113,98                                                    |
|  G1; speed             grid                                0,997/ 176,46                                                    |
|                                                                                                                              |
|System Mode  10     Tp=  19,033 s    Dp=    0,473        A1/A2=   8113,176                                                   |
|  avr ESAC8B; xder      Plant_G1                            0,051/-180,00                                                    |
|  avr ESAC8B; xe        Plant_G1                            0,045/ -33,10                                                    |
|  avr ESAC8B; xi        Plant_G1                            1,000/   0,00                                                    |
|  avr ESAC8B; xr        Plant_G1                            0,012/  32,04                                                    |
|  G1; phi               grid                                0,007/ -71,53                                                    |
|  G1; psiD              grid                                0,005/  66,94                                                    |
|  G1; psie              grid                                0,995/ 178,64                                                    |
|  G1; speed             grid                                0,008/-156,07                                                    |
```

Figure B.2: Participations G1

Participations G2

Modal-Analysis, Participations;			Max.Damping: 10,000 Max. Period: 30,00 s Min.Part: 0,001
		DIgSILENT PowerFactory 14.1.6	Project: Date: 4/20/2015
System Stage: Study Case	Study Case: Study Case		Annex: / 1

Element	Folder	Magnitude/Angle	Participation
System Mode 8 Tp= 1,060 s Dp= -0,034		A1/A2= 0,965	
avr ESAC8B; xder	Plant_G2	0,037/-174,38	
avr ESAC8B; xe	Plant_G2	0,046/ -1,51	
avr ESAC8B; xi	Plant_G2	0,007/ 5,62	
avr ESAC8B; xr	Plant_G2	0,016/ -0,83	
G2; phi	grid	1,000/ 0,00	
G2; psiD	grid	0,009/ 101,28	
G2; psiQ	grid	0,002/ 52,54	
G2; psie	grid	0,043/-139,65	
G2; speed	grid	0,998/ 178,73	
System Mode 10 Tp= 18,333 s Dp= 0,474		A1/A2= 5994,455	
avr ESAC8B; xder	Plant_G2	0,052/-180,00	
avr ESAC8B; xe	Plant_G2	0,040/ -32,49	
avr ESAC8B; xi	Plant_G2	1,000/ 0,00	
avr ESAC8B; xr	Plant_G2	0,013/ 31,62	
G2; phi	grid	0,006/ -12,99	
G2; psiD	grid	0,005/ 162,49	
G2; psiQ	grid	0,001/ 34,91	
G2; psie	grid	0,994/ 178,90	
G2; speed	grid	0,005/ -96,51	

Figure B.3: Participations G2

PWM model

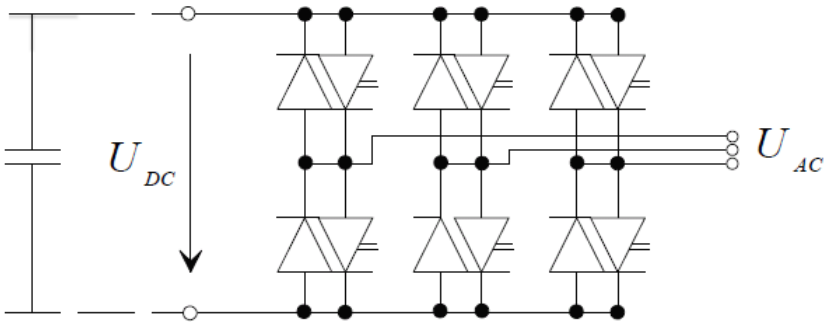

Figure B.4: PWM converter equivalent circuit [18].

For values $[Pm] < 1$ [18]:

$$U_{ACr} = K_0 Pm_r U_{DC} U_{ACi} = K_0 Pm_i U_{DC} \tag{B.1}$$

Where:

- U_{ACr}: Real part of AC-voltage (RMS value)
- U_{ACi}: Imaginary part og AC-voltage (RMS-value)
- K_0: Constant depending on the modulation method
- Pm_r: Real part of modulation index
- Pm_i: Imaginary part of modulation index
- U_{DC}: DC-voltage

"The fundamental frequency equations are completed by the active-power conservation between AC- and DC-side" [18]:

$$P_{AC} = Re(U_{ac}I^*_{AC}) = U_{DC}I_{DC} = P_{DC} \tag{B.2}$$

Where:

- U_{AC}: AC-voltage phasor (RMS-vaue)
- I^*_{AC}: Conjugate complex value of AC-current phasor (RMS-value)
- U_{DC}: DC-voltage
- I_{DC}: DC-current
- P_{DC}: DC-power

Appendix C

3333 kVA Generator MatLab/SimPowerSystems Model

C.1 Components and Parameters

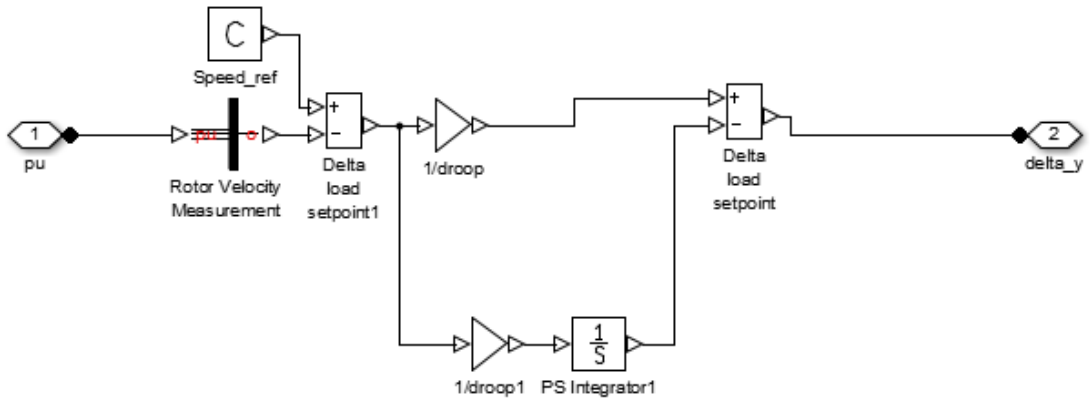

Figure C.1: One line diagram of the governor used in the 3333 kVA generator model in SimPowerSystems

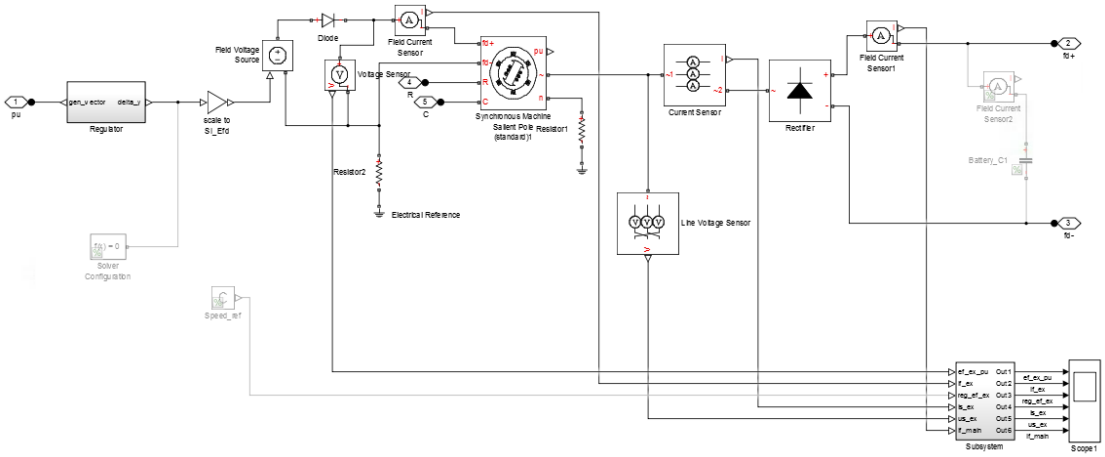

Figure C.2: One line diagram of the AVR and exciter used in the 3333 kVA generator model in SimPowerSystems

Table C.1: Parameter settings for 17.1 kVA exciter generator used in G1-model

Symbol	Unit	Parameter	Description
f	[Hz]	88	Rated electrical frequency
S	[VA]	17.1e3	Rated apparent power
V	[V]	194	Rated voltage
n	[-]	6	Number of pole pairs
I	[A]	3.15	Field circuit current
R_a	[pu]	0.015	Stator resistance
X_l	[pu]	0.15	Stator leakage reactance
X_d	[pu]	0.591	d-axis synchronous reactance
X_q	[pu]	0.315	q-axis synchronous reactance
X_0	[pu]	0.225	Zero-sequence reactance
$X‘_d$	[pu]	0.135	d-axis transient reactance
$X“_d$	[pu]	0.134	d-axis subtransient reactance
$X“_q$	[pu]	0.314	q-axis subtransient reactance
$T‘_{d0}$	[s]	0.229	d-axis transient open circuit
$T“_d$	[s]	0.0001	d-axis subtransient short circuit
$T“_q$	[s]	0.0001	q-axis subtransient schort circuit
V	[V]	1	Terminal voltage magnitude

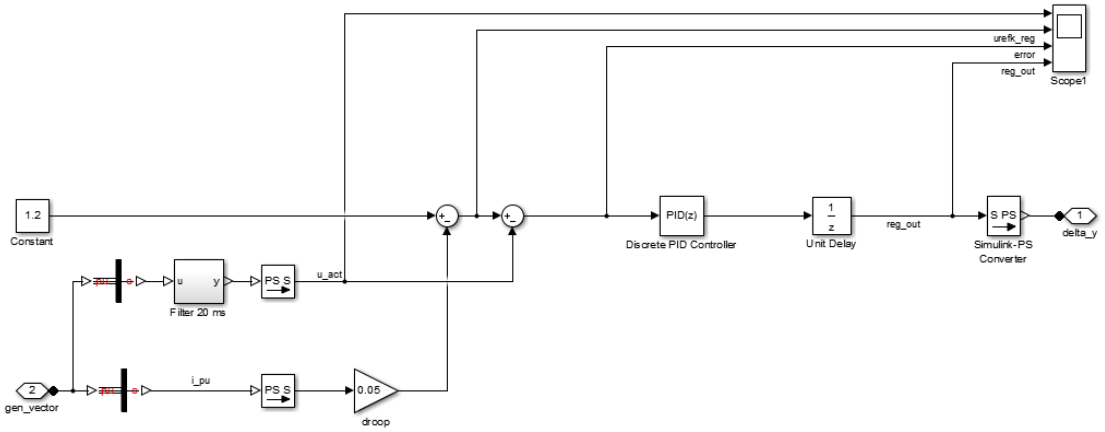

Figure C.3: One line diagram of the voltage regulator used in the 3333 kVA generator model in SimPowerSystems

Table C.2: Parameter settings for voltage regulator used in 3333 kVA generator model

Symbol	Unit	Parameter	Description
Constant			
Constant	[-]	1.2	Referance value
Filter 20ms			
$1/T$	[-]	50	PS gain
$1/S$	[-]	0	PS Integrator
droop			
d	[-]	0.05	Gain
Discrete PID controller			
P	[-]	1.19	Proportional
I	[-]	0.43	Integral
D	[-]	0.57	Derivative
N	[-]	10000	Filter coefficient

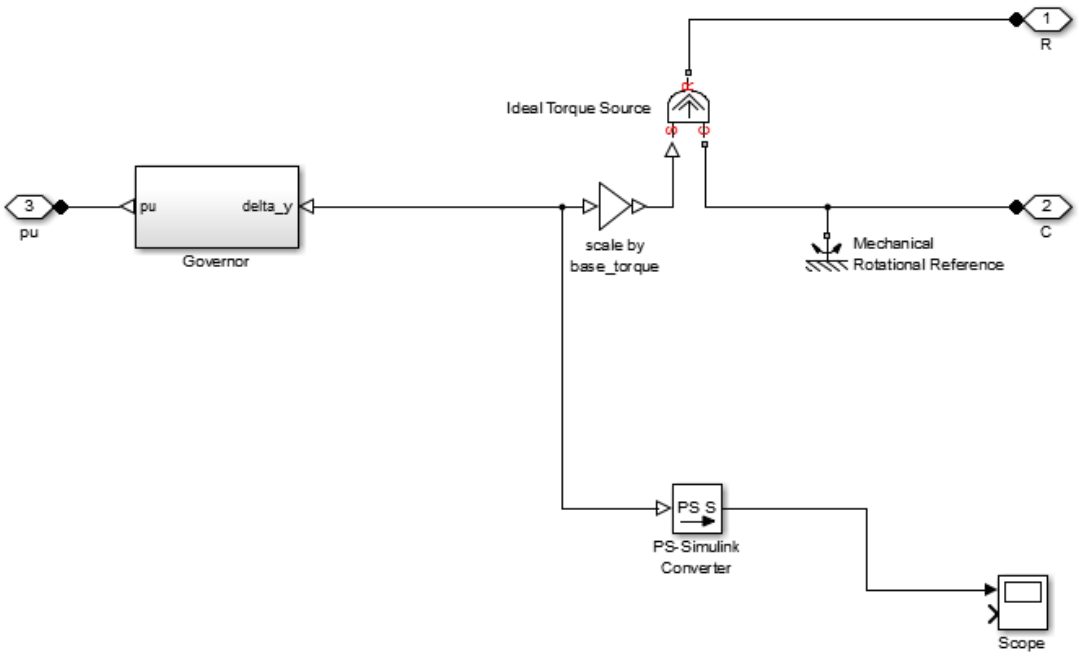

Figure C.4: One line diagram of the governor used to control the speed from the 3333 kVA generator used in the SimPowerSystems model. The ideal Torque Source converts the torque into the two ports R and C.

Table C.3: Parameter settings for governor used in G1-model

Symbol	Unit	Parameter	Description
s_{ref}	[pu]	0.998	Speed reference
p	[%]	5	percentage droop
L	[pu]	0.5	Load reference setpoint
T_{gov}	[s]	0.002	Time constant of governor
T	[s]	0.003	Time constant of main inlet volumes and steam chest
τ_b	[kNm]	16.615	Base torque
τ_i	[pu]	0.451061	Initial torque

C.2 Simulation Results from the Governor, Voltage Regulator and Exciter

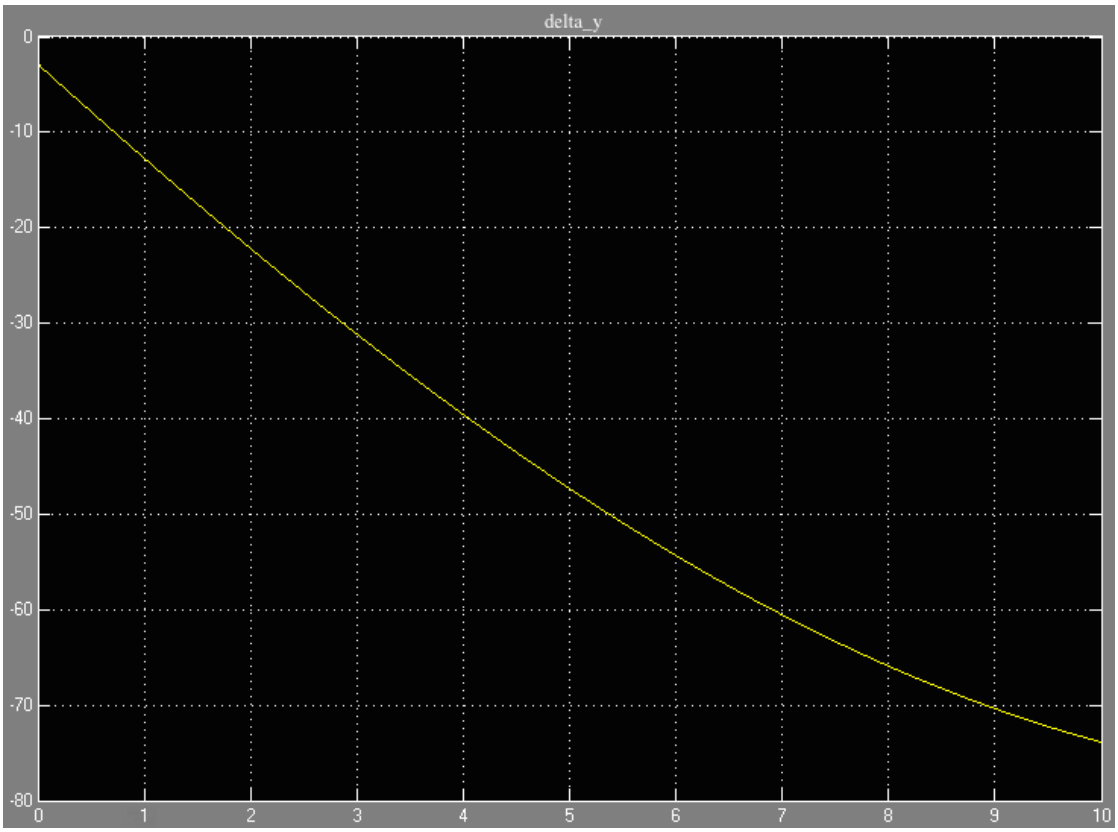

Figure C.5: 3333 kVA generator system output values from the governor, where $delta_y$ is the signal output from the governor.

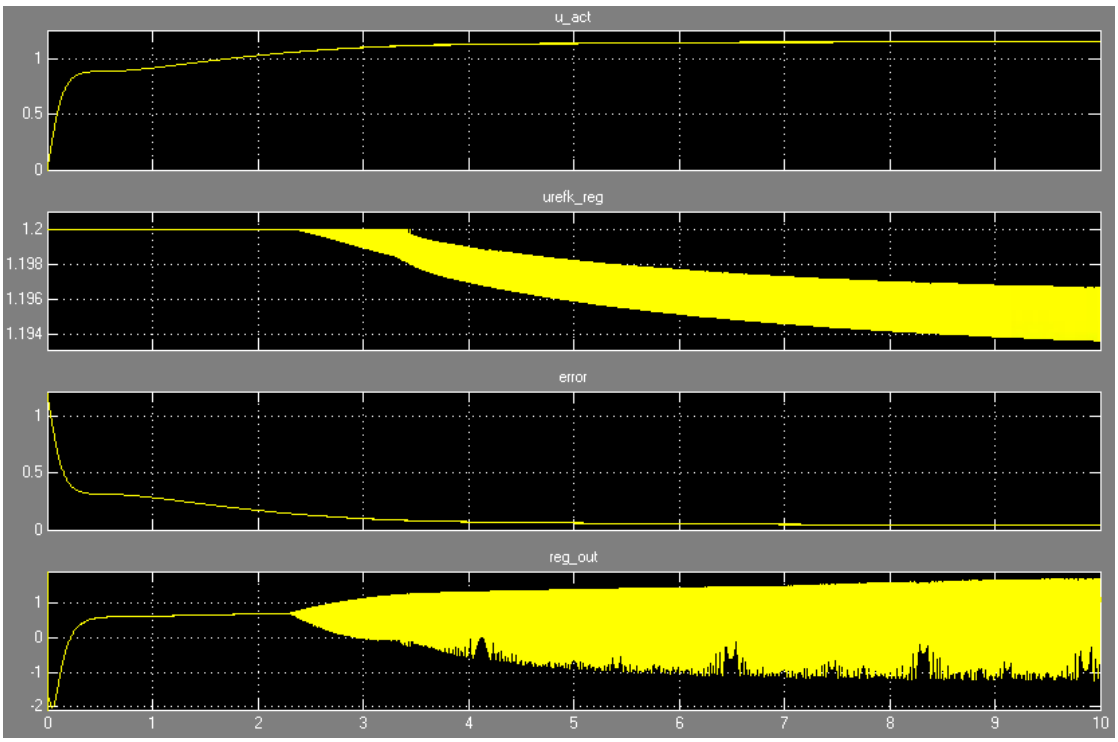

Figure C.6: 3333 kVA generator system output values from the voltage regulator, where u_act is the result of the filtered terminal voltage from the 3333kVA generator, $u_{refk}reg$ is the reference value signal, $error$ is the signal before the PID-controller in the voltage regulator, and reg_{out} is the output signal from the voltage regulator.

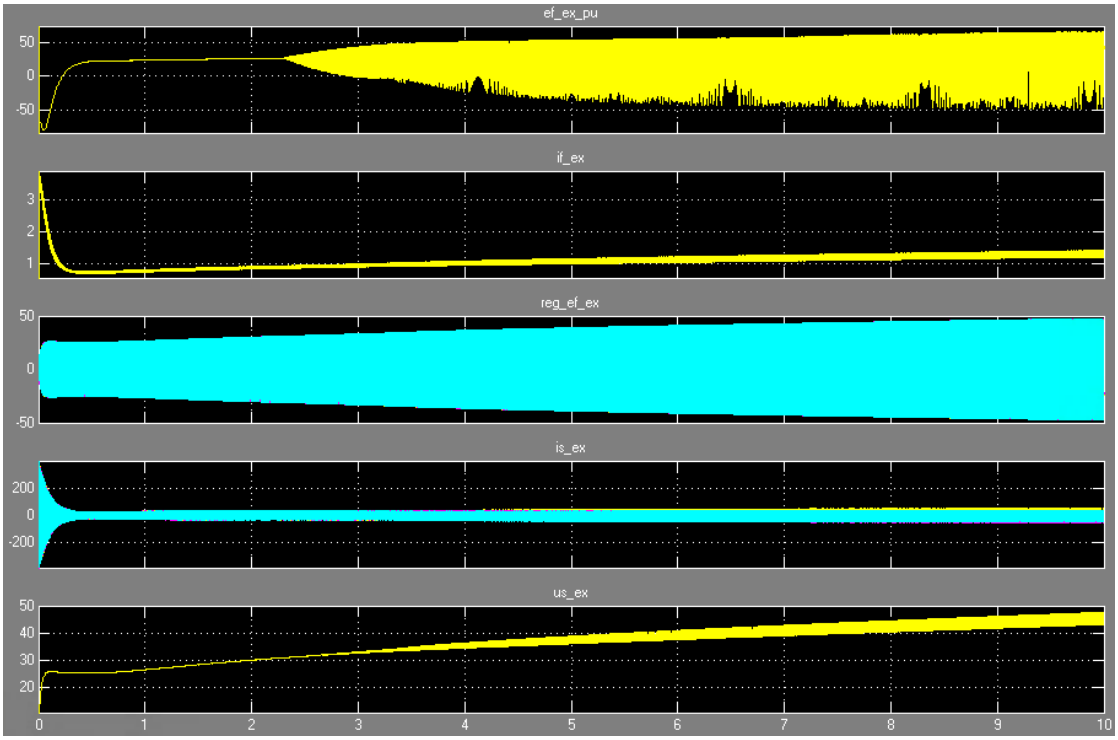

Figure C.7: 3333 kVA generator system output values from the exciter, where: e_f is the field voltage that excites the exciter-generator modeled as a salient pole, i_f is the field current that excites the exciter-generator modeled as a salient pole, i_s is the line current from the exciter generator output, u_s is the line voltage from the exciter generator output, and I_f is the current output from the rectifier after the exciter generator.

Appendix D

1940 kVA Generator MatLab/SimPowerSystems Model

D.1 Components and Parameters

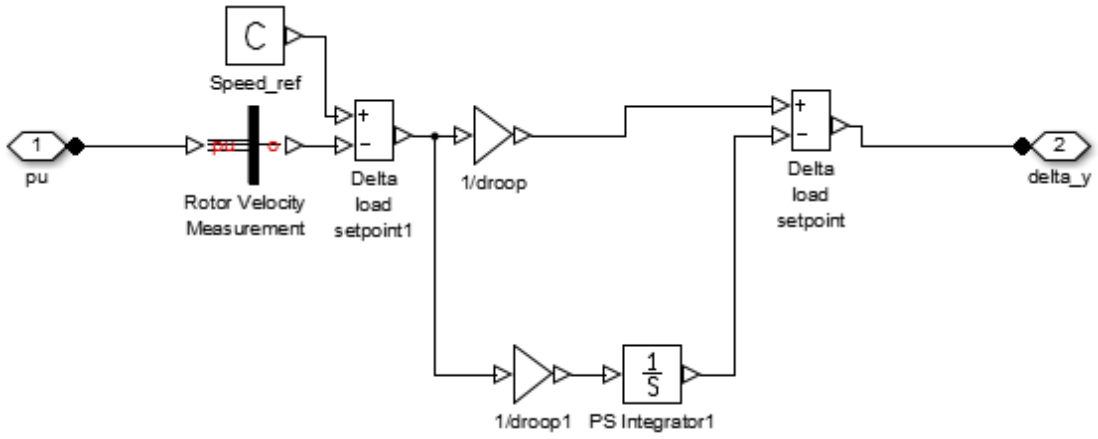

Figure D.1: One line diagram of the governor used in the 1940 kVA generator model in SimPowerSystems

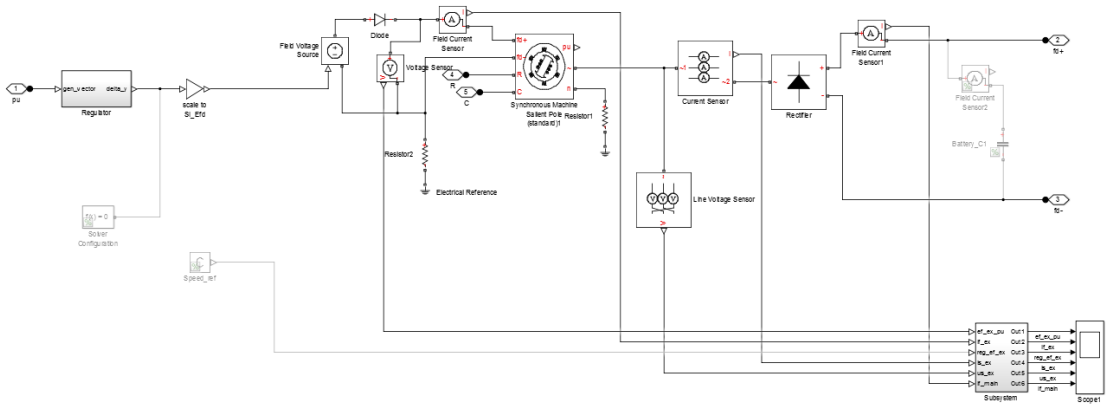

Figure D.2: One line diagram of the AVR and exciter used in the 1940 kVA generator model in SimPowerSystems

Table D.1: Parameter settings in 27.3 kVA exciter generator used in G2-model

Symbol	Unit	Parameter	Description
f	[Hz]	100	Rated electrical frequency
S	[VA]	27.3e3	Rated apparent power
V	[V]	128	Rated voltage
n	[-]	6	Number of pole pairs
I	[A]	3.15	Field circuit current
R_a	[pu]	0.015	Stator resistance
X_l	[pu]	0.15	Stator leakage reactance
X_d	[pu]	1.049	d-axis synchronous reactance
X_q	[pu]	0.543	q-axis synchronous reactance
X_0	[pu]	0.371	Zero-sequence reactance
$X‘_d$	[pu]	0.199	d-axis transient reactance
$X“_d$	[pu]	0.199	d-axis subtransient reactance
$X“_q$	[pu]	0.54	q-axis subtransient reactance
$T‘_{d0}$	[s]	0.509	d-axis transient open circuit
$T“_d$	[s]	0.0001	d-axis subtransient short circuit
$T“_q$	[s]	0.0001	q-axis subtransient schort circuit
V	[V]	1	Terminal voltage magnitude

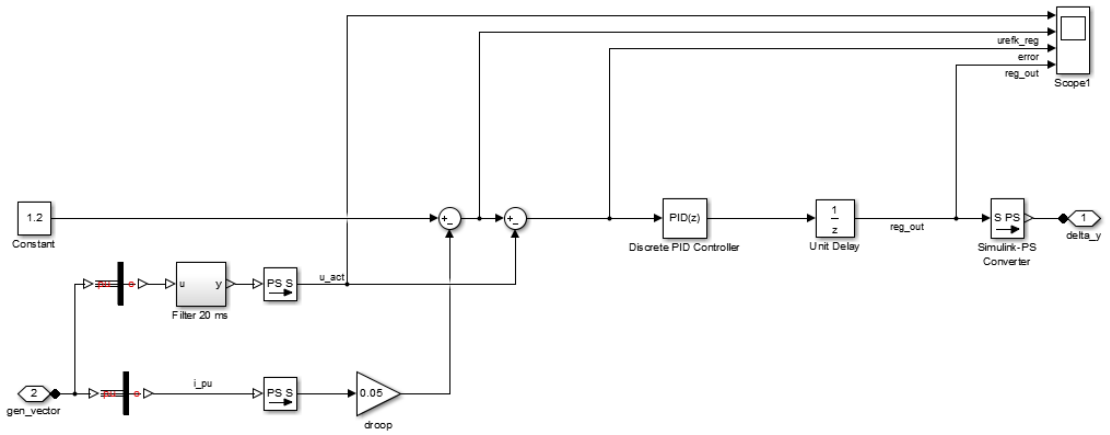

Figure D.3: One line diagram of the voltage regulator used in the 1940 kVA generator model in SimPowerSystems

Table D.2: Parameter settings for voltage regulator used in 1940 kVA generator model

Symbol	Unit	Parameter	Description
Constant			
Constant	[-]	1.2	Referance value
Filter 20ms			
$1/T$	[-]	50	PS gain
$1/S$	[-]	0	PS Integrator
droop			
d	[-]	0.05	Gain
Discrete PID controller			
P	[-]	1.19	Proportional
I	[-]	0.43	Integral
D	[-]	0.57	Derivative
N	[-]	10000	Filter coefficient

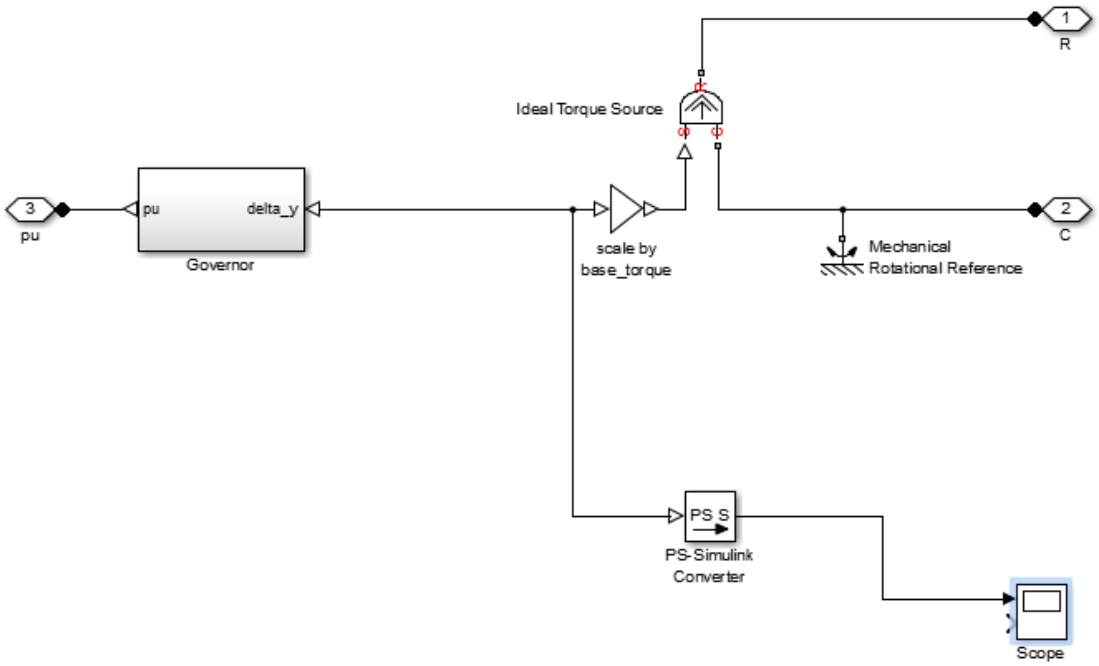

Figure D.4: One line diagram of the governor used to control the speed from the 1940 kVA generator used in the SimPowerSystems model.

Table D.3: Parameter settings for governor used in G2-model

Symbol	Unit	Parameter	Description
s_{ref}	[pu]	0.998	Speed reference
p	[%]	5	percentage droop
L	[pu]	0.5	Load reference setpoint
T_{gov}	[s]	0.002	Time constant of governor
T	[s]	0.003	Time constant of main inlet volumes and steam chest
τ_b	[kNm]	16.615	Base torque
τ_i	[pu]	0.451061	Initial torque

D.2 Simulation Results Measured from the Voltage Regulator, Exciter and Governor

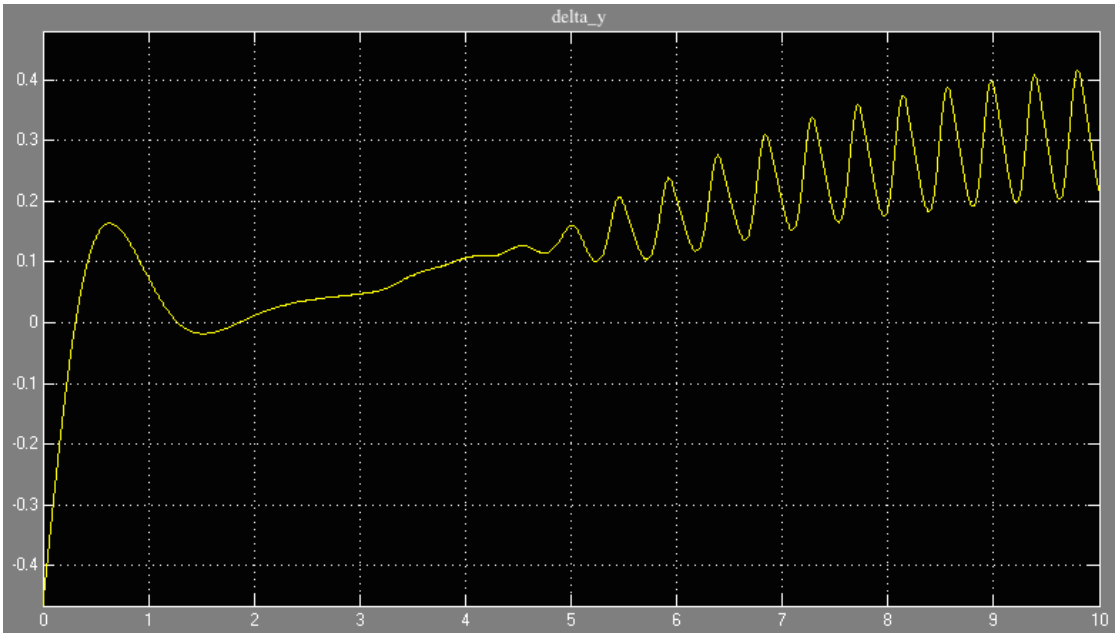

Figure D.5: 1940 kVA generator system output values from the governor, where $delta_y$ is the signal output from the governor.

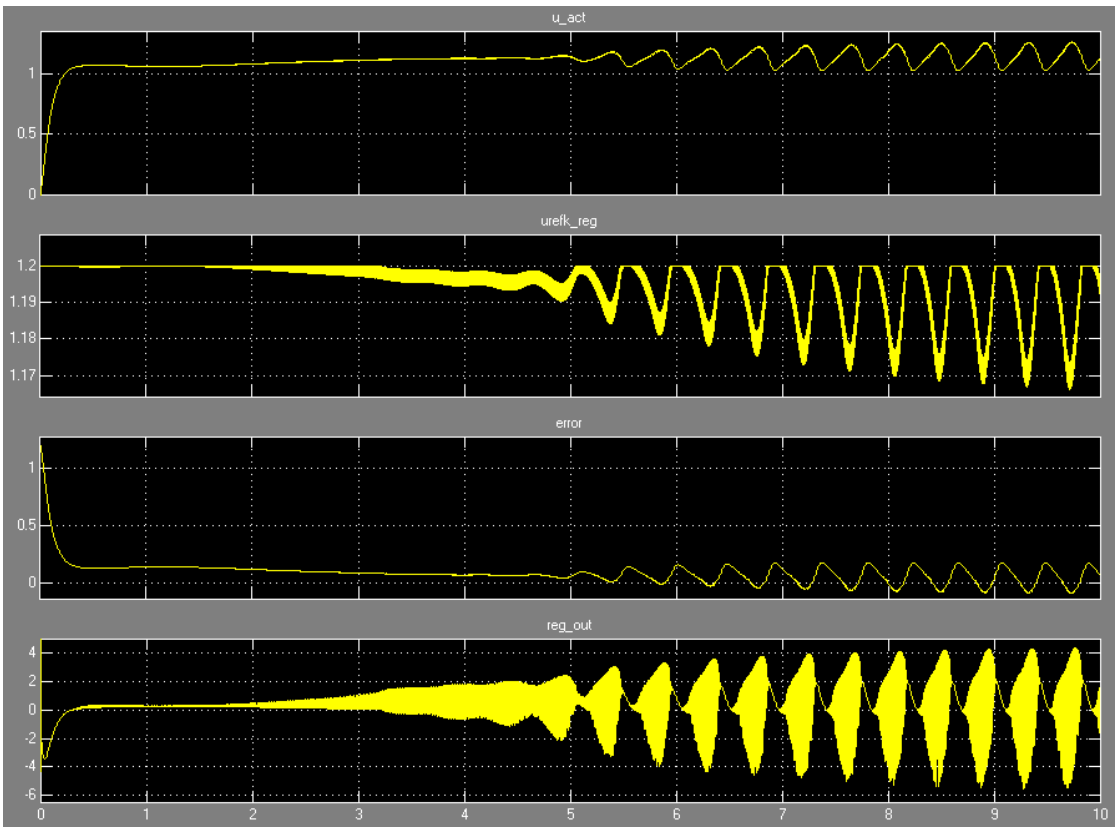

Figure D.6: 1940 kVA generator system output values from the voltage regulator, where u_act is the result of the filtered terminal voltage from the 1940kVA generator, $u_{refk}reg$ is the reference value signal, $error$ is the signal before the PID-controller in the voltage regulator, and reg_{out} is the output signal from the voltage regulator.

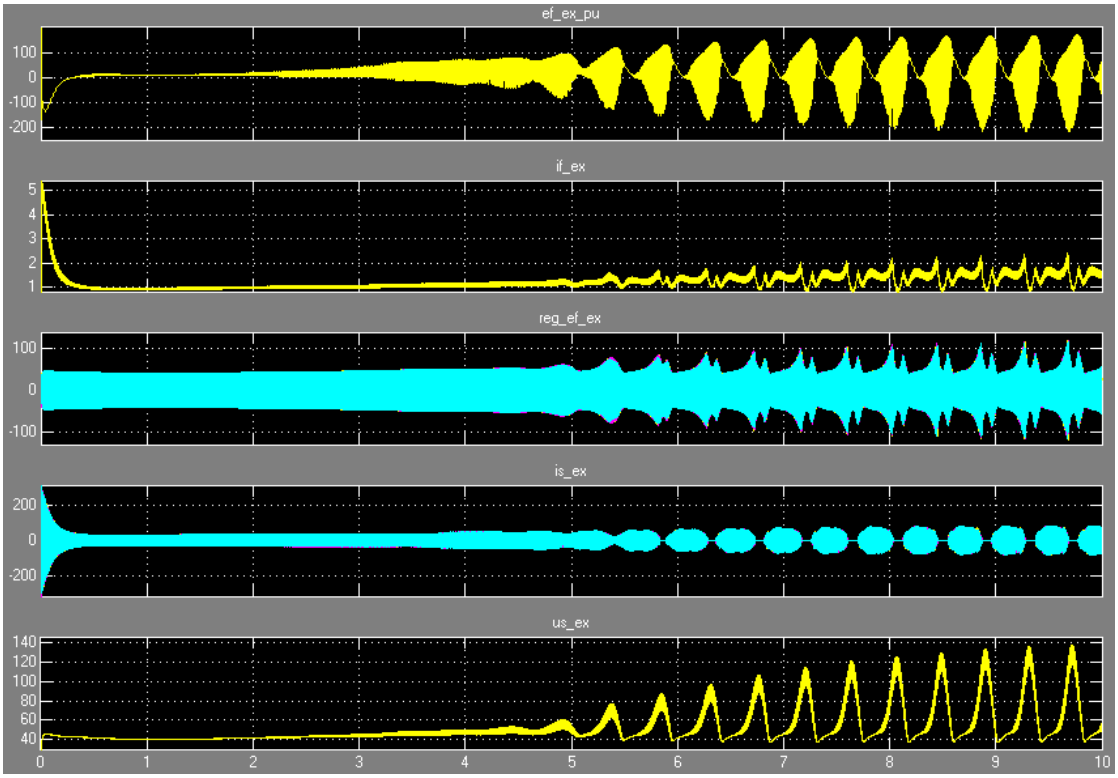

Figure D.7: 1940 kVA generator system output values from the exciter, where: e_f is the field voltage that excites the exciter-generator modeled as a salient pole, i_f is the field current that excites the exciter-generator modeled as a salient pole, i_s is the line current from the exciter generator output, u_s is the line voltage from the exciter generator output, and I_f is the current output from the rectifier after the exciter generator

Appendix E

Voltage Regulator ESAC8B used in PowerFactory

E.1 Block Diagram of AVR ESAC8B

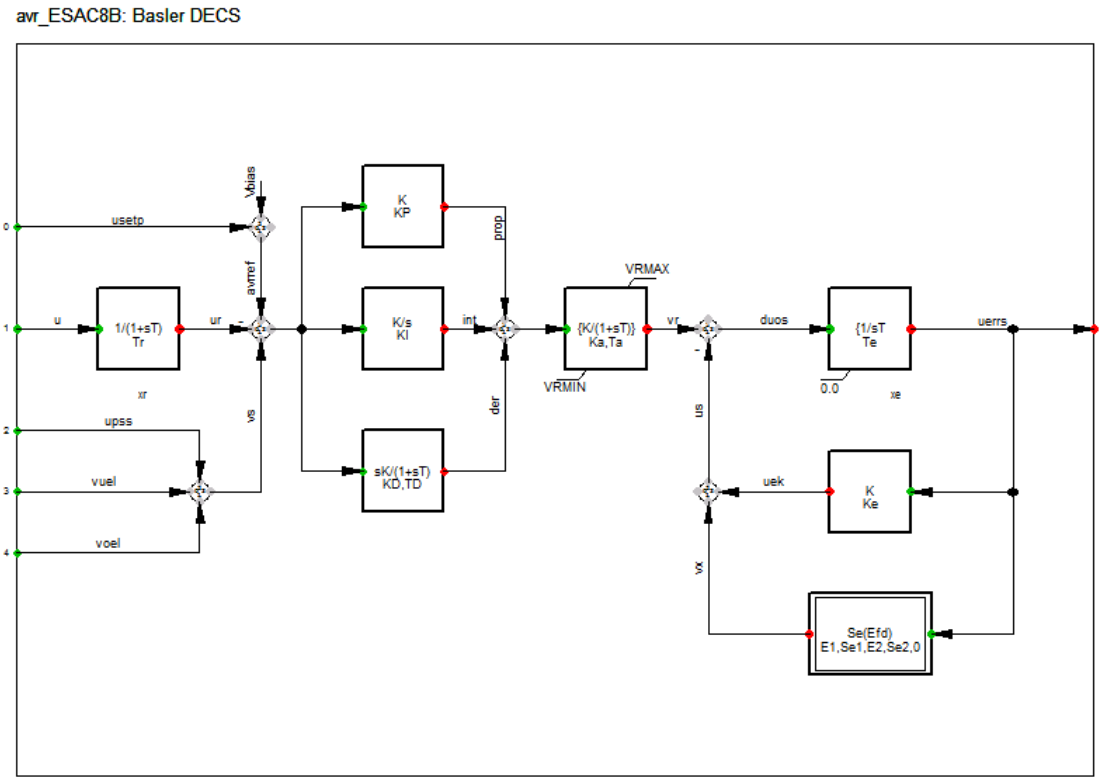

Figure E.1: The block diagram of the AVR ESAC8B.

E.2 Parameter Setting of AVR ESAC8B

Table E.1: Voltage regulator ESAC8B parameters settings

Symbol	Unit	Parameter	Description
K_p	[pu]	120.5	PID proportional gain
K_I	[pu]	165.5	PID integral gain
T_I	[s]	1	PID integral time constant
K_D	[pu]	25	PID derivative gain
T_D	[s]	0.01	PID derivative time constant
K_A	[pu]	1	Voltage regulator gain
T_A	[s]	0	Regulator time constant
V_{Rmax}	[pu]	35	Maximium regulator output
V_{Rmin}	[pu]	0	Minimum regulator output
K_E	[pu]	1.0	Exciter constant
T_E	[s]	0.5	Exciter time constant
S_{E1}	[pu]	1.346	Saturation curve value at point 1
E_1	[pu]	2.222	Voltage value at point 1
S_{E2}	[pu]	1.9	Saturation curve value at point 2
E_2	[pu]	2.962	Voltage value at point 2

Appendix F

System Component Parameters

F.1 Rectifier

Table F.1: Parameter settings in the rectifier block

Symbol	Unit	Parameter	Description
V	[V]	0.8	Forward voltage
r	[Ω]	0.0001	On-resistance
c	$[\frac{1}{\Omega}]$	1e-5	Off-conductance

F.2 Battery-Arrangement C1

Table F.2: Parameter settings in the battery-arrangement

Symbol	Unit	Parameter	Description
C	[F]	2100	Capacitance
r	[Ω]	1e-9	Series resistance
c	$[\frac{1}{\Omega}]$	0	Parallel conductance
V	[V]	1030	Capacitor voltage

F.3 Resistance

Table F.3: Parameter settings in the resistor

Symbol	Unit	Parameter	Description
r	[Ω]	0.0625	Resistance

Appendix G

SimScape Lithium-Ion Battery Model

G.1 Equivalent Circuit

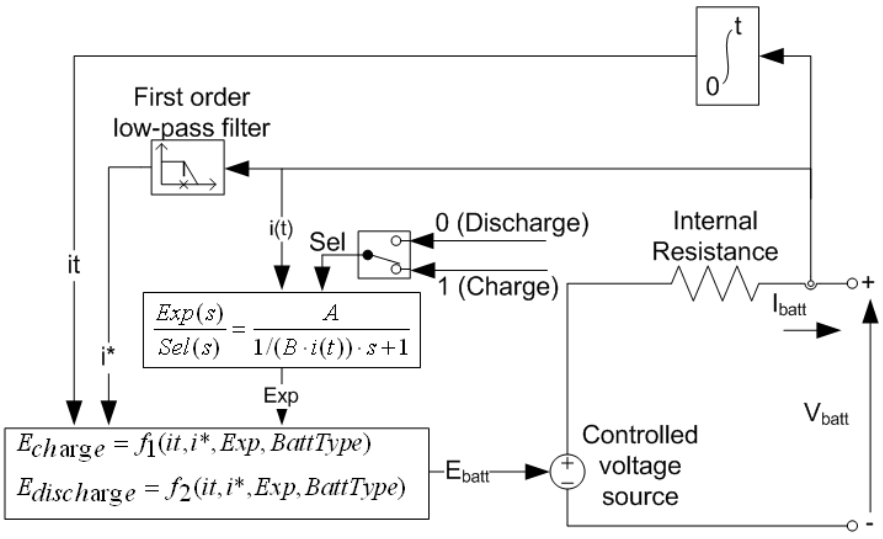

Figure G.1: The equivalent circuit of the SimScape-block lithium-ion type battery used in the SimPowerSystems model.

G.2 Lithium-Ion Battery Model

Discharge model (i*>0)

$$f_1(it, i*, i) = E_0 - K * \frac{Q}{Q - it} * i * -KK * \frac{Q}{Q - it} * it + A * exp(-B * it) \tag{G.1}$$

Charge model (i*<0)

$$f_2(it, i*, i) = E_0 - K * \frac{Q}{it + 0.1 * Q} * i * -KK * \frac{Q}{Q - it} * it + A * exp(-B * it) \tag{G.2}$$

Where:

- E_0 = Constant voltage
- K = Polarization constant (Ah^-1) or polarization resistance (Ohms)
- $i*$ = Low frequency current dynamics (A)
- i = Battery current (A)
- it = Extracted capacity (Ah)
- Q = Maximum battery capacity (Ah)
- A = Exponential voltage (V)
- B = Exponential capacity $(Ah)^(- 1)$

G.3 Rated Capacity=300Ah, $V_{initial} = 1030V$

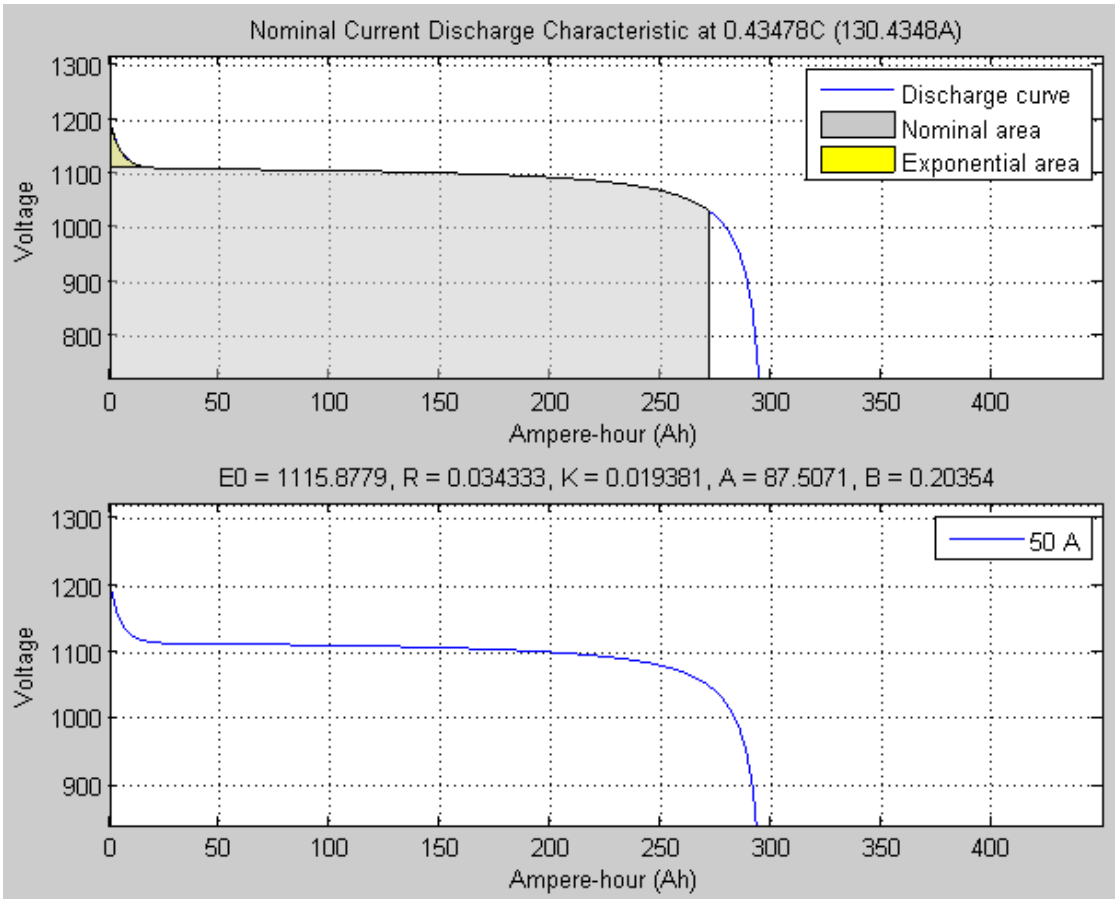

Figure G.2: The nominal current discharge characteristics of the battery with C=300Ah, $V_{initial} = 1030V$.

G.4 Rated Capacity=300Ah, $V_{initial} = 950V$

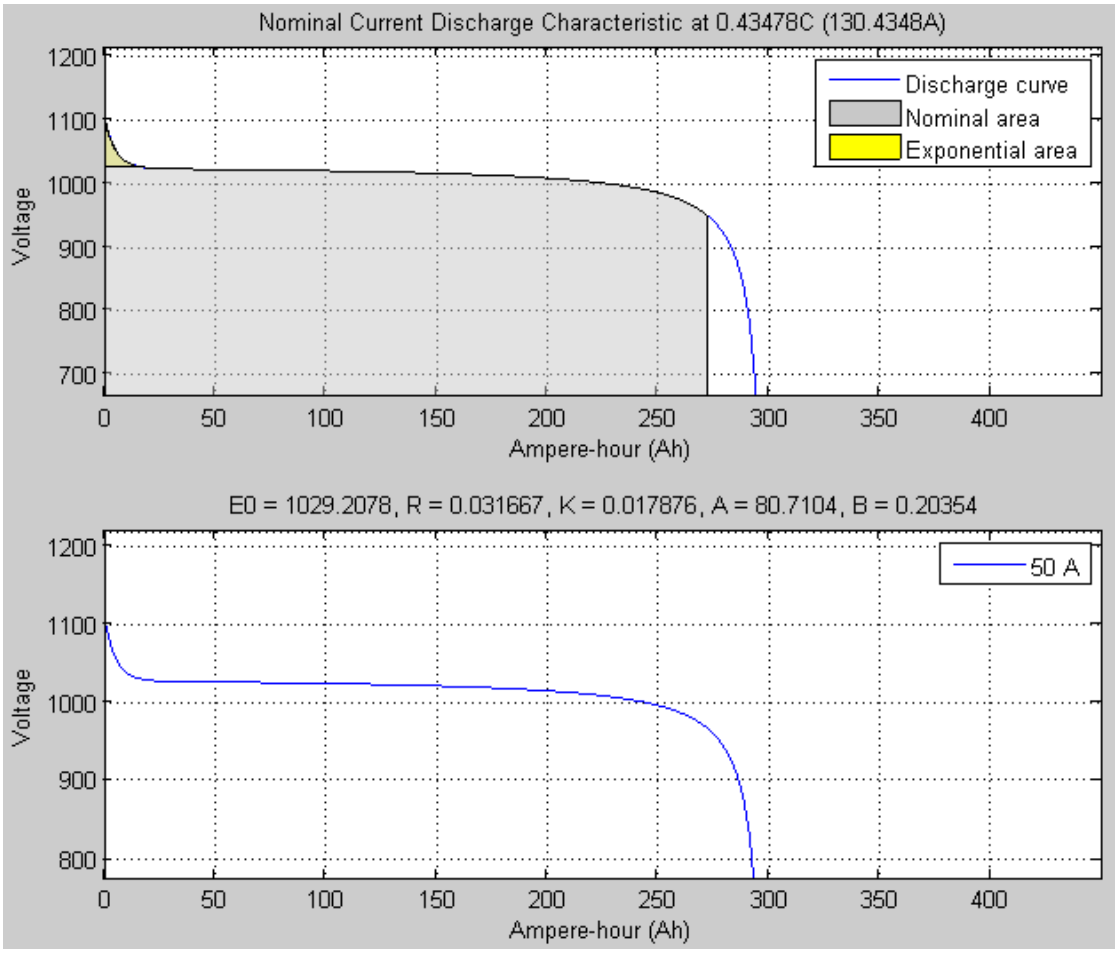

Figure G.3: The nominal current discharge characteristics of the battery with C=300Ah, $V_{initial} = 950V$.

G.5 Rated Capacity=150Ah, $V_{initial} = 950V$

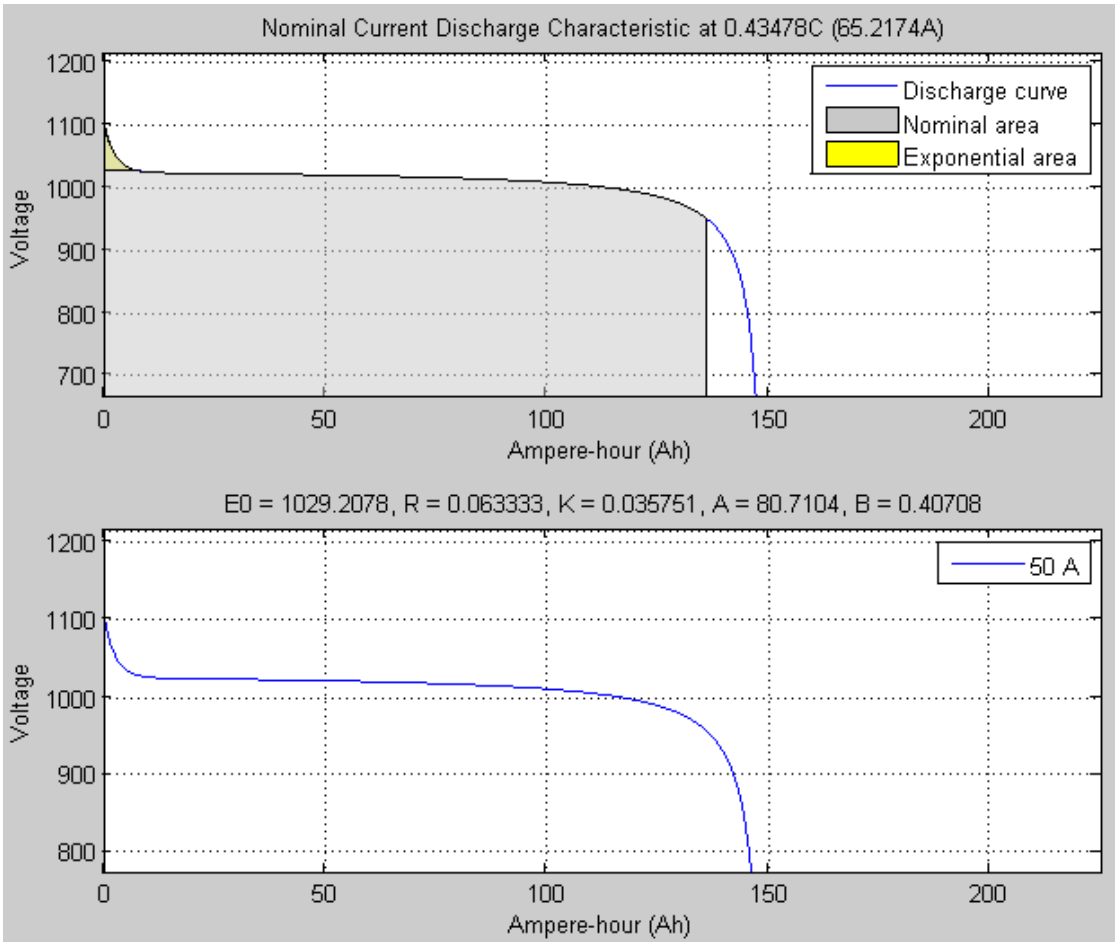

Figure G.4: The nominal current discharge characteristics of the battery with C=150Ah, $V_{initial} = 950V$.

Appendix H

Voltage Regulator AC5A in MatLab/SimPowerSystems

H.1 One-Line Diagram of AVR AC5A

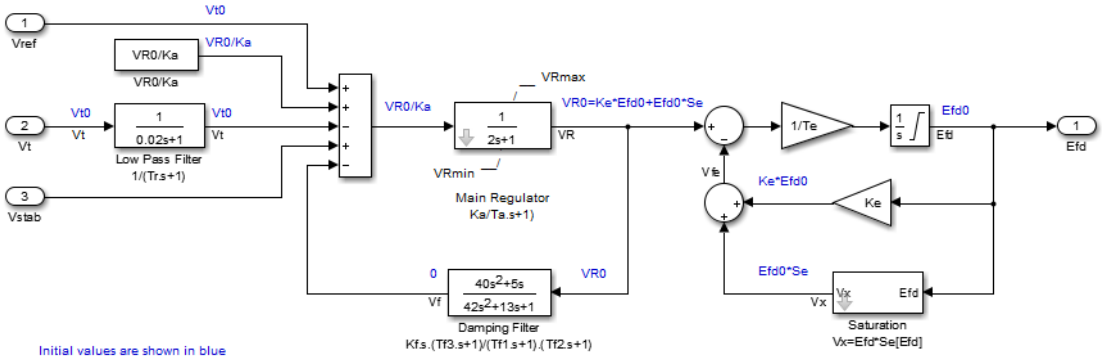

Figure H.1: The line diagram of the AVR AC5A.

H.2 Parameter Settings of AVR AC5A

Table H.1: Parameter settings for AVR type AC5A. Terminal voltage transducer: $T_R = 0, R_C = 0; X_C = 0$ [23]

Symbol	Unit	Parameter	Description
K_A	[pu]	400	Regulator output gain
T_A	[s]	0.02	Regulator output time constant
V_{RMAX}	[pu]	7.3	Maximum controller output voltage
V_{RMIN}	[pu]	-7.3	Minimum controller output voltage
T_E	[s]	0.8	Exciter field time constant
K_E	[pu]	1.0	Exciter field proportional constant
$S_E[E_{FD1}]$	[pu]	0.86	Saturation factor at E_{FD1}
E_{FD1}	[pu]	5.6	Exciter flux at $S_E[E_{FD1}]$
$S_E[E_{FD2}]$	[pu]	0.5	Saturation factor at E_{FD2}
E_{FD2}	[pu]	$0.75 * E_{FD1}$	Exciter flux at $S_E[E_{FD2}]$
K_F	[pu]	0.03	Rate feedback gain
T_{F1}	[pu]	1.0	Rate feedback time constant
T_{F2}	[pu]	0	Rate feedback time constant
T_{F3}	[pu]	0	Rate feedback time constant

H.3 G2 Output Parameters when AC5A is Added, and $V_{ref} = 1.0$ at No-Load. The Battery Arrangement is Included

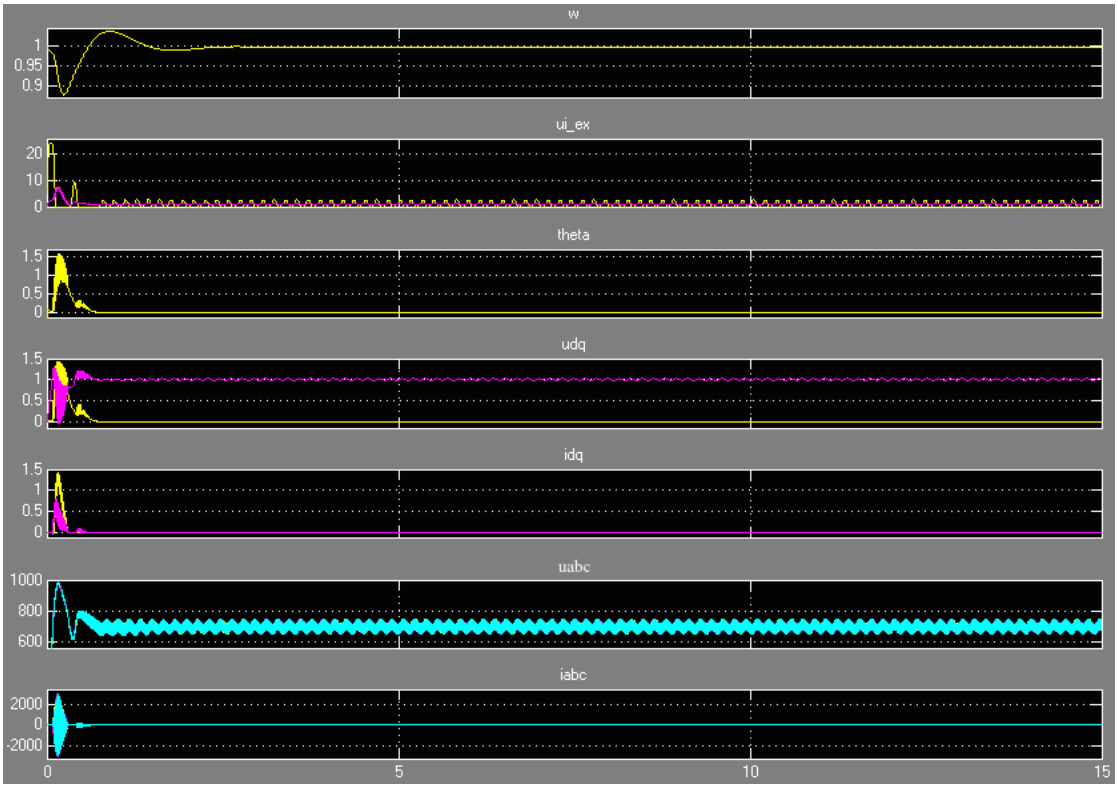

Figure H.2: The 1940kVA round rotor generator outputs when the AVR AC5A is added to the model, no load is attached to the dc-side of the rectifier, and the reference value of the regulator is 1.0. w is the rotor velocity, u_iex is the field voltage of the exciter, *theta* is the rotor angle, u_{dq} is the stator voltage in the d- and q-axis, i_{dq} is the stator current in the d- and q-axis, u_{abc} and i_{abc} is the terminal voltage in rms and the current, respectively.

H.4 G2 Output Parameters when AC5A is Added, and $V_{ref} = 1.2$ at No-Load. The 150Ah Battery Model is Included.

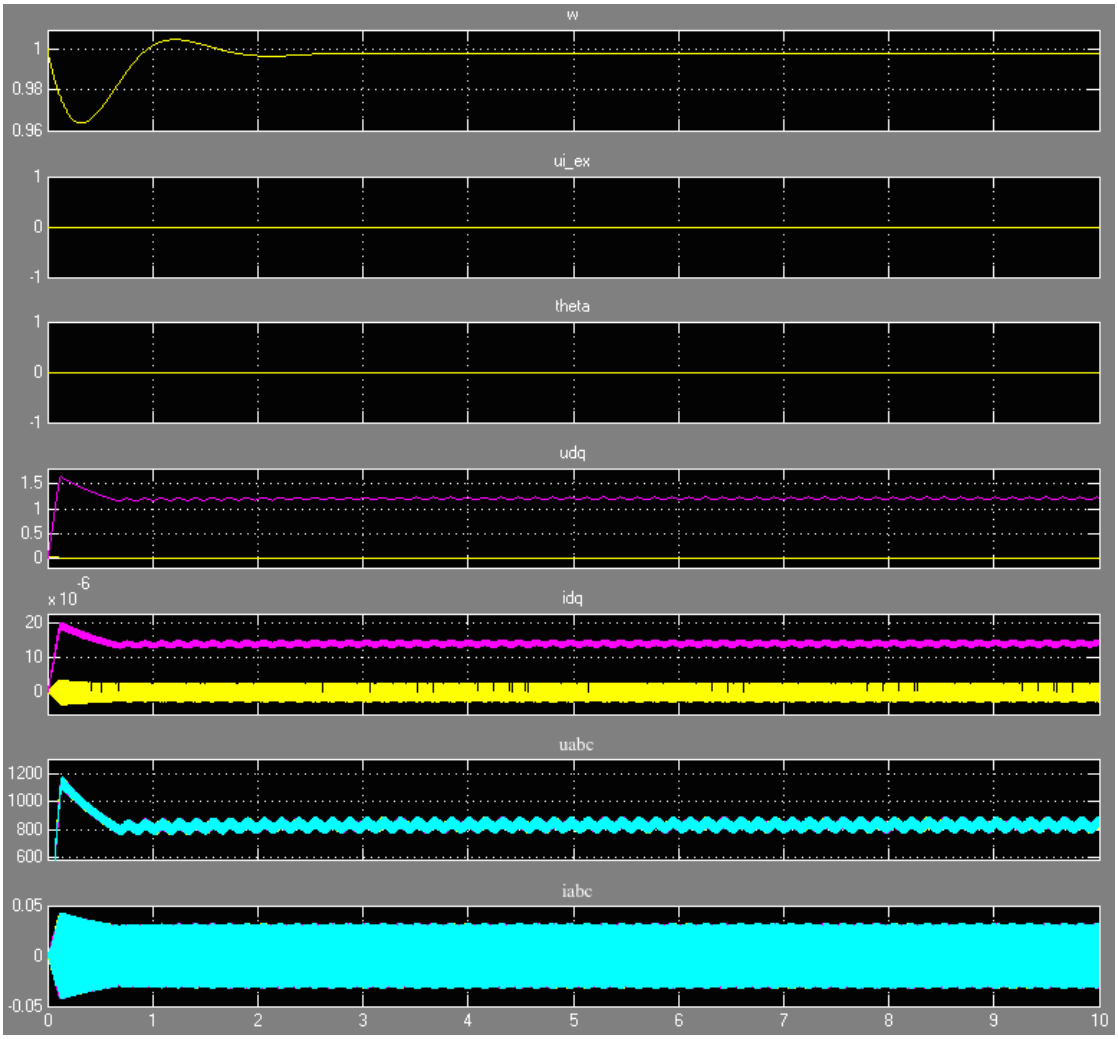

Figure H.3: The 1940kVA round rotor generator outputs when the AVR AC5A is added to the model, no load is attached to the dc-side of the rectifier, and the reference value of the regulator is 1.2. w is the rotor velocity, u_iex is the field voltage of the exciter, *theta* is the rotor angle, u_{dq} is the stator voltage in the d- and q-axis, i_{dq} is the stator current in the d- and q-axis, u_{abc} and i_{abc} is the terminal voltage in rms and the current, respectively.